A STABLE ISOTOPE APPROACH TO INVESTIGATE ECOHYDROLOGICAL PROCESSES IN NAMIBIA

Kudzai Farai Kaseke

Submitted to the faculty of the University Graduate School
in partial fulfillment of the requirements
for the degree
Doctor of Philosophy
in the Department of Earth Sciences
Indiana University

December 2018

Accepted by the Graduate Faculty, Indiana University, in partial fulfilment of the requirements for the degree of Doctor of Philosophy.

Doctoral Committee

_____

Lixin Wang, Ph.D., Chair

_____

Pierre-André Jacinthe, Ph.D.

_____

William P. Gilhooly, Ph.D.

April 23, 2018

_____

Jeffrey Wilson, Ph.D.

_____

Keir Soderberg, Ph.D.

ACKNOWLDGEMENTS

I would like to thank all the people that were instrumental in the culmination of this dissertation, without whom none of this work would have been possible. I appreciate the academic, financial and spiritual encouragement I have received over the years by my support groups. Unfortunately, I cannot mention everyone by name but rest assured of my love and gratitude.

First and foremost, I would like to express my gratitude to my advisor Dr. Lixin Wang for giving me the opportunity to pursue my studies under his mentorship. Thank you for the guidance, opportunities, collaborations, general advice on life and patience during this remarkable journey. The U.S National Science Foundation grants (IIA-1427642 and EAR-1554894) awarded to Dr. Lixin Wang and funded this work. This financial support was greatly appreciated as I was able to focus on the science and not worry about financial matters.

I would also like to thank my committee members: Professor Pierre-André Jacinthe, Professor Jeffrey Wilson, Dr. William P. Gilhooly and Dr. Keir Soderberg for their support and insightful comments that improved the quality of this dissertation. My collaborators: Dr. Heike Wanke, Veronika Turewicz, Dr. Paul Koeniger, Dr. Eugene Marais, Dr. Sujith Ravi, Dr. Mary Seely, Dr. Roland Vogt, Dr. Xuefei Lu, Dr. Chao Tian, Dr. Wenzhe Jiao, Bonan Li, Matthew Lanning, Theo Wassenaar and Roland Mushi; I will be forever indebted to you for all the input and support. My heart felt gratitude to Gobabeb Research and Training Centre: Gillian Maggs-Kölling, Novald Kandali, Ritha Kapitango and Jessica Sack for hosting me, assistance during fieldwork and unwavering support during this work.

The Earth Science Department staff for the many conversations and advice, all greatly appreciated and cherished. Special mention to Kevin Mandernack and Gabe Filippelli for the advice and assistance. A big thank you to Cathy Chouinard and Cheryl Montgomery for all the assistance with travel, paperwork and making my stay at IUPUI comfortable. Thank you to Dr. Patricia Clark for the opportunity and experience leading the ecology lab.

I would also like to thank the many friends and colleagues I have made during graduate school, far too many to mention. Please accept my apologies for not mentioning individuals in the fear of omitting a name. A big thank you to you all for keeping me sane

during this journey. My church family, The Blended Church and S.A.L.T, I love and appreciate you guys and thanks for making me feel at home. My family, Baba namai Kaseke, Baba namai Mutapanduwa, Baba namai Tadiwa, Taremekedzwa, Tadiwa and Anashe thank you for the love, support and patience. Last but certainly not least, I thank the Lord God for bringing me this far. Thank you, *tatenda*, *siyabonga*.

"Trust in the Lord with all your heart, and lean not on your own understanding; in all your ways acknowledge Him and He shall direct your paths." (Proverbs 3^{5-6})

Kudzai Farai Kaseke

A STABLE ISOTOPE APPROACH TO INVESTIGATE ECOHYDROLOGICAL PROCESSES IN NAMIBIA

Drylands cover 40% of the earth's terrestrial surface supporting over 2 billion people, the majority of whom reside in developing nations characterised by high population growth rates. This imposes pressure on the already limited water resources and in some dryland regions such as southern Africa, the origins and dynamics of rainfall are not well understood. Research has also tended to focus on factors limiting (e.g., rainfall) than sustaining productivity in drylands. However, non-rainfall water (NRW) e.g., fog and dew can supplement and/or exceed rainfall in these environments and could potentially be exploited as potable water resources. Much remains unknown in terms of NRW formation mechanisms, origins, evolution, potability and potential impact of global climate change on these NRW dependent ecosystems.

Using Namibia as a proxy for drylands and developing nations, this dissertation applies stable isotopes of water (δ^2H, $\delta^{18}O$, $\delta^{17}O$ and d-excess), cokriging and trajectory analysis methods to understand ecohydrological processes. Results suggest that locally generated NRW may be a regular occurrence even in coastal areas such as the Namib Desert, and that what may appear as a single fog event may consist of different fog types co-occurring. These results are important because NRW responses to global climate change is dependent on the source, groundwater vs. ocean, and being able to distinguish the two will allow for more accurate modelling. I also demonstrate, that fog and dew formation are controlled by different fractionation processes, paving the way for plant water use strategy studies and modelling responses to global climate change. The study also suggests that current NRW harvesting technologies could be improved and that the potability of this water could raise some public health concerns related to trace metal and biological contamination. At the same time, the dissertation concludes that global precipitation isoscapes do not capture local isotope variations in Namibia, suggesting caution when applied to drylands and developing nations. Finally, the dissertation also reports for the first time, $\delta^{17}O$ precipitation results for Namibia, novel isotope methods to differentiate

synoptic from local droughts and suggests non-negligible moisture contributions from the Atlantic Ocean due to a possible sub-tropical Atlantic Ocean dipole.

Lixin Wang, Ph.D., Chair

TABLE OF CONTENTS

LIST OF TABLES

LIST OF FIGURES

CHAPTER 1: INTRODUCTION

Drylands are water scarce regions, often defined on the basis of the ratio of mean annual precipitation to mean annual evaporative demand (UNEP and Thomas 1992, Wang et al. 2012, Ojima et al. 1993). They account for over 40% of the earth's terrestrial surface (Slaymaker and Spencer 1998), and despite the limitations to productivity imposed by water scarcity (Louw and Seely 1982, Whitford 2002), contribute about 40% of global net primary productivity (Grace et al. 2006). In these ecosystems, non-fall water (e.g., fog and dew) is an important component of the hydrological cycle that can exceed annual rainfall (Agam and Berliner 2006, Wang et al. 2016, Kidron et al. 2011). It is thus not surprising that the ecophysiology of desert organisms is adapted to obtaining non-rainfall water (Henschel and Seely 2008). However, rainfall is still the major water input and driver of biological processes in these ecosystems (Noy-Meir 1973, Li et al. 2016), thus non-rainfall water plays a supplementary role and sustains flora and fauna during the absence of rainfall (Seely et al. 2005). Despite its acknowledged importance, non-rainfall water is often the least studied component of the hydrological cycle as research often focuses on limiting factors rather than factors sustaining productivity. Therefore, there are large gaps in knowledge related to the origins and formation mechanisms of non-rainfall water especially in drylands.

It is often assumed that non-rainfall water in coastal drylands is advected from the ocean (Olivier 1995, Dawson 1998), but many dryland regions have groundwater resources (Yang et al. 2010, Houston 2002) that could contribute to non-rainfall water in these areas (Cereceda et al. 2002, Eckardt et al. 2013). However, we are not aware of any systematic studies that have investigated this possibility. How fog and dew will change in the future is dependent on their formation and origins, groundwater versus ocean. At the same time, because non-rainfall water is often not well characterised, most ecological studies tend to group fog and dew as the same input (Brown et al. 2008), although they are different meteorological phenomena. This distinction is important because vegetation may be differentially adapted to harvesting fog and dew (Roth-Nebelsick et al. 2012, Ebner et al. 2011, Esler et al. 1999). Therefore, the increase in frequency of one of these components does not necessarily translate to the same species composition or distribution. To better

understand plant functioning under current or future climates and develop sound ecological models for arid environments, it is therefore important to identify the origins non-rainfall water and be able to differentiate non-rainfall components.

Advective fog is a prominent feature of the south-west coast of Africa (Olivier 2004, Jacobson et al. 2015, Seely 1979) and is thought to be the architect of the Namib fog-zone, an area of the most visible impacts of fog on ecophysiology extending up-to 60 km inland (Seely 1979, Lancaster 1984, Olivier 1995, Hamilton and Seely 1976). However, there is speculation that other fog types may be a regular occurrence, especially along ephemeral rivers and other low laying areas (Eckardt et al. 2013). Furthermore, fog classification is often subjective (George 1951, Tardif and Rasmussen 2007) and may be complicated by co-occurrence of different types of fog over large geographic areas (Bari et al. 2016). There is thus a need for an objective method to classify fog as we may be under-estimating the significance of other fog types, which might hinder modelling of the potential impact of global climate change on these fog dominated environments. For example, satellite imagery and models tend to underestimate fog occurrence in the Namib Desert, especially inland (Haensler et al. 2011). This could be related to the formation of locally generated fog that may not be detectable from satellite imagery. If and how this locally generated fog combines with advective fog is unclear and so is the composition of this fog. This is surprising given the ecohydrological significance of fog to many arid and semi-arid ecosystems, coastal regions and tropical montane forests (Schemenauer and Cereceda 1991, Dawson 1998, Ebner et al. 2011, Nørgaard et al. 2012, Li et al. 2018). However, this has not prevented efforts to model the potential impacts of global climate change on fog dominated systems. For example, fog frequency in the Namib Desert is predicted to increase at the coast and decrease inland (Haensler et al. 2011). This will undoubtedly impact flora and fauna species composition and distribution negatively, especially inland. However, because these models are based on the assumption that advective fog is the only fog type affecting this region, they may be overly simplistic and or dramatic in their predictions. Therefore, it is important to determine the spatial distribution and evolution of fog, which should allow for the generation of more realistic models.

Given the importance of non-rainfall water to dryland ecosystems, its potential as a potable source of water has been acknowledged since ancient times e.g., the legend of the rain tree of Ferro Island (Hutchinson 1919). Even more recently, there has been strong interest in utilising fog and dew as supplementary water resources (Schutte 1971, Fessehaye et al. 2014, Abdul-Wahab et al. 2007a, Muselli et al. 2006, Schemenauer and Cereceda 1994, Sharan et al. 2017). However, whereas most research and reviews suggest that this water is potable (Klemm et al. 2012, Abdul-Wahab et al. 2007b, Sharan et al. 2011), fog and dew quality is a function of air quality and gas-liquid-solid heterogeneous interactions (Herckes et al. 2007, Lekouch et al. 2011, Nath and Yadav 2017). Therefore, non-rainfall water could be susceptible to trace metal contamination which could be of concern to human health. However, most of the non-rainfall water studies do not conduct any trace metal or biological analyses thus we do not know the extent of this problem. At the same time, fog and dew harvesting technologies have been driven by convenience and local availability than innovation, thus these technologies and harvesting could be improved by the use of materials specifically designed for fog and or dew harvesting (Sharan et al. 2017). Therefore, we provide a perspective on fog and dew harvesting improvements and concerns on potability.

Despite the potential of non-rainfall water as potable water resources, they are unlikely to replace traditional water sources in drylands. Drylands support 1.2-2 billion people (WWAP 2012, Gilbert 2011, MEA 2005), 90% of whom reside in developing nations with population growth rates above the global average, exacerbating the already tight limitations imposed by water availability on water and food security in these regions (Wang et al. 2012). Given the threat of global climate change, the response of dryland ecosystems is therefore important as global water resources are inherently related to and affected by population growth (Vörösmarty et al. 2000). Water scarcity is thus one of the major threats to mankind in the 21st century (Prinz 2000) and there is a need to understand hydrological processes at both global and local scales to create an inventory of available water resources and encourage efficient management of these resources. Understanding the spatio-temporal variation of precipitation isotope patterns (isoscapes) could provide information on regional and global hydrologic processes that may enable preparation for potential global climate change impacts (Sánchez-Murillo et al. 2013). The basis for most

global isoscapes is the Global Network for Isotopes in Precipitation (GNIP) database. However, the dataset has inherent deficiencies related to but not limited to coarse spatio-temporal resolution and station unevenness (West et al. 2014). This results in insufficient data coverage for many regions that are of interest to hydrologists, geologists and ecologists (Wassenaar et al. 2009, Zhao et al. 2012). Unfortunately, most of these data deficient regions are located in drylands and developing nations, thus the accuracy and relevance of global isoscapes is questionable, at least to these regions. At the same time, these regions may have precipitation isotope data that may not meet the GNIP standards or scope. Therefore, could these data be utilized somehow to generate regional or local isoscapes, and how do these isoscapes compare to global isoscapes for the same region and do these localised isoscapes reflect synoptic systems influencing rainfall in the area or should these data be discarded?

Although global isoscapes reproduce reasonably well the global distribution of mean annual isotope contents of modern precipitation (Risi et al. 2010, Werner et al. 2011), they do not fully explain observed seasonal or inter-annual variations at regional or locale scale (Field 2010, Vuille et al. 2003, Schmidt et al. 2005, Risi et al. 2010). Recent work also suggests intra-storm variability (Barras and Simmonds 2009, Coplen et al. 2008), thus event scale studies capture day-to-day synoptic variation that may be lost or diluted in monthly samples (Liu et al. 2010, Noone and Simmonds 2002). Therefore, event-scale comparisons with monthly or annual data may help define underlying uncertainties in relationships between the isotopic composition of precipitation and climate variables (Soderberg et al. 2013). At the same time, event-scale samples enable the use of backward trajectory analyses to determine precipitation origins and when coupled with isotope data, evaporative conditions (Sinclair et al. 2011, Baldini et al. 2010, Soderberg et al. 2013). Given that the climate of southern Africa is not well constrained and the influence of the Atlantic Ocean on precipitation events in the region is unknown (Reason et al. 2006), event-scale precipitation isotopes coupled with trajectory analysis may give new insights to precipitation patterns in southern Africa, at least Windhoek.

This dissertation applies stable water isotopes ($\delta^{18}O$ and $\delta^{2}H$), environmental tracers that have been used to understand dynamics and processes in hydrology, geology, ecology and climate research (Stumpp et al. 2014, Soderberg et al. 2013, Gat 1996). Isotope

fractionation processes impart unique signatures on meteoric water that can be combined with deuterium excess (*d*), a second order parameter defined as $d = \delta D - 8 \times \delta^{18}O$ (Dansgaard 1964) to determine vapour source evaporative conditions (Merlivat and Jouzel 1979). The study also applies $\delta^{17}O$ as an additional parameter as recent work suggests it is indicative of humidity conditions at the evaporative source, independent of temperature (Angert et al. 2004, Barkan and Luz 2007). Thus the inclusion of ^{17}O to stable water isotopes could lead to new insights and understanding of ecohydrological processes in addition to those obtained from $\delta^{18}O$, $\delta^{2}H$ and *d*. The location of the study, Namibia, was chosen because the country is classified as both a dryland and developing nation, is represented by a single sampling point in the GNIP database, and has several short-term precipitation isotope studies that have been conducted in the country. At the same time, the Central Namib Desert is characterised by an abundance of fog and dew (Henschel and Seely 2008). While groundwater along the ephemeral Kuiseb and Swakop rivers is derived from the interior (Jacobson et al. 1995), at higher elevation, "altitude effect" (Friedman and Smith 1970). This would result in distinct isotopic compositions of groundwater, rainfall and the ocean; thus non-rainfall water derived from these waters should reflect these differences, making the Central Namib an ideal site for non-rainfall water research suing isotope methods. Therefore, Namibia was the perfect proxy for an isotope approach to investigate dryland ecohydrological processes.

The dissertation has the following main objectives and will be structured as: 1) Determination of non-rainfall water origins and formation mechanisms (Chapter 2), 2) Development of novel isotope methods to differentiate fog from dew (Chapter 2), 3) Determination of the spatial variation and evolution of fog in the Namib Desert (Chapter 3), 4) A perspective on fog and dew as potable water resources (Chapter 4), 5) Determination of the relevance and applicability of global precipitation isoscapes to drylands and developing nations (Chapter 5) 6) The origins and key drivers of precipitation isotopes over Windhoek (Chapter 6) and 7) Conclusions (Chapter 7).

References

Abdul-Wahab, Sabah A, Hilal Al-Hinai, Khalid A Al-Najar, and Mohammed S Al-Kalbani. 2007a. "Feasibility of fog water collection: a case study from Oman." *Journal of Water Supply: Research and Technology-AQUA* 56 (4):275-280.

Abdul-Wahab, Sabah A, Hilal Al-Hinai, Khalid A Al-Najar, and Mohammed S Al-Kalbani. 2007b. "Fog water harvesting: quality of fog water collected for domestic and agricultural use." *Environmental Engineering Science* 24 (4):446-456.

Agam, N, and PR Berliner. 2006. "Dew formation and water vapor adsorption in semi-arid environments—a review." *Journal of Arid Environments* 65 (4):572-590.

Angert, Alon, Christopher D Cappa, and Donald J DePaolo. 2004. "Kinetic ^{17}O effects in the hydrologic cycle: Indirect evidence and implications." *Geochimica et cosmochimica acta* 68 (17):3487-3495.

Baldini, Lisa M, Frank McDermott, James UL Baldini, Matthew J Fischer, and Martin Möllhoff. 2010. "An investigation of the controls on Irish precipitation $\delta^{18}O$ values on monthly and event timescales." *Climate dynamics* 35 (6):977-993.

Bari, Driss, Thierry Bergot, and Mohamed El Khlifi. 2016. "Local Meteorological and Large-Scale Weather Characteristics of Fog over the Grand Casablanca Region, Morocco." *Journal of Applied Meteorology and Climatology* 55 (8):1731-1745.

Barkan, Eugeni, and Boaz Luz. 2007. "Diffusivity fractionations of $H_2{}^{16}O/H_2{}^{17}O$ and $H_2{}^{16}O/ H_2{}^{18}O$ in air and their implications for isotope hydrology." *Rapid Communications in Mass Spectrometry* 21:2999-3005.

Barras, Vaughan, and Ian Simmonds. 2009. "Observation and modeling of stable water isotopes as diagnostics of rainfall dynamics over southeastern Australia." *J. Geophys. Res.* 114 (D23):D23308. doi: 10.1029/2009jd012132.

Brown, Roger, Anthony J Mills, and Chris Jack. 2008. "Non-rainfall moisture inputs in the Knersvlakte: methodology and preliminary findings: short communication." *Water SA* 34 (2):275-278.

Cereceda, P, P Osses, H Larrain, M Farıas, M Lagos, R Pinto, and RS Schemenauer. 2002. "Advective, orographic and radiation fog in the Tarapacá region, Chile." *Atmospheric Research* 64 (1):261-271.

Coplen, Tyler B., Paul J. Neiman, Allen B. White, Jurate M. Landwehr, F. Martin Ralph, and Michael D. Dettinger. 2008. "Extreme changes in stable hydrogen isotopes and precipitation characteristics in a landfalling Pacific storm." *Geophysical Research Letters* 35:L21808, doi:10.1029/2008GL035481.

Dansgaard, W. 1964. "Stable isotopes in precipitation." *Tellus, 16*:436-468.

Dawson, T.E. 1998. "Fog in the California redwood forest: ecosystem inputs and use by plants." *Oecologia* 117:476-485.

Ebner, M, T Miranda, and A Roth-Nebelsick. 2011. "Efficient fog harvesting by Stipagrostis sabulicola (Namib dune bushman grass)." *Journal of Arid Environments* 75 (6):524-531.

Eckardt, FD, K Soderberg, LJ Coop, AA Muller, KJ Vickery, RD Grandin, C Jack, TS Kapalanga, and J Henschel. 2013. "The nature of moisture at Gobabeb, in the central Namib Desert." *Journal of Arid Environments* 93:7-19.

Esler, Karen J, Phillip W Rundel, and Piet Vorster. 1999. "Biogeography of prostrate-leaved geophytes in semi-arid South Africa: hypotheses on functionality." *Plant Ecology* 142 (1-2):105-120.

Fessehaye, Mussie, Sabah A Abdul-Wahab, Michael J Savage, Thomas Kohler, Tseggai Gherezghiher, and Hans Hurni. 2014. "Fog-water collection for community use." *Renewable and Sustainable Energy Reviews* 29:52-62.

Field, Robert D. 2010. "Observed and modeled controls on precipitation $\delta^{18}O$ over Europe: From local temperature to the Northern Annular Mode." *Journal of Geophysical Research: Atmospheres* 115 (D12).

Friedman, Irving, and George I Smith. 1970. "Deuterium content of snow cores from Sierra Nevada area." *Science* 169 (3944):467-470.

Gat, Joel R. 1996. "Oxygen and hydrogen isotopes in the hydrologic cycle." *Annual Review of Earth and Planetary Sciences* 24 (1):225-262.

George, Joseph J. 1951. "Fog." In *Compendium of meteorology*, 1179-1189. Springer.

Gilbert, Natasha. 2011. "United Nations considers creating advisory panel on land degradation akin to IPCC." *Nature* 477:262-264, doi:10.1038/477262a.

Grace, J., J. San José, P. Meir, H. S. Miranda, and R. A. Montes. 2006. "Productivity and carbon fluxes of tropical savannas." *Journal of Biogeography* 33:387–400, doi:10.1111/j.1365-2699.2005.01448.x.

Haensler, Andreas, Jan Cermak, Stefan Hagemann, and Daniela Jacob. 2011. "Will the southern African west coast fog be affected by future climate change? Results of an initial fog projection using a regional climate model." *Erdkunde*:261-275.

Hamilton, William J, and Mary K Seely. 1976. "Fog basking by the Namib Desert beetle, Onymacris unguicularis."

Henschel, Joh R, and Mary K Seely. 2008. "Ecophysiology of atmospheric moisture in the Namib Desert." *Atmospheric Research* 87 (3):362-368.

Herckes, Pierre, Hui Chang, Taehyoung Lee, and Jeffrey L Collett. 2007. "Air pollution processing by radiation fogs." *Water, air, and soil Pollution* 181 (1-4):65-75.

Houston, John. 2002. "Groundwater recharge through an alluvial fan in the Atacama Desert, northern Chile: mechanisms, magnitudes and causes." *Hydrological processes* 16 (15):3019-3035.

Hutchinson, J. 1919. "The Rain Tree of Hierro, Canary Islands.(Oreodaphne foetens.)." *Bulletin of Miscellaneous Information (Royal Botanic Gardens, Kew)* 1919 (3):153-164.

Jacobson, Kathryn, Anne van Diepeningen, Sarah Evans, Rachel Fritts, Philipp Gemmel, Chris Marsho, Mary Seely, Anthony Wenndt, Xiaoxuan Yang, and Peter Jacobson. 2015. "Non-Rainfall Moisture Activates Fungal Decomposition of Surface Litter in the Namib Sand Sea."

Jacobson, P.J, Kathryn M. Jacobson, and M. K Seely. 1995. *Ephemeral rivers and their catchments : sustaining people and development in western Namibia*. Edited by P.J Jacobson, Kathryn M. Jacobson and M. K Seely. Windhoek: Desert Research Foundation of Namibia.

Kidron, Giora J, Marina Temina, and Avraham Starinsky. 2011. "An investigation of the role of water (rain and dew) in controlling the growth form of lichens on cobbles in the Negev Desert." *Geomicrobiology Journal* 28 (4):335-346.

Klemm, Otto, Robert S Schemenauer, Anne Lummerich, Pilar Cereceda, Victoria Marzol, David Corell, Johan van Heerden, Dirk Reinhard, Tseggai Gherezghiher, and Jana

Olivier. 2012. "Fog as a fresh-water resource: overview and perspectives." *Ambio* 41 (3):221-234.

Lancaster, MK. 1984. "Climate of the central Namib Desert." *Madoqua* 14 (1):5-61.

Lekouch, Imad, Marc Muselli, Belkacem Kabbachi, Jalil Ouazzani, Iryna Melnytchouk-Milimouk, and Daniel Beysens. 2011. "Dew, fog, and rain as supplementary sources of water in south-western Morocco." *Energy* 36 (4):2257-2265.

Li, Bonan, Lixin Wang, Kudzai F Kaseke, Lin Li, and Mary K Seely. 2016. "The Impact of Rainfall on Soil Moisture Dynamics in a Foggy Desert." *PloS one* 11 (10):e0164982.

Li, Bonan, Lixin Wang, Kudzai F Kaseke, Roland Vogt, Lin Li, and Mary Seely. 2018. "The impact of fog on soil moisture dynamics in the Namib Desert." *Advances in Water Resources*.

Liu, J., G. Fu, X. Song, S. P. Charles, Y. Zhang, D. Han, and S. Wang. 2010. "Stable isotopic compositions in Australian precipitation." *Journal of Geophysical Research D: Atmospheres* 115 (23).

Louw, Gideon, and Mary Seely. 1982. "Ecology of desert organisms."

MEA. 2005. *Ecosystems and human well-being: desertification synthesis*. Washington, DC: World Resources Institute.

Merlivat, Liliane, and Jean Jouzel. 1979. "Global Climatic Interpretation of the Deuterium-18O Relationship for Precipitation." *J. Geophys. Res.* 84:5029-5033. doi: 10.1029/JC084iC08p05029.

Muselli, Marc, Daniel Beysens, Emmanuel Soyeux, and Owen Clus. 2006. "Is dew water potable? Chemical and biological analyses of dew water in Ajaccio (Corsica Island, France)." *Journal of environmental quality* 35 (5):1812-1817.

Nath, Supriya, and Sudesh Yadav. 2017. "A Comparative Study on Fog and Dew Water Chemistry at New Delhi, India." *Aerosol and Air Quality Research*.

Noone, David, and I Simmonds. 2002. "Associations between δ 18O of water and climate parameters in a simulation of atmospheric circulation for 1979–95." *Journal of Climate* 15 (22):3150-3169.

Nørgaard, Thomas, Martin Ebner, and Marie Dacke. 2012. "Animal or plant: which is the better fog water collector?" *PloS one* 7 (4):e34603.

Noy-Meir, I. 1973. "Desert ecosystems: environment and producers." *Ann. Rev. Ecol. Systemat.* 4:25-51.

Ojima, Dennis S, Bjørn OM Dirks, Edward P Glenn, Clenton E Owensby, and Jonathan O Scurlock. 1993. "Assessment of C budget for grasslands and drylands of the world." *Water, Air, and Soil Pollution* 70 (1-4):95-109.

Olivier, Jana. 1995. "Spatial distribution of fog in the Namib." *Journal of Arid Environments* 29 (2):129-138.

Olivier, Jana. 2004. "Fog harvesting: An alternative source of water supply on the West Coast of South Africa." *GeoJournal* 61 (2):203.

Prinz, Dieter. 2000. "Global and European water challenges in the 21st century." 3rd Inter-Regional Conference on Environment Water "Water Resources Management in the 21st Century", Budapest.

Reason, CJC, W Landman, and W Tennant. 2006. "Seasonal to decadal prediction of southern African climate and its links with variability of the Atlantic Ocean." *Bulletin of the American Meteorological Society* 87 (7):941-955.

Risi, Camille, Sandrine Bony, Françoise Vimeux, and Jean Jouzel. 2010. "Water-stable isotopes in the LMDZ4 general circulation model: Model evaluation for present-day and past climates and applications to climatic interpretations of tropical isotopic records." *Journal of Geophysical Research: Atmospheres* 115 (D12).

Roth-Nebelsick, A, M Ebner, T Miranda, V Gottschalk, D Voigt, S Gorb, T Stegmaier, J Sarsour, M Linke, and W Konrad. 2012. "Leaf surface structures enable the endemic Namib desert grass Stipagrostis sabulicola to irrigate itself with fog water." *Journal of The Royal Society Interface*.

Sánchez-Murillo, Ricardo, Germain Esquivel-Hernández, Kristen Welsh, Erin S Brooks, Jan Boll, Rosa Alfaro-Solís, and Juan Valdés-González. 2013. "Spatial and temporal variation of stable isotopes in precipitation across Costa Rica: An analysis of historic GNIP records." *Open Journal of Modern Hydrology* 2013.

Schemenauer, Robert S, and Pilar Cereceda. 1991. "Fog-water collection in arid coastal locations." *Ambio*:303-308.

Schemenauer, Robert S, and Pilar Cereceda. 1994. "Fog collection's role in water planning for developing countries." Natural Resources Forum.

Schmidt, Gavin A, Georg Hoffmann, Drew T Shindell, and Yongyun Hu. 2005. "Modeling atmospheric stable water isotopes and the potential for constraining cloud processes and stratosphere-troposphere water exchange." *Journal of Geophysical Research: Atmospheres* 110 (D21).

Schutte, JM. 1971. Die onttrekking van water uit die lae wolke op Mariepskop. Technical note.

Seely, Mary, Joh R Henschel, and William J Hamilton III. 2005. "Long-term data show behavioural fog collection adaptations determine Namib Desert beetle abundance: research letter." *South African Journal of Science* 101 (11 & 12):570-572.

Seely, MK. 1979. "Irregular fog as a water source for desert dune beetles." *Oecologia* 42 (2):213-227.

Sharan, Girja, Owen Clus, S Singh, M Muselli, and D Beysens. 2011. "A very large dew and rain ridge collector in the Kutch area (Gujarat, India)." *Journal of Hydrology* 405 (1):171-181.

Sharan, Girja, Anil Kumar Roy, Laurent Royon, Anne Mongruel, and Daniel Beysens. 2017. "Dew plant for bottling water." *Journal of Cleaner Production* 155:83-92.

Sinclair, KE, SJ Marshall, and TA Moran. 2011. "A Lagrangian approach to modelling stable isotopes in precipitation over mountainous terrain." *Hydrological Processes* 25 (16):2481-2491.

Slaymaker, Olav, and Tom Spencer. 1998. *Physical geography and global environmental change*: Longman Harlow, UK.

Soderberg, Keir, Stephen P. Good, Molly O'Connor, Lixin Wang, Kathleen Ryan, and Kelly K. Caylor. 2013. "Using atmospheric trajectories to model the isotopic composition of rainfall in central Kenya." *Ecosphere* 4 (3):art33. doi: 10.1890/ES12-00160.1.

Stumpp, C, J Klaus, and W Stichler. 2014. "Analysis of long-term stable isotopic composition in German precipitation." *Journal of Hydrology* 517:351-361.

Tardif, Robert, and Roy M Rasmussen. 2007. "Event-based climatology and typology of fog in the New York City region." *Journal of applied meteorology and climatology* 46 (8):1141-1168.

UNEP, N Middleton, and D Thomas. 1992. "World Atlas of Desertification." *Edward Arnold, London*:15-45.

Vörösmarty, Charles J., Pamela Green, Joseph Salisbury, and Richard B. Lammers. 2000. "Global Water Resources: Vulnerability from Climate Change and Population Growth." *Science* 289 (5477):284-288. doi: 10.1126/science.289.5477.284.

Vuille, M, Raymond S Bradley, Martin Werner, R Healy, and F Keimig. 2003. "Modeling δ18O in precipitation over the tropical Americas: 1. Interannual variability and climatic controls." *Journal of Geophysical Research: Atmospheres* 108 (D6).

Wang, L, P D'Odorico, JP Evans, DJ Eldridge, MF McCabe, KK Caylor, and EG King. 2012. "Dryland ecohydrology and climate change: critical issues and technical advances." *Hydrology and Earth System Sciences* 16:2585-2603. doi: 10.5194/hess-16-2585-2012.

Wang, Lixin, Kudzai Farai Kaseke, and Mary K Seely. 2016. "Effects of non-rainfall water inputs on ecosystem functions." *WIREs*:doi:10.1002/wat2.1179.

Wassenaar, LI, SL Van Wilgenburg, K Larson, and KA Hobson. 2009. "A groundwater isoscape (δD, $\delta^{18}O$) for Mexico." *Journal of Geochemical Exploration* 102 (3):123-136.

Werner, Martin, Petra M Langebroek, Tim Carlsen, Marcus Herold, and Gerrit Lohmann. 2011. "Stable water isotopes in the ECHAM5 general circulation model: Toward high-resolution isotope modeling on a global scale." *Journal of Geophysical Research: Atmospheres* 116 (D15).

West, AG, EC February, and GJ Bowen. 2014. "Spatial analysis of hydrogen and oxygen stable isotopes ("isoscapes") in ground water and tap water across South Africa." *Journal of Geochemical Exploration* 145:213-222.

Whitford, W.G. 2002. *Ecology of desert systems*: Academic Pr.

WWAP. 2012. "The United Nations World Water Development Report 4: Managing Water under Uncertainity and Risk." In. Paris: UNESCO.

Yang, Xiaoping, Nina Ma, Jufeng Dong, Bingqi Zhu, Bing Xu, Zhibang Ma, and Jiaqi Liu. 2010. "Recharge to the inter-dune lakes and Holocene climatic changes in the Badain Jaran Desert, western China." *Quaternary Research* 73 (1):10-19. doi: http://dx.doi.org/10.1016/j.yqres.2009.10.009.

Zhao, Liangju, Honglang Xiao, Maoxian Zhou, Guodong Cheng, Lixin Wang, Li Yin, and Juan Ren. 2012. "Factors controlling spatial and seasonal distributions of precipitation $\delta^{18}O$ in China." *Hydrological Processes* 26 (1):143-152. doi: 10.1002/hyp.8118

CHAPTER 2: NON-RAINFALL WATER ORIGINS AND FORMATION MECHANISMS

2.1 Introduction

Non-rainfall water (fog, dew, vapour) is an important ecohydrological component of arid ecosystems (Wang et al. 2016, Kidron et al. 2011), where any additional source of water may have a positive impact on productivity (Wang, D'Odorico, et al. 2010). However, non-rainfall water is less studied because research often focuses on factors limiting rather than sustaining productivity in arid environments. As such, non-rainfall water is often not well characterised and most ecological research tends to consider fog and dew inputs as one (Brown et al. 2008), although the two are derived from different meteorological phenomena.

For many coastal regions the obvious source of fog and dew is the ocean (i.e., advective fog and dew). However, many desert regions with reported non-rainfall water inputs have groundwater resources (Houston 2002, Yang et al. 2010), which could be a source of non-rainfall water (i.e., radiation fog and dew). It is often assumed that fog confined to river valleys in coastal deserts is advected inland from the ocean, but there is speculation it may be generated locally as radiation fog (Eckardt et al. 2013). However, few studies address the sources of non-rainfall water and as far we are aware, no studies have investigated the possibility of groundwater contribution to non-rainfall water formation. How fog and dew will change in the future is dependent on their formation from their respective sources, ocean vs. groundwater. Vegetation water-use of both rainfall and non-rainfall components is essential for developing sound ecological models for arid environments (Schroder et al. 2009) and key to understanding plant function under current or future climates (Feddes et al. 2001). Differentiation of non-rainfall inputs will help build better ecological prediction models because the effect of global climate change on these ecosystems has not been adequately addressed (Giannini et al. 2008).

Although stable isotopes ($\delta^{2}H$ and $\delta^{18}O$) have been applied widely to fog research (Fischer and Still 2007), the application to dew research is minimal. To our knowledge, multiple stable isotope measurements have never been applied jointly to include both fog and dew within a given ecosystem. Because fog and dew involve condensation reactions,

it is often assumed that their formation is similar to the liquid-vapour equilibrium state in clouds (Stewart 1975, Jouzel 1986). The equilibrium assumption is likely true for fog formation (Gonfiantini and Longinelli 1962); however, recent theoretical work suggests that dew formation could be dominated by kinetic fractionation processes (Deshpande et al. 2013). Because of the differences in fractionation processes, it is possible to differentiate fog and dew formation using the relationships of triple oxygen isotopes (^{16}O, ^{17}O and ^{18}O) since a recent study shows that the $\delta^{17}O$-$\delta^{18}O$ slope is different for kinetic and equilibrium fractionation processes (Angert et al. 2004).

Like many dryland ecosystems worldwide, the Namib Desert is likely to experience changes in its hydrological cycle response to global climate change (Engelbrecht et al. 2009, Hulme 1996). Given the abundance and importance of fog and dew in this desert (Henschel and Seely 2008), it provides an ideal location to study both components of non-rainfall water as part of the same ecosystem. Here we collect diverse water samples (i.e., rain, fog, dew, river water and groundwater) and apply stable isotopes of hydrogen and oxygen ($\delta^{2}H$, $\delta^{17}O$ and $\delta^{18}O$) to differentiate fog from dew and determine source waters of these inputs in the Namib Desert at Gobabeb Research and Training Centre (Fig. 2.1). These findings provide a new experimental framework to identify the origins of non-rainfall waters and differentiate fog and dew. These findings will assist in predicting dryland responses to global climate change by providing information about the sources of non-rainfall waters.

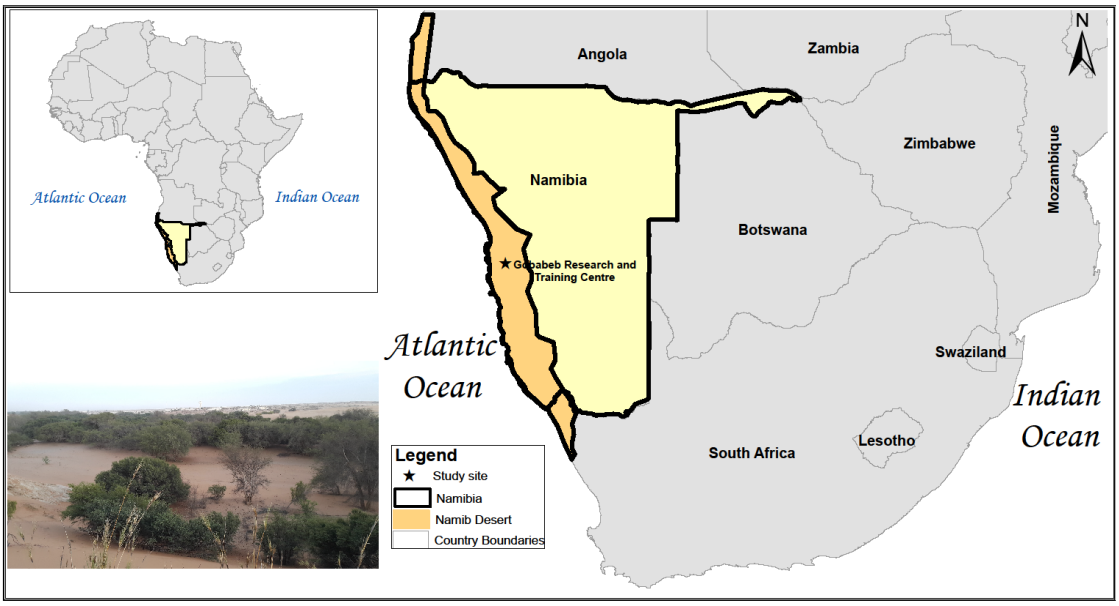

Figure 2. 1 Extent of the Namib Desert and location of the study site. The map shows the location of the Gobabeb Research and Training Centre and the extent of the Namib Desert, as well as an inset showing the general landscape characteristics around the study area: the Kuiseb River and the gravel plains. CREDIT: K.F.Kaseke/Indiana University–Purdue University Indianapolis.

2.2 Materials and Methods

2.2.1 Site description

This study was conducted in the Central Namib Desert at the Gobabeb Research and Training Centre (lat. -23.55°, long. 15.04° and elv. 405 m a.s.l.). The centre is located about 60 km from the Atlantic Ocean, on the outer edge of the Namib fog-zone, annual precipitation < 20 mm. The fog zone is an area of the most visible impacts of advective fog characteristic of the Namib coast (Olivier 1995); however, there are suggestions that other types of fog could occur regularly in the Namib (Eckardt et al. 2013). The centre is surrounded by three distinct ecosystems: to the north and east the gravel plains (91% sand, 0.6% clay and 8.4% silt), to the west and south the sand dune sea (74.8% sand, 5.5% clay, 19.7% silt) and the ephemeral Kuiseb river (91.5% sand, 2.1% clay, 6.4% silt) lies south of the centre separating the gravel plains and sand dune sea. The Kuiseb river is one of the largest ephemeral rivers (~560 km) in Namibia, draining the western Great Escarpment with a 420 km long catchment area of approximately 15 500 km^2 (Jacobson et al. 1995). It

drains the high plateau (~2000 m a.s.l) westward through the escarpment to the Atlantic Ocean near Walvis Bay. Mean annual rainfall at the headwater is > 300 mm yr^{-1} and decreases to less than 20 mm yr^{-1} in the low lands (Dahan et al. 2008). The Kuiseb river has flowed past Gobabeb at least once a year for an average of 12 day yr^{-1} with a maximum of 33 days in 1997 (Dahan et al. 2008). Rainfall and groundwater availability are often the primary determinants of species distribution in the Namib Desert (Schachtschneider and February 2010), with large trees confined to the eastern edge of the desert and along ephemeral watercourses (Burke 2006) where they access the shallow alluvial aquifers (Lange 2005). The ephemeral vegetation at Gobabeb Research and Training Centre is dominated by four species: *Faiderbia albida, Acacia erioloba, Euclea pseudobenus* and *Tamarix usneoides* (Jacobson et al. 1995).

2.2.2 Sample collection

Samples were collected within the vicinity of the Gobabeb Research and Training Centre from January 2014 – January 2015. Groundwater samples were collected during field campaigns from two boreholes located in the Kuiseb River. River water was obtained on the 23rd December 2013, when the river flowed for two days. Precipitation was collected immediately after a rain event to minimise evaporation effects at the centre. Fog samples were collected from fog collectors designed after Schemenauer and Cereceda (1994), 1 m^2 metal frames covered by a polyethylene mesh raised 2 m from the ground surface and oriented in the direction of the dominant fog bearing wind. The mesh intercepts fog droplets which coalesce and flow into a collecting trough, directing the flow to an outlet pipe and into a container where samples were collected daily at 08:00 hrs. Dew was collected from a dew collector, which was made of 1 m^2 metal sheet, overlain by a glass plate at a 30^0 angle and raised 0.5 m from the soil surface. The glass plate is able to achieve or go below the ambient dew point temperature, facilitating dew formation which collects in a trough placed at the end of the collector. Attached to the trough is a collecting pipe which directs this flow into a container. Dew samples were obtained opportunistically during field campaigns at 06:00 hrs to minimise evaporation. All samples were then transferred into 15 ml Qorpak clear French square bottles with black phenolic polycone lined caps, labelled appropriately with the sample type, location and date and stored at Gobabeb Research and

Training Centre until shipment to the Indiana University-Purdue University Indianapolis (IUPUI) Ecohydrology Lab for isotope analysis. HYSPLIT (Stein et al. 2015) was used to track the origin of the five precipitation events captured during the study period (Fig. A2.1) with monthly rainfall that may have influenced fog and dew formation displayed in Table A2.3.

2.2.3 Practical considerations for dew and fog water collection

The major difference between fog and dew formation is the dependence of dew formation on the receiving substrate surface attaining or falling below ambient dew point temperature while fog formation is independent of the receiving substrate surface. The receiving surface of the dew collector has a high thermal conductivity, which facilitates dew condensation on the dew collector compared to the fog collector using polyethylene mesh. Therefore, when water was collected in the dew collector and absent from the fog collector, this input was classified as dew. Because interception by objects projecting into the fog droplet stream is the dominant avenue for fog deposition onto a surface, it is possible to collect appreciable amounts of fog in the dew collector. However, fog collectors are more efficient in harvesting this, input, collecting significantly more fog water compared to dew collectors during fog events. Furthermore, fog water collected in the dew collector easily exceeds the theoretical dew maximum yield of 0.8 mm per night (Monteith 1957). Therefore, when water was collected in both the dew and fog collectors but the dew collector had significantly more than 0.8 mm of input we classified this as fog and discarded the sample and collected that in the fog collector.

2.2.4 Isotope analysis

We used a Triple Water Vapor Analyzer (Los Gatos Research Inc., Mountain View, CA, USA), for isotopic analysis with a precision of 0.2‰ $\delta^{18}O$, 0.8‰ $\delta^{2}H$ and 0.4‰ $\delta^{17}O$ similar to those reported elsewhere (Wang et al. 2009, Tian 2016). Data was reported in δ notation relative to VSMOW-SLAP scale as

$$\delta = \frac{R_{\text{sample}}}{R_{\text{VSMOW}}} - 1, \qquad (1)$$

where R_{sample} and R_{VSMOW} are the molar ratios of heavy to light isotopes ($^{2}H/H$, $^{18}O/^{16}O$ or $^{17}O/^{16}O$) of the sample and international standard - Vienna Standard Mean Ocean Water

(V-SMOW). However, it has been demonstrated that when dealing with high precision ratios in multiple systems a modified δ is preferred (Miller 2002, Luz and Barkan 2005, Hulston and Thode 1965) hereafter designated as δ' and defined as

$$\delta'^{*}O = \ln(\delta + 1) = \ln\left(\frac{R_{\text{sample}}}{R_{\text{VSMOW}}}\right), \quad (2)$$

where *O is either ^{17}O or ^{18}O.

2.2.5 Differentiation of non-rainfall vectors based on isotopes

Differentiation of fog type was based on the knowledge that fog is a first stage condensate controlled by equilibrium fractionation processes and plots on a meteoric water line reflecting its origins (Majoube 1971, Stewart 1975, Jouzel 1986). Because the Namib fog-zone is characterised by advective fog originating from the Atlantic Ocean and the sampling location is close to the ocean (~60 km) (Olivier 1995), we expect advective fog to plot on the global meteoric water line (GMWL) while locally generated (radiation) fog should plot on the LMWL reflecting local meteoric water origins. Because fog is a derivative of the meteoric water lines, we excluded fog from defining the LMWL for the site, thus the LMWL was based on groundwater and rain samples.

Similar to fog, dew can be classified isotopically based on the samples position relative to the GMWL and LMWL. In any ecosystem, dew has at least three sources: lower atmosphere, shallow soil layer and deep soil layer/groundwater (Wen et al. 2012). During evaporative enrichment of water, vapour will have a reciprocal depletion and plot on the same evaporative line but opposite the initial composition of water (i.e., left of the meteoric water line). Condensation of this vapour on a sufficiently cooled substrate surface results in dew and in theory should plot along the evaporative line but to the left of the relevant meteoric water line. Based on this, we can classify dew by calculating the isotopic composition of the dew source and comparing it to the isotopic signatures of the different pools of water to identify its origins.

Differentiation of fog from dew water was based on the knowledge that different $\delta'^{17}O$ vs $\delta'^{18}O$ slopes indicate different fractionation processes, 0.528 (equilibrium) and 0.515 (kinetic) (Angert et al. 2004, Luz and Barkan 2010). Therefore, $\delta'^{17}O$ vs $\delta'^{18}O$ was used to separate bulk fog and dew samples.

2.2.6 Statistical Analyses

All statistical analyses were performed using non-parametric methods in PAST 3 (Paleontological Statistics, Natural History Museum, University of Oslo), the Kruskal-Wallis test followed by a *post-hoc* Mann-Whitney U test with a p-value of 0.05 for significance. Because advective and radiation fog were derived from different meteoric waters we compared each fog to its respective meteoric water line e.g. advective fog *d* to that of the GMWL while that of the radiation fog was compared to the LMWL. Using the *d* of advective fog we can determine the evaporation conditions over the ocean and if significantly greater than that of the GMWL we can conclude that evaporation occurred under low humidity (< 85% RH) (Araguás-Araguás et al. 2000). If the *d* of the radiation generated fog is significantly greater than that of the LMWL we can conclude that the fog was generated by admixture with advecting moisture. ANCOVA ($p < 0.05$) was used to compare differences in slopes between radiation fog and the LMWL. Isotopic characteristics of all meteoric water samples (river, groundwater, rain, fog and dew) were based on arithmetic means and the associated standard deviations.

2.3 Results and Discussion

2.3.1 Isotopic characteristics of various ecosystem waters.

Rain, fog, dew, groundwater and Kuiseb River water were isotopically distinct, with rain being the most enriched in ^{2}H, ^{17}O and ^{18}O compared to all other waters (Table 2.1). Groundwater had two distinct isotope signatures (Table 2.1), indicating the existence of two alluvial aquifers at the study site. Both aquifers are likely dependent on recharge through the ephemeral river bed (Scanlon 2004) via short-duration water flow (Mizuno 2010). Backward trajectory analyses showed that rain events sampled during this period originated from the Atlantic Ocean (Fig. A2.1); thus, isotopic enrichment of rain relative to all other waters is attributed to the 'continental effect' and sub-cloud evaporation (Stewart 1975, Dansgaard 1964, Kaseke et al. 2016) (Table 2.1). The ephemeral Kuiseb River water was depleted in ^{2}H, ^{17}O and ^{18}O compared to local rainfall (Table 2.1), indicating this water was sourced from headwaters at higher altitudes in the interior, exhibiting the 'altitude effect' (Friedman and Smith 1970). Non-rainfall water had the largest variability in all three isotopes and when separated into fog and dew, these samples

still exhibited large variability suggesting the existence of different groups within these composite classes (Table 2.1).

Table 2. 1 Isotopic characteristics (mean ± standard deviation) of the various water samples at the Gobabeb Research and Training Centre, Central Namib Desert.

Sample Type	$\delta^{18}O$ ‰	$\delta^{2}H$ ‰	$\delta^{17}O$ ‰	n
Rain	+2.16 ± 3.0	+12.72 ± 28.84	+0.83 ± 2.9	5
Non-rainfall water	+0.39 ± 3.5	+3.74 ± 17.8	+0.11 ± 1.9	53
Dew (composite)	-1.25 ± 3.1	-7.97 ±13.7	-1.22 ± 1.6	15
Fog (composite)	+1.03 ± 3.4	+8.37 ± 17.3	+0.64 ± 1.8	38
River water (Kuiseb)	-11.49	-85.11	-6.51	1
*Groundwater	-9.33 ± 0.3	-63.97 ± 2.0	-4.54 ± 0.2	4
†Groundwater	-6.80 ± 0.2	-45.88 ± 0.7	-3.43 ± 0.2	2

Note: 1. Non-rainfall water refers to combined fog and dew samples.

2. ***** refers to the shallow aquifer and † refers to the deep aquifer.

2.3.2 Fog types and their origins

We identified three types of fog: advective, radiation and mixed fog (Fig. 2.2). There are no local open water sources close to the study site except the ephemeral Kuiseb River when in flow, thus the only source of advective fog is the ocean. Fog formed from oceanic vapour is depleted in ^{18}O relative to ocean water (1-3‰) (Aravena et al. 1989) (Fig. 2.2 and Table 2.2). Furthermore, the isotopic composition of these samples (Table 2.2) was similar to those collected from the Namibian coast ($\delta^{18}O$: -0.86 to -0.39‰ and $\delta^{2}H$: +0.80 to +3.30‰) (Eckardt et al. 2013). The Mann-Whitney U *post hoc* test showed that d-excess ($d = \delta^{2}H - 8.0 \times \delta^{18}O$) of advective fog (+7.2‰) was significantly lower than that of the GMWL (+10‰) (Bonferroni corrected $p < 0.05$) suggesting evaporation at the source occurred at a relative humidity (RH) > 85% or near-equilibrium (Merlivat and Jouzel 1979). Advective fog is usually enriched in ^{2}H and ^{18}O compared to local rainfall (Dawson 1998) but our results show that advective fog was depleted in ^{2}H, ^{17}O and ^{18}O compared to rainfall (Table 2.1 and Table 2.2). Because of the close proximity of the study site to the Atlantic Ocean, both rain and advective fog could be considered first stage

condensates. However, whereas fog droplets remain at equilibrium with vapour, rain may experience sub-cloud evaporation due to aridity of the Namib Desert resulting in enrichment of the rain compared to fog. This is supported by the low *d* exhibited by individual rain events (Table A2.1) and the precipitation isoscape for Namibia (Kaseke et al. 2016).

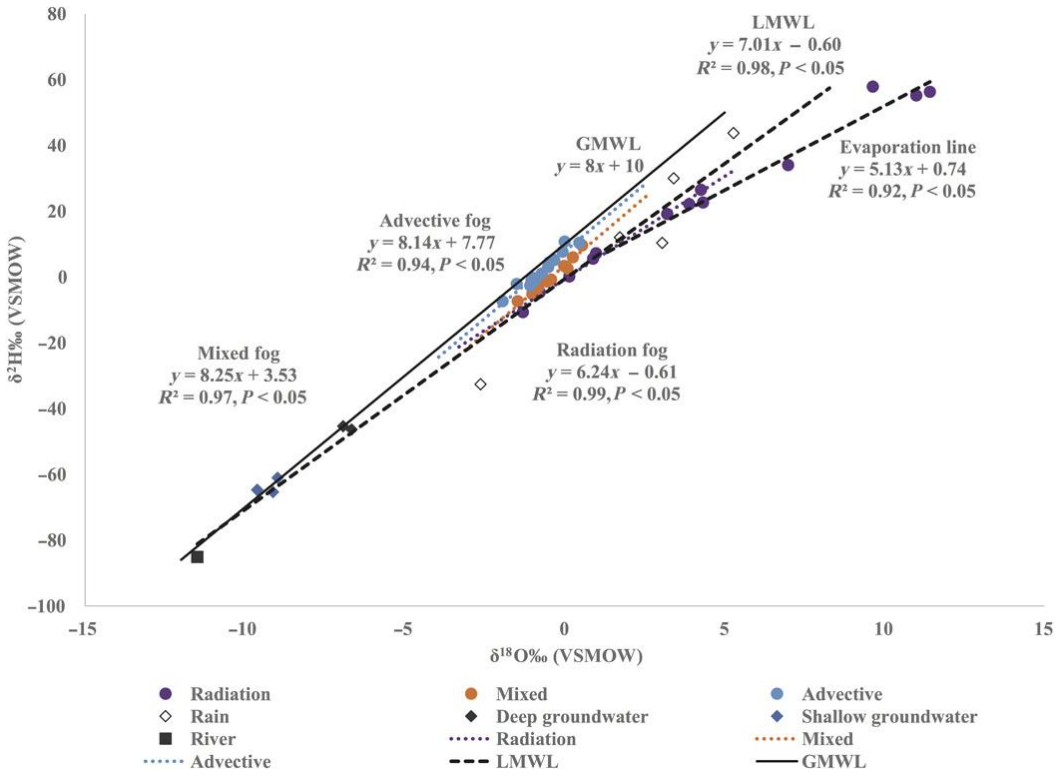

Figure 2. 2 Origins of fog water. The isotopic distribution of fog samples collected from the Gobabeb Research and Training Centre in relation to the GMWL and the LMWL, river water, and groundwater during the observation period (2014–2015). Fog regression lines indicate the source and classification of the fog. VSMOW, Vienna Standard Mean Ocean Water.

Table 2. 2 Classification and isotopic characteristics (mean ± standard deviation) of fog collected from Gobabeb Research and Training Centre in the Namib Desert, 2014-2015.

Classification	$\delta^{18}O$ ‰	$\delta^{2}H$ ‰	$\delta^{17}O$ ‰	*d* ‰	n
Advective	-0.74 ± 0.6	+1.76 ± 5.1	-0.20 ± 0.5	+7.67 ± 1.3	15
Mixed	-0.43 ± 0.6	+0.01 ± 5.3	-0.23 ± 0.5	+3.42 ±1.0	10
Radiation	+1.41 ± 2.1	+8.18 ± 13.3	+0.78 ± 1.1	-2.24 ± 3.4	8

The LMWL defined for this study (Fig. 2.2), was similar to that defined as $\delta^{2}H = 7.2 \times \delta^{18}O - 0.6$‰ (Schachtschneider and February 2010), although the latter LMWL included fog in its definition. Because the LMWL slope was less than 8, this indicates evaporative enrichment of local waters, a characteristic of arid environments (Fig. 2.2). Radiation fog *d* (-1.2‰) was significantly depleted than advective fog *d* (+7.2‰) (Mann-Whitney U *post hoc,* Bonferroni corrected $p < 0.05$), which suggests the two have different moisture sources as equilibrium fractionation does not change *d* (Dansgaard 1964). There was no significant difference between LMWL *d* (-0.6‰) and radiation fog *d* (-1.2‰) (Table 2.2 and Fig. 2.2), suggesting radiation fog was generated from local water sources (rainfall, ephemeral rivers or shallow aquifers). Figure 2.2 shows two clusters of radiation fog: one cluster plots among the rain samples ($\delta^{18}O$ (+3.78 ± 0.5‰), $\delta^{2}H$ (+22.6 ± 3.72‰) and $\delta^{17}O$ (+1.75 ± 0.6‰)) indicating local rainfall origins (Cui et al. 2009) and the second cluster plots below the rain samples eliminating local precipitation as the source origin (($\delta^{18}O$ (-0.02 ± 1.0‰), $\delta^{2}H$ (-0.48 ± 7.4‰) and $\delta^{17}O$ (+0.20 ± 0.9‰)) (Fig. 2.2 and Table A2.2). This fog cluster occurred when the river was dry, suggesting groundwater as the possible origin, hence classification as groundwater derived radiation fog (Fig. 2.2). There were a few radiation fog samples that showed evidence of evaporative enrichment, plotting to the right of the LMWL (Fig. 2.2). We thus calculated the source isotopic composition of these evaporated fog samples ($\delta^{18}O$ +0.71‰ and $\delta^{2}H$ +4.40‰), similar to that of groundwater derived fog and plotted below the rain samples (Fig. 2.2). These samples were thus classified as groundwater derived fog but excluded from characterisation of radiation fog. Radiation fog is thus a composite of fog derived from local water sources, each with a unique isotopic signature reflecting the source water (Fig. 2.2 and Table 2.2).

The classification of groundwater derived fog can be verified through theoretical calculations and basic isotope principles (Fig. 2.2). It is estimated that 48-80% of local rainfall in tropical regions is from recycling of water to the atmosphere via evapotranspiration (Shuttleworth et al. 1984, Salati et al. 1979), with transpiration being the largest component of the evapotranspiration flux (Wang et al. 2014, Jasechko et al. 2013). Transpiration is non-fractionating. Therefore, transpired water vapour is isotopically similar to xylem water (Yakir and Sternberg 2000) and reflects the isotopic signature of the source water utilised (Craig 1966). Because the isotopic composition of fog is related to equilibrium with atmospheric vapour, similar to the liquid-vapour equilibrium state found in clouds (Jouzel 1986, Stewart 1975), we assume the fog condensate is at equilibrium with transpired vapour, and transpired vapour reflects the groundwater isotopic signature. In support of this assumption, recent spectroscopy-based transpiration studies have shown that the isotopic composition of transpiration vapour is similar to that of the source waters (Wang et al. 2012, Wang, Caylor, et al. 2010).

$$\alpha_{\mathrm{l-v}} = \frac{1000+\delta_{\mathrm{l}}}{1000+\delta_{\mathrm{v}}}, \qquad (3)$$

where α_l is isotopic composition of the fog condensate and α_v is the isotopic composition of the transpired vapour which reflects the groundwater isotopic composition (Table 2.1).

Using the average isotopic composition of the groundwater derived fog ($\delta^{18}O$, -0.02‰ and $\delta^{2}H$, -0.48‰) and applying the groundwater isotopic compositions from Table 2.1 to equation 3 we obtained ${}^{18}\alpha_{l\text{-}v}$ = 1.0094 and ${}^{2}\alpha_{l\text{-}v}$= 1.0678 for shallow groundwater and ${}^{18}\alpha_{l\text{-}v}$ =1.0068 and ${}^{2}\alpha_{l\text{-}v}$ = 1.0478 for deep groundwater. The fractionation factors obtained using the shallow groundwater were similar to the equilibrium fractionation factors at 20ºC (1.0098 for $\delta^{18}O$ and 1.084 for $\delta^{2}H$) determined from experimental work (Majoube 1971). We further estimated the RH conditions during fog formation based on the observed fractionation factors. We assumed equilibrium fractionation occurs at 100% RH for the experimental work (Majoube 1971), then ${}^{2}\alpha$ / ${}^{18}\alpha$ = 84‰/9.8‰ = 8.57. Combining this information and our calculated fractionation factors, RH during fog formation in our study was (67.8‰/9.4‰)/8.57 = 84.2%, which was within the range of observed RH for fog events at this site (Kaseke et al. 2012). At the same time, a previous study showed that most ephemeral vegetation in the lower Kuiseb is reliant on the shallow aquifer depending on stage of growth and species (Schachtschneider and February 2010).

As advective fog dissipates downwind, it persists as a high humidity air mass (Kaseke et al. 2012) which mixes with local moisture from the vicinity of the study site. Radiative cooling of this mixed air then results in mixed (advective-radiation) fog, which plots between the GMWL and the LMWL (Fig. 2.2). Mixed fog *d* (+3.2‰) was significantly enriched than LMWL *d* (-0.6‰) but significantly depleted than advective fog *d* (+7.2‰) (Mann-Whitney U *post hoc* test, Bonferroni corrected $p < 0.05$) (Fig. 2.2, Table 2.2), providing evidence of the mixing of different air masses (Gat and Matsui 1991, Liu et al. 2007) to generate this fog. There were no significant differences in all three isotopes ($\delta^{18}O$, $\delta^{2}H$ and $\delta^{17}O$) between mixed fog and either advective or radiation fog, suggesting that mixed fog retains characteristics of both moisture sources (Fig. 2.2). However, radiation fog ^{18}O (+0.98‰) and ^{17}O (+1.08‰) was significantly enriched compared to advective fog ^{18}O (-0.94‰) and ^{17}O (+1.08‰) (Mann-Whitney U *post hoc* test, Bonferroni corrected $p < 0.05$, Table 2.2).

This isotope based fog classification was consistent with associated meteorological parameters: wind speed and direction (Note A2.1 and Table A2.2). The Atlantic Ocean is located on the western side of the study site (Fig. 2.1), while advective and mixed fog had western origins: median 230° and median 260°, respectively (Table A2.2). Radiation fog on the other-hand had southern origins (median 180°), consistent with the location of the Kuiseb River in relation to the sampling site. Wind speeds attributed to advective fog (4.0 m/s) were higher than both those for mixed (3.8 m/s) and radiation fog, which is also consistent with expectation.

Based on the samples collected, fog type frequency was as follows: advective fog (39.5%), radiation fog (34.2%) and mixed fog (26.3%). However, mixed fog could be considered as a form of radiation fog because it is generated by radiative cooling and localised. Therefore, radiation fog accounted for 60.5% of the fog occurrence during this period and was thus the dominant fog type, during the study period at the site. This result was surprising in that the study site lies on the edge of the Namib fog-zone and is thought to be influenced by advective fog. Our results thus suggest that advective fog is dissipating closer to the coast than the 60 km inland boundary used to define the fog-zone (Fig. 2.1). There is corroborative evidence from our site which suggests a receding range in the occurrence of fog harvesting beetles to less than 60 km inland. Increasing global air

temperatures would increase soil temperatures and result in a 0-20% decline in RH and decrease in cloud immersion in cloud forests (Foster 2001). Although not a cloud forest, the principle is applicable to the Namib fog-zone and could be evidence that global climate change is diminishing this fog-zone. If true, we expect to observe more changes in the flora and fauna composition over the outer edge of the Namib Desert fog-zone. This is because radiation fog is spatially variable and its dominance is related to a decrease in advective fog rather than an increase in frequency of radiation fog. Consequently, fog input to the area is decreasing, with fog frequency dropping 56% from 2001 (Henschel and Seely 2008) to the time of this study. In addition, radiation fog is confined to topographic lows and ephemeral channels (Eckardt et al. 2013) while behavioural adaptations of fauna (e.g., fog harvesting beetles) shows that they position themselves on dune crests to harvest fog. This advective-radiation fog shift may necessitate redefining the extent of the Namib fog-zone and provide an opportunity to study the effects of global climate change on fog dependent systems.

2.3.3 Dew types and their origins.

We identified three types of dew: groundwater derived, advective and shallow soil water derived dew (Fig. 2.3). Extending the evaporation line of groundwater derived radiation fog beyond the LMWL, some dew samples plot along this line, suggesting similar origins: groundwater derived dew (Fig. 2.3a and Fig. 2.3b). In addition, the source isotopic composition of groundwater derived dew ($\delta^{18}O$ +0.35‰ and $\delta^{2}H$ +1.84‰) and groundwater derived fog ($\delta^{18}O$ -0.02 ± 1.0‰ and $\delta^{2}H$ -0.48 ± 7.4‰) were similar and can be viewed as evidence that the two have the same origin. Wen *et al.* (2012) demonstrates theoretically that dew formation under super-saturated conditions is controlled by kinetic fractionation processes but detection using $\delta^{2}H$ and $\delta^{18}O$ is difficult. We did not find any significant differences in both $\delta^{18}O$ and $\delta^{2}H$ between groundwater derived dew ($\delta^{18}O$ -2.32‰ and $\delta^{2}H$ -12.33‰) and groundwater derived radiation fog ($\delta^{18}O$ +0.14‰ and $\delta^{2}H$ -12.33‰) (Kruskal-Wallis test, $p > 0.05$). However, groundwater derived dew ^{17}O (-1.86‰) was significantly depleted compared to groundwater radiation fog ^{17}O (+0.39‰) (Mann-Whitney U *post hoc* test, Bonferroni corrected $p < 0.05$), suggesting $\delta^{17}O$ could be the key to differentiation of fog and dew isotopically. Groundwater derived dew *d* (+6.21‰) was

significantly enriched than both the LMWL *d* (-0.6‰) and groundwater derived radiation fog *d* (-0.6‰) (Mann-Whitney U *post hoc* test, Bonferroni corrected $p < 0.05$) (Fig. 2.3b and Table 2.3). Because groundwater has an inherently low *d*, the unusually high *d* of groundwater derived dew suggests strong kinetic fractionation processes during its formation similar to that reported for liquid condensation (Deshpande et al. 2013).

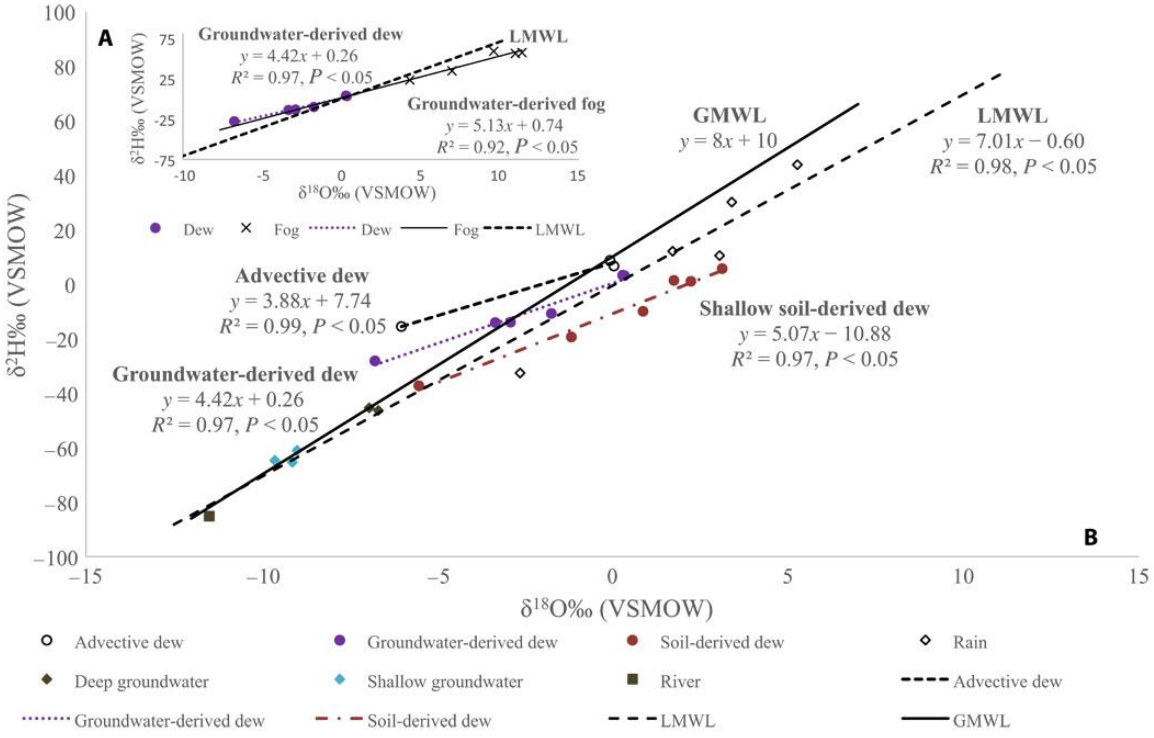

Figure 2. 3 Origins of dew water. a) Groundwater derived dew and fog lines indicating similar origins and plotting along the same evaporation line. b) The local meteoric water line (LMWL) at Gobabeb Research and Training Centre with groundwater, Kuiseb River water, rain, and dew isotopes collected from 2014-2015. The GMWL was included as a reference.

Table 2. 3 Isotopic characteristics (mean ± SD) and classification of dew samples from the Gobabeb Research and Training Centre in the Namib Desert (2014-2015).

Dew classification	$\delta^{18}O$ ‰	$\delta^{2}H$ ‰	$\delta^{17}O$ ‰	*d* ‰	n
Advective	-2.01 ± 3.5	-0.07 ± 13.5	-1.77 ± 1.7	16.0±14.3	3
Groundwater derived	-2.35 ± 2.7	-10.12 ± 11.9	-1.75 ± 1.4	8.67±9.7	6

Some dew samples plotted to left of the GMWL, while the source isotopic composition of these samples ($\delta^{18}O$ -0.56‰ and $\delta^{2}H$ +5.53‰) was similar to that of advective fog derived from the ocean, suggesting similar origins: advective dew (Fig. 2.3b and Table 2.2). The *d* value of advective dew (+16.0‰) was much higher than expected (Table 2.3), and was likely influenced by kinetic fractionation processes during two stages: evaporation of moisture from the ocean and during condensation. This combined kinetic isotope effect could then account for the unusually large *d* (Table 2.3). The source water isotopic composition and the advective dew line (Fig. 2.3b) were similar to those reported for the Negev desert ($\delta^{18}O$ -0.68‰ and $\delta^{2}H$ +4.54‰; $\delta^{2}H = 3.9 \times \delta^{18}O + 7.2$) (Hill et al. 2015), suggesting this could be universal for advective dew from the ocean.

The isotopic composition of shallow water derived dew ($\delta^{18}O$ -5.30‰ and $\delta^{2}H$ -37.75‰) did not match any of the water sources identified for the ecosystem (Table 2.1), but was likely formed from evaporative discharge from the shallow alluvial aquifer (Schachtschneider and February 2010) (Fig. 2.3). $\delta^{18}O$ was similar to that indicated for soil at 0.5 m depth in the Kuiseb river in a $\delta^{18}O$ vs depth profile (Schachtschneider and February 2010), however, $\delta^{2}H$ was not reported. Therefore, we applied the LMWL defined in this study to calculate $\delta^{2}H$, 37.81‰, which was similar to the calculated source water value. Our data thus suggests these dew samples were derived from shallow soil water at about 0.5 m. However, we did not characterise the isotopic composition for shallow soil derived dew because most of these samples plotted to the right of the LMWL and this suggests they had undergone evaporative enrichment (Fig. 2.3b).

This isotope based dew classification was consistent with associated meteorological parameters: wind speed and direction (Note A2.1 and Table A2.2). In general, advective dew originated from the south-west (median 205°) while locally derived dew originated from the south-east (median 166°) (Table A2.2). We expected higher wind

speeds would transport moisture to the site resulting in advective dew formation while locally generated dew would have slower speeds or calm conditions. The data generally supports this, 6.5 m/s vs 2.1 m/s for advective and locally generated dew, respectively (Table A2.2).

2.3.4 Separation of fog and dew.

Some fog and dew samples were excluded from isotopic characterisation due to evidence of evaporative enrichment (Fig. 2.2 and Fig. 2.3), but because all samples were handled in the same manner, this enrichment could have been formation induced. Therefore, all samples were included in the $\delta'^{17}O$-$\delta'^{18}O$ analysis of bulk or composite fog (n = 38) and dew (n = 15) samples (Fig. 2.4). The $\delta'^{17}O$-$\delta'^{18}O$ slope of the bulk fog samples, 0.528 (Fig. 2.4), indicates meteoric waters condensed under isotopic equilibrium conditions (Angert et al. 2004, Luz and Barkan 2010). This is in agreement with earlier conclusions on advective and radiation fog based on interpretations of *d* and the calculated fractionation factors. Therefore, the isotopic composition of fog is determined by equilibrium fractionation processes regardless of fog type. Meanwhile, the $\delta'^{17}O$-$\delta'^{18}O$ slope of bulk dew samples was 0.516 (Fig. 2.4), indicating that dew formation is dominated by kinetic fractionation processes (Angert et al. 2004), regardless of dew type. Kinetic fractionation during the vapour-liquid phase change is related to the degree of super-saturation and differences in diffusive velocities of isotopic molecular species through super saturated air (Deshpande et al. 2013), similar to the vapour-solid phase change (Jouzel and Merlivat 1984, Petit et al. 1991). This is the first reported field evidence of kinetic fractionation dominating the oxygen isotope composition of dew during natural formation. There were no significant differences between $\delta^{18}O$ values in bulk fog (-0.38‰) and bulk dew (-0.07‰), as well as *d* values in bulk fog (+3.75‰) and bulk dew (+3.17‰) (Kruskal-Wallis test, $p > 0.05$). However, fog ^{2}H (+2.82‰) and ^{17}O (+0.08‰) were significantly enriched compared to dew ^{2}H (-10.06‰) and ^{17}O (-0.09‰) (Mann-Whitney U *post hoc* test, Bonferroni corrected $p < 0.05$).

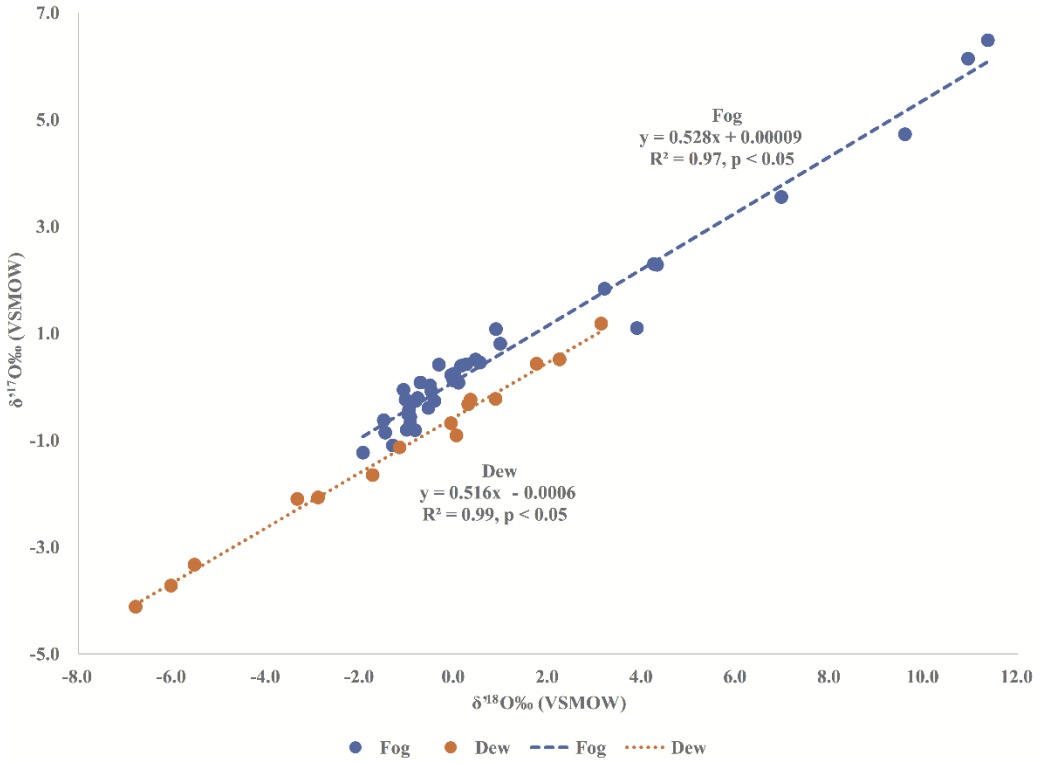

Figure 2. 4 Differentiation of fog and dew. $\delta'^{17}O$ vs $\delta'^{18}O$ plots for bulk fog and dew samples showing fog and dew are controlled by different fractionation processes, equilibrium and kinetic, respectively.

Although most previous research tends to treat dew inputs as fog (Brown et al. 2008) or vice versa in dewy deserts such as the Negev, where fogs are often regarded as dew (Kidron et al. 2014), due to technical constraints. Our results demonstrate that fog and dew are dominated by different fractionation processes, equilibrium and kinetic, respectively, and this can be used as a basis for differentiation of the two inputs using the ^{17}O-^{18}O relationship. This distinction is important because vegetation may be differentially adapted to harvesting fog and dew. For example, Esler et al. (1999) postulates that the ecophysiology of prostrate-leaved geophytes in arid environments may enhance dew formation by lowering leaf temperature while grasses such as *Stipagrostis sabulicola* are adapted for efficient fog harvesting due to surface traits and upright structure (Ebner et al. 2011, Roth-Nebelsick et al. 2012). Therefore, the increase in frequency of one of these components does not necessarily translate to the same species composition or distribution. To better understand plant functioning under current or future climates and develop sound

ecological models for arid environments, it is therefore important to differentiate non-rainfall components and water use strategies. The new $\delta'^{17}O$-$\delta'^{18}O$ method developed here to differentiate fog and dew will thus enhance the understanding of vegetation water-use strategies in non-rainfall water dependent ecosystems.

2.4 Conclusions

Non-rainfall water in coastal drylands such as the Central Namib Desert have multiple origins and types. Based on our estimated source origins of fog and dew; groundwater in alluvial aquifers may have a much larger impact than often acknowledged in arid environments. Groundwater is evapotranspired through riparian vegetation, forming radiation fog and/or dew and is redistributed into the upper few cm of the soil profile making it available for use by other life forms. At the same time, although the ecophysiology of dryland organisms is geared towards obtaining non-rainfall water (Henschel and Seely 2008), vegetation may be differentially adapted to harvesting non-rainfall water (Roth-Nebelsick et al. 2012, Ebner et al. 2011, Esler et al. 1999). Therefore, the non-rainfall form, fog vs. dew, has important implications for species survival and distribution. By determining the significance of each non-rainfall water input to specific plant species we could more accurately model the potential climate change impact on plant species and fauna that depend on it. The $\delta'^{17}O$-$\delta'^{18}O$ method developed here demonstrates for the first time that fog and dew are controlled by different formation mechanisms: equilibrium and kinetic fractionation processes, respectively. This $\delta'^{17}O$-$\delta'^{18}O$ method will enhance the understanding of vegetation water-use strategies in non-rainfall water dependent ecosystems and the potential impact of global climate change on species survival and distribution.

The suggested decrease in fog frequency and potential shift in advection-radiation fog may necessitate redefining the extent of the Namib fog-zone, and provide an opportunity to study the effects of global climate change on these non-rainfall water dependent ecosystems. At the same time, fog and dew should be excluded from determination of the LMWL as these non-rainfall waters or moisture could be transported from other areas and are thus not derived from the local meteoric waters. For example, inclusion of advective and mixed fog samples in determining the LMWL for the Central

Namib Desert could result in a slope ≥ 8, uncharacteristic of arid environments whose LMWL slope < 8 due to the strong atmospheric demand (Kendall and McDonnell 2012).

We acknowledge that direct isotopic measurements of transpiration vapour would strengthen our estimates of the fractionation factors (equation 3). However, such measurements would not change our conclusions. We also note that recent spectroscopy-based transpiration studies have shown that the isotopic composition of transpiration vapour closely approximates its source waters (Wang, Caylor, et al. 2010, Wang et al. 2012), supporting the assumptions made in the fractionation factor calculations. In addition, coherent multiple lines of evidence provided here (e.g., positions on isotopic water lines, theoretical fractionation factor calculations, wind speed/direction and *d* values) provide strong support for our estimates on the source origins of fog and dew.

References

Angert, Alon, Christopher D Cappa, and Donald J DePaolo. 2004. "Kinetic ^{17}O effects in the hydrologic cycle: Indirect evidence and implications." *Geochimica et cosmochimica acta* 68 (17):3487-3495.

Araguás-Araguás, L, K. Froehlich, and K. Rozanski. 2000. "Deuterium and $\delta^{18}O$ isotope composition of precipitation and atmospheric moisture." *Hydrological Processes* 14 (8):1341-1355.

Aravena, R, O Suzuki, and A Pollastri. 1989. "Coastal fog and its relation to groundwater in the IV region of northern Chile." *Chemical Geology: Isotope Geoscience Section* 79 (1):83-91.

Brown, Roger, Anthony J Mills, and Chris Jack. 2008. "Non-rainfall moisture inputs in the Knersvlakte: methodology and preliminary findings: short communication." *Water SA* 34 (2):275-278.

Burke, A. 2006. "Savanna trees in Namibia - Factors controlling their distribution at the arid end of the spectrum." *Flora* 201:189-201.

Craig, Harmon. 1966. "Isotopic composition and origin of the Red Sea and Salton Sea geothermal brines." *Science* 154 (3756):1544-1548.

Cui, Jun, Shuqing An, Zhongsheng Wang, Changming Fang, Yuhong Liu, Haibo Yang, Zhen Xu, and Shirong Liu. 2009. "Using deuterium excess to determine the sources of high-altitude precipitation: Implications in hydrological relations between sub-alpine forests and alpine meadows." *Journal of hydrology* 373 (1):24-33.

Dahan, Ofer, Boaz Tatarsky, Yehouda Enzel, Christoph Kulls, Mary Seely, and Gererdo Benito. 2008. "Dynamics of flood water infiltration and ground water recharge in hyperarid desert." *Groundwater* 46 (3):450-461.

Dansgaard, W. 1964. "Stable isotopes in precipitation." *Tellus, 16*:436-468.

Dawson, T.E. 1998. "Fog in the California redwood forest: ecosystem inputs and use by plants." *Oecologia* 117:476-485.

Deshpande, RD, AS Maurya, B Kumar, A Sarkar, and SK Gupta. 2013. "Kinetic fractionation of water isotopes during liquid condensation under super-saturated condition." *Geochimica et Cosmochimica Acta* 100:60-72.

Ebner, M, T Miranda, and A Roth-Nebelsick. 2011. "Efficient fog harvesting by Stipagrostis sabulicola (Namib dune bushman grass)." *Journal of Arid Environments* 75 (6):524-531.

Eckardt, FD, K Soderberg, LJ Coop, AA Muller, KJ Vickery, RD Grandin, C Jack, TS Kapalanga, and J Henschel. 2013. "The nature of moisture at Gobabeb, in the central Namib Desert." *Journal of Arid Environments* 93:7-19.

Engelbrecht, FA, JL McGregor, and CJ Engelbrecht. 2009. "Dynamics of the Conformal-Cubic Atmospheric Model projected climate-change signal over southern Africa." *International Journal of Climatology* 29 (7):1013-1033.

Esler, Karen J, Phillip W Rundel, and Piet Vorster. 1999. "Biogeography of prostrate-leaved geophytes in semi-arid South Africa: hypotheses on functionality." *Plant Ecology* 142 (1-2):105-120.

Feddes, R.A, H. Hoff, and M Bruen. 2001. "Modelling root water uptake in hydrological and climate models." *Bulletin of the American Meteorological Society* 82:2797-2809.

Fischer, Douglas T, and Christopher J Still. 2007. "Evaluating patterns of fog water deposition and isotopic composition on the California Channel Islands." *Water Resources Research* 43 (4).

Foster, Pru. 2001. "The potential negative impacts of global climate change on tropical montane cloud forests." *Earth-Science Reviews* 55 (1):73-106.

Friedman, Irving, and George I Smith. 1970. "Deuterium content of snow cores from Sierra Nevada area." *Science* 169 (3944):467-470.

Gat, JR, and E Matsui. 1991. "Atmospheric water balance in the Amazon Basin: an isotopic evapotranspiration model." *Journal of Geophysical Research: Atmospheres* 96 (D7):13179-13188.

Giannini, Alessandra, Michela Biasutti, Isaac M Held, and Adam H Sobel. 2008. "A global perspective on African climate." *Climatic Change* 90 (4):359-383.

Gonfiantini, R, and A Longinelli. 1962. "Oxygen isotopic composition of fogs and rains from the North Atlantic." *Experientia* 18 (5):222-223.

Henschel, Joh R, and Mary K Seely. 2008. "Ecophysiology of atmospheric moisture in the Namib Desert." *Atmospheric Research* 87 (3):362-368.

Hill, Amber J, Todd E Dawson, Oren Shelef, and Shimon Rachmilevitch. 2015. "The role of dew in Negev Desert plants." *Oecologia*:1-11.

Houston, John. 2002. "Groundwater recharge through an alluvial fan in the Atacama Desert, northern Chile: mechanisms, magnitudes and causes." *Hydrological processes* 16 (15):3019-3035.

Hulme, Mike. 1996. "Recent climatic change in the world's drylands." *Geophysical Research Letters* 23 (1):61-64.

Hulston, JR, and HG Thode. 1965. "Variations in the S^{33}, S^{34}, and S^{36} contents of meteorites and their relation to chemical and nuclear effects." *Journal of Geophysical Research* 70 (14):3475-3484.

Jacobson, P.J, Kathryn M. Jacobson, and M. K Seely. 1995. *Ephemeral rivers and their catchments : sustaining people and development in western Namibia*. Edited by P.J Jacobson, Kathryn M. Jacobson and M. K Seely. Windhoek: Desert Research Foundation of Namibia.

Jasechko, Scott, Zachary D. Sharp, John J. Gibson, S. Jean Birks, Yi Yi, and Peter J. Fawcett. 2013. "Terrestrial water fluxes dominated by transpiration." *Nature*:doi: 10.1038/nature11983.

Jouzel, J, and L. Merlivat. 1984. "Deuterium and $\delta^{18}O$ in precipitation: modeling of the isotopic effects during snow formation." *Journal of Geophysical Research-Atmospheres* 89 (11):749–757 doi:10.1029/JD089iD07.

Jouzel, JEAN. 1986. "Isotopes in cloud physics: Multiphase and multistage condensation processes." *Handbook of Environmental Isotope Geochemistry* 2:61-112.

Kaseke, KF, AJ Mills, K Esler, J Henschel, MK Seely, and R Brown. 2012. "Spatial Variation of "Non-Rainfall" Water Input and the Effect of Mechanical Soil Crusts on Input and Evaporation." *Pure and Applied Geophysics* 169 (12):2217-2229.

Kaseke, Kudzai Farai, Lixin Wang, Heike Wanke, Veronika Turewicz, and Paul Koeniger. 2016. "An Analysis of Precipitation Isotope Distributions across Namibia Using Historical Data." *PloS one* 11 (5). doi: http://dx.doi.org/10.1371/journal.pone.0154598.

Kendall, Carol, and Jeffrey J McDonnell. 2012. *Isotope tracers in catchment hydrology*: Elsevier.

Kidron, Giora J, Abraham Starinsky, and Dan H Yaalon. 2014. "Cyanobacteria are confined to dewless habitats within a dew desert: Implications for past and future climate change for lithic microorganisms." *Journal of Hydrology* 519:3606-3614.

Kidron, Giora J, Marina Temina, and Avraham Starinsky. 2011. "An investigation of the role of water (rain and dew) in controlling the growth form of lichens on cobbles in the Negev Desert." *Geomicrobiology Journal* 28 (4):335-346.

Lange, J. 2005. "Dynamics of transmission losses in a large and stream channel." *Journal of Hydrology* 306:112-126.

Liu, Wen Jie, Wen Yao Liu, Peng Ju Li, Lei Gao, You Xin Shen, Ping Yuan Wang, Yi Ping Zhang, and Hong Mei Li. 2007. "Using stable isotopes to determine sources of fog drip in a tropical seasonal rain forest of Xishuangbanna, SW China." *Agricultural and Forest Meteorology* 143 (1):80-91.

Luz, Boaz, and Eugeni Barkan. 2005. "The isotopic ratios $^{17}O/^{16}O$ and $^{18}O/^{16}O$ in molecular oxygen and their significance in biogeochemistry." *Geochimica et Cosmochimica Acta* 69 (5):1099-1110.

Luz, Boaz, and Eugeni Barkan. 2010. "Variations of $^{17}O/^{16}O$ and $^{18}O/^{16}O$in meteoric waters." *Geochimica et Cosmochimica Acta* 74 (22):6276-6286.

Majoube, M. 1971. "$\delta^{18}O$ and deuterium fractionation between water and steam " *Journal De Chimie Physique Et De Physico-Chimie Biologique* 68 (10):1423.

Merlivat, Liliane, and Jean Jouzel. 1979. "Global Climatic Interpretation of the Deuterium-18O Relationship for Precipitation." *J. Geophys. Res.* 84:5029-5033. doi: 10.1029/JC084iC08p05029.

Miller, Martin F. 2002. "Isotopic fractionation and the quantification of ^{17}O anomalies in the oxygen three-isotope system: an appraisal and geochemical significance." *Geochimica et Cosmochimica Acta* 66 (11):1881-1889.

Mizuno, Kazuharu. 2010. "Environmental change and vegetation succession along an ephemeral river: The Kuiseb in the Namib Desert." *African study monographs. Supplementary issue.* 40:3-18. doi: http://dx.doi.org/10.14989/96301.

Monteith, JL. 1957. "Dew." *Quarterly Journal of the Royal Meteorological Society* 83 (357):322-341.

Olivier, Jana. 1995. "Spatial distribution of fog in the Namib." *Journal of Arid Environments* 29 (2):129-138.

Petit, JR, JWC White, NW Young, J Jouzel, and Ye S Korotkevich. 1991. "Deuterium excess in recent Antarctic snow." *Journal of Geophysical Research: Atmospheres* 96 (D3):5113-5122.

Roth-Nebelsick, A, M Ebner, T Miranda, V Gottschalk, D Voigt, S Gorb, T Stegmaier, J Sarsour, M Linke, and W Konrad. 2012. "Leaf surface structures enable the endemic Namib desert grass Stipagrostis sabulicola to irrigate itself with fog water." *Journal of The Royal Society Interface*.

Salati, Eneas, Attilio Dall'Olio, Eiichi Matsui, and Joel R Gat. 1979. "Recycling of water in the Amazon basin: an isotopic study." *Water Resources Research* 15 (5):1250-1258.

Scanlon, B. R., ed. 2004. *Evaluation of methods of estimating recharge in semiarid and arid regions in the southwestern US.* . Edited by JE Hogan, Fred Melville Phillips, Bridget R Scanlon and JF Hogan, *Groundwater Recharge in a Desert Environment: The Southwestern United States*: Publisher American Geophysical Union.

Schachtschneider, Klaudia, and Edmund C February. 2010. "The relationship between fog, floods, groundwater and tree growth along the lower Kuiseb River in the hyperarid Namib." *Journal of Arid Environments* 74 (12):1632-1637.

Schemenauer, Robert S, and Pilar Cereceda. 1994. "A proposed standard fog collector for use in high-elevation regions." *Journal of Applied Meteorology* 33 (11):1313-1322.

Schroder, T, M Javaux, J Vanderborght, B. Korfgen, and H Vereecken. 2009. "Implementation of of a microscopic soil root hydraulic conductivity drop function in a three-dimensional soil root architecture water transport model." *Vadose Zone J.* 8 (3):783-792. doi:10.2136/vzj2008.0116.

Shuttleworth, W James, John HC Gash, Colin R Lloyd, Christopher J Moore, John Roberts, Marques Ari De O Filho, Gilberto Fisch, Vicente De Paula Silva Filho, Maria De Nazaré Góes Ribeiro, and Luiz CB Molion. 1984. "Eddy correlation measurements of energy partition for Amazonian forest." *Quarterly Journal of the Royal Meteorological Society* 110 (466):1143-1162.

Stein, AF, RR Draxler, GD Rolph, BJB Stunder, MD Cohen, and F Ngan. 2015. "NOAA's HYSPLIT atmospheric transport and dispersion modeling system." *Bulletin of the American Meteorological Society* 96 (12):2059-2077.

Stewart, Michael K. 1975. "Stable isotope fractionation due to evaporation and isotopic exchange of falling waterdrops: Applications to atmospheric processes and evaporation of lakes." *Journal of Geophysical Research* 80 (9):1133-1146.

Tian, C., Wang, L. & Novick, K. A. 2016. "Water vapor δ^2H, $\delta^{18}O$ and $\delta^{17}O$ measurements using an off-axis integrated cavity output spectrometer – sensitivity to water vapor concentration, delta value and averaging-time." *Rapid Communications in Mass Spectrometry*:doi: 10.1002/rcm.7714.

Wang, Lixin, Kelly Caylor, and Danilo Dragoni. 2009. "On the calibration of continuous, high-precision $\delta^{18}O$ and δ^2H measurements using an off-axis integrated cavity output spectrometer " *Rapid Communications in Mass Spectrometry* 23:530-536. doi: 10.1002/rcm.3905.

Wang, Lixin, Kelly K Caylor, Juan Camilo Villegas, Greg A Barron-Gafford, David D Breshears, and Travis E Huxman. 2010. "Partitioning evapotranspiration across gradients of woody plant cover: Assessment of a stable isotope technique." *Geophysical Research Letters* 37 (9).

Wang, Lixin, Paolo D'Odorico, Lydia Ries, Kelly Caylor, and Stephen Macko. 2010. "Combined effects of soil moisture and nitrogen availability variations on grass productivity in African savannas." *Plant and Soil* 328:95-108, 10.1007/s11104-009-0085-z.

Wang, Lixin, Stephen P Good, and Kelly K Caylor. 2014. "Global synthesis of vegetation control on evapotranspiration partitioning." *Geophysical Research Letters* 41 (19):6753-6757.

Wang, Lixin, Stephen P. Good, Kelly K. Caylor, and Lucas A. Cernusak. 2012. "Direct quantification of leaf transpiration isotopic composition." *Agricultural and Forest Meteorology* 154-155:127-135. doi: http://dx.doi.org/10.1016/j.agrformet.2011.10.018.

Wang, Lixin, Kudzai Farai Kaseke, and Mary K Seely. 2016. "Effects of non-rainfall water inputs on ecosystem functions." *WIREs*:doi:10.1002/wat2.1179.

Wen, X. F., X. Lee, X. M. Sun, J. L. Wang, Z. M. Hu, S. G. Li, and G. R. Yu. 2012. "Dew water isotopic ratios and their relationships to ecosystem water pools and fluxes in a cropland and a grassland in China." *Oecologia* 168 (2):549-61. doi: 10.1007/s00442-011-2091-0.

Yakir, D., and L. da S. L. Sternberg. 2000. "The use of stable isotopes to study ecosystem gas exchange." *Oecologia* 123 (3):297-311. doi:10.1007/s004420051016.

Yang, Xiaoping, Nina Ma, Jufeng Dong, Bingqi Zhu, Bing Xu, Zhibang Ma, and Jiaqi Liu. 2010. "Recharge to the inter-dune lakes and Holocene climatic changes in the Badain Jaran Desert, western China." *Quaternary Research* 73 (1):10-19. doi: http://dx.doi.org/10.1016/j.yqres.2009.10.009

CHAPTER 3: FOG SPATIAL DISTRIBUTIONS OVER THE CENTRAL NAMIB DESERT – AN ISOTOPE APPROACH

3.1 Introduction

Non-rainfall waters (e.g., fog and dew) are the least studied hydrological components in most ecosystems. However, these non-rainfall water components play an important role in ecosystem dynamics and are particularly important for water-limited ecosystems (Wang et al. 2017). In arid ecosystems, non-rainfall waters can exceed rainfall and can be the sole source of water for plants (Agam and Berliner 2006), thus the ecophysiology of these organisms is geared towards obtaining non-rainfall waters (Henschel and Seely 2008)

According to Byers (1959), it is challenging to provide an exact definition of fog because fog formation occurs under a variety of conditions and is dependent on the observer's perspective and research interests (George 1951, Tardif and Rasmussen 2007). However, for practical purposes, fog is defined as the suspended water droplets or ice crystals that are near the surface and lead to horizontal visibility below 1 km (WMO 1992). Fog formation is influenced by thermodynamic or radiative cooling, aerosol concentration, microphysical processes and surface conditions (Gultepe, Tardif, et al. 2007), thus classification is often based on different combinations of these factors. George (1951) restricted fog classification to six categories: advection, radiation (restricted heating or air drainage), advection-radiation, pre-warmfrontal and mixed radiation. However, given the location of the Central Namib Desert (the region of interest in this study), advective and radiation fog are of interest, thus we present general definitions of these categories. Advective fog is formed in one area and transported to the site of interest (Degefie et al. 2015). Radiation fog is formed from radiative cooling of stagnant air close to the surface (Gultepe, Pagowski, et al. 2007). Advection-radiation fog occurs in coastal areas and is formed from the advection of moist air inland during daylight hours followed by radiative cooling (Ryznar 1977).

Fog has been recognized as an important component of hydrologic and nutrient cycling in forest ecosystems of coastal areas (Dawson 1998, Wang et al. 2017, Weathers and Likens 1996). It is often assumed that fog in these coastal regions is advected from the

ocean and the majority of authors agree that advective sea fog dominates the south-west coast of Africa (Jacobson et al. 2015, Olivier 2004, Seely 1979). The most visible impacts of this advective fog on ecophysiology in the Namib Desert are thought to extend about 60 km inland, a region known as the fog-zone (Lancaster 1984, Olivier 1995, Seely 1979). However, recent studies show that other fog types may be a regular occurrence in the Namib fog-zone, especially along ephemeral rivers and other low laying areas (Eckardt et al. 2013, Kaseke et al. 2017). Therefore we could be under-estimating the significance of other fog types, which hinders the understanding of the potential impact of global climate change on these fog dominated environments.

Despite the ecohydrological significance of fog to many arid and semi-arid ecosystems, coastal regions and tropical montane forests (Dawson 1998, Ebner et al. 2011, Nørgaard et al. 2012, Schemenauer and Cereceda 1991), we still do not fully understand the spatial variation and/or origin of fog in these environments. Cereceda et al. (2002) suggests advective fog in the Atacama Desert dissipates and persists as an area of high humidity, which can be transported further inland. If the high humidity is radiatively cooled, it can result in localized condensation and forms radiation fog (some would call it advection-radiation fog (George 1951, Ryznar 1977). Alternatively, inland fog could be generated from condensation of localized evaporation from the salt flats of the Atacama Desert and classified as radiation fog (Cereceda et al. 2002). The inland fog could also be generated from possible mixing of different air masses to form mixed fog (Degefie et al. 2015). Therefore, in addition to the traditional fog classification techniques, there is a critical need for an objective method that will enable reliable fog differentiation over a large geographic area.

Stable isotopes are one of the best tools available to trace fog water movement because isotope fractionation imparts unique signatures that can be used as environmental tracers (Ingraham and Matthews 1988). Over the years, stable isotopes have been successfully applied to different fog studies and have shown that in some environments fog contributes to groundwater recharge (Ingraham and Matthews 1988, 1990, Scholl et al. 2002) and vegetation water use (Dawson 1998, Limm et al. 2009, Simonin et al. 2009). Although the spatial variation of fog has been investigated at some sites (Bari et al. 2016, Tardif and Rasmussen 2007), the classification methods are often based on subjective

algorithms. As George (1951) points out, there will always be exceptions to classification based on meteorology or aviation forecasting. Here we utilize a classification system based on the isotope approach composed of three fog classes: advective (externally sourced), radiation (locally generated), mixed fog (advection + radiation). The objectives of this study were to identify the fog classes of each fog event at multiple sites, identify source waters of different fog types during each fog event and understand the spatial distribution of these fog types within the Namib Desert.

3.2 Materials and Methods

3.2.1 Site description

This study was conducted in the central Namib Desert located on the south-western edge of the summer rainfall zone (Schulze 1969) (Fig. 3.1). The central Namib Desert receives less than 25 mm annual rainfall (Eckardt et al. 2013), while the western half receives less than 12 mm (Henschel and Seely 2008), resulting in an east-west decreasing rainfall gradient (Hachfeld et al. 2000, Lancaster 1984). Fog occurs throughout the year but peak seasons differ between the coast and the interior. The peak fog season for the coast is winter while that for the interior is summer. However, the greatest fog intensity for all sites is between June and July (Lancaster, 1984). There is a west-east gradient with decreasing fog frequency (Lancaster 1984). Rainfall and groundwater availability are often the primary determinants of species distribution in the Namib Desert (Schachtschneider and February 2010), with large trees confined to the eastern edge of the desert and along ephemeral water courses (Burke 2006) where they access the shallow alluvial aquifers (Lange 2005). The sampling sites were located between the Swakop and Kuiseb ephemeral rivers (Fig. 3.1).

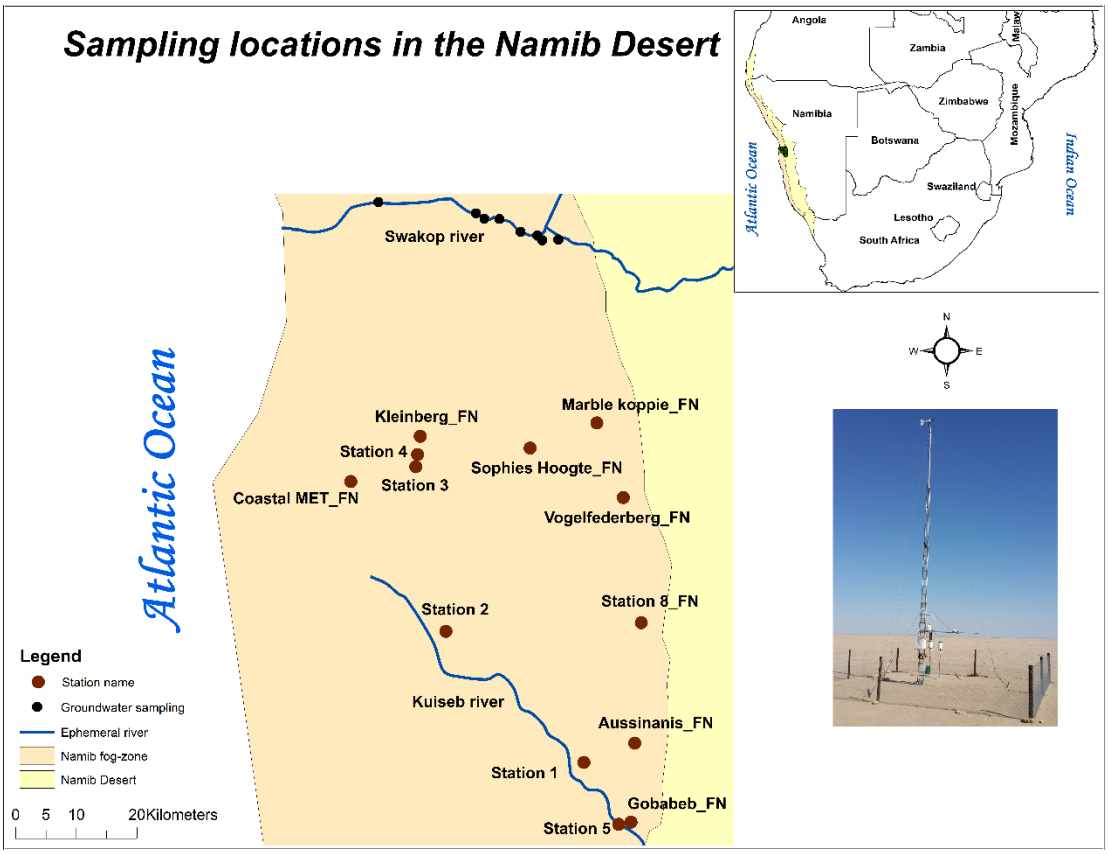

Figure 3. 1 Map indicating the location and extent of the Namib Desert and Namib fog-zone in southern Africa, with the spatial distribution of the individual sampling stations. FN (FogNet) denotes a station that is part of the SASSCAL network and the photo shows a typical setup of the automated weather station. The Swakop River groundwater sampling points were obtained from Marx (2009).

3.2.2 Sample collection

Fog samples were collected from a total of 13 stations. Eight stations were part of the Southern African Science Service Centre for Climate Change and Adaptive Land Management (SASSCAL) or FogNet (FN) project, while the remaining five were temporary stations (Fig. 3.1 and Table B3.1). The FN stations were equipped with automated meteorological instrumentation along with a passive cylindrical fog collector facilitating fog collection and correlation with local meteorological conditions (Fig. 3.1). Data was recorded at hourly intervals from the FN stations and consisted of wind speed, air temperature, soil temperature (10 cm depth), rainfall, relative humidity (RH) and leaf

wetness. Because atmospheric pressure was only recorded at Coastal MET FN and Vogelfederberg FN stations, specific humidity was only computed for these two stations. Each temporary station (station 1 to 5) consisted of a passive flat fog collector (1 m^2) after Schemenauer and Cereceda (1994) and was established primarily to increase spatial sampling coverage. The total area covered by all fog stations was about 1700 km^2 and a roundtrip visit was about 250 km (Fig. 3.1). Fieldwork was conducted from the 9th June–22nd June 2016 and involved daily site visits to all stations to inspect and collect fog samples (Fig. 3.1). Fog events were identified by the presence of sample in the fog collectors. At the FN stations this was in conjunction with wetness recorded on the leaf wetness sensor (0.1 m above the ground). The leaf wetness data enabled determination of the duration of the fog event and associated meteorological conditions. Fog samples were transferred into 15 mL Qorpak clear French square bottles with black phenolic polycone lined caps, labelled appropriately with the sample type location and date and stored at the Gobabeb Research and Training Centre (Gobabeb), until they were shipped to Indiana University-Purdue University Indianapolis (IUPUI) Ecohydrology Lab for isotope analysis.

3.2.3 Isotope analysis

We used a Triple Water Vapor Analyzer (Los Gatos Research Inc., Mountain View, CA, USA), for isotopic analysis with a precision of 0.2‰ $\delta^{18}O$ and 0.8‰ $\delta^{2}H$ similar to those reported elsewhere (Wang et al. 2009). Data was reported in δ notation relative to VSMOW-SLAP scale as

$$\delta = \frac{R_{\text{sample}}}{R_{\text{VSMOW}}} - 1 \qquad , \qquad (1)$$

where R_{sample} and R_{VSMOW} are the molar ratios of heavy to light isotopes international ($^{2}H/H$ or $^{18}O/^{16}O$) of the sample and standard - Vienna Standard Mean Ocean Water (VSMOW).

3.2.4 Differentiation of fog sources based on isotopes

Isotope fractionation imparts unique signatures on meteoric water that can be combined with deuterium excess, defined as $d = \delta 2H - 8 \times \delta^{18}O$ (Dansgaard 1964), to determine source origins and evaporative conditions (Merlivat and Jouzel 1979). Because fog is a first-stage condensate controlled by equilibrium fractionation processes, it should

plot on a meteoric water line reflecting its origins (Gonfiantini and Longinelli 1962, Jouzel 1986, Majoube 1971, Stewart 1975). We thus assumed fog formed from oceanic vapour would plot on the global meteoric water line (GMWL), fog formed from local meteoric waters on the local meteoric water line (LMWL) and fog formed from a mixture of the two air masses would plot between the two meteoric water lines (Kaseke et al. 2017). Since transpiration and equilibrium fractionation do not alter *d* (Dansgaard 1964, Gat 2005), fog *d* derived from locally transpired vapour would be similar to LMWL *d*, while advective *d* would be similar to that of GMWL, +10‰. However, because evaporation increases *d* of vapour relative to evaporating water (Gat and Matsui 1991, Salati et al. 1979), fog formed from evaporated vapour should have a larger *d* than the LMWL. Therefore if radiation fog plots on the LMWL we assume it did not undergo evaporative enrichment after formation. If its *d* is smaller or equal to the LMWL *d*, this suggests transpiration is the main vapour transport pathway and transpired vapour is used for fog formation. If its *d* is larger than the LMWL, this suggests a significant contribution of vapour from evaporation of local water sources. Admixture of different air masses will lead to significantly greater *d* compared to LMWL *d* (Gat and Matsui 1991, Liu et al. 2007, Martinelli et al. 1996), thus we expect mixed fog *d* to have a larger *d* than LMWL. From Kaseke et al. (2017), despite being transported 60 km inland, advective fog plotted around the GMWL and had an isotopic composition similar to that sampled from the coast. Therefore, we should be able to identify advective fog isotopically from all sampling sites as the furthest sites were located about 60 km inland (Fig. 3.1).

Because the stations were remote and receive similar amounts of rainfall, typically less than 20 mm annual rainfall (Henschel and Seely 2008), defining a LMWL for each site would be challenging. Instead, we assumed similar meteorological conditions across the sites given their close proximity (Fig. 3.1). This assumption enabled the application of the LMWL defined for Gobabeb, $\delta^2H = 7.01 \times \delta^{18}O - 0.6$ (Kaseke et al. 2017), to all sites. This LMWL was generated from precipitation, ephemeral water and groundwater samples obtained from Gobabeb (2014–2015) and excluded fog and dew. Because transpiration is non-fractionating, transpired vapour is isotopically similar to source waters (Wang et al. 2010, Wang et al. 2012), hence groundwater was included to the LMWL to account for possible vegetation groundwater uptake along the riverbeds (Fig. 3.1).

3.2.5 Trajectory Analyses

All FN stations received rainfall on the 6th and 7th June 2016, supporting the assumption of similar meteorological conditions across sites (Table 3.1). Hybrid Single Particle Lagrangian Trajectory Model (HYSPLIT) (Stein et al. 2015) was used to model the origin of these rain events for each of the FN stations. Based on the data from each FN station, we calculated dewpoint temperature (Berry et al. 1945) at the start of the rainfall event at each station. We used this value to calculate an approximate cloud height, lifted condensation level (LCL), for the rain event at the station. The back-trajectory of the rain producing air-mass was then computed based on the LCL to identify origins (Soderberg et al. 2013). However, because there may be microclimatological differences among sites, we analysed air temperature, soil temperature and RH among sites and classified the sites into two groups: northern (Coastal MET, Kleinberg, Station 3, Station 4, Sophies Hoogte and Marble Koppie) and southern sites (Vogelfederberg, Station 8, Aussinanis, Gobabeb, Station 1, Station 2 and Station 5) (Fig. 3.1). Statistical analysis was performed in PAST 3 (Paleontological Statistics, Natural History Museum, University of Oslo), with parametric methods for normally distributed data and non-parametric methods for non-normally distributed data.

3.3 Results and Discussion

3.3.1 Classification of fog on the 10th June 2016

Sufficient sample for isotopic analysis on the 10th June 2016 was obtained from eleven of the twelve sites (station 5 was not set up yet). Nine of these fog samples plotted on the LMWL, suggesting they were derived from local meteoric waters (Fig. 3.2). These samples were defined by the regression line $\delta^2H = 6.17 \times \delta^{18}O - 1.2$ and we did not find any significant differences in either slope or intercept between the fog line and LMWL (One-Way ANCOVA, $p > 0.05$). There were also no significant differences between fog *d* (–0.9‰ ± 1.2) and LMWL (+3.6‰ ± 8.8) (One-way ANOVA, Welch F test $p > 0.05$), thus we concluded these samples were generated entirely from local meteoric waters, radiation fog ($\delta^{18}O$ (–0.2‰ ± 0.4), δ^2H (–2.4‰ ± 2.7) and *d* (–0.9‰ ± 1.2) ($n = 9$) (Fig. 3.2 and Fig. 3.3) (Kaseke et al. 2017).

The remaining fog samples plotted between the GMWL and LMWL, suggesting admixture of different air masses (Gat and Matsui 1991, Liu et al. 2007, Martinelli et al. 1996), mixed fog (Kaseke et al. 2017) (Fig. 3.2). However, the Aussinanis sample plotted to the right of the mixed fog line suggesting evaporative enrichment of the sample (Fig. 3.2). The enriched isotopic composition and low *d* (–1.8‰) of the Aussinanis sample relative to other samples was consistent with this conclusion (Table B3.1). Therefore we did not characterise mixed fog because the Gobabeb fog sample was the only unevaporated mixed fog sample, *d* (+5.5‰). Both mixed fog and radiation fog require similar conditions for formation e.g., radiative cooling and calm winds (< 2.5 ms^{-1}) (Meyer and Lala 1990, Roach et al. 1976, Tardif and Rasmussen 2007), conditions that were prevalent during the fog events at all sites (Table B3.2). However, there was a noticeable difference in the degree of radiative cooling and RH during the fog event between the mixed fog sites and the radiation fog sites. Mixed fog sites had a 6.5°C temperature drop with 94.6% RH while radiation fog sites had a 3.2°C temperature drop with 98.8% RH (Table B3.2). The dominant wind direction was variable among sites indicating micro-climatological differences (Table B3.2).

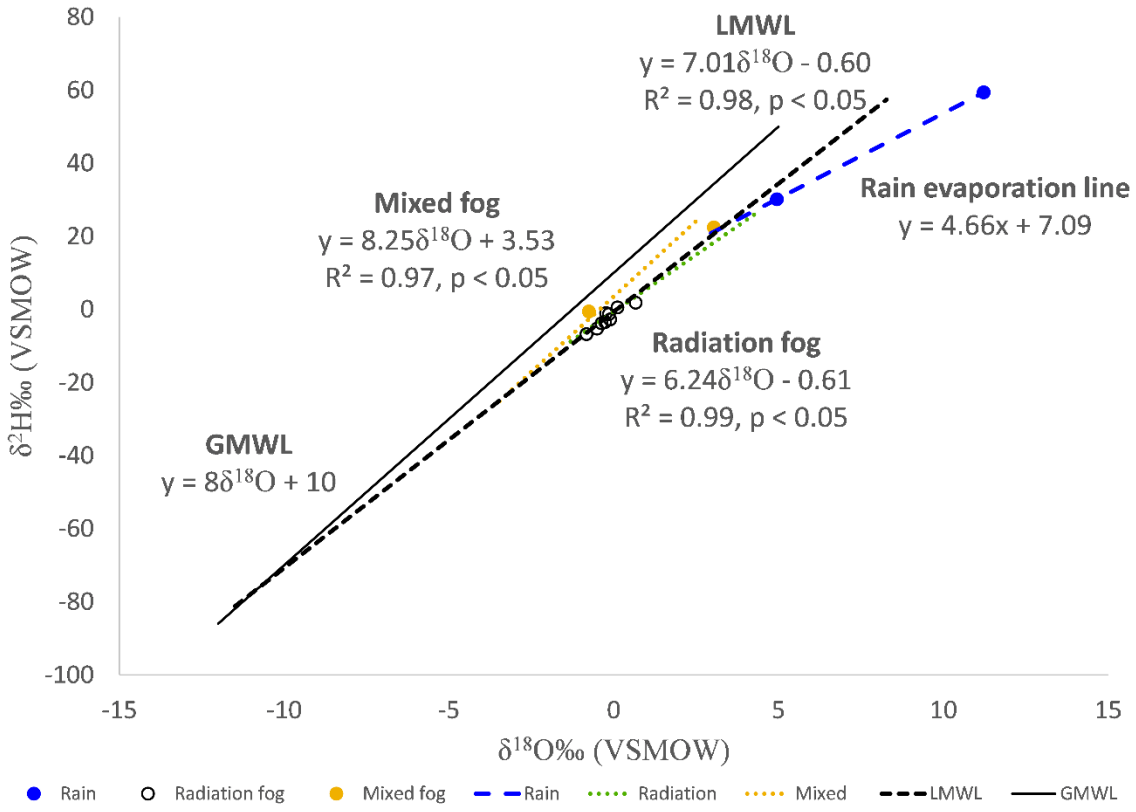

Figure 3. 2 Isotopic classification of fog samples collected from 10 sites in the Central Namib Desert on the 10th June 2016 into mixed fog and radiation fog. The GMWL, LMWL, and radiation fog line were used as references and adapted from Kaseke et al. (2017).

Figure 3. 3 Temporal and spatial variation of fog classification in the Central Namib Desert, June 2016.

Kaseke et al. (2017) attributed radiation fog around Gobabeb to local evapotranspiration from the ephemeral Kuiseb River and/or recent rainfall. Vegetation is restricted to ephemeral water courses and the eastern edge of the Namib Desert (Burke 2006). Therefore, radiation fog originating from groundwater would be restricted to sites along the ephemeral rivers e.g., Stations 1, 2, 5 and Gobabeb, while that from rainfall would be widespread but generally restricted to topographic lows e.g., inter dunes (Eckardt et al. 2013) (Fig. 3.1). Given the location of the study area, between two ephemeral rivers, transpiration of groundwater by ephemeral vegetation could be a source of moisture that generated this fog. This would account for the similarity between radiation fog *d* and LMWL. However, because the area received rainfall on the 6th and 7th June (Table 3.1 and Fig. B3.1), the high soil moisture coupled with conducive micro-climatological conditions at each site could also account for the formation of radiation fog over such a large area (Fig. 3.3). Therefore, radiation fog on the 10th June 2016 could have been derived from either the soil evaporate and/or transpired vapour from the ephemeral rivers. The groundwater isotopic composition of the Swakop River (Marx 2009) plotted on the LMWL defined for Gobabeb, suggesting similar sources and conditions (Fig. B3.2).

Table 3. 1 Rainfall amounts recorded at each FogNet site in the Central Namib Desert, June 2016.

	Rainfall (mm)	
Site	**6 June 2016**	**7 June 2016**
Coastal MET	2.4	1.7
Kleinberg	3.8	0.3
Sophies Hoogte	4.7	3.7
Marble koppie	4.4	3.0
Vogelfedeberg	3.1	4.6
Station 8	4.4	9.0
Aussinanis	3.7	13.3
Gobabeb	3.8	8.7

The source isotopic composition of rainfall ($\delta^{18}O$ +3.27‰ and +22.34‰) received on the 6th and 7th June was enriched relative to radiation fog sampled on the 10th June 2016 (Fig. 3.2). Fog has been reported to be isotopically enriched relative to local rainfall (if they are from the same source) because it is a first stage condensate and formed at generally higher temperatures than rainfall (Gonfiantini and Longinelli 1962, Ingraham and Matthews 1988, Scholl et al. 2011). However, local rainfall can be more enriched isotopically than fog in some arid environments because sub-cloud evaporation could result in in enrichment beyond that observed in the first stage condensates alone (Kaseke et al. 2017). Backward trajectory analysis of rainfall received on the 6th and 7th June 2016 showed that both rainfall events originated from the Indian Ocean (Fig. 3.4). The rain isotopic composition was consistent with enrichment predictions due to sub-cloud evaporation for the Namib Desert since its *d* (-3.8‰) was lower than the LMWL (+3.6‰) (Fig. 3.4) (Kaseke et al. 2017). We thus concluded that fog observed on the 10th June 2016 was derived from local meteoric waters through evapotranspiration (Fig. 3.2).

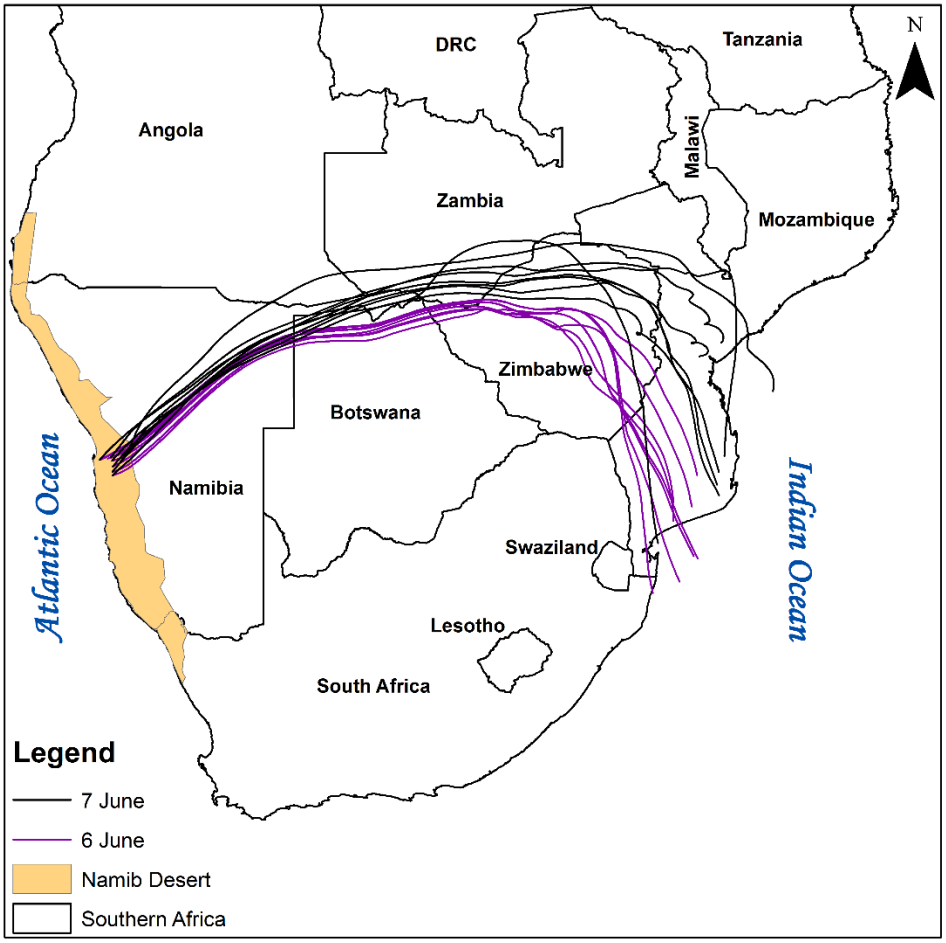

Figure 3. 4 Map of Southern Africa showing origins of rain that fell over the Central Namib Desert on the 6th, 7th and 14th June 2016. These trajectories were calculated using HYSPLIT for each of the eight FogNet stations that were included in the study.

3.3.2 Classification of fog on the 17th June 2016

Fog collected on the 17th June 2016 was observed at s even sites and the majority of samples showed evidence of evaporative enrichment but plotted close to the LMWL (Fig. 3.5). This was supported by the significantly lower fog *d* (–4.1‰ ± 3.3) compared to the LMWL (+3.6‰) and the low fog yield at Sophies Hoogte, Marble Koppie and Vogelfederberg (Table B3.3) (One-way ANOVA, Welch test $p < 0.05$). Therefore we did not characterise the isotopic composition of fog sampled on the 17th June. However, we defined a fog evaporation line $\delta^2H = 6.24\delta^{18}O - 5.98$ ($r^2 = 0.99$) for these fog samples and found no significant difference in either slope or intercept between the fog evaporation line and the LMWL (One-way ANCOVA, $p > 0.05$). Coupled with the puddle in Fig. B3.1

which persisted until the 19th June 2016, these results suggest that the rainfall events on the 6th and 7th may have had an ecohydrological impact beyond their onset date. Therefore, we concluded these fog samples were derived from local meteoric waters and classified it as radiation fog.

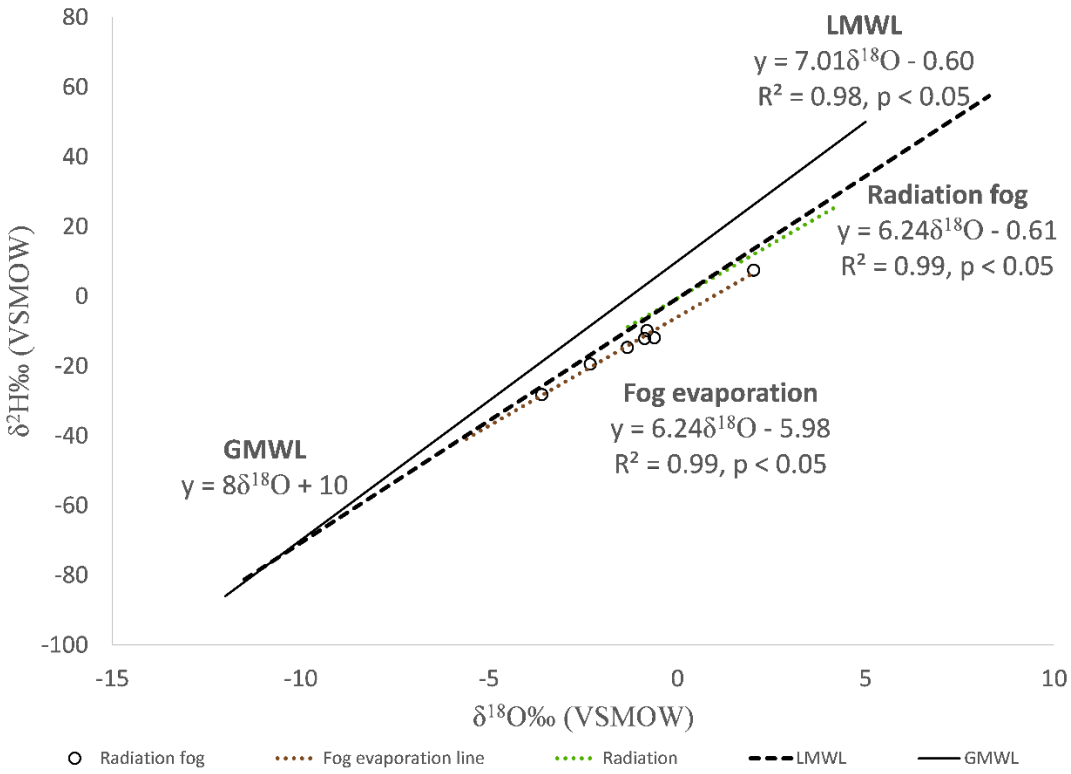

Figure 3. 5 Isotopic classification of fog samples collected from the Central Namib Desert on the 17th June 2016. The GMWL, LMWL, and radiation fog lines were used as references and adapted from Kaseke et al. (2017).

Wind speeds during the fog event on the 17th June 2016 were generally calm (< 2.5 ms^{-1}) with the exception of Vogelfederberg (Table B3.2). However, the dominant wind direction for all sites had easterly origins eliminating the ocean as the source because advective fog would have either north-westerly (Seely and Henschel 1998) or south-westerly origins (Eckardt et al. 2013) (Table B3.2). Advection-radiation fog is associated with an increase in specific humidity due to inflow from the ocean during the daylight hours (Bari et al. 2016). However, although Volgefederberg showed an initial increase in specific humidity on the 16th June 2016, by end of the daylight hours this had decreased

and only increased during the night by 0.8 g kg^{-1} just before fog onset at 0:00 hrs (Fig. B3.3). In the hours preceding fog onset, the wind originated from an easterly direction. The Coastal MET site showed a similar but smaller increase (0.4 g kg^{-1}) in specific humidity during the fog event. These results therefore do not support advection-radiation (mixed) fog classification but support our classification of fog on the 17th June 2016 being radiation fog.

Fog on the 17th June 2016 was restricted to the northern sections of the study area while absent from the southern sections (Fig. 3.3). Because fog occurs only when particular atmospheric conditions are met (Jacobs et al. 2002), this implies conditions conducive for fog formation were not met in the southern sites on the 17th June 2016 (Fig. 3.3). We analyzed 2016 meteorological data and did not find any significant differences in RH, air and soil temperature (Mann Whitney U tests, Bonferroni $p > 0.05$) among the northern sites or among the southern sites indicating similar meteorological conditions within the northern and southern sites. However, inter-region (north versus south) comparisons showed that RH in the northern sites (66.95%) was significantly higher than in the southern sites (53.60%) (Mann Whitney U test, $p < 0.05$). Air temperature was significantly lower at the northern sites (18.87°C ± 2.6) compared to the southern sites (20.72°C ± 2.4) (ANOVA, $p < 0.05$). There was no significant difference in soil temperature at 10 cm depth between the sites: northern sites (24.6°C ± 3.5) compared to southern sites (25.8°C ± 3.8). These results suggest that conditions in the northern sites were more conducive for radiation fog formation than the southern sites because of the higher RH and lower air temperature. Therefore, we attribute the absence of radiation fog in the southern sites on the 17th June, to microclimatological differences between the northern (cooler and more humid) and southern (warmer and drier) sites (Fig. 3.3). However, the differences between the northern and southern sites in air temperature and RH could also be due to higher fog frequency at the northern sites.

3.3.3 Classification of fog on the 18th June 2016

Fog on the 18th June 2016 was observed at all sites; however, isotopic analysis suggested three types of fog occurred over the area (Fig. 3.3). Advective fog was observed at four sites, radiation fog at seven sites and mixed fog at one site (Fig. 3.6). The sample

obtained from Station 8 was insufficient for isotopic analysis and was not classified (Fig. 3.3). Advective fog plotted close but to the right of the GMWL and the advective fog line from (Kaseke et al. 2017), suggesting evaporative enrichment of the samples (Fig. 3.6). The advective fog samples were defined by the regression line $\delta^2H = 9.93\delta^{18}O + 7.74$ ($r^2 = 0.77$) and there was no significant difference in slope between this line and the advective fog line from Kaseke et al. (2017) (ANCOVA, $p > 0.05$). However, *d* of these samples (+6‰) was significantly lower than that of the advective fog line (+7.6‰) and GMWL (10‰) (One-way ANOVA, Welch F test, $p < 0.05$), which could be taken as evidence of evaporative enrichment, thus we did not characterise advective fog. Wind data was consistent with this classification, showing westerly and north-westerly origins of fog for Coastal MET and Kleinberg stations (Fig. 3.3 and Table B3.2).

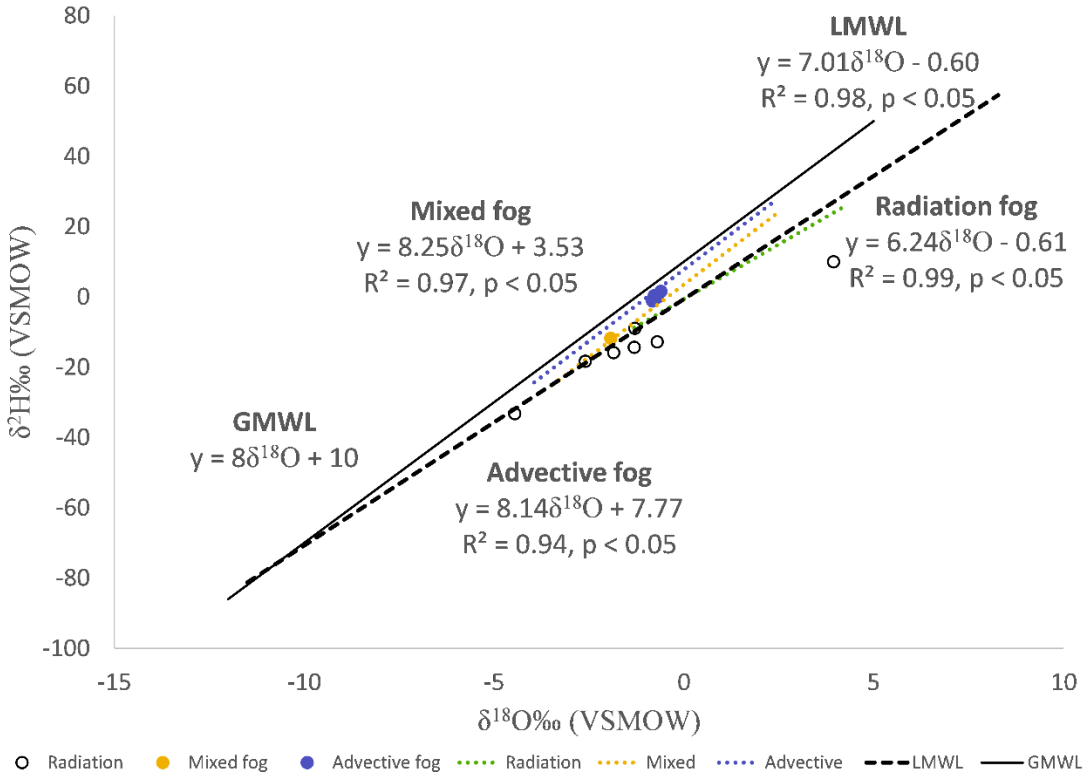

Figure 3. 6 Isotopic classification of fog samples collected from 12 sites in the Central Namib Desert on the 18th June 2016 into advective fog, mixed fog and radiation fog. The GMWL, LMWL, advective fog line, mixed fog line and radiation fog line were used as references and adapted from Kaseke et al. (2017).

Computing forward trajectories of advective fog observed at Coastal MET and Kleinberg based on the dominant winds, we expected the fog to extend to Sophies Hoogte (~50 km inland) but the sample obtained from Sophies Hoogte was classified as mixed fog based on isotopes (Fig. 3.6). This suggests either, dissipation of advective fog downwind and the mixing of residual humidity with locally derived moisture followed by radiative cooling of the mixed air mass to generate mixed fog, or, advective fog incorporating substantial amounts of local moisture along its inland trajectory altering its isotopic composition to that of mixed fog while maintaining the same RH (Fig. 3.3 and Table B3.2). The dominant wind direction at Sophies Hoogte (342°) suggests advective fog or residual moisture may have entered the Namib Desert north of the Swakop River, incorporating transpired vapour along the river transforming into mixed fog as it extended southwards (Fig. 3.1 and Table B3.2). As the fog extended south, it may have also incorporated soil evaporate (Fig. B3.1), resulting in the mixed fog isotopic composition of the sample obtained from Sophies Hoogte (Fig. 3.3).

Seven fog samples from the 18th June were classified as locally generated, radiation fog samples (Fig. 3.3). Three samples plotted directly on the LMWL consistent with local origins of fog ($\delta^{18}O$ –2.8‰, $\delta^{2}H$ –20.1‰), while the remaining plotted to the right of the LMWL suggesting evaporative enrichment and were excluded from isotopic characterisation (Fig. 3.6). Radiation fog *d* (+2.1‰ ± 0.6) was similar to LMWL (+3.6‰ ± 8.8) (One-way ANOVA, Welch F test $p > 0.05$) suggesting local origins of the fog. Interestingly, all sites classified as having received radiation fog had on average lower RH during the fog event than sites with samples classified as advective and mixed fog (Fig. 3.3 and Table B3.2).

Marble Koppie was dominated by westerly winds during the fog event, suggesting extension of mixed fog further inland (~60 km), but the isotopic composition was consistent with local origins (Fig. 3.3 and Table B3.2). Coupled with the decrease in RH, these results suggest that the advecting mixed fog/moisture incorporated more local moisture increasing its contribution while RH decreased. This resulted in a change in the isotopic composition to reflect the dominance of the local moisture contribution to fog ~60 km inland, radiation fog (Fig. 3.3 and Fig. 3.6). Taking into account the west-east and north-south wind trajectories during the fog occurrence at Kleinberg and Sophies Hoogte,

respectively (Table B3.2), it suggests convergence of these systems about 50 km inland, extending fog in a south-easterly direction to about 60 km inland (Fig. 3.3). However, fog samples obtained from sites 60 km inland were classified as radiation fog, suggesting that either the fog observed at Sophies Hoogte dissipated before 60 km and the fog observed at these sites was generated from local moisture (6th and 7th June rains) or the mixed fog observed at Sophies Hoogte incorporated more local moisture along its trajectory inland altering the isotopic composition to that of radiation fog (Fig. 3.3 and Fig. 3.6). The dominant winds during the fog event at the southern sites (~60 km inland) was variable e.g., Gobabeb and Station 8 had southerly origins, Aussinanis (north-westerly) while Vogelfederberg had easterly origins (Table B3.2). The southerly wind origins at Gobabeb suggest that transpiration from the Kuiseb River may have contributed moisture to radiation fog (Fig. 3.1 and Fig. 3.3).

Interestingly, Station 2 (~30 km inland, 215 m a.s.l) was classified as radiation fog and received less input than Stations 3 and 4 (~ 33 km inland, 185 m a.s.l) which were classified as advective fog (Fig. 3.3 and Table B3.4). This suggests substantial amounts of locally derived moisture was added to advective fog/moisture within ~30 km from the coast, altering the isotopic composition to reflect the dominance of the local moisture input component to the fog observed at Station 2 (Fig. 3.3). This local moisture could have been generated from the residual soil moisture (6th and 7th June rains) and the ephemeral vegetation given the proximity of Station 2 to the Kuiseb River (Fig. 3.1). Similarly, the fog samples from Station 1, 5 and Gobabeb located along the Kuiseb River were also classified as locally generated fog (Fig. 3.1 and Fig. 3.3).

These results suggest that the observed widening or extension of the Namib fog-zone to about 60 km inland between the Swakop and Kuiseb rivers could be due to the perpetuation of 'advective' fog by evapotranspiration from river vegetation in addition to the effect of topography (Cermak 2012, Lancaster 1984) (Fig. 3.1).

3.3.4 Classification of Fog on the 19th June 2016

Fog on the 19th June 2016 was experienced at all 13 stations. However, there was insufficient sample for analysis from the Coastal MET station (Fig. 3.3). The five fog samples classified as mixed fog: $\delta^{18}O$ (–1.1‰ ± 0.4), $\delta^{2}H$ (–5.1‰ ± 3.4) and *d* (+3.9‰ ±

0.8) (Fig. 3.3 and Fig. 3.7) were restricted to the northern sites (Fig. 3.3). Although mixed fog *d* (+3.9‰) was not significantly larger than the LMWL (+3.6‰) (One-way ANOVA, Welch F test, $p > 0.05$), the samples plotted between the GMWL and LMWL on the mixed fog line from Kaseke et al. (2017) suggesting admixture of different air masses, mixed fog (Fig. 3.7). Although somewhat similar to the 18th June fog, the fog on the 19th June was unique in that local moisture inputs to advective moisture/fog was substantial to alter the isotopic composition of the fog at all northern sites, to form mixed fog (Fig. 3.3). Because the fog yield on the 19th was generally lower than on the 18th June 2016, suggests a light advective fog (low preciptable water) and the local moisture additions along the trajectory increased the fog preciptable water resulting in a west-east increasing fog yield gradient (Table B3.3).

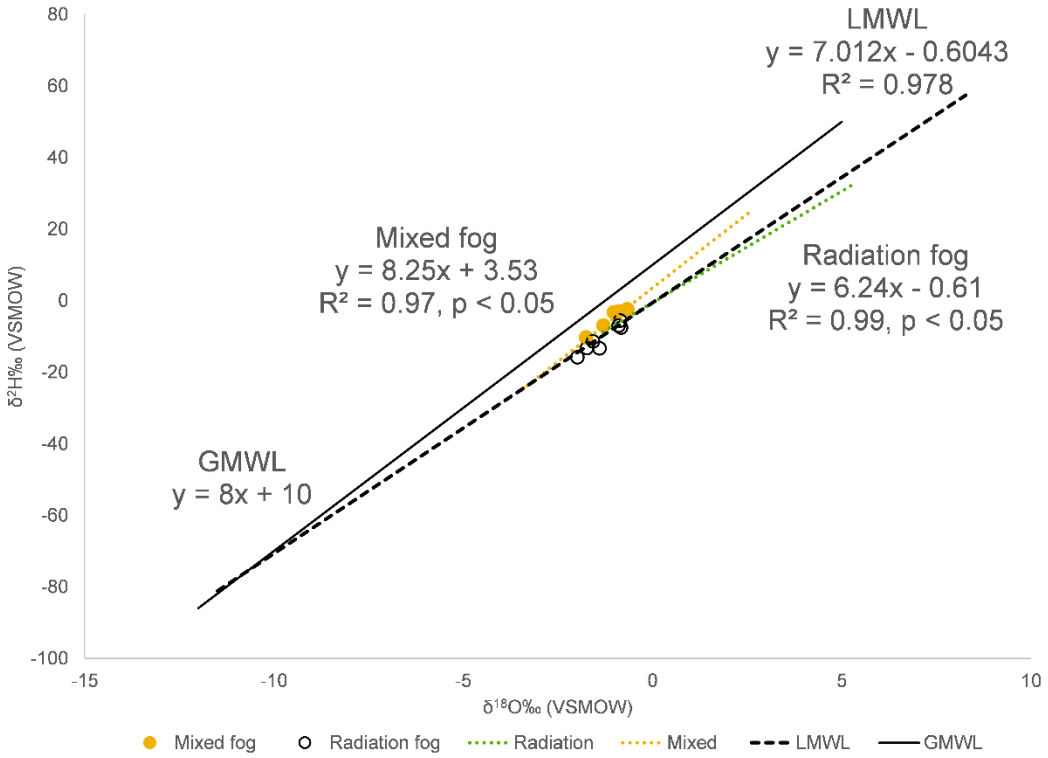

Figure 3. 7 Isotopic classification of fog samples collected from 13 sites in the Central Namib Desert on the 19th June 2016 into mixed and radiation fog types. The GMWL, LMWL, mixed fog line and radiation fog line were used as references and adapted from Kaseke et al. (2017).

All fog samples collected from the southern sites plotted on the LMWL and there was no significant difference between fog *d* (+0.1‰ ± 1.2) and LMWL (+3.6‰), hence classified as radiation fog ($\delta^{18}O$ (–1.3‰ ± 1.7), $\delta^{2}H$ (–10.5‰ ± 3.9)) (Fig. 3.3 and Fig. 3.7). This fog may have been formed by radiative cooling of moisture derived from local waters as wind directions were variable among sites while wind speeds at each site were consistent with those associated with radiation fog (< 2.5 ms^{-1}) (Meyer and Lala 1990, Roach et al. 1976, Tardif and Rasmussen 2007) (Table B3.2). Or, this fog was formed by the perpetuation of mixed fog inland with addition of local moisture along its trajectory similar to that proposed for the 18th June 2016. Therefore, although fog observed over the area on the 19th June may appear like a single fog event, the isotopic data suggests this was composed of mixed fog in the northern sections and radiation fog in the southern sites (Fig. 3.3).

3.3.5 The Relationships between radiation fog isotopic compositions and physical factors

We analysed meteorological data of all FN radiation fog samples that did not show evidence of evaporative enrichment (plotted on the LMWL) and defined these as $\delta^{2}H = 7.15 \times \delta^{18}O - 1.42$ ($r^2 = 0.99$, n =13). There was no significant difference between the LMWL and the radiation fog line in either slope or intercept (One-way ANCOVA, $p > 0.05$). There was also no significant difference between the *d* of the LMWL (+3.6‰) and the radiation fog line (–0.1‰ ± 1.6) (One-way ANOVA Welch F test, $p > 0.05$). Therefore, we concluded that these fog samples were derived from local meteoric waters.

Our results show that radiation fog $\delta^{18}O$ and $\delta^{2}H$ were positively correlated with soil temperature (at 10 cm depth) ($p < 0.05$) (Fig. 3.8a and Fig. 3.8b). The recent rains received over the area (Table 3.1 and Fig. 3.4) resulted in saturation of the soil surface with surface storage at some sites (Fig. B3.1). However, these soils were exposed to evaporative conditions, which resulted in drying of the soil, creating unsaturated conditions from the surface. Overtime, soil tortuosity increases and vapour movement becomes the dominant avenue for water transfer to the surface (Philip 1957). Vapour movement in arid soils is an important means of water transfer (Evans and Thames 1981) and nocturnal cooling may generate a thermal gradient sufficient for upward vapour movement from soil to atmosphere (Francis et al. 2007, Philip 1957). On average, our sites show a 4.9°C night

time soil-atmosphere temperature gradient during radiation fog events, which would facilitate night time evaporation from the soil (Table B3.2). Soil water becomes enriched in both ^{18}O and ^{2}H at the soil surface due to evaporation that is dominated by kinetic fractionation effects (Allison and Barnes 1983). The resulting vapour transferred into the atmosphere is thus isotopically depleted in ^{18}O and ^{2}H compared to the soil water. Condensation of this vapour during fog formation (equilibrium fractionation) results in a condensate that is depleted in ^{18}O and ^{2}H compared to the soil water or rain (Fig. 3.2). As soil temperatures increase, kinetic fractionation effects are reduced causing an increase in $\delta^{18}O$ and $\delta^{2}H$ in the vapour and consequently ^{18}O and ^{2}H enrichment in fog condensed from this vapour (Fig. 3.8a and Fig. 3.8b). Interestingly, we did not find any significant correlation between radiation fog $\delta^{18}O$ and $\delta^{2}H$ and air temperature.

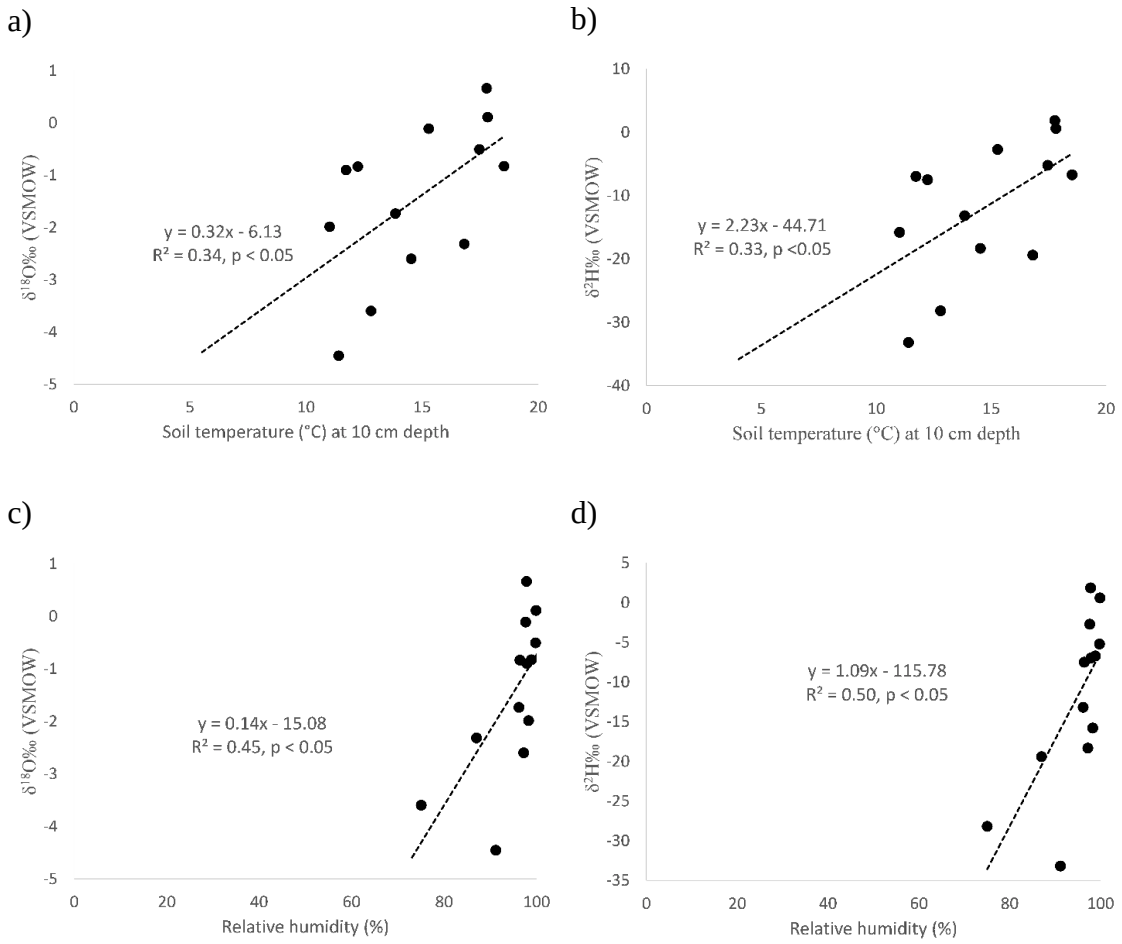

Figure 3. 8 The relationship between soil temperature at 10 cm depth and radiation fog isotopes a) δ18O and b) δ2H. The relationship between relative humidity and radiation fog c) δ18O and d) δ2H).

Radiation fog $\delta^{18}O$ and $\delta^{2}H$ was also positively correlated with RH (Fig. 3.8c and Fig. 3.8d, $p < 0.05$). Since the observed radiation fog was likely derived from soil moisture, this means RH was related to the amount of soil moisture transferred into the atmosphere. Because evaporation from the drying soil is dominated by kinetic fractionation effects resulting in a vapour depleted in ^{18}O and ^{2}H, condensation at low humidity results in fog with low $\delta^{18}O$ and $\delta^{2}H$ values. However, as more moisture is transferred into the atmosphere increasing RH, this also increases vapour $\delta^{18}O$ and $\delta^{2}H$ values and condensation of this vapour under equilibrium conditions should result in an increase in $\delta^{18}O$ and $\delta^{2}H$ in the resulting condensate (Fig. 3.8c and Fig. 3.8d).

We acknowledge the limitations of our study such as the limited dataset and the unusually large winter rainfall, which may not reflect typical conditions over the study area. However, despite these limitations, this study demonstrated that besides advective fog, radiation and mixed fog occurred regularly in this section of the Namib Desert, at least during the observation period. Furthermore, stable isotope analysis of fog suggests co-occurrence of different types of fog during what appears as a single fog event over a large geographic area, similar to the observations of Bari et al. (2016) in Morocco. This suggests that our current understanding of fog dominated ecosystems could be overly simplistic thus there is a need for further studies to understand spatial variability of fog types, their significance to ecohydrology and how shifts or changes might affect the composition of endemic flora and fauna in the future. The study also suggests a north-south decreasing fog gradient similar to that reported by Olivier (1995).

3.4 Conclusions

Local precipitation over the Namib Desert had impacts on fog formation beyond their onset resulting in localized fog, radiation fog. Formation of this localized fog was dependent on micro-climatological conditions at each site and occurred more frequently in the more humid and cooler northern sites compared to the southern sites. Evapotranspiration from the Swakop and Kuiseb rivers could be influential in perpetuating fog inland, creating the observed extension/bulge of the fog-zone inland, in the area between these ephemeral rivers. It is important to acknowledge the short span of the observations in this study, thus future studies using this novel isotope framework are needed to confirm the observed spatial trend. Nonetheless, isotope analyses have demonstrated spatial variations of fog over this area and that what appears as a single fog event may be a mix of different fog types with different formation processes. Such information is particularly important for the Namib Desert because the response of fog dependent desert organisms to climate change is dependent or linked to the source of the fog: ocean or locally generated.

References

Agam, N, and PR Berliner. 2006. "Dew formation and water vapor adsorption in semi-arid environments—a review." *Journal of Arid Environments* 65 (4):572-590.

Allison, GB, and CJ Barnes. 1983. "Estimation of evaporation from non-vegetated surfaces using natural deuterium."

Bari, Driss, Thierry Bergot, and Mohamed El Khlifi. 2016. "Local Meteorological and Large-Scale Weather Characteristics of Fog over the Grand Casablanca Region, Morocco." *Journal of Applied Meteorology and Climatology* 55 (8):1731-1745.

Berry, Frederic Aroyce, Eugene Bollay, and Norman R Beers. 1945. "Handbook of meteorology."

Burke, A. 2006. "Savanna trees in Namibia - Factors controlling their distribution at the arid end of the spectrum." *Flora* 201:189-201.

Byers, Horace Robert. 1959. "General meteorology." In *General meteorology*. McGraw-Hill.

Cereceda, P, P Osses, H Larrain, M Farıas, M Lagos, R Pinto, and RS Schemenauer. 2002. "Advective, orographic and radiation fog in the Tarapacá region, Chile." *Atmospheric Research* 64 (1):261-271.

Cermak, Jan. 2012. "Low clouds and fog along the South-Western African coast—Satellite-based retrieval and spatial patterns." *Atmospheric Research* 116:15-21.

Dansgaard, W. 1964. "Stable isotopes in precipitation." *Tellus, 16*:436-468.

Dawson, T.E. 1998. "Fog in the California redwood forest: ecosystem inputs and use by plants." *Oecologia* 117:476-485.

Degefie, DT, T-S El-Madany, J Hejkal, M Held, J-C Dupont, M Haeffelin, and O Klemm. 2015. "Microphysics and energy and water fluxes of various fog types at SIRTA, France." *Atmospheric Research* 151:162-175.

Ebner, M, T Miranda, and A Roth-Nebelsick. 2011. "Efficient fog harvesting by Stipagrostis sabulicola (Namib dune bushman grass)." *Journal of Arid Environments* 75 (6):524-531.

Eckardt, FD, K Soderberg, LJ Coop, AA Muller, KJ Vickery, RD Grandin, C Jack, TS Kapalanga, and J Henschel. 2013. "The nature of moisture at Gobabeb, in the central Namib Desert." *Journal of Arid Environments* 93:7-19.

Evans, Daniel D, and John L Thames. 1981. "Water in Desert Ecosystems." *Water in Desert Ecosystems*. (11).

Francis, ML, MV Fey, HP Prinsloo, F Ellis, AJ Mills, and TV Medinski. 2007. "Soils of Namaqualand: compensations for aridity." *Journal of Arid Environments* 70 (4):588-603.

Gat, JR. 2005. "Some classical concepts of isotope hydrology." In *Isotopes in the Water Cycle*, 127-137. Springer.

Gat, JR, and E Matsui. 1991. "Atmospheric water balance in the Amazon Basin: an isotopic evapotranspiration model." *Journal of Geophysical Research: Atmospheres* 96 (D7):13179-13188.

George, Joseph J. 1951. "Fog." In *Compendium of meteorology*, 1179-1189. Springer.

Gonfiantini, R, and A Longinelli. 1962. "Oxygen isotopic composition of fogs and rains from the North Atlantic." *Experientia* 18 (5):222-223.

Gultepe, I, M Pagowski, and J Reid. 2007. "A satellite-based fog detection scheme using screen air temperature." *Weather and forecasting* 22 (3):444-456.

Gultepe, I, R Tardif, SC Michaelides, J Cermak, A Bott, J Bendix, MD Müller, M Pagowski, B Hansen, and G Ellrod. 2007. "Fog research: A review of past achievements and future perspectives." *Pure and Applied Geophysics* 164 (6-7):1121-1159.

Hachfeld, Berit, Norbert Jürgens, U Deil, and J Loidi. 2000. "Climate patterns and their impact on the vegetation in a fog driven desert: the Central Namib Desert in Namibia." Vegetation and climate. A selection of contributions presented at the 42nd Symposium of the International Association of Vegetation Science, Bilbao, Spain, 26-30 July 1999.

Henschel, Joh R, and Mary K Seely. 2008. "Ecophysiology of atmospheric moisture in the Namib Desert." *Atmospheric Research* 87 (3):362-368.

Ingraham, Neil L., and Robert A. Matthews. 1988. "Fog drip as a source of groundwater recharge in northern Kenya." *Water Resources Research* 24 (8):1406-1410. doi: 10.1029/WR024i008p01406.

Ingraham, Neil L., and Robert A. Matthews. 1990. "A stable isotopic study of fog: the Point Reyes Peninsula, California, U.S.A." *Chemical Geology: Isotope Geoscience section* 80 (4):281-290. doi: http://dx.doi.org/10.1016/0168-9622(90)90010-A.

Jacobs, Adrie FG, Bert G Heusinkveld, and Simon M Berkowicz. 2002. "A simple model for potential dewfall in an arid region." *Atmospheric Research* 64 (1):285-295.

Jacobson, Kathryn, Anne van Diepeningen, Sarah Evans, Rachel Fritts, Philipp Gemmel, Chris Marsho, Mary Seely, Anthony Wenndt, Xiaoxuan Yang, and Peter Jacobson. 2015. "Non-Rainfall Moisture Activates Fungal Decomposition of Surface Litter in the Namib Sand Sea."

Jouzel, JEAN. 1986. "Isotopes in cloud physics: Multiphase and multistage condensation processes." *Handbook of Environmental Isotope Geochemistry* 2:61-112.

Kaseke, Kudzai Farai, Lixin Wang, and Mary K Seely. 2017. "Nonrainfall water origins and formation mechanisms." *Science Advances* 3 (3):e1603131.

Lancaster, MK. 1984. "Climate of the central Namib Desert." *Madoqua* 14 (1):5-61.

Lange, J. 2005. "Dynamics of transmission losses in a large and stream channel." *Journal of Hydrology* 306:112-126.

Limm, Emily Burns, Kevin A. Simonin, Aron G. Bothman, and Todd E. Dawson. 2009. "Foliar water uptake: a common water acquisition strategy for plants of the redwood forest." *Oecologia* 161:449-459.

Liu, Wen Jie, Wen Yao Liu, Peng Ju Li, Lei Gao, You Xin Shen, Ping Yuan Wang, Yi Ping Zhang, and Hong Mei Li. 2007. "Using stable isotopes to determine sources of fog drip in a tropical seasonal rain forest of Xishuangbanna, SW China." *Agricultural and Forest Meteorology* 143 (1):80-91.

Majoube, M. 1971. "$\delta^{18}O$ and deuterium fractionation between water and steam " *Journal De Chimie Physique Et De Physico-Chimie Biologique* 68 (10):1423.

Martinelli, Luiz Antonio, Reynaldo Luiz Victoria, Leonel Silveira Lobo Sternberg, Aristides Ribeiro, and Marcelo Zacharias Moreira. 1996. "Using stable isotopes to determine sources of evaporated water to the atmosphere in the Amazon basin." *Journal of hydrology* 183 (3):191-204.

Marx, V. 2009. "Impacts of upstream uses on the alluvial aquifer of the Swakop River, Namibia." *Germany: Diplomarbeit, Albert Ludwig University of Freiburg*.

Merlivat, Liliane, and Jean Jouzel. 1979. "Global Climatic Interpretation of the Deuterium-18O Relationship for Precipitation." *J. Geophys. Res.* 84:5029-5033. doi: 10.1029/JC084iC08p05029.

Meyer, Michael B, and G Garland Lala. 1990. "Climatological aspects of radiation fog occurrence at Albany, New York." *Journal of Climate* 3 (5):577-586.

Nørgaard, Thomas, Martin Ebner, and Marie Dacke. 2012. "Animal or plant: which is the better fog water collector?" *PloS one* 7 (4):e34603.

Olivier, J. 2004. "Fog-water harvesting along the West Coast of South Africa: A feasibility study." *Water SA* 28 (4):349-360.

Olivier, Jana. 1995. "Spatial distribution of fog in the Namib." *Journal of Arid Environments* 29 (2):129-138.

Philip, John R. 1957. "Evaporation, and moisture and heat fields in the soil." *Journal of meteorology* 14 (4):354-366.

Roach, WT, R Brown, SJ Caughey, JA Garland, and CJ Readings. 1976. "The physics of radiation fog: I–a field study." *Quarterly Journal of the Royal Meteorological Society* 102 (432):313-333.

Ryznar, Edward. 1977. "Advection-radiation fog near Lake Michigan." *Atmospheric Environment (1967)* 11 (5):427-430.

Salati, Eneas, Attilio Dall'Olio, Eiichi Matsui, and Joel R Gat. 1979. "Recycling of water in the Amazon basin: an isotopic study." *Water Resources Research* 15 (5):1250-1258.

Schachtschneider, Klaudia, and Edmund C February. 2010. "The relationship between fog, floods, groundwater and tree growth along the lower Kuiseb River in the hyperarid Namib." *Journal of Arid Environments* 74 (12):1632-1637.

Schemenauer, Robert S, and Pilar Cereceda. 1991. "Fog-water collection in arid coastal locations." *Ambio*:303-308.

Schemenauer, Robert S, and Pilar Cereceda. 1994. "A proposed standard fog collector for use in high-elevation regions." *Journal of Applied Meteorology* 33 (11):1313-1322.

Scholl, Martha A, Stephen B Gingerich, and Gordon W Tribble. 2002. "The influence of microclimates and fog on stable isotope signatures used in interpretation of regional hydrology: East Maui, Hawaii." *Journal of Hydrology* 264 (1):170-184.

Scholl, Martha, Werner Eugster, and Reto Burkard. 2011. "Understanding the role of fog in forest hydrology: stable isotopes as tools for determining input and partitioning of cloud water in montane forests." *Hydrological Processes* 25 (3):353-366.

Schulze, BR. 1969. "The climate of Gobabeb." *Scientific Papers of the Namib Desert Research Station* 1969 (38):5-12.

Seely, M, and JR Henschel. 1998. "The climatology of Namib fog." Proceedings of the First International Conference on Fog and Fog Collection.

Seely, MK. 1979. "Irregular fog as a water source for desert dune beetles." *Oecologia* 42 (2):213-227.

Simonin, Kevin A, Louis S Santiago, and Todd E Dawson. 2009. "Fog interception by Sequoia sempervirens (D. Don) crowns decouples physiology from soil water deficit." *Plant, cell & environment* 32 (7):882-892.

Soderberg, Keir, Stephen P. Good, Molly O'Connor, Lixin Wang, Kathleen Ryan, and Kelly K. Caylor. 2013. "Using atmospheric trajectories to model the isotopic composition of rainfall in central Kenya." *Ecosphere* 4 (3):art33. doi: 10.1890/ES12-00160.1.

Stein, AF, RR Draxler, GD Rolph, BJB Stunder, MD Cohen, and F Ngan. 2015. "NOAA's HYSPLIT atmospheric transport and dispersion modeling system." *Bulletin of the American Meteorological Society* 96 (12):2059-2077.

Stewart, Michael K. 1975. "Stable isotope fractionation due to evaporation and isotopic exchange of falling waterdrops: Applications to atmospheric processes and evaporation of lakes." *Journal of Geophysical Research* 80 (9):1133-1146.

Tardif, Robert, and Roy M Rasmussen. 2007. "Event-based climatology and typology of fog in the New York City region." *Journal of applied meteorology and climatology* 46 (8):1141-1168.

Wang, Lixin, Kelly Caylor, and Danilo Dragoni. 2009. "On the calibration of continuous, high-precision $\delta^{18}O$ and $\delta^{2}H$ measurements using an off-axis integrated cavity output spectrometer " *Rapid Communications in Mass Spectrometry* 23:530-536. doi: 10.1002/rcm.3905.

Wang, Lixin, Kelly K Caylor, Juan Camilo Villegas, Greg A Barron-Gafford, David D Breshears, and Travis E Huxman. 2010. "Partitioning evapotranspiration across

gradients of woody plant cover: Assessment of a stable isotope technique." *Geophysical Research Letters* 37 (9).

Wang, Lixin, Stephen P. Good, Kelly K. Caylor, and Lucas A. Cernusak. 2012. "Direct quantification of leaf transpiration isotopic composition." *Agricultural and Forest Meteorology* 154-155:127-135. doi: http://dx.doi.org/10.1016/j.agrformet.2011.10.018.

Wang, Lixin, Kudzai Farai Kaseke, and Mary K Seely. 2017. "Effects of non-rainfall water inputs on ecosystem functions." *WIREs*:doi:10.1002/wat2.1179.

Weathers, Kathleen C, and Gene E Likens. 1996. "Clouds in southern Chile: an important source of nitrogen to nitrogen-limited ecosystems?" *Environmental Science & Technology* 31 (1):210-213.

WMO. 1992. *International Meteorological Vocabulary*. 2 ed: World Meteorological Organization.

CHAPTER 4: FOG AND DEW AS POTABLE WATER RESOURCES - HARVESTING TECHNIQUE IMPROVEMENTS AND WATER QUALITY CONCERNS

4.1 Introduction

Water is a critical resource upon which all socioeconomic activities depend, thus universal access to potable water and water resources is an imperative in all internationally agreed development objectives (WWAP 2012). It is estimated that 1.2 billion people live in areas of physical water scarcity (WWAP 2012), 90% of whom live in developing nations with population growth rates above the global average, exerting more pressure on water resources and exacerbating the situation (Wang et al. 2012). Furthermore, it is estimated an additional 500 million people are approaching physical water scarcity (WWAP 2012), while 1.6 billion people face economic water shortages (Water 2007).Water scarcity is thus one of the major threats to mankind in the 21st century (Prinz 2000) and harvesting of ancillary potable water resources may ameliorate water scarcity. Fog and dew are two such potentially exploitable ancillary water resources.

4.2 Discussion

4.2.1 Definitions and harvesting

Although often considered as the same input (Brown et al. 2008), fog and dew are different meteorological phenomena, controlled by different formation processes (Kaseke et al. 2017, Wang et al. 2016). Fog is the suspended water droplets in the atmosphere reducing visibility to less than 1 km (WMO 1992), while dew is the formation of water droplets on a sufficiently cooled substrate surface (Beysens 1995). Interest in fog as a potable water resource often eclipses interest in dew (Fig. 4.1). This is attributable to differences in the potential yield per event e.g., fog can be as high as 50 L m^{-2} day^{-1} (Abdul-Wahab et al. 2007), while dew has a theoretical maximum of 0.8 L m^{-2} day^{-1} (Monteith 2013). However, in some places such as Mirleft (Morocco), dew may present a better harvesting potential: annual frequency dew (48.8%) and yield (20 L m^{-2} yr^{-1}) vs. fog frequency (5.5%) and yield is (1.4 L m^{-2} yr^{-1}) (Lekouch et al. 2012). Nonetheless, some regions have an abundance of both fog and dew e.g., the Central Namib Desert (Henschel

and Seely 2008). In these environments, both fog and dew harvesting could augment groundwater resources which can be brackish during certain times of the year (Shanyengana et al. 2002). In addition, dew harvesting can be integrated into or conducted from existing infrastructure like roofs, combined with rain harvesting, and result in financial savings (Fig. 4.2) (Clus et al. 2013).

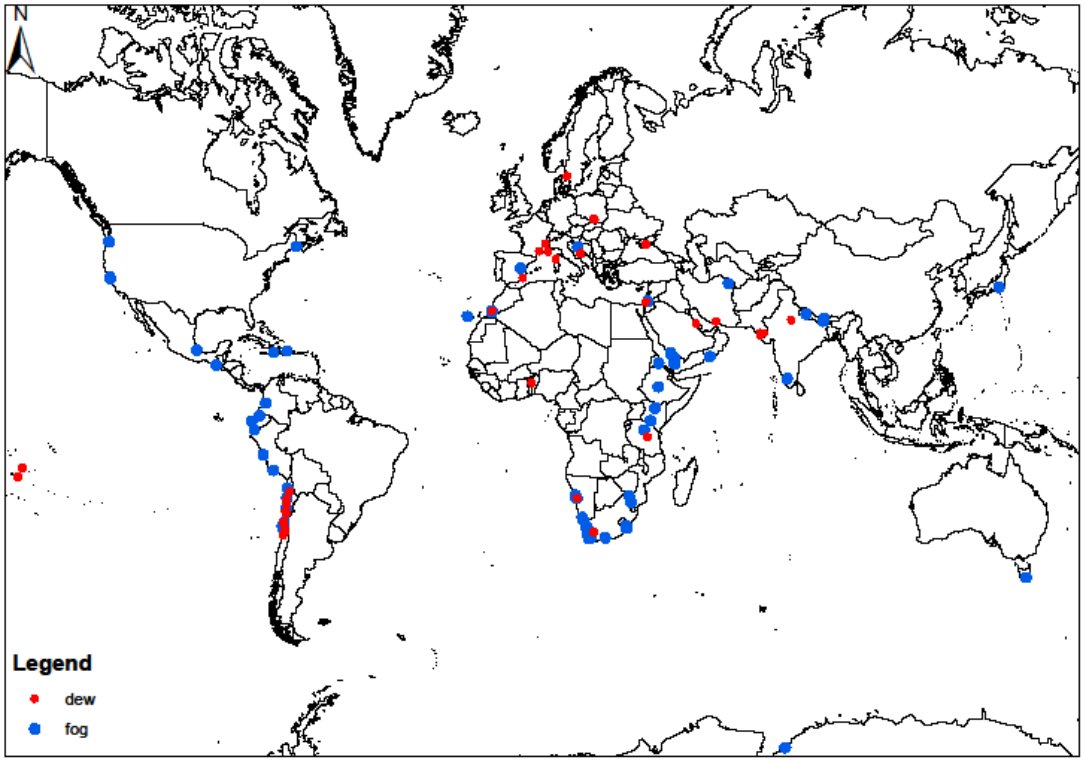

Figure 4. 1 Global distribution of fog and dew collection and or evaluation projects, both operational and non-operational.

a) b)

Figure 4. 2 Dew collection project in Manquehua Chile, a) rooftop dew collection and b) pipes and storage system. The same system is used for rainfall harvesting. CREDIT: Carvajal D. / Universidad de La Serena, Chile (with permission).

4.2.2 Potential of harvesting technique improvements

Fog and dew yield are functions of the prevailing meteorological conditions, as well as the efficiencies of the fog collecting mesh (de Dios Rivera 2011) and receiving substrate surface characteristics of the dew collector (Beysens 1995). However, the de facto fog harvesting mesh material, Raschel mesh, was not developed specifically for this purpose and in fact, the properties of the material in relation to fog harvesting require further investigation (Briassoulis et al. 2007). Its adoption and that of local variants is thus more of convenience and local availability than suitability. Therefore, fog harvesting technologies could benefit from the use of materials specifically designed for fog harvesting which could increase yields by as much as five-fold (Park et al. 2013). Similarly, dew could also benefit from advancements in material science and collector designs developed specifically for passive dew collection (Sharan et al. 2017). For example, origami shaped roofs could increase dew yield efficiency by as much as 400% compared to planar surfaces for low yields (< 0.02 L $m^{-2}day^{-1}$) (Beysens et al. 2013). Assuming ceteris paribus, Table 4.1 and Table 4.2 demonstrate potential fog and dew yields, as well as populations potentially supported by re-evaluations of past projects. The potential fog yields may appear high, however, a recent mesh developed specifically for fog harvesting collected up to 66 $Lm^{-2}day^{-1}$ (https://www.youtube.com/watch?time_continue=5&v=D_kXxGCi2-Q). This

demonstrates that such yields are achievable. However, yields will undoubtedly be limited by the fog liquid water content and duration of the event.

Table 4. 1 Summary and re-evaluation of fog water harvesting potential for select locations and potential number of people supported by a single 40 m^2 fog collector, based on minimum water requirements (7.5 L $person^{-1}$ day^{-1}) (Gleick 1996).

Site	Yield L/m^2/ day		Estimated population, supported by a 40 m^2 LFC		Source
Cape Verde	12	60	64	320	(Sabino 2007)
South Africa, Lepelfontein	4.5	22.5	24	120	(Olivier 2004)
Nepal, Pathivara	3.6	18	19	96	(MacQuarrie et al. 2001)
Namibia	2.4	12	13	64	(Shanyengana et al. 2002)
India, Coimbatore	7.7	38.5	36	205	(Abhiram et al. 2015)
Saudi Arabia	4	20	21	107	(Gandhidasan and Abualhamayel 2012)

Note: SFC is standard fog collector, SFCM is a standard fog collector modified with a mesh that increases collection efficiency five-fold (Park et al. 2013) and LFC is a large fog collector.

Table 4. 2 Average dew yields from planar radiative condensers from different field studies vs projected yields using a hollow funnel condenser and origami (40% and 200% increase in efficiency, respectively).

Site	Average Dew yield [L/ m^2/ day]			Source
	Planar	Cone	Origami	
Kungsbacka, Sweden	0.15	0.21	0.30	(Nilsson 1996)
Dodoma, Tanzania	0.06	0.08	0.12	(Nilsson 1996)
Ajaccio, France	0.12	0.17	0.24	(Muselli et al. 2002)
Jerusalem, Israel	0.2	0.28	0.4	(Berkowicz et al. 2007)
Kothara, India	0.46	0.64	*	(Sharan et al. 2017)

Note: Plane is planar surface and * indicates values not calculated because efficiency calculation is not valid for reference (planar) values > 0.2 L/ m^2/ day (Beysens et al. 2013).

4.2.3 Water quality concerns

Most fog and dew research suggests that this water meets World Health Organisation (WHO) standards (Klemm et al. 2012), mainly based on major cation and anion analyses. However, it must be noted that fog and dew act as atmospheric scrubbers, thus their chemistry is a function of the air quality and gas-liquid-solid heterogeneous interactions in the region (Lekouch et al. 2011, Nath and Yadav 2017). This can result in fogs with acidic pH and high ion concentrations due to either oxidation of dimethyl sulphides from oceanic emissions to sulphates especially along coastal sites (Schemenauer and Cereceda 1992) or anthropogenic emissions due to industrial activities (Sträter et al. 2010). These gas-liquid-phase interactions in the atmosphere contribute more to fog because it remains suspended, while in dew, are restricted to the surface of the condensate (Lekouch et al. 2011, Nath and Yadav 2017).

Whereas acidity on its own is not a major human health concern, Sträter et al. (2010) note that acidic pH may result in extraction of heavy metals from aerosol particulates incorporated into fog and result in trace metal concentrations that may exceed local and/or WHO drinking water guidelines. The data on trace metal concentrations in fog and dew waters are extremely limited. However, the existing data does pose serious concerns in this regard. For example, acidic pH, high levels of selenium, arsenic and nitrates that exceed Chilean guidelines for potable water have been reported in fog water (Sträter et al. 2010). Elevated concentrations of aluminium and iron in excess of European Union drinking standards and lead concentrations on the WHO threshold have also been reported in water harvested from dew (Muselli et al. 2006). Unfortunately, most fog and dew studies do not include trace metals in their analyses thus we do not know how prevalent this problem is. At the same time, biological aspects of fog and dew water are also often ignored but the few studies that have investigated them suggest susceptibility to biological contamination, including coliform and enterococcus forms (Fuzzi et al. 1997, Muselli et al. 2006). Therefore, we urge cautionary practices e.g., increasing pH, use of filters and non-corrosive pipes and storage facilities as well as disinfection to make this water potable (Muselli et al. 2006, Sharan et al. 2011). Although these processes increase the cost of producing water from these systems, there are still cost effective compared to traditional

water sources in countries such as Chile (Cereceda et al. 1992), southwest Morocco (Lekouch et al. 2012) and India (Sharan et al. 2011, Sharan et al. 2017).

4.3 Summary and Recommendations

Can fog and dew harvesting replace traditional water resources? Probably not. However, they can supplement existing water resources, especially during the driest periods and collection efficiency can be significantly improved by adoption of materials specifically designed for these purposes. Based on the existing data, although we believe fog and dew to be potable after some treatments, we encourage trace metal analyses especially in samples collected from areas influenced by industrial activities or areas with fog and or dew that exhibits very low pH values since acidic pH of these waters could extract and elevate trace metal concentrations to levels harmful to human health. Although fog and dew harvesting aim to address the same problem, there are often not implemented together and yet any additional water sources in these arid environments is important. It is thus no surprise that despite the many fog and dew reviews, there hasn't been a single review paper that addresses the potability of both fog and dew in the same context. There is no coordination in either fog and/or dew harvesting projects worldwide such that it is difficult to analyse or access information about these projects. As an example, the authors of this paper reached out to 21 fog and dew researchers enquiring additional information on the status of different projects with the intention of generating a more detailed map for Fig. 4.1, but only received 4 responses or 14% of the requests. This was also partly attributable to the fact that some listed contact information was not current and despite our best efforts to locate these, emails went unanswered or we could not find alternative contact information. Therefore, it would be beneficial to have a coordinated and updated database where such information is readily available. This could later be expanded to include chemical and biological information for samples collected from these sites and this could help answer important questions such as how prevalent trace metal toxicity and biological contamination may be and what are the global trends.

References

Abdul-Wahab, Sabah A, Hilal Al-Hinai, Khalid A Al-Najar, and Mohammed S Al-Kalbani. 2007. "Fog water harvesting: quality of fog water collected for domestic and agricultural use." *Environmental Engineering Science* 24 (4):446-456.

Abhiram, M, N Dhivya Priya, and P Geetha. 2015. "Fog Harvesting–A Wind Flow Perspective in Western Ghats, Coimbatore, Tamil Nadu." *Indian Journal of Science and Technology* 8 (28).

Berkowicz, Simon, Daniel Beysens, Irène Milimouk, Bert Heusinkveld, Marc Muselli, Adrie Jacobs, and O Clus. 2007. "Urban dew collection in Jerusalem: a three-year analysis." 4th Conference on Fog, Fog Collection and Dew.

Beysens, D. 1995. "The formation of dew." *Atmospheric Research* 39 (1):215-237.

Beysens, Daniel, Filippo Brogginib, Iryna Milimouk-Melnytchoukc, Jalil Ouazzanid, and Nicolas Tixiere. 2013. "New architectural forms to enhance dew collection." *Chem. Eng* 34:79-84.

Briassoulis, D, A Mistriotis, and D Eleftherakis. 2007. "Mechanical behaviour and properties of agricultural nets. Part II: Analysis of the performance of the main categories of agricultural nets." *Polymer Testing* 26 (8):970-984.

Brown, Roger, Anthony J Mills, and Chris Jack. 2008. "Non-rainfall moisture inputs in the Knersvlakte: methodology and preliminary findings: short communication." *Water SA* 34 (2):275-278.

Cereceda, Pilar, Robert S Schemenauer, and Marcela Suit. 1992. "An alternative water supply for Chilean coastal desert villages." *International Journal of Water Resources Development* 8 (1):53-59.

Clus, Owen, Imad Lekouch, Marc Muselli, I Milimouk-Melnytchouk, and Daniel Beysens. 2013. "Dew, fog and rain water collectors in a village of S-Morocco (Idouasskssou)." *Desalination and Water Treatment* 51 (19-21):4235-4238.

de Dios Rivera, Juan. 2011. "Aerodynamic collection efficiency of fog water collectors." *Atmospheric research* 102 (3):335-342.

Fuzzi, Sandro, Paolo Mandrioli, and Antonio Perfetto. 1997. "Fog droplets—an atmospheric source of secondary biological aerosol particles." *Atmospheric Environment* 31 (2):287-290.

Gandhidasan, P, and HI Abualhamayel. 2012. "Exploring fog water harvesting potential and quality in the Asir Region, Kingdom of Saudi Arabia." *Pure and applied geophysics* 169 (5-6):1019-1036.

Gleick, Peter H. 1996. "Basic water requirements for human activities: Meeting basic needs." *Water international* 21 (2):83-92.

Henschel, Joh R, and Mary K Seely. 2008. "Ecophysiology of atmospheric moisture in the Namib Desert." *Atmospheric Research* 87 (3):362-368.

Kaseke, Kudzai Farai, Lixin Wang, and Mary K Seely. 2017. "Nonrainfall water origins and formation mechanisms." *Science Advances* 3 (3):e1603131.

Klemm, Otto, Robert S Schemenauer, Anne Lummerich, Pilar Cereceda, Victoria Marzol, David Corell, Johan van Heerden, Dirk Reinhard, Tseggai Gherezghiher, and Jana Olivier. 2012. "Fog as a fresh-water resource: overview and perspectives." *Ambio* 41 (3):221-234.

Lekouch, Imad, Khalid Lekouch, Marc Muselli, Anne Mongruel, Belkacem Kabbachi, and Daniel Beysens. 2012. "Rooftop dew, fog and rain collection in southwest Morocco and predictive dew modeling using neural networks." *Journal of Hydrology* 448:60-72.

Lekouch, Imad, Marc Muselli, Belkacem Kabbachi, Jalil Ouazzani, Iryna Melnytchouk-Milimouk, and Daniel Beysens. 2011. "Dew, fog, and rain as supplementary sources of water in south-western Morocco." *Energy* 36 (4):2257-2265.

MacQuarrie, KIA, A Pokhrel, Y Shrestha, P Osses, RS Schemenauer, F Vitez, K Kowalchuk, and R Taylor. 2001. "R. 2001. Results from a high elevation fog water supply project in Nepal." Proceedings of the 2nd International Conference on Fog and Fog Collection.

Monteith, J. L. and Unsworth, M. H. 2013. *Principles of environmental physics*. New York: Routledge Chapman & Hall Inc.

Muselli, Marc, Daniel Beysens, Jacques Marcillat, Irina Milimouk, Torbjörn Nilsson, and Alain Louche. 2002. "Dew water collector for potable water in Ajaccio (Corsica Island, France)." *Atmospheric Research* 64 (1):297-312.

Muselli, Marc, Daniel Beysens, Emmanuel Soyeux, and Owen Clus. 2006. "Is dew water potable? Chemical and biological analyses of dew water in Ajaccio (Corsica Island, France)." *Journal of environmental quality* 35 (5):1812-1817.

Nath, Supriya, and Sudesh Yadav. 2017. "A Comparative Study on Fog and Dew Water Chemistry at New Delhi, India." *Aerosol and Air Quality Research*.

Nilsson, Torbjörn. 1996. "Initial experiments on dew collection in Sweden and Tanzania." *Solar Energy Materials and Solar Cells* 40 (1):23-32.

Olivier, Jana. 2004. "Fog harvesting: An alternative source of water supply on the West Coast of South Africa." *GeoJournal* 61 (2):203.

Park, Kyoo-Chul, Shreerang S Chhatre, Siddarth Srinivasan, Robert E Cohen, and Gareth H McKinley. 2013. "Optimal design of permeable fiber network structures for fog harvesting." *Langmuir* 29 (43):13269-13277.

Prinz, Dieter. 2000. "Global and European water challenges in the 21st century." 3rd Inter-Regional Conference on Environment Water "Water Resources Management in the 21st Century", Budapest.

Sabino, A. 2007. "Fog collection in the natural park of Serra Malagueta. An alternative source of water for the communities." Proceedings of the 4th International Conference on Fog, Fog Collection and Dew.

Schemenauer, Robert S, and Pilar Cereceda. 1992. "The quality of fog water collected for domestic and agricultural use in Chile." *Journal of Applied Meteorology* 31 (3):275-290.

Shanyengana, ES, JR Henschel, MK Seely, and RD Sanderson. 2002. "Exploring fog as a supplementary water source in Namibia." *Atmospheric Research* 64 (1):251-259.

Sharan, Girja, Owen Clus, S Singh, M Muselli, and D Beysens. 2011. "A very large dew and rain ridge collector in the Kutch area (Gujarat, India)." *Journal of Hydrology* 405 (1):171-181.

Sharan, Girja, Anil Kumar Roy, Laurent Royon, Anne Mongruel, and Daniel Beysens. 2017. "Dew plant for bottling water." *Journal of Cleaner Production* 155:83-92.

Sträter, Ellen, Anna Westbeld, and Otto Klemm. 2010. "Pollution in coastal fog at Alto Patache, Northern Chile." *Environmental Science and Pollution Research* 17 (9):1563-1573.

Wang, L, P D'Odorico, JP Evans, DJ Eldridge, MF McCabe, KK Caylor, and EG King. 2012. "Dryland ecohydrology and climate change: critical issues and technical advances." *Hydrology and Earth System Sciences* 16:2585-2603. doi: 10.5194/hess-16-2585-2012.

Wang, Lixin, Kudzai Farai Kaseke, and Mary K Seely. 2016. "Effects of non-rainfall water inputs on ecosystem functions." *WIREs*:doi:10.1002/wat2.1179.

Water, UN. 2007. "Coping with water scarcity: challenge of the twenty-first century." *Prepared for World Water Day*.

WMO. 1992. *International Meteorological Vocabulary*. 2 ed: World Meteorological Organization.

WWAP. 2012. "The United Nations World Water Development Report 4: Managing Water under Uncertainity and Risk." In. Paris: UNESC

CHAPTER 5: AN ANALYSIS OF PRECIPITATION ISOTOPE DISTRIBUTIONS ACROSS NAMIBIA USING HISTORICAL DATA

5.1 Introduction

Drylands are often defined on the basis of the ratio of mean annual precipitation to mean annual evaporative demand (UNEP and Thomas 1992, Ojima et al. 1993, Wang et al. 2012) and the aridity index (AI) is used to classify drylands as regions with AI < 0.65. Globally, they account for over 40% of the earth's terrestrial surface (Slaymaker and Spencer 1998) and are characterised by low and often seasonal rainfall resulting in permanent or seasonal soil water deficit (D'Odorico and Porporato 2006) and ephemeral drainage. Despite limitations to dryland productivity due to water scarcity (Louw and Seely 1982), they contribute approximately 40% of global net primary productivity (Grace et al. 2006) supporting more than 2 billion people worldwide (Gilbert 2011, MEA 2005). Global water resources are inherently related to and affected by population growth (Vörösmarty et al. 2000). 90% of the dryland population resides in developing countries which have an above average population density growth, exacerbating the already tight limitations imposed by water availability and food security on these systems (Wang et al. 2012). Therefore, there is a need to understand hydrological processes at both global and local scales to create an inventory of available water resources and encourage efficient management of these resources.

Stable isotopes ($\delta^{18}O$ and $\delta^{2}H$) in precipitation and groundwater are valuable environmental tracers that can be used to understand dynamics and processes in hydrology, geology, ecology and climate research (Stumpp et al. 2014, Gat 1996, Soderberg et al. 2013). Isotope fractionation processes impart unique signatures on meteoric water that can be combined with deuterium excess (*d*), a second-order isotope parameter defined as $d = \delta D - 8 \times \delta^{18}O$ (Dansgaard 1964) to determine vapour source origins and evaporative conditions (Merlivat and Jouzel 1979). Points that fall on the Global Meteoric Water Line (GMWL) have a constant *d* of 10‰ because rainout isotopic fractionation is considered an equilibrium process. Since the effect of equilibrium Rayleigh condensation processes roughly follows the GMWL slope of 8, variations in *d* can provide information about the environmental conditions (e.g., relative humidity and temperature) during non-equilibrium

processes in oceanic moisture source regions (Welp et al. 2012). Stable isotope hydrology is therefore based on interpreting isotope variations (δ^2H, $\delta^{18}O$ and *d*) in precipitation which are governed by the origins and conditions during cloud formation and rainout (Stumpp et al. 2014), thus the distribution of precipitation isotopes measured from a particular location reflect the local temperature, latitude and altitude (Clark and Fritz 1997, Friedman et al. 1964, Dansgaard 1964). The relationship between water isotope ratios, meteorological and geographical parameters allows for the production of regional and global isotopic landscapes - isoscapes (Bowen and Revenaugh 2003, Liu et al. 2010, Bowen and Wilkinson 2002b, Bowen and West 2008). These isoscapes enable the documentation and visualization of large-scale hydrological processes and provide point estimates. The examination of deviant values from the trend surface can highlight values that are unusual in their geographic context (Bowen and Revenaugh 2003). However, recent research suggests that *d* can be significantly altered by local processes and is thus not a true reflection (conservative tracer) of humidity at the source region as previously assumed (Welp et al. 2012, Lai and Ehleringer 2011, Zhao et al. 2014).

Understanding the spatio-temporal variation of precipitation patterns (isotopes) could provide further information on regional and global hydrologic processes that enable better planning and preparation for climate change (Sánchez-Murillo et al. 2013). The basis for most global isoscapes is the Global Network for Isotopes in Precipitation (GNIP) dataset, initiated by the International Atomic Energy Agency (IAEA) and the World Meteorological Organisation (WMO) in 1961. However, the dataset has a coarse spatio-temporal resolution in some areas and is also affected by station unevenness (West et al. 2014) resulting in insufficient data coverage for many regions that are of interest to hydrologists, geologists and ecologists (Wassenaar et al. 2009, Zhao et al. 2012). These inconsistencies in data continuity complicate efforts to evaluate seasonal and long-term trends in isotope distributions as accuracy and precision of geostatistical estimation is linked to data density. To overcome the temporal heterogeneity of data, studies have adopted the use of long-term average values rather than specific months or years thus greatly increasing the sampling density by integrating data across time (Bowen 2010). The integration of data over time is achieved via two methods: weighted by amount approach (Bowen and Wilkinson 2002a) which gives a measure of the net flux of isotopes to the land

surface (Bowen 2010) and the alternative unweighted approach (Dutton et al. 2005) used as a last resort when handling historical data and amounts are scarce or not reported. However, regardless the method applied, data aggregation although advantageous in some circumstances will inevitably cause data reduction and details of data reduction should be carefully considered as they could potentially introduce random or systematic error within the reduced data set (Bowen 2010).

Modelling of global hydrologic isoscapes has evolved over the years (Dutton et al. 2005, Bowen and Wilkinson 2002b, Terzer et al. 2013, Bowen and Wilkinson 2002a); however, each of these models suffers some degree of uncertainty due to dataset problems mentioned previously. Additionally, isotope ratios show a strong correlation with mean annual temperature in nontropical regions (Bowen and Wilkinson 2002b), and global isoscapes do not always work well in the tropics explaining 58-61% of the global isotopic variance in precipitation (Terzer et al. 2013). Furthermore, there is often a mismatch between observed isotope data and modelled results when models are downscaled especially in data deficient regions (e.g., Africa, Asia and the topics) (Terzer et al. 2013). Researchers have employed various strategies to reduce the mismatch between the observed data and model results at regional or country level. These approaches include constraining the geographical extent of the models and adding meteorological data as explanatory variables to improve interpolations at local scales (Liu et al. 2008, Liebminger et al. 2006, Lykoudis and Argiriou 2007, Terzer et al. 2013, IAEA 2015).

The Regionalised Cluster-based Water Isotope Prediction (RCWIP) model (IAEA 2015, Terzer et al. 2013) is a recent precipitation isoscape model which out performs traditional modelling approaches 67% of the time. However, the RCWIP model (IAEA 2015, Terzer et al. 2013) coverage is limited to specific regions thus for many regions we still have to rely on the fixed regression-interpolation models of global rainfall isoscapes such as the Bowen and Wilkinson model (Bowen and Revenaugh 2003, Bowen and Wilkinson 2002a). Spatial interpolation allows estimation of the isotopic composition of precipitation where data is not available by generating a smoothed trend surface that captures the geographic variability of the data. Therefore, despite the inherent problems of the GNIP dataset, improvements in model processing and data interpolation techniques make it a valuable resource and starting point to understanding hydrological isoscapes and

processes at a global scale. However, refinement of these models at a local scale is necessary especially in data scarce regions as these models may fail to capture important local trends due to the coarse resolution of the models.

The goal of this study is to develop precipitation isoscapes that reflect local meteorological and physical conditions of a typical arid environment (Namibia) based on historical data from different isotope studies and use the generated isoscapes to address the following questions: 1) what are the differences between the globally fitted isoscape (GFI) and our precipitation isoscape? 2) is there a coherent spatial pattern in precipitation isoscapes across Namibia and what are the mechanisms responsible for the spatial pattern?

5.2 Materials and Methods

5.2.1 Site description

Namibia is located on the south-western tip of the Southern African subcontinent. The country covers an area of over 825 000 km^2 but is represented by only two stations in the GNIP network. Its position is strongly influenced by the aridifying nature of the cold Benguela current and dry descending air of the Global Hadley Circulation which limits convectional rainfall throughout much of the country's interior (Thuiller et al. 2006, Eckardt et al. 2013). Namibia is officially classified as dryland (Morton and Anderson 2008), although climate varies from arid and semi-arid in the west to a more subtropical summer-rainfall climate in the north-east (Thuiller et al. 2006) (Fig. 5.1c). The hyper arid Namib Desert stretches over 2000 km, from southern Angola through Namibia into South Africa with a variable width (80 – 200 km) and gradual rise from the Atlantic coast to the foot of the Namib Escarpment (Goudie 2009). The Namib Escarpment runs north to south along the Atlantic coast and is characterised by a steep elevation gradient to over 2000 m (Fig. 5.1b). Fig. 5.1 shows the administrative geographical regions and some physical and meteorological parameters across Namibia.

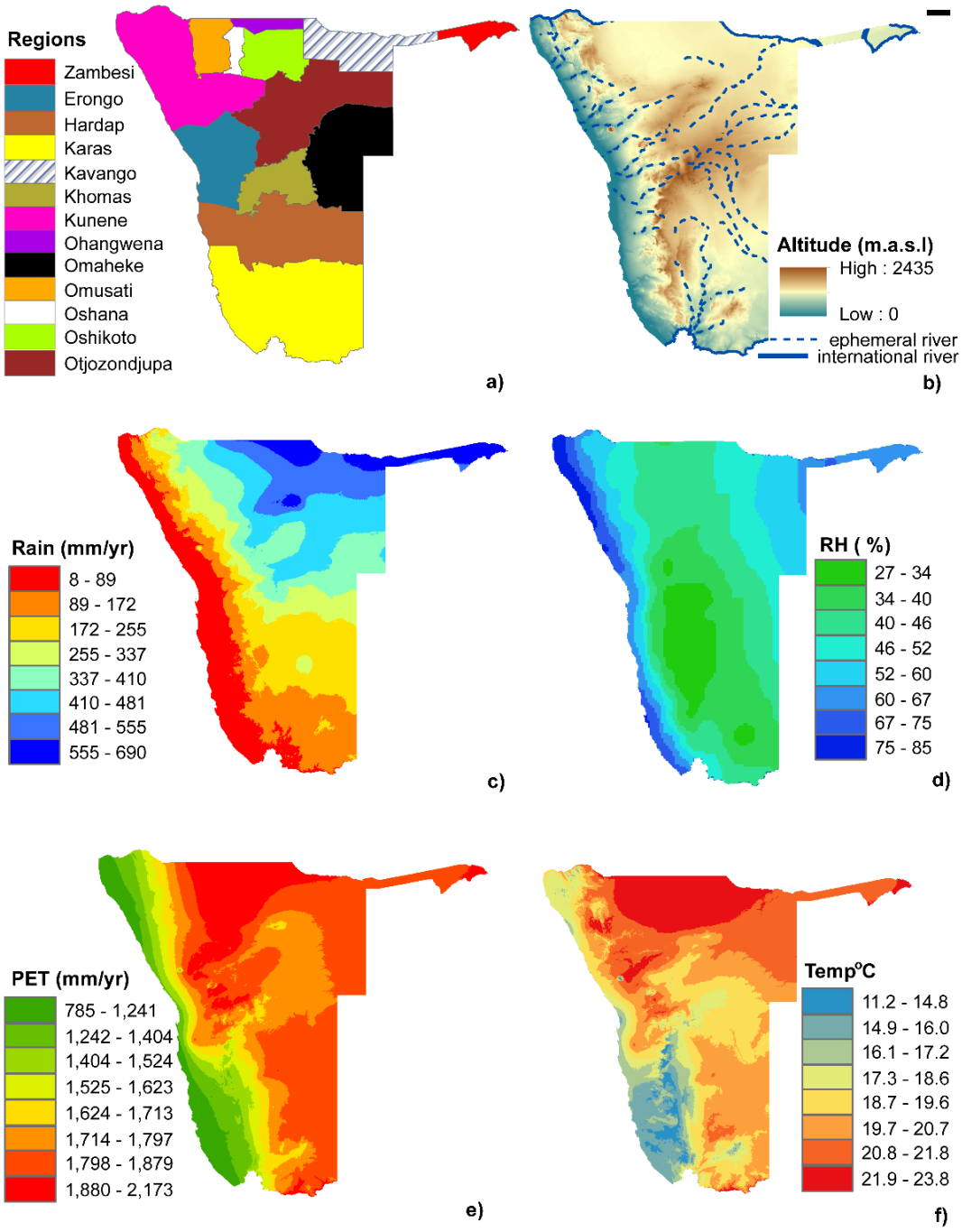

Figure 5. 1 Geographical and meteorological data for Namibia. (a) Namibia's administrative regions, (b) digital elevation model (DEM), (c) mean annual rainfall, (d) mean annual relative humidity (RH%), (e) mean annual potential evapotranspiration (PET) and (f) mean annual temperature.

5.2.2 $\delta^{18}O$ and $\delta^{2}H$ data sources and data processing

We compiled a database of rainfall isotopic studies conducted in Namibia from a literature review from 1960 – 2010 (Turewicz 2013). Additional isotopic data for the Central Namib Desert at Gobabeb Research Centre was collected from a 2014 field campaign, where samples were collected immediately after the rain event, stored in vials and analysed using laser spectrometery (SD 0.2 ‰ $\delta^{18}O$ and 1.1‰ $\delta^{2}H$) (Wang et al. 2009). We acknowledge discontinuity of the data and that the studies often differed in their scope and analysis methods but the fundamental principles remained constant. Data was and is reported in δ notation relative to VSMOW-SLAP scale defined as,

$$\delta‰ = \left(\frac{R_{sample}}{R_{standard}} - 1\right) x\ 10^{3} \qquad (1)$$

where R_{sample} and $R_{standard}$ are the molar ratios of heavy to light isotopes ($^{2}H/H$ or $^{18}O/^{16}O$) of the sample and standard.

Given the limited availability of isotopic data in this region, and that most of this historical data did not report rainfall amounts, we made an effort to integrate and conserve as much data as possible by adopting the unweighted approach (Dutton et al. 2005). Before adopting the unweighted approach, we discarded data when either $\delta^{18}O$ or $\delta^{2}H$ was not reported for a site or when geographic coordinates were not provided. Because the southern and south-eastern parts of Namibia were inadequately represented in the database, we incorporated data from nearby studies conducted in Botswana and South Africa to increase robustness of the database (Cape Town, Wolkop, Uitkyyk, Twatuin (Harris et al. 2010) and Lobastse (Talma and van Wyk 2013)). The final rainfall dataset consisted of 45 locations (40 in Namibia and 5 outside, Dataset C1).

5.2.3 Meteorological data

A matrix of physical and meteorological variables plausibly related to precipitation isotope ratios were obtained at 30 arc second raster resolution for these variables. These variables included: elevation, mean annual precipitation, mean annual temperature, minimum temperature, maximum temperature (worldclim.org), mean annual potential evapotranspiration (PET), Aridity Index (AI) (www.cgiar-csi.org/data/global-aridity-and-pet-database) and mean annual relative humidity (RH) (www.cru.uea.ac.uk/~markn/cru05/cru05_intro.html). Data from each of these raster

datasets was extracted for each of the 45 data points and we also calculated the straight-line distance from each data point to the Atlantic Ocean (Dataset C1).

5.2.4 Isoscape cokriging

Models were generated based on multiple regressions of location-based rainfall isotopes and associated physical and meteorological data followed by cokriging (interpolation) of the best performing models (West et al. 2014, Terzer et al. 2013). The meteorological and physical data extracted from the raster datasets were used as predictors for the isoscapes and we did not compute non-linear combinations with the exception of the multiplicative combination of elevation and distance to the coast as we expected significant interaction between the two (West et al. 2014). We performed exploratory regression of the data followed by ordinary least squares (OLS) regression which assessed the model residuals for normalcy, the major assumption of the statistical methods employed. The passing models were recalculated using geographic weighted regression analysis (GWR) to improve model performance and ranked using the Akaike Information Criterion (AICc). The AICc enables model selection by balancing r^2 and simplicity thus giving an estimate of the quality of the model.

We selected the top five models (Table 5.1) and looked for the highest ranking models that appeared in both $\delta^{18}O$ and $\delta^{2}H$, based on the AICc (highlighted in bold Table 5.1). Selection of the highest ranking models common to both $\delta^{18}O$ and $\delta^{2}H$ would ensure no strange artifacts when cokriging was done to produce the *d* isoscape (West et al. 2014) as *d* integrates $\delta^{18}O$ and $\delta^{2}H$. The highlighted models (Table 5.1) were then used in the ordinary cokriging interpolation to produce rainfall $\delta^{18}O$ and $\delta^{2}H$ isoscapes using ArcGIS 10.2.2 (Fig. 5.2a and Fig. 5.2c). The Gaussian kernel function (goodness of fit = 4.17) was used and anisotropy accounted for in the interpolation process, mean error (0.98), mean standardised error (0.37), root-mean-square-error (6.08), average-standard error (2.57). Because the root-mean-square-error is greater than the average-standard error, variability was likely under-estimated because spatial distribution of observations was uneven as determined by the availability of data. The *d* isoscapes (Fig. 5.2e and Fig. 5.2f) were calculated using the formula $d = \delta D - 8 \times \delta^{18}O$ (Dansgaard 1964) from the $\delta^{18}O$ and $\delta^{2}H$ isoscapes and were similar to those obtained from cokriging the best performing model

(Table 5.1). We then restricted the geographic extent of the precipitation cokriging isoscapes to Namibia after interpolation. We downloaded the RCWIP model (IAEA 2015, Terzer et al. 2013) and restricted it to the geographic extent of Namibia and according to the model, this portion actually represents a globally fitted isoscape (GFI). We thus made a side by side comparison of our precipitation cokriging isoscape to the GFI for the geographic extent of Namibia overlain with the observed precipitation isotope data (Fig. 5.2).

Table 5. 1 Model parameters and goodness of fit statistics for regression models of predictive environmental variables. The model selected for interpolation and generation of a predictive surface (cokriging) for rainfall isoscapes are indicated in bold.

Isoscape	Parameters			OLS Model			GWR Model		
				AICc	r^2	Rank	AICc	r^2	Rank
$\delta^{18}O$ rain	**elev. x coast**	**RH**		**215.5**	**0.34**	**1**	**214.7**	**0.36**	**1**
$\delta^{18}O$ rain	elev. x coast	PPT		222.1	0.24	4	216.2	0.38	2
$\delta^{18}O$ rain	PET	PPT		217.8	0.30	2	217.8	0.31	3
$\delta^{18}O$ rain	PET	RH		224.0	0.20	5	219.6	0.28	4
$\delta^{18}O$ rain	MT	RH	elev.	221.5	0.27	3	221.5	0.27	5
$\delta^{2}H$ rain	**elev. x coast**	**RH**		**397.8**	**0.33**	**3**	**392.6**	**0.43**	**2**
$\delta^{2}H$ rain	elev. x coast	PPT-PET	RH	392.5	0.42	1	392.4	0.42	1
$\delta^{2}H$ rain	PET	RH		394.1	0.38	2	394.1	0.38	3
$\delta^{2}H$ rain	PET	coast		395.9	0.35	4	395.4	0.36	4
$\delta^{2}H$ rain	MT	coast		398.0	0.32	5	1221.0	0.63	5

Note: PPT-PET – precipitation minus potential evapotranspiration; MAP – mean annual precipitation; RH – relative humidity, Elev. x coast – elevation x distance to coast; T – mean annual temperature; Elev. – elevation; PPT– mean annual precipitation; OLS – ordinary least regression; GWR – geographic weighted regression.

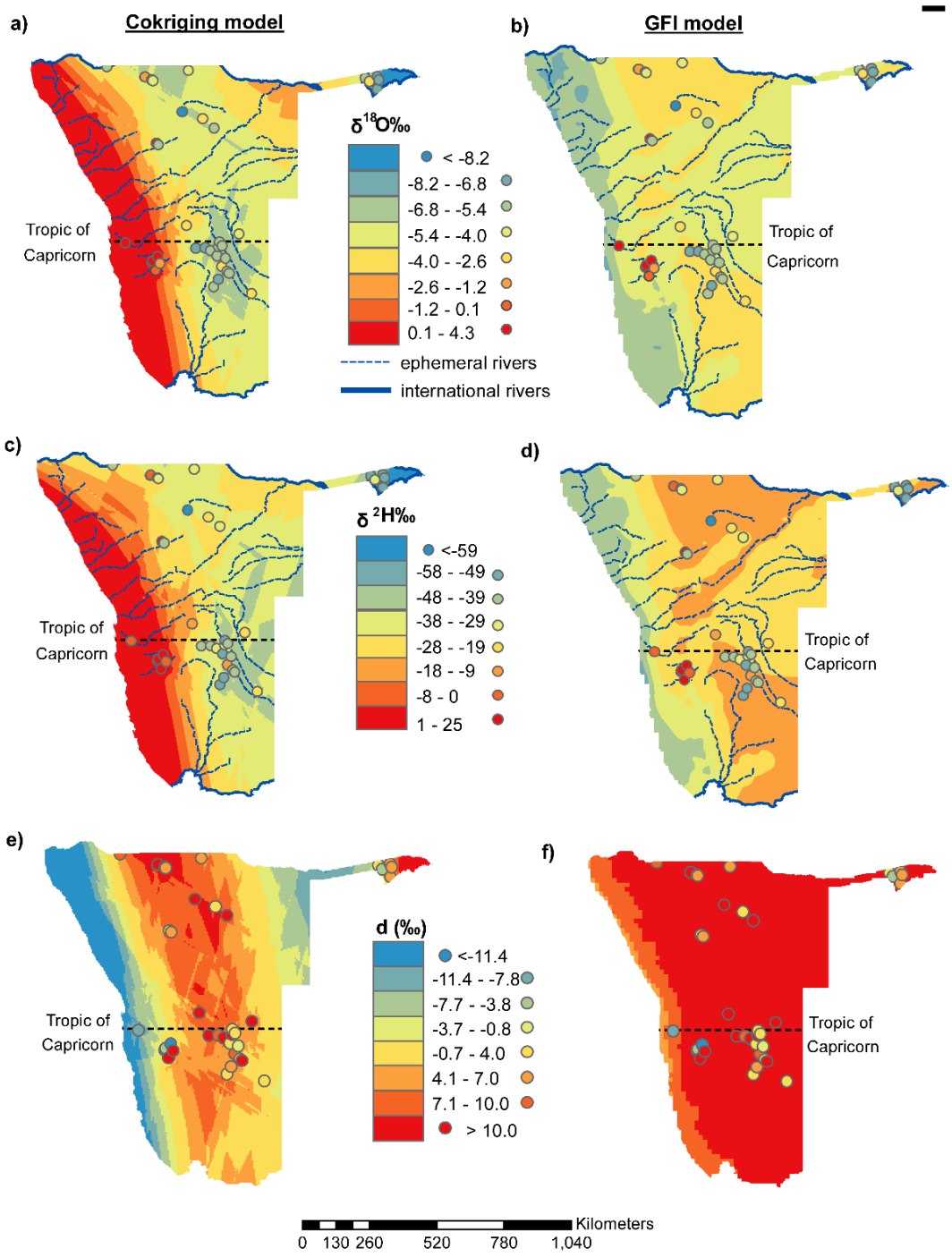

Figure 5. 2 Rainfall cokriging isoscapes and the globally fitted isoscape (GFI) overlain with observed data. (a) $\delta^{18}O$ cokriging isoscape, (b) $\delta^{18}O$ GFI, (c) $\delta^{2}H$ cokriging isoscape, (d) $\delta^{2}H$ GFI, (e) d-excess (*d*) cokriging isoscape, and (f) d-excess (*d*) GFI.

5.3 Results and Discussion

5.3.1 Cokriging models for rainfall isotopes across Namibia

Precipitation across terrestrial Southern Africa originates as vapour from the Indian and Atlantic Oceans (Van Wyk et al. 2011) and weather synoptics in this region are heavily influenced by the unique geomorphology and landmass orientation relative to the southern hemisphere's atmospheric system (Thomas and Shaw 1991). The influence of the Namibian geomorphology and landmass orientation on rainfall is evident by the dominance of elevation (Namib Escarpment) and distance from the Atlantic coast on the rainfall models. The two best-performing models out of the top five δ^2H and $\delta^{18}O$ precipitation models have the elevation and distance to the coast parameters (Table 5.1 and Fig. 5.1c) which suggests orographic rainfall patterns. The best performing model common to both δ^2H and $\delta^{18}O$ was selected to enable calculations of *d*, which would be affected if different models were used to calculate δ^2H and $\delta^{18}O$ isoscapes resulting in strange artifacts. The selected models used for cokriging are highlighted in Table 5.1 and shown in Fig. 5.2.

5.3.2 Comparison and interpretation of the cokriging and GFI isoscapes

5.3.2.1 Atlantic Ocean maritime vapour (Westerly winds)

The cokriging model predicts rainfall isotopic depletion in both $\delta^{18}O$ and δ^2H from several directions (Fig. 5.2) suggesting that rainfall across the Namibian landscape is influenced by several synoptic weather systems. The cokriging model predicts $\delta^{18}O$ and δ^2H enrichment along the west coast with progressive depletion inland (Fig. 5.2a and Fig. 5.2c). Rainfall isotopic gradients show a negative correlation with increasing distance from the vapour source due to progressive rainout also known as the 'continental effect' (Dansgaard 1964, Kazmierz Rozanski and Gonftanttni 1993, Ingraham and Taylor 1991). Therefore, the cokriging model suggests that some rainfall over terrestrial Namibia originates from the Atlantic Ocean and is progressively isotopically depleted as it moves inland (Fig. 5.2a and Fig. 5.2c).

Although the 'continental effect' could be used to explain the rainfall isotopic trend predicted by the cokriging model from the coast inland, the degree of isotopic enrichment predicted and observed along the west coast is extreme and could be indicative of secondary processes affecting the isotopic signature (Fig. 5.2a and Fig. 5.2c). Rain drops

can re-evaporate below the cloud if in disequilibrium with the surrounding atmospheric humidity and the resulting kinetic fractionation effects can lead to enrichment of $\delta^{18}O$ and $\delta^{2}H$ in the droplets (Ehhalt et al. 1963, Stewart 1975). Sub-cloud evaporation is common in short lived rain events where sub-cloud humidity does not achieve equilibrium with the falling droplets before the storm is over (Kendall and McDonnell 2012, Stewart 1975). According to the cokriging isoscape the most extreme enrichment in $\delta^{18}O$ and $\delta^{2}H$ rainfall isotopes is confined to the hyper-arid Namib Desert (Fig. 5.2a and Fig. 5.2c) where annual precipitation is variable, 50-100 mm in the south, 5-18 mm in the Central Namib and < 50 mm in the north (Eckardt et al. 2013). Low annual rainfalls suggest short-lived events which would create conditions that would be favourable for further isotopic enrichment due to sub-cloud evaporation hence the extreme degree of enrichment predicted and observed in the cokriging model and the observed isotopic values.

Rainfall in the Namib Desert is spatially and temporally variable although a general decreasing rainfall gradient east to west has been reported (Henschel and Seely 2008, Pietruszka and Seely 1985, Southgate et al. 1996, Lovegrove and Siegfried 1993). The isotopic range predicted by the cokriging model for the Namib Desert (0.1-4.3 ‰ $\delta^{18}O$ and 1-25‰ $\delta^{2}H$) probably reflects this gradient and the 'continental effect' (Fig. 5.2a and Fig. 5.2c). However, beyond the eastern edge of the Namib there is a narrow region of rapid isotopic depletion which coincides with the Namib Escarpment (Fig. 5.1b, Fig. 5.2a and Fig. 5.2c). The steep elevation changes from the Namib Desert to the Namib Escarpment cause orographic lift of the Atlantic maritime air mass resulting in orographic rainfall over the region. The west to east gradient extends beyond the Namib Desert to the interior Central Plateau (Eckardt et al. 2013) and this is captured by the cokriging model which shows continued $\delta^{18}O$ and $\delta^{2}H$ depletion over the Namib Escarpment (Fig. 5.2a and Fig. 5.2c).

5.3.2.2 Indian Ocean maritime vapour (Easterly winds)

The GFI model generally predicts a rainfall isotopic depletion gradient from east-west, with the most depleted values occurring along the Atlantic Coast in contrast to the cokriging model (Fig. 5.2b and Fig. 5.2d). Because the GFI predicts isotopic depletion from east-west, this suggests Indian Oceanic origins of the maritime vapour which is

progressively depleted and modified along its trajectory towards the Namibian coast due to rainout and evapotranspiration (Fig. 5.2b and Fig. 5.2d). Summer rainfall over Southern Africa is dominated by cold dry westerlies flowing over warm moist easterlies which create instability and thunderstorms over South Africa, central and southern Botswana and central and south-east Namibia (Williams et al. 1984). Furthermore, it has been indicated that at latitudes greater than 18°S in Namibia, most rainfall is supplied by the slow westward advance of tropical easterly disturbances peaking in February and March (Dyer and Marker 1978). However, these storms seldom reach the west coast bordered by the eastern edge of the Namib Escarpment and are thus confined to the Central Plateau (Eckardt et al. 2013) in contrast to the depictions of the GFI model predictions (Fig. 5.2b and Fig. 5.2d). This is because by the time the easterly winds get to the Namib Escarpment they would have lost most of their moisture as they advect over terrestrial Southern Africa resulting in warm, dry winds incapable of cloud formation and generating rain. Therefore the GFI model could be exaggerating the extent of the influence of the easterly winds on rainfall dynamics over Namibia (Fig. 5.2).

The cokriging model on the other hand, predicts a similar east-west depletion in both $\delta^{18}O$ and $\delta^{2}H$ precipitation signatures but differs from the GFI model in that the predicted isotopic depletion does not extend all the way to the coast (Fig. 5.2). According to the cokriging model, the Indian Ocean maritime vapour generated rainfall (convectional) exhausts before the Namib resulting in the most isotopically depleted rainfalls from this system occurring in the Khomas and central Hardap regions due to rainout effects (Fig. 5.2a and Fig. 5.2c). The resulting warm dry winds develop into berg winds as they continue on a westward trajectory into the Namib Desert where they supress the convectional rise of the underlaying cool humid Atlantic vapour advecting inland, preventing cloud formation and rain (von Willert 1992). This partially explains the low rainfall observed over the Namib Desert despite its close proximity to its rainfall vapour source, the Atlantic Ocean (Fig. 5.1c). The cokriging isoscapes also predict convergence of the westerly (orographic) and easterly (convectional) derived rainfall over the same areas in the Central Plateau resulting in the most isotopically depleted rainfall occurring in the Khomas and central Hardap regions (Fig. 5.2a and Fig. 5.2c). Therefore, according to the cokriging model convectional rainfall will not extend beyond these locations and vice versa for the

orographic rainfall, which is in agreement with an earlier study (Eckardt et al. 2013). Furthermore, observed rainfall isotopic values are similar to those predicted in the cokriging than the GFI model suggesting that the latter model could be overestimating the extent of the influence of the Indian Ocean on rainfall patterns in the Namib Desert (Fig. 5.2a and Fig. 5.2c).

5.3.2.3 Zaire Air Boundary (ZAB) and the Intertropical Convergence Zone (ITCZ)

Rainfall in the wetter northern parts of Namibia is associated with the southward migration of the Intertropical Convergence Zone (ITCZ) and the Zaire Air Boundary (ZAB) which extends to about 18^{o}S between January and February (Tyson 1986). This is defined as a convergence of tropical and subtropical circulation over central and southern Africa associated with convective activity, cloud formation and precipitation (Lindesay et al. 1998, Tyson and Preston-Whyte 2000). The ZAB system generates rainfall that extends into the northern parts of Namibia from Angola hence the high rainfall observed (Fig. 5.1c) and the depleted signatures in the Oshana, Oshikoto and Ohangwena regions which can be attributed to rainout effects (Dansgaard 1964) (Fig. 5.2a and Fig. 5.2c). Convergence of the ZAB and ITCZ during the austral summer generate rains that could be responsible for the north-east to south-west rainfall gradient across Namibia (Fig. 5.1c). These convective thunderstorms enter Namibia via the Kavango region hence the relatively enriched isotopic signature but this is not as enriched as that observed over the Namib Desert because kinetic fraction effects are minimised due to the higher rainfall (Fig. 5.1c). The rains decrease in a south-west direction which is reflected by the progressive radial depletion of the isotopic signatures predicted in the cokriging model (Fig. 5.2a and Fig. 5.2c). The most depleted signatures are observed in the Zambesi region and this can be attributed to the amount effect (Fig. 5.2a and Fig. 5.2c) as this region receives the highest rainfall in Namibia (Fig. 5.1c).

5.3.2.4 Tropical Temperate Troughs (TTTs)

The TTTs are considered as the dominant summer rainfall producing system over southern Africa (Reason et al. 2006, Mason and Jury 1997, Todd et al. 2004) accounting for about 39% of mean annual rainfall over the region (Harrison 1984). Tropical Temperate

Troughs link an easterly wave in the tropics to a westerly wave in the in the south (Lindesay et al. 1998) an event associated with a cloud band and precipitation (Todd et al. 2004). Development of a continental low over central southern Africa in late summer enhances low level westerly flow from western southern Africa at 10°S facilitating anomalous water vapour convergence over eastern southern Africa (Todd et al. 2004). This links with the TTT cloud band, such that the resulting rain extends further west over the region including Namibia than early summer (Todd et al. 2004). The cokriging isoscapes depict an area of isotopically depleted rainfall in a general northwest-southeast direction which could be reflecting the cloud band and resulting rainfall from the TTTs (Fig. 5.2a and Fig. 5.2c). The GFI model also appears to depict the influence of the TTTs over Namibia but in this case we observe isotopic enrichment in the northwest and southeast regions which does not match the observed data (Fig. 5.2b and Fig. 5.2d).

5.3.3 Modelled isotopic relationships

By extracting modelled isotopic values from both isoscapes we can investigate the classic isotope relations such as the 'continental' and 'amount' effects across the Namibian landscape (Fig. 5.3). The "amount effect" is the negative relationship between precipitation isotopes and the amount of precipitation (Dansgaard 1964) and is observable at intra-seasonal or longer timescales (Risi et al. 2008). Although the "amount effect' is predominately due to sub-cloud evaporation and the recycling of the sub-cloud vapour layer (Risi et al. 2008) combining the two gives the opportunity to evaluate our modelled relationships. Given that the cokriging isoscape suggests that some orographic rainfall across Namibia originates in the Atlantic in a general west-east direction (Fig. 5.2a and Fig. 5.2c), we modelled the 'continental effect' by calculating distance from the Atlantic Ocean to the extent of the Atlantic influence on rainfall isotopes as determined by the cokriging isoscape (Fig. 5.2a and Fig. 5.2c). Figure 5.3a shows a strong negative correlation ($r^2 = 0.93$, $p < 0.05$) between isotopic value and distance travelled inland from the Atlantic Ocean until the Central Plateau. This can be attributed to progressive rainout or 'continental effect' (Dansgaard 1964, Ingraham and Taylor 1991, Kazmierz Rozanski and Gonftanttni 1993), thus Fig. 5.3a supports the Atlantic origins of orographic rainfall over the western sections of Namibia as depicted in the cokriging isoscapes (Fig. 5.2a and

Fig. 5.2c). We did not consider the ‘continental effect’ from the Indian Ocean for the cokriging isoscape because the east-west rainfall isotope gradient extends to about 400 km in Namibia while distance to the Indian Ocean is over 1000 km. Therefore, the rainfall isotopic signature would certainly have been altered before reaching Namibia because of the distance involved (Lai and Ehleringer 2011, Welp et al. 2012).

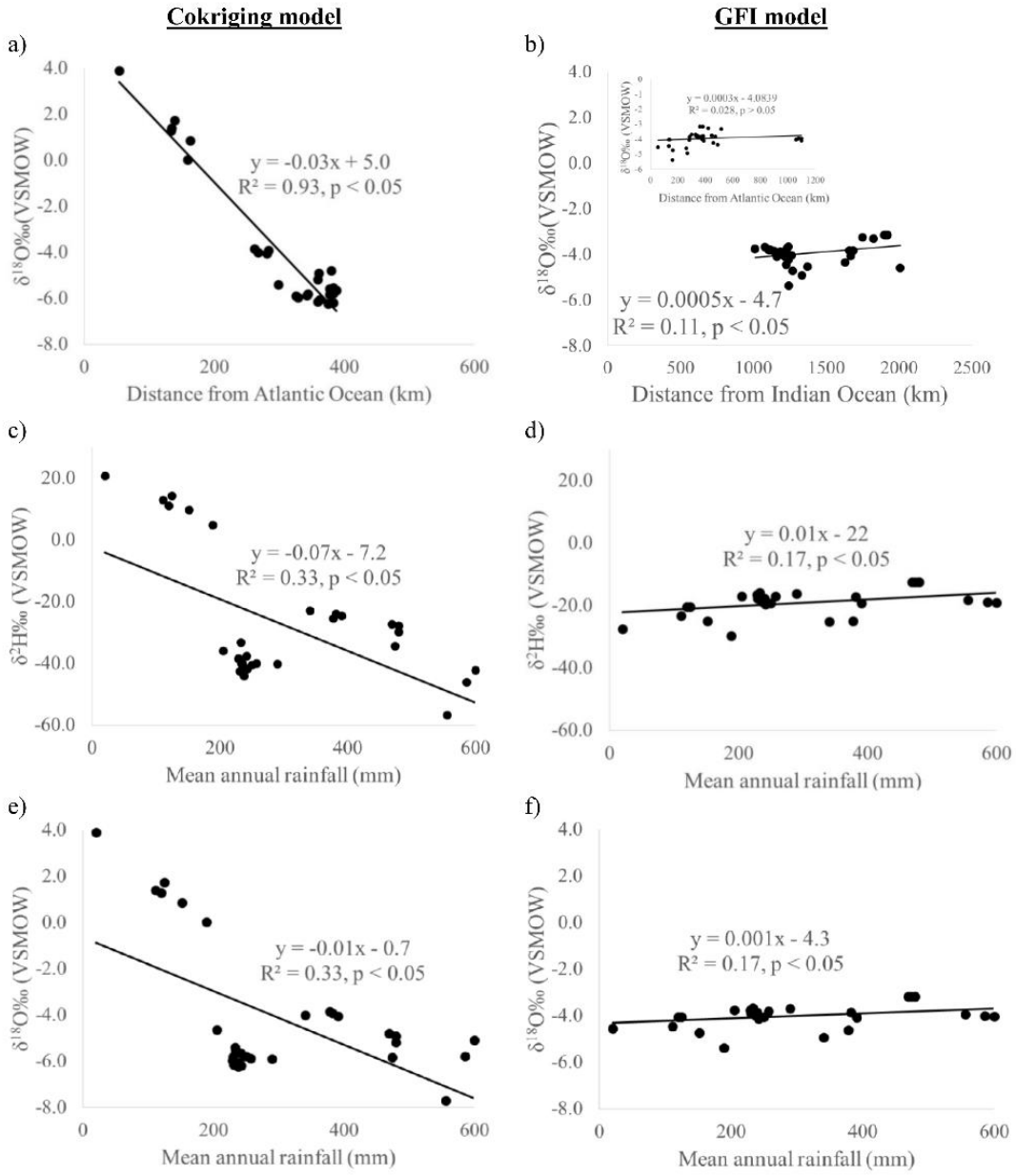

Figure 5. 3 Modelled rainfall isotope relationships with distance from coast (continental effect) and rainfall amount (amount effect) across Namibia. (a) $\delta^{18}O$ cokriging model 'continental effect', (b) $\delta^{18}O$ GFI model 'continental effect', (c) $\delta^{2}H$ cokriging model 'amount effect', (d) $\delta^{2}H$ GFI model 'amount effect', (e) $\delta^{18}O$ cokriging model 'amount effect', and (f) $\delta^{18}O$ GFI model 'amount effect'.

Given that the GFI model predicts a general east-west rainfall isotopic depletion gradient (Fig. 5.2b and Fig. 5.2d), we did not expect to observe the "continental effect"

from the Atlantic coast inland. The inset in Fig. 3b confirms that there was no significant correlation between rainfall isotopic signature and distance from the Atlantic coast ($p > 0.05$). We thus evaluated the 'continental effect' using the distance from the Indian Ocean for the GFI model (Fig. 5.3b). Figure 5.3b does not show the 'continental effect' instead showing a weak positive correlation ($r^2 = 0.11$, $p < 0.05$) between isotopic signatures and distance from the Indian Ocean. The 'continental effect' is not always pronounced even in regions with strong rainfall gradients en route as reported for the Amazon (Salati et al. 1979). This could be due to the return flux of moisture by transpiration and this invalidates the effect of rainout in subsequent rains further inland (Gat et al. 2001). However, in the case of the GFI model the 'continental effect' is masked or interrupted by the enrichment observed in the north and south central portions of Namibia probably related to the TTTs (Fig. 5.2b and Fig. 5.2d). Therefore, although we can observe a general east-west rainfall isotopic gradient on the GFI model, it is difficult to model the 'continental effect' from the Indian Ocean because of the influence of the TTTs and the distance involved which result in possible alterations of the isotopic signature.

Extracting the modelled isotopic values from both the cokriging and GFI models (Fig. 5.2) we evaluated the 'amount effect' (Fig. 5.3c - Fig. 5.3f). The cokriging model shows a negative correlation between rainfall isotopic signature and rainfall amount (Fig. 5.3c and Fig. 5.3e), the classic 'amount effect'. The GFI model on the other hand depicts the opposite trend, a positive correlation between isotopes and annual rainfall contrary to expectation (Fig. 5.3d and Fig. 5.3f). This suggests that the GFI model could be flawed in this region or could be reflecting convective precipitation which cannot be adequately explained by the 'amount effect' (Miyake 1968). In addition, the opposite slope in GFI models could be related to the insufficient representation of topography at local scale. For example, higher latitudes tend to have less precipitation and lower delta values and vice versa on an annual basis, an effect opposite to the amount effect. Therefore if the topography was not represented in sufficient detail, this latitude effect may mask the "amount effect".

5.3.4 D-excess, d

The *d* cokriging isoscape depicts extremely low values along the west coast of Namibia (Fig. 5.2e) and this could be related to the negative correlation between *d* and RH (Gat et al. 2003, Uemura et al. 2008, Pfahl and Sodemann 2014) (Fig. 5.1d). The high RH over the Namib Desert can be attributed to the frequent fog occurrences along Namibia's west coast (Olivier 1995) that penetrate to about 60 km inland (Hachfeld et al. 2000) and their dissipation downwind could result in the observed high RH beyond the fog zone. Meanwhile, the rainfall gradient decreases from east to west (Henschel and Seely 2008, Pietruszka and Seely 1985, Southgate et al. 1996, Lovegrove and Siegfried 1993) (Fig. 5.1c) contrary to the RH trend. Therefore, the low *d* over the Namib Desert could be due to the negative correlation between *d* and RH from the frequent fog and its dissipation in this area (Fig. 5.2e). At the same time, because $\delta^{18}O$ and $\delta^{2}H$ enrichment along the coast was attributed to sub-cloud evaporation (Fig. 5.2a and Fig. 5.2c) this also means the low *d* could be also attributed to sub-cloud evaporation of falling raindrops through an unsaturated air column (Dansgaard 1964, Ehhalt et al. 1963, Kazmierz Rozanski and Gonftanttni 1993) as $d = \delta D - 8 \times \delta^{18}O$ (Dansgaard 1964). Therefore, *d* in this area could be a result of the combined effects of RH (fog induced) and sub-cloud evaporation, depending on the prevailing conditions during the particular rainfall event.

The cokriging *d* isoscape also depicts extremely low values in the north eastern regions of Namibia (Kavango, Otjozondjupa and Omaheke) (Fig. 5.2e). Because these regions have a subtropical climate (Thuiller et al. 2006) and high rainfall (Fig. 5.1c), the prospects of sub-cloud evaporation are minimal. Therefore the low *d* values are unlikely caused by sub-cloud evaporation and they could be related to the negative correlation between *d* and RH (Gat et al. 2003, Uemura et al. 2008, Pfahl and Sodemann 2014). The high RH in this region is due to evapotranspiration from the abundance of vegetation, which are supported by the higher rainfall in this area (Fig. 5.1c and Fig. 5.1d). We, however, acknowledge the limited data in this region. Although both the $\delta^{18}O$ and $\delta^{2}H$ cokriging isoscapes generally agree and predict isotope enrichment in the north east region (Fig. 5.2), there could be isoscape digression undetectable in the individual isoscapes but amplified in the *d* isoscape (Fig. 5.2e). Thus, there is need for more field observations for some of the locations to attain a better prediction model.

There is large variability in *d* across the Central Plateau in the cokriging isoscape (Fig. 5.2e) and this can be attributed to the multiple sources of precipitation over this area as depicted in Fig. 5.2a and Fig. 5.2c. The GFI *d* model, on the other hand, although not showing variability in the Central Plateau and eastern parts of Namibia depicting $d > 10‰$ for these areas (Fig. 5.2f). This suggests either evaporation under low humidity or moisture recycling in the area (Martinelli et al. 1996, Gat and Matsui 1991). Therefore although different both *d* isoscapes demonstrate that *d* cannot be considered as a truly conservative tracer of environmental conditions at the vapour source as it could be significantly altered before the vapour arrives in Namibia (Lai and Ehleringer 2011, Welp et al. 2012, Zhao et al. 2014) and because there are multiple sources of rain for Namibia.

5.3.5 Rainfall isoscape validation

Because of the scarcity and quality (e.g., precipitation amounts were not reported) of data, apart from comparing the cokriging and GFI models to classic isotopic relationships as a means of evaluating the model performance, we also regressed unweighted observed isotopic values to the modelled data and compared the slope to the 1:1 line (Fig. 5.4) (Piñeiro et al. 2008). The observed $\delta^{18}O‰$ values ranged between -9.6‰ and +4.3‰ (mean = -4.4‰), while the cokriging model values ranged between -7.9‰ and +3.9‰ (mean = -4.5‰) and those of the GFI model ranged between -5.4‰ and -3.2‰ (mean = -4.0‰) (Fig. 5.4a). The observed $\delta^{2}H‰$ values ranged between -59‰ and +25‰ (mean = -30‰), while the cokriging model values ranged between -58‰ and +21‰ (mean = -30‰) and the GFI model values ranged between -30‰ and -13‰ (mean = -19‰) (Fig. 5.4b). The modelled cokriging values of both $\delta^{18}O‰$ and $\delta^{2}H‰$ explain a larger proportion of the linear variance in the observed values ($r^2 = 0.67$) in both cases compared to the GFI model ($r^2 = 0.17$ and 0.19 for $\delta^{18}O‰$ and $\delta^{2}H‰$, respectively, Fig. 5.4). The poor r^2 between predicted and observed values of the GFI model (Fig. 5.4) could be due to the fact that although the model was restricted to Namibia, it still reflected the global isotope distributions and not necessarily those specific to Namibia. We acknowledge the bias of the cokriging model towards the observed values because the model was not evaluated with an independent set of data because of data scarcity. However, the modelled cokriging values show expected large variations as the samples were collected from environmentally

and climatically diverse locations (Fig. 5.1 and Fig. 5.2) and closely follow the 1:1 line (Fig. 5.4). The modelled values from the GFI model on the other hand do not correlate well with either of the observed $\delta^{18}O‰$ and $\delta^{2}H‰$ values (Fig. 5.4) and do not show much variation despite the meteorological and physical differences in sampling locations (Fig. 5.1). This suggests that the GFI model values are not a realistic estimate of the observed local values.

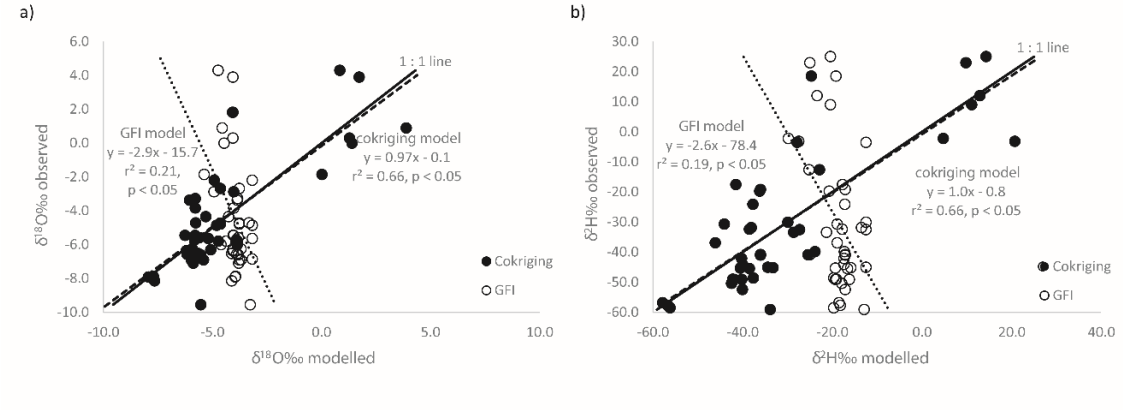

Figure 5. 4 Rainfall cokriging and globally fitted isoscape (GFI) model validation using the observed data. (a) $\delta^{18}O$ validation with 1:1 line as a reference; (b) $\delta^{2}H$ validation with 1:1 line as a reference.

We used the GMWL ($\delta^{2}H=8 \times \delta^{18}O +10$) (Craig 1961) to further validate our models. Because Namibia is classified as arid (Anderson et al. 2010) we expect its local meteoric water line (LMWL) to plot below the GMWL (slope < 8). We thus constructed a LMWL based on data from the two Namibian GNIP stations (GNIP_LMWL) which had a slope of 7.2 consistent with our predictions (Fig. 5.5). However, the GNIP_LMWL cannot be representative of the larger geographic area given that the data is from only two locations. Therefore, we calculated a second LMWL based on the observed data (Observed_LMWL) (slope 7.1), which was similar to the GNIP_LMWL with the only major difference being the intercept. However, the slopes point to some degree of aridity and this was similar to the modelled LMWL from the cokriging model (Fig. 5.5). The GFI_LMWL was almost identical to the long term weighted mean GMWL defined as $\delta^{2}H = 8.2 \times \delta^{18}O + 10.35$ (Kazmierz Rozanski and Gonftanttni 1993, Craig 1961) but different

from the Observed_LMWL. The GMWL (Kazmierz Rozanski and Gonftanttni 1993) is a weighted global average constructed from the GNIP database. Therefore, the modelled Namibian GFI_LMWL reflects the average isotopic composition of global meteoric waters and does not account for local variations even when scaled down to a smaller geographic area. We cannot determine how much lower the slope would be because Namibia has different eco-regions ranging from hyper-arid desert to more subtropical (Fig. 5.1) and the LMWL would intergrate these to provide an average which plots below the GMWL slope as that depicted by Observed_LMWL and the Cokriging_LMWL (Fig. 5.5).

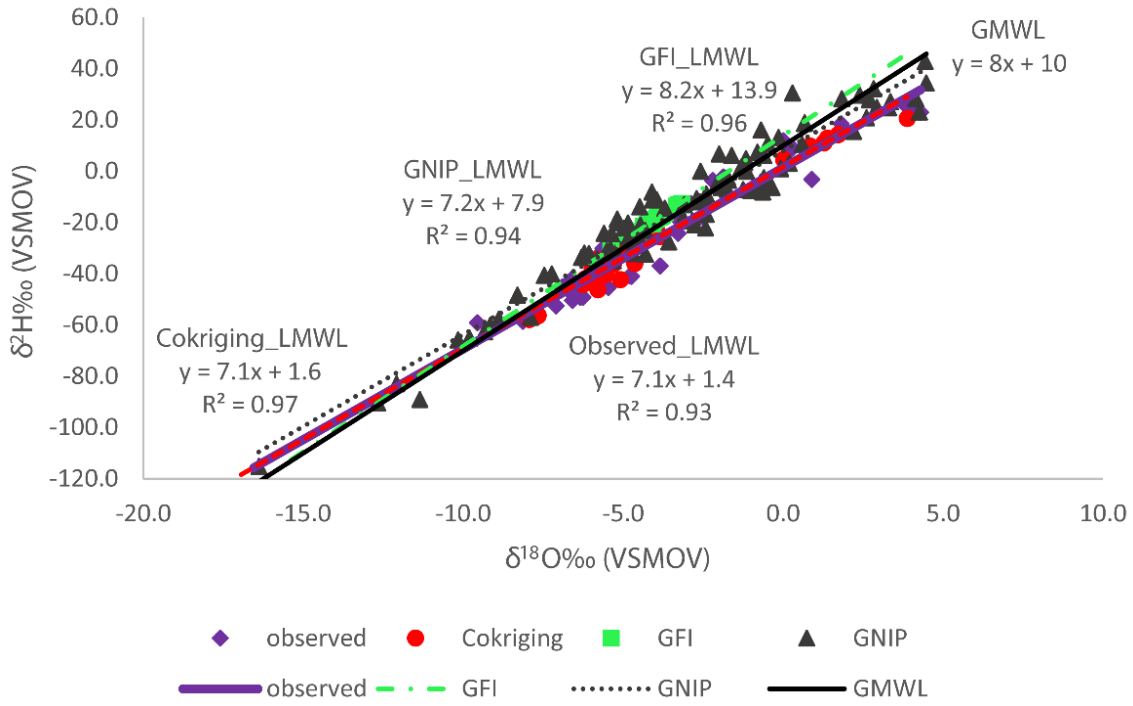

Figure 5. 5 Modelled local meteoric water lines (LMWL) compared to observation-based LMWL with the global meteoric water line (GMWL) shown as a reference.

The differences between the cokriging and global models can be quantified to show areas of similarity and dissimilarity (Fig. 5.6). The two models differ on their predictions of both $\delta^{18}O$ and $\delta^{2}H$ along the west coast varying by orders of magnitude 2-15‰ and 11-100‰ for $\delta^{18}O$ and $\delta^{2}H$, respectively (Fig. 5.6). These differences are largely because the two models exhibit different trends in this area with the cokriging model showing progressive rainfall isotopic depletion inland while the GFI model shows the opposite trend

hence the maximum difference is observed along Namibia's coast (Fig. 5.6). In the north east (Zambesi region) there is a difference of -6.8 to -11.8‰ for $\delta^{18}O$ between the models, which is also observed on the north central portions (Ohangwena and Oshikoto regions). The latter difference is because the cokriging model predicts depletion in this area due to rains originating from Angola along the TTTs while the GFI model predicts relatively enriched rains in the same area. Areas with ± 2‰ difference $\delta^{18}O$ can be considered as areas of similar isotopic composition while areas of ±10‰ difference in $\delta^{2}H$ similar in isotopic composition because the cokriging model uses unweighted averages while the global isoscape makes use of weighted averages (Fig. 5.6).

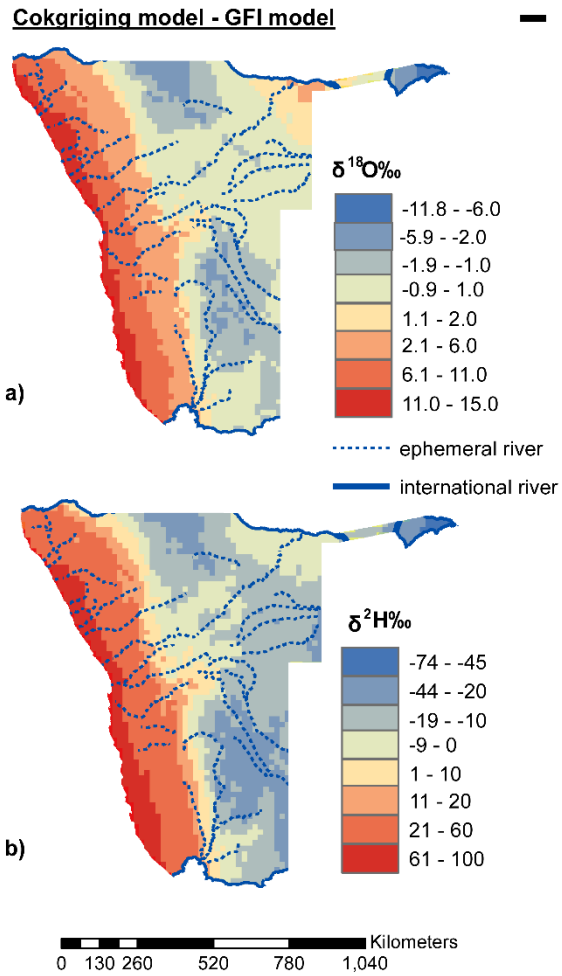

Figure 5. 6 Calculated differences between the cokriging model and the globally fitted isoscape (GFI) model.

5.4 Conclusions

Rainfall isotopes across Namibia show coherent spatial distribution patterns that can be modelled and interpreted as isoscapes. Although global isoscape models are useful in depicting global trends of isotopic distributions they do not scale-down well and fail to capture or account for local variations. These global isoscapes often do not take into account local geographical features or meteorological parameters which could influence local rainfall patterns leading to low correlations between observed and modelled data. The relevance of global rainfall isoscapes to hydrologically interesting but under-represented regions is thus questionable. Although not ideal, the unweighted cokriging approach showed stronger r^2 values with observed data (67 % vs. < 24 % for cokriging and GFI

models, respectively) and this could be attributed to the inclusion of elevational data which generated local geographic features (Namib Escarpment) that have a profound effect on rainfall patterns across Namibia. The rainfall cokriging isoscapes also show that rainfall in Namibia is influenced by several synoptic weather systems originating from both the Atlantic and Ocean Oceans while the GFI isoscape suggests origins from the Indian Ocean alone. Therefore, although the absolute values may be subject to improvements; the trends of the local isoscape models appear more consistent with the synoptic systems affecting rainfall patterns in Namibia and the unweighted approach could be considered a viable alternative especially when dealing with historical data in data deficient regions.

References

Anderson, Simon, John Morton, and Camilla Toulmin. 2010. "Climate change for agrarian societies in drylands: implications and future pathways." *Social dimensions of climate change: equity and vulnerability in a warming world*:199-230.

Bowen, G. J. 2010. "Statistical and geostatistical mapping of precipitation water isotope ratios." In *Isoscapes: understanding movement, pattern, and process on earth through isotope mapping*, edited by J. B. West, Bowen, G. J., Dawson, T. E., Tu, K. P., 139-160. New York: Springer.

Bowen, Gabriel J, and Jason B West. 2008. "Isotope landscapes for terrestrial migration research." *Terrestrial Ecology* 2:79-105.

Bowen, Gabriel J, and Bruce Wilkinson. 2002a. "Spatial distribution of $\delta^{18}O$ in meteoric precipitation." *Geology* 30 (4):315-318.

Bowen, Gabriel J., and Bruce Wilkinson. 2002b. "Spatial distribution of $\delta^{18}O$ in meteoric precipitation." *Geology* 30 (4):315-318. doi: 10.1130/0091-7613(2002)030<0315:sdooim>2.0.co;2.

Bowen, GJ, and J Revenaugh. 2003. "Interpolating the isotopic composition of modern meteoric precipitation." *Water Resources Research* 39:1299, doi:10.129/2003WR002086.

Clark, Ian D, and Peter Fritz. 1997. *Environmental isotopes in hydrogeology*: CRC press.

Craig, H. 1961. "Isotopic variations in meteoric waters." *Science* 133:1702-1703.

D'Odorico, P, and A Porporato. 2006. *Dryland Ecohydrology*. Dordrecht, Netherlands: Springer.

Dansgaard, W. 1964. "Stable isotopes in precipitation." *Tellus, 16*:436-468.

Dutton, Andrea, Bruce H Wilkinson, Jeffrey M Welker, Gabriel J Bowen, and Kyger C Lohmann. 2005. "Spatial distribution and seasonal variation in 18O/16O of modern precipitation and river water across the conterminous USA." *Hydrological Processes* 19 (20):4121-4146.

Dyer, TGJ, and ME Marker. 1978. "On the variation of rainfall over South West Africa." *South African Geographical Journal* 60 (2):144-149.

Eckardt, FD, K Soderberg, LJ Coop, AA Muller, KJ Vickery, RD Grandin, C Jack, TS Kapalanga, and J Henschel. 2013. "The nature of moisture at Gobabeb, in the central Namib Desert." *Journal of Arid Environments* 93:7-19.

Ehhalt, D, K Knott, JF Nagel, and JC Vogel. 1963. "Deuterium and $\delta^{18}O$ in rain water." *Journal of Geophysical Research* 68 (13):3775-3780.

Friedman, Irving, Alfred C Redfield, Beatrice Schoen, and Joseph Harris. 1964. "The variation of the deuterium content of natural waters in the hydrologic cycle." *Reviews of Geophysics* 2 (1):177-224.

Gat, Joel R, Willem G Mook, and Harm AJ Meijer. 2001. "Environmental isotopes in the hydrological cycle." *Principles and Applications UNESCO/IAEA Series* 2:63-67.

Gat, JR. 1996. "Oxygen and hydrogen isotopes in the hydrologic cycle." *Annual Review of Earth and Planetary Sciences* 24:225–262.

Gat, JR, B Klein, Y Kushnir, W Roether, H Wernli, R Yam, and A Shemesh. 2003. "Isotope composition of air moisture over the Mediterranean Sea: an index of the air–sea interaction pattern." *Tellus B* 55 (5):953-965.

Gat, JR, and E Matsui. 1991. "Atmospheric water balance in the Amazon Basin: an isotopic evapotranspiration model." *Journal of Geophysical Research: Atmospheres* 96 (D7):13179-13188.

Gilbert, Natasha. 2011. "United Nations considers creating advisory panel on land degradation akin to IPCC." *Nature* 477:262-264, doi:10.1038/477262a.

Goudie, Andrew. 2009. "Namib sand sea: large Dunes in an ancient desert." In *Geomorphological Landscapes of the World*, 163-169. Springer.

Grace, J., J. San José, P. Meir, H. S. Miranda, and R. A. Montes. 2006. "Productivity and carbon fluxes of tropical savannas." *Journal of Biogeography* 33:387–400, doi:10.1111/j.1365-2699.2005.01448.x.

Hachfeld, Berit, Norbert Jürgens, U Deil, and J Loidi. 2000. "Climate patterns and their impact on the vegetation in a fog driven desert: the Central Namib Desert in Namibia." Vegetation and climate. A selection of contributions presented at the 42nd Symposium of the International Association of Vegetation Science, Bilbao, Spain, 26-30 July 1999.

Harris, C , C Burgers, J Miller, and F Rawoot. 2010. "O- and H-isotope record of Cape Town rainfall from 1996 to 2008, and its application to recharge studies of Table mountian groundwater, South Africa." *South African Journal of Geology* 113:33-56

Harrison, MSJ. 1984. "The annual rainfall cycle over the central interior of South Africa." *South African Geographical Journal* 66 (1):47-64.

Henschel, Joh R, and Mary K Seely. 2008. "Ecophysiology of atmospheric moisture in the Namib Desert." *Atmospheric Research* 87 (3):362-368.

IAEA. 2015. "RCWIP (Regionalized Cluster-Based Water Isotope Prediction) Model – gridded precipitation $\delta^{18}O$ and $\delta^{2}H$ isoscape data. ." IAEA Accessed 03/04/2015. http://www.iaea.org/water.

Ingraham, Neil L., and Bruce E. Taylor. 1991. "Light stable isotope systematics of large-scale hydrologic regimes in California and Nevada." *Water Resour. Res.* 27 (1):77-90. doi: 10.1029/90wr01708.

Kazmierz Rozanski, Luis Araguas-Araguas, and Roberto Gonftanttni. 1993. "Isotopic Patterns in Modern Global Precipitation."

Kendall, Carol, and Jeffrey J McDonnell. 2012. *Isotope tracers in catchment hydrology*: Elsevier.

Lai, C. T., and J. R. Ehleringer. 2011. "Deuterium excess reveals diurnal sources of water vapor in forest air." *Oecologia* 165 (1):213-223.

Liebminger, Andreas, Georg Haberhauer, Wolfgang Papesch, and Gerhard Heiss. 2006. "Correlation of the isotopic composition in precipitation with local conditions in alpine regions." *Journal of Geophysical Research: Atmospheres (1984–2012)* 111 (D5).

Lindesay, JA, JE Hobbs, JA Lindesay, and HA Bridgman. 1998. "Present climates of southern Africa." *Cliamtes of the Southern Continents: Present, Past and Future. Wiley press, Ed. JE Hobbs, JA Lindesay y HA Bridgman* 297.

Liu, J., G. Fu, X. Song, S. P. Charles, Y. Zhang, D. Han, and S. Wang. 2010. "Stable isotopic compositions in Australian precipitation." *Journal of Geophysical Research D: Atmospheres* 115 (23).

Liu, Zhongfang, Lide Tian, Xurong Chai, and Tandong Yao. 2008. "A model-based determination of spatial variation of precipitation δ18O over China." *Chemical Geology* 249 (1):203-212.

Louw, Gideon, and Mary Seely. 1982. "Ecology of desert organisms."

Lovegrove, Barry, and Roy Siegfried. 1993. *The living deserts of southern Africa*: Fernwood Press.

Lykoudis, SP, and AA Argiriou. 2007. "Gridded data set of the stable isotopic composition of precipitation over the eastern and central Mediterranean." *Journal of Geophysical Research: Atmospheres (1984–2012)* 112 (D18).

Martinelli, Luiz Antonio, Reynaldo Luiz Victoria, Leonel Silveira Lobo Sternberg, Aristides Ribeiro, and Marcelo Zacharias Moreira. 1996. "Using stable isotopes to determine sources of evaporated water to the atmosphere in the Amazon basin." *Journal of hydrology* 183 (3):191-204.

Mason, SJ, and MR Jury. 1997. "Climatic variability and change over southern Africa: a reflection on underlying processes." *Progress in Physical Geography* 21 (1):23-50.

MEA. 2005. *Ecosystems and human well-being: desertification synthesis*. Washington, DC: World Resources Institute.

Merlivat, Liliane, and Jean Jouzel. 1979. "Global Climatic Interpretation of the Deuterium-18O Relationship for Precipitation." *J. Geophys. Res.* 84:5029-5033. doi: 10.1029/JC084iC08p05029.

Miyake, Y., Matsubaya, O., Nishihara, C. 1968. "An isotopic study on meteoric precipitation." *Pop. Meteor. Geophysics* 19:243-266.

Morton, John, and Simon Anderson. 2008. "Climate Change and Agrarian Societies in Drylands." Workshop on Social Dimensions of Climate Change. Washington DC: World Bank.

Ojima, Dennis S, Bjørn OM Dirks, Edward P Glenn, Clenton E Owensby, and Jonathan O Scurlock. 1993. "Assessment of C budget for grasslands and drylands of the world." *Water, Air, and Soil Pollution* 70 (1-4):95-109.

Olivier, Jana. 1995. "Spatial distribution of fog in the Namib." *Journal of Arid Environments* 29 (2):129-138.

Pfahl, S, and H Sodemann. 2014. "What controls deuterium excess in global precipitation?" *Climate of the Past* 10 (2):771-781.

Pietruszka, RD, and MK Seely. 1985. "Predictability of two moisture sources in the Namib Desert." *South African journal of science*.

Piñeiro, Gervasio, Susana Perelman, Juan P Guerschman, and Jose M Paruelo. 2008. "How to evaluate models: observed vs. predicted or predicted vs. observed?" *Ecological Modelling* 216 (3):316-322.

Reason, CJC, W Landman, and W Tennant. 2006. "Seasonal to decadal prediction of southern African climate and its links with variability of the Atlantic Ocean." *Bulletin of the American Meteorological Society* 87 (7):941-955.

Risi, Camille, Sandrine Bony, and Françoise Vimeux. 2008. "Influence of convective processes on the isotopic composition ($\delta^{18}O$ and δD) of precipitation and water vapor in the tropics: 2. Physical interpretation of the amount effect." *Journal of Geophysical Research: Atmospheres (1984–2012)* 113 (D19).

Salati, Eneas, Attilio Dall'Olio, Eiichi Matsui, and Joel R Gat. 1979. "Recycling of water in the Amazon basin: an isotopic study." *Water Resources Research* 15 (5):1250-1258.

Sánchez-Murillo, Ricardo, Germain Esquivel-Hernández, Kristen Welsh, Erin S Brooks, Jan Boll, Rosa Alfaro-Solís, and Juan Valdés-González. 2013. "Spatial and temporal variation of stable isotopes in precipitation across Costa Rica: An analysis of historic GNIP records." *Open Journal of Modern Hydrology* 2013.

Slaymaker, Olav, and Tom Spencer. 1998. *Physical geography and global environmental change*: Longman Harlow,, UK.

Soderberg, Keir, Stephen P. Good, Molly O'Connor, Lixin Wang, Kathleen Ryan, and Kelly K. Caylor. 2013. "Using atmospheric trajectories to model the isotopic composition of rainfall in central Kenya." *Ecosphere* 4 (3):art33. doi: 10.1890/ES12-00160.1.

Southgate, RI, P Masters, and MK Seely. 1996. "Precipitation and biomass changes in the Namib Desert dune ecosystem." *Journal of Arid Environments* 33 (3):267-280.

Stewart, Michael K. 1975. "Stable isotope fractionation due to evaporation and isotopic exchange of falling waterdrops: Applications to atmospheric processes and evaporation of lakes." *Journal of Geophysical Research* 80 (9):1133-1146.

Stumpp, C, J Klaus, and W Stichler. 2014. "Analysis of long-term stable isotopic composition in German precipitation." *Journal of Hydrology* 517:351-361.

Talma, AS, and E van Wyk. 2013. Rainfall and groundwater isotope atlas. In *The use of isotope hydrology to characterize and assess water resources in South(ern) Africa*, edited by Tamiru Abiye. South Africa: Water Research Commission.

Terzer, S, LI Wassenaar, LJ Araguás-Araguás, and PK Aggarwal. 2013. "Global isoscapes for δ 18 O and δ 2 H in precipitation: improved prediction using regionalized climatic regression models." *Hydrology and Earth System Sciences* 17 (11):4713-4728.

Thomas, David SG, and Paul A Shaw. 1991. *The Kalahari Environment*: Cambridge University Press.

Thuiller, Wilfried, Guy F Midgley, Greg O Hughes, Bastian Bomhard, Gill Drew, Michael C Rutherford, and Fian Woodward. 2006. "Endemic species and ecosystem sensitivity to climate change in Namibia." *Global Change Biology* 12 (5):759-776.

Todd, Martin C, Richard Washington, and Paul I Palmer. 2004. "Water vapour transport associated with tropical–temperate trough systems over southern Africa and the southwest Indian Ocean." *International Journal of Climatology* 24 (5):555-568.

Turewicz, Veronika. 2013. "Stable isotopes of waters in Namibia." BSc., Geology and Mineralogy, University of Cologne.

Tyson, Peter Daughtrey. 1986. *Climatic change and variability in southern Africa*: Oxford University Press, USA.

Tyson, Peter Daughtrey, and Robert A Preston-Whyte. 2000. *weather and climate of southern Africa*: Oxford University Press.

Uemura, Ryu, Yohei Matsui, Kei Yoshimura, Hideaki Motoyama, and Naohiro Yoshida. 2008. "Evidence of deuterium excess in water vapor as an indicator of ocean surface conditions." *Journal of Geophysical Research: Atmospheres (1984–2012)* 113 (D19).

UNEP, N Middleton, and D Thomas. 1992. "World Atlas of Desertification." *Edward Arnold, London*:15-45.

Van Wyk, E, GJ Van Tonder, and D Vermeulen. 2011. "Characteristics of local groundwater recharge cycles in South African semi-arid hard rock terrains-rainwater input." *Water SA* 37 (2):147-154.

von Willert, Dieter J. 1992. *Life strategies of succulents in deserts: with special reference to the Namib Desert*: CUP Archive.

Vörösmarty, Charles J., Pamela Green, Joseph Salisbury, and Richard B. Lammers. 2000. "Global Water Resources: Vulnerability from Climate Change and Population Growth." *Science* 289 (5477):284-288. doi: 10.1126/science.289.5477.284.

Wang, L, P D'Odorico, JP Evans, DJ Eldridge, MF McCabe, KK Caylor, and EG King. 2012. "Dryland ecohydrology and climate change: critical issues and technical advances." *Hydrology and Earth System Sciences* 16 (8):2585-2603.

Wang, Lixin, Kelly Caylor, and Danilo Dragoni. 2009. "On the calibration of continuous, high-precision $\delta^{18}O$ and $\delta^{2}H$ measurements using an off-axis integrated cavity output spectrometer " *Rapid Communications in Mass Spectrometry* 23:530-536. doi: 10.1002/rcm.3905.

Wassenaar, LI, SL Van Wilgenburg, K Larson, and KA Hobson. 2009. "A groundwater isoscape (δD, δ 18 O) for Mexico." *Journal of Geochemical Exploration* 102 (3):123-136.

Welp, Lisa R., Xuhui Lee, Timothy J. Griffis, Xue-Fa Wen, Wei Xiao, Shenggong Li, Xiaomin Sun, Zhongmin Hu, Maria Val Martin, and Jianping Huang. 2012. "A meta-analysis of water vapor deuterium-excess in the midlatitude atmospheric surface layer." *Global Biogeochem. Cycles* 26 (3):GB3021. doi: 10.1029/2011gb004246.

West, AG, EC February, and GJ Bowen. 2014. "Spatial analysis of hydrogen and oxygen stable isotopes ("isoscapes") in ground water and tap water across South Africa." *Journal of Geochemical Exploration* 145:213-222.

Williams, FR, RJ Renard, GH Jung, RD Tomkins, and RR Picard. 1984. Forecasters Handbook for the Southern African Continent and Atlantic/Indian Ocean Transit. DTIC Document.

worldclim.org. Accessed 23/02/2015. www.worldclim.org.

www.cgiar-csi.org/data/global-aridity-and-pet-database.

www.cru.uea.ac.uk/~markn/cru05/cru05_intro.html. Accessed 23/02/2015.

Zhao, L, Lixin Wang, X Liu, H Xiao, Y Ruan, and M Zhou. 2014. "The patterns and implications of diurnal variations in the d-excess of plant water, shallow soil water and air moisture." *Hydrology and Earth System Sciences* 18 (10):4129-4151.

Zhao, Liangju, Honglang Xiao, Maoxian Zhou, Guodong Cheng, Lixin Wang, Li Yin, and Juan Ren. 2012. "Factors controlling spatial and seasonal distributions of precipitation $\delta^{18}O$ in China." *Hydrological Processes* 26 (1):143-152. doi: 10.1002/hyp.8118.

CHAPTER 6: PRECIPITATION ORIGINS AND KEY DRIVERS OF PRECIPITATION ISOTOPE (^{18}O, ^{2}H, ^{17}O) COMPOSITIONS OVER WINDHOEK

6.1 Introduction

The climate of southern Africa, defined as the land area bound by the region 15°S–35°S; 12.5°E–42.5°E, is complex and involves the interaction of several factors that alternate in importance (Allan et al. 2003, Reason and Rouault 2002, Richard et al. 2000). Traditionally, Atlantic influences on southern African precipitation have been downplayed and this could be attributed to data paucity, lack of awareness of the complexities of the atmosphere-ocean coupling and associated tropical-extratropical interactions as well as perceptions that Atlantic influences were secondary to those from the Indian or Pacific Oceans (ENSO) (Reason et al. 2006). Therefore, precipitation over southern Africa has been associated with sea surface temperatures (SST) from the Indian Ocean (D'Abreton and Lindesay 1993, Reason and Mulenga 1999). However, there is growing consensus that the South Atlantic Ocean may play a significant role on climate in the region, although the exact influences are unknown (Reason et al. 2006). Given this uncertainty in moisture origins, it is not surprising that model estimates of precipitation over the region vary depending on a model's representation of the Angola Low, a regional circulation feature which can account for as much as 60% of the inter-model variability (Munday and Washington 2017). The ability to capture this ocean-atmospheric circulation feature might drive the disagreement between models. Therefore, despite the tight coupling between precipitation and society in southern Africa (Conway et al. 2015), our knowledge of precipitation patterns and their climate controls for the region are limited (Reason et al. 2006).

Stable isotopes of hydrogen and oxygen ($\delta^{2}H$ and $\delta^{18}O$) are unique environmental tracers that can be used to understand dynamics and processes in hydrology, geology, ecology and climate research (Gat 1996, Stumpp et al. 2014, Zhao et al. 2012). However, relatively few studies across Africa have applied stable isotopes of precipitation to climate research. Although global isoscapes reproduce reasonably well the global distribution of mean annual isotope contents of modern precipitation (Risi et al. 2010, Werner et al. 2011),

they do not explain observed seasonal or inter-annual variations at a regional or local scale (Field 2010, Lee et al. 2007, Risi et al. 2010, Schmidt et al. 2005, Vuille et al. 2003) and do not down-scale well in data scarce regions (Kaseke et al. 2016, Terzer et al. 2013). Furthermore, multi-scale influences on the isotopic composition of precipitation do not conform well to univariate regression analysis in mid-latitude and subtropical locations (Alley and Cuffey 2001, Fricke and O'Neil 1999, Sturm et al. 2010). However, event-scale studies capture day-to-day synoptic variation that may be lost or diluted in monthly samples (Liu et al. 2010, Noone and Simmonds 2002). Therefore, event-scale comparisons with aggregated data may help define underlying uncertainties in relationships between the isotopic composition of precipitation and climate variables (Soderberg et al. 2013).

The moisture that eventually becomes precipitation is derived primarily from the oceans and/or evapotranspiration from the terrestrial surface (Sjostrom and Welker 2009). Therefore, traditional approaches have suggested air-mass history may influence the isotopic composition of precipitation (Dansgaard 1964). In addition to δ^2H and $\delta^{18}O$, d-excess defined as $d = \delta^2H - 8 \times \delta^{18}O$ (Dansgaard 1964) has been used to determine evaporative conditions (Merlivat and Jouzel 1979). However, recent work suggests *d* may not be a true conservative tracer of evaporation conditions (Lai and Ehleringer 2011, Welp et al. 2012, Zhao et al. 2014). Until recently, it was assumed that $\delta^{17}O$ in precipitation did not carry any additional information to that of $\delta^{18}O$ (Angert et al. 2004). However, recent work indicates that $\delta^{17}O$-$\delta^{18}O$ is independent of temperature and can be used to differentiate fractionation processes (Angert et al. 2004, Kaseke et al. 2017). Therefore, $\delta^{17}O$-excess ($^{17}\Delta$), $^{17}\Delta = \delta'^{17}O - 0.528 \times \delta'^{18}O$, could be a conservative tracer of humidity changes at the vapour source origin and complement $\delta^{18}O$, δ^2H and *d* (Angert et al. 2004, Barkan and Luz 2007). In addition, air mass trajectories have been used to explain precipitation isotope variations in North America (Burnett et al. 2004, Sinclair et al. 2011, Sjostrom and Welker 2009), Europe (Baldini et al. 2010, Gat and Carmi 1970), Asia (Fudeyasu et al. 2011, Liu et al. 2011), Australia (Barras and Simmonds 2008, Barras and Simmonds 2009) and Africa (Lewis et al. 2010, Soderberg et al. 2013). However, despite the complexities of southern African climate, we are not aware of any studies that have investigated the influence of atmospheric trajectories on southern African precipitation isotope compositions. We are also not aware of any studies that have reported $\delta^{17}O$ values

in precipitation for the region. Using a four-year (2012-2016) precipitation dataset, the objectives of this study were thus to determine storm-to-storm isotopic variability and composition ($\delta^{18}O$, $\delta^{2}H$ $\delta^{17}O$) of precipitation in Windhoek (Namibia), identify the local controls of precipitation isotopes, apply trajectory analysis to determine vapour source origins and $\delta'^{17}O$-$\delta'^{18}O$ relationships to infer evaporation conditions at the source region. The observation period covered three drought years of which two occurred during the 2014-2016 El Niño Southern Oscillation (ENSO) event. This provided the opportunity to test whether novel $\delta'^{17}O$-$\delta'^{18}O$ techniques could be used to differentiate different types of droughts. We are not aware of any isotope studies that have done this, although a few have focused exclusively on isotope compositions and variability during ENSO events (Sánchez-Murillo et al. 2017).

6.2 Materials and Methods

6.2.1 Site description

Namibia is located on the south-western tip of the African continent and the study site (22.6137° S and 17.09753° E, elevation 1720 m a.s.l) is located in the capital, Windhoek (3 133km^2) (Fig. 6.1a). According to the Köppen Climate classification system, Windhoek is a hot semi-arid climate (*BSh*) characterised by hot wet summers and cool dry winters. Based on data from the Southern Africa Science Service Centre for Climate Change and Adaptive Land-use (SASSCAL) Windhoek weather station (22.5706° S and 17.0957° E, elevation 1722 m a.s.l), 2012-2016 had the following monthly meteorological characteristics: temperature range (-0.2–36.3°C), average temperature (20.7°C), relative humidity (RH) range (0.4-99.6%) and average RH (29.5%) (Fig. 6.1b and Fig. 6.1c). Because precipitation is highly seasonal and precipitation events are concentrated between October and April (Lu et al. 2016, Sturm et al. 2009), our analyses were based on the hydrologic year (October to September). Windhoek has not experienced any significant changes in precipitation intensity, frequency or total amount between 1998 and 2015 (Lu et al. 2016), and because the current study falls within this timeframe, results should be comparable to this relatively long-term study.

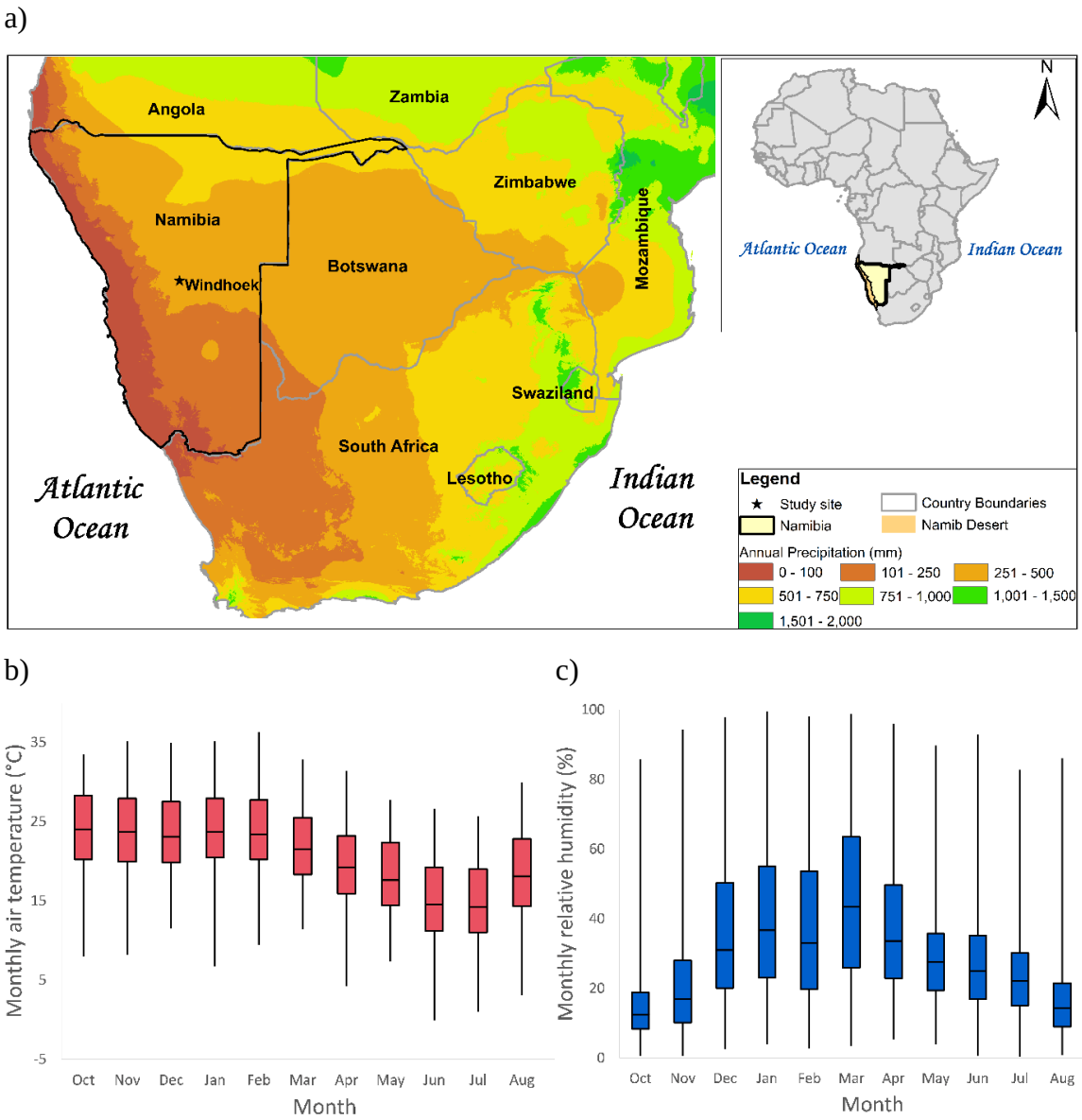

Figure 6. 1 a) Map showing regional mean annual precipitation, location of the study site and Namibia (insert) (http://www.worldclim.org/bioclim), b) monthly temperature and c) monthly relative humidity for Windhoek (2012-2016). Median represented by dark line in box, while box represents 1st and 3rd quartile range. Whiskers indicate the maximum and minimum values per month.

A total of 109 discrete precipitation events were sampled during the observation period (Dataset D1). These precipitation events were matched based on the date of sampling to the SASSCAL weather data which showed 138 events during this period. This

total excluded 42 precipitation events recorded by the SASSCAL weather station because there were less than 0.2 mm per day and may have resulted in either insufficient sample for analyses or were localised events that did not occur at the sampling site. When possible, samples were collected immediately after the event or the next morning from a manual rain gauge and transferred into 15 ml Qorpak clear French square bottles with black phenolic polycone lined caps. The bottles were labelled with the appropriate site name, date and amount and stored at 5°C at the University of Namibia (UNAM) Windhoek campus. Samples were stored for about 6 months and either shipped or retrieved during field campaigns and transported to Indiana University-Purdue University Indianapolis (IUPUI) Ecohydrology lab for isotope analysis.

6.2.2 Isotope analysis

Isotope analysis was performed using the Triple Water Vapor Analyzer coupled to the Water Vapor Isotope Standard Source (WVISS) (Los Gatos Research Inc., Mountain View, CA, USA) with a reported precision of 0.2‰ $\delta^{18}O$, 0.8‰ $\delta^{2}H$ and 0.4‰ $\delta^{17}O$ similar to those reported elsewhere (Tian 2016, Wang et al. 2009). Data was reported in δ notation relative to VSMOW-SLAP scale as

$$\delta = \left(\frac{R_{\text{sample}}}{R_{\text{VSMOW}}} - 1\right) \times 10^3, \qquad (1)$$

where R_{sample} and R_{VSMOW} are the molar ratios of heavy to light isotopes ($^{2}H/H$, $^{18}O/^{16}O$ or $^{17}O/^{16}O$) of the sample and international standard – Vienna Standard Mean Ocean Water (V-SMOW). However, it has been demonstrated that when dealing with high precision ratios in multiple systems a modified δ is preferred (Hulston and Thode 1965, Luz and Barkan 2005, Miller 2002) hereafter designated as δ' and defined as

$$\delta'^{*}O = \ln(\delta + 1) = \ln\left(\frac{R_{\text{sample}}}{R_{\text{VSMOW}}}\right), \qquad (2)$$

where *O is either ^{17}O or ^{18}O.

We computed mean annual isotopic composition as arithmetic and weighted means, adapted from Kazmierz Rozanski and Gonftanttni (1993):

$$\delta Annual\ weighted = \sum_{September}^{October} \delta\text{Event}\, X \frac{ppt_{(Event)}}{ppt_{(Annual\ Total)}}, \quad (3)$$

where $ppt_{(Event)}$ is the event precipitation amount and $ppt_{(Annual\ Total)}$ is the annual total precipitation amount as defined by the hydrologic year.

6.2.3 Local meteoric water lines (LMWLs)

Multiple statistical methods have been proposed to calculate the LMWL (Crawford et al. 2014). These methods include the unweighted and precipitation weighted versions of the ordinary least squares (OLSR), reduced major axis (RMA) and major axis (MA) regression models. However, because each method has its merits, we present all versions generated from the Local Meteoric Water Line Freeware programme (Crawford et al. 2014), based on event samples (Table D6.1). A long term LMWL (2012-2016) was calculated and used as a reference for the site for comparisons to annual LMWLs from the same period. For statistical comparisons, the unweighted OLSR LMWL (annual and inter-annual) was adopted to perform the analysis of covariance (ANCOVA). Similarly, annual $\delta'^{17}O$-$\delta'^{18}O$ lines were calculated based on the unweighted OLSR to complement interpretation of the $\delta^{18}O$-$\delta^{2}H$ LMWLs.

6.2.4 Precipitation classification: stratiform versus convective

Tropical Rainfall Measuring Mission (TRMM) 2A25 V7 and Global Precipitation Measurement (GPM) 2AKu band satellite data products covering the study area during 2012-2016 were downloaded and analysed. Because the sampling site was located roughly in the centre of Windhoek, the sampling site was taken as the centre of a 0.5° x 0.5° square centroid (3025 km^2) for data retrieval. The level 2 data products of TRMM and GPM have a temporal resolution of 16 orbits a day and a total of 24 satellite products showed precipitation over the area that corresponded to the Windhoek SASSCAL weather station. Data from both TRMM and GPM classify precipitation into three types: stratiform, convective and other. However, the third precipitation type 'other' was not encountered during our analyses and according to Aggarwal et al. (2016), it exists at higher levels and may not contribute significantly to precipitation near the surface. Therefore, for the purposes of this study we excluded the third classification. Average conditional precipitation rates were calculated for each event based on conditional stratiform and convective precipitation rates over the area. The stratiform fraction was defined as the ratio

of stratiform rainfall to total conditional precipitation rates. Therefore, stratiform fraction as applied to this paper translates to 0% stratiform = 100% convective except during non-precipitation days and vice-versa.

6.2.5 Trajectory analyses

Analysis of discrete precipitation events permits the use of back trajectory models to determine source origins and inference of source evaporation conditions that may influence the isotopic composition of precipitation when coupled with secondary parameters such as *d*. We assumed similar meteorological conditions between the site and the National Botanic Research Institute Windhoek (NBRI), located 5 km away. This enabled the use of hourly meteorological data from the SASSCAL weather station located at the NBRI. Using this approach, 99 of the 109 precipitation events (91%) at the site were consistent with NBRI data, sampling dates and general volumes, providing an approximation of local meteorological conditions. The associated meteorological data and event times were then used to calculate the approximate cloud base height of each individual storm based on the lifted condensation level (LCL) (Lawrence 2005, Romps 2017):

$$LCL = z + \left(20 + \frac{T-273.15}{5}\right)(100)(1 - RH), \quad (4)$$

where LCL is the cloud base height in metres, T is absolute temperature, RH is relative humidity ranging between 0 and 1 and z is the height where RH and T were measured.

Using LCL to determine the parcels origin height (n = 99), ten-day air mass back-trajectories were computed using the Hybrid Single-Particle Lagrangian Integrated Trajectory (HYSPLIT) model (Stein et al. 2015) and meteorological data from the Global Data Assimilation System (GDAS1). Because LCL ranged between 83 and 2154 m above ground level, no trajectories were disqualified for reaching the top of the atmosphere. Global estimates for mean atmospheric moisture residence times range from 4 – 9 days (Läderach and Sodemann 2016, Trenberth 1998), while Miralles et al. (2016) estimates an optimal 6 day residence time for the Kalahari ecoregion. The average time for each trajectory from land intersection to Windhoek was about 140 hrs (~6 days), thus trajectory cluster analysis time was set at 140 hrs at six hour intervals. The total spatial variance (TSV) for this process was 30%, indicating there was no forcing and misclassification of

cluster trajectories (Stein et al. 2015). Trajectory analyses in this study were used primarily to provide the spatial history of an air parcel.

6.2.6 Statistical analyses

Statistical analyses were performed in PAST 3 (Hammer 2001) with parametric methods for normally distributed data and non-parametric methods for non-normally distributed data. Multiple linear regression analyses were performed in XLSTAT 2017 v 4, while trajectory cluster analysis was performed in HYSPLIT (Stein et al. 2015). All data pertaining to this study is provided as Dataset D1.

6.3 Results and discussion

6.3.1 Precipitation anomalies

Three of the four years under observation received below normal precipitation amounts and were classified as meteorological droughts, with the exception of 2013-2014 (Fig. 6.2 and Table D6.2). Based on the Oceanic Niño Index (ONI) (CPC 2016), two of the three drought years (2014-2015 and 2015-2016) occurred during weak and strong El Niño years, respectively (Fig. D6.1). Given the well documented effects of ENSO on southern African precipitation (i.e., decrease in precipitation amount) (Allan et al. 2003, Nicholson and Entekhabi 1986, Reason and Rouault 2002), the 2014-2015 and 2015-2016 meteorological droughts could be El Niño related. However, the 2012-2013 meteorological drought occurred during an El Niño neutral year suggesting that the cause of this drought was different from that of the 2014-2016 droughts (Fig. 6.2, Table D6.2 and Fig. D6.1). Precipitation was highly seasonal over the sampling period with 89.4 – 99.5% of annual precipitation occurring during the rainy season, Oct-Apr (Table D6.3). About 55% of the annual precipitation in Windhoek occurs between Feb-Apr (late summer), with peak rainfall amounts and largest inter-annual variability occurring in February (Lu et al. 2016). However, according to the data presented here, with the exception of 2013-2014, less than 50% of annual precipitation occurred during late summer, suggesting droughts resulted in precipitation distribution anomalies over the area (Table D6.3). Consequently, peak rainfall amounts differed among the years: March for 2012-2013, February for 2013-2014 and January for 2014-2015 and 2015-2016. Interestingly, most precipitation during 2012-2013

occurred during late summer while for 2014-2015 and 2015-2016 this occurred during early summer (October - January; Table D6.3). This difference in precipitation distribution among the drought years also suggests that the causes of these droughts, 2012-2013 and 2014-2016, were different with the 2012-2013 drought being the most severe (Fig. 6.2 and Table D6.2).

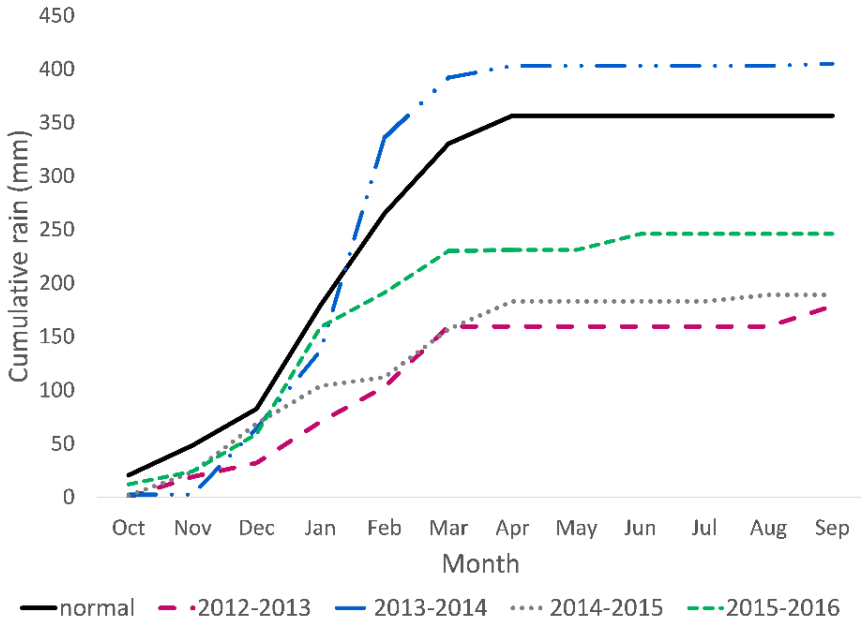

Figure 6. 2 Annual cumulative precipitation totals measured from the site for Windhoek 2012-2016 (Oct-Sept) compared to long-term average 'normal' precipitation from the Namibia Meteorological Services.

6.3.2 Precipitation isotope ($\delta^{18}O$, $\delta^{2}H$ and $\delta^{17}O$) variations

The long-term "2012-2016" weighted precipitation isotope compositions from this study (Table 6.1) were comparable to those from Kazmierz Rozanski and Gonftanttni (1993) ($\delta^{18}O$ -5.0‰) and the Online Isotopes in Precipitation Calculator (OIPC) ($\delta^{18}O$ -5.2‰ and $\delta^{2}H$ -27.0‰) (Bowen 2017, Bowen and Revenaugh 2003). Similarly, the unweighted precipitation isotope compositions were comparable to those extracted from the Namibia precipitation isoscape ($\delta^{18}O$ -2.9‰ and $\delta^{2}H$ -12.6‰) (Kaseke et al. 2016) and Kazmierz Rozanski and Gonftanttni (1993) ($\delta^{18}O$ -2.7‰) (Table 6.1). Therefore, the precipitation isotope results presented in this study are consistent with long term data presented elsewhere, thus comparisons of event scale with aggregated data may help define

underlying uncertainties between isotopic compositions and climatic variables at longer time scales (Soderberg et al. 2013).

Storm-to-storm isotopic variability over the four year period, $\delta^{18}O$ 25‰, $\delta^{2}H$ 180‰ and $\delta^{17}O$ 13‰, was similar to that reported elsewhere (Benson and Klieforth 1989, Friedman et al. 2002, Liu et al. 2010) (Table 6.1). However, at annual scales storm-to-storm isotopic variation was lower for the meteorological drought years while those for the 'normal year' 2013-2014 were similar to the four year overall isotopic variability (Table 6.1). The 2013-2014 precipitation was significantly depleted in $\delta^{18}O$, $\delta^{2}H$ and $\delta^{17}O$ (-5.97‰, -42.44‰, -3.14‰) compared to 2012-2013 (+0.94‰, +9.51‰, +0.48‰), 2014-2015 (-0.41‰, +1.73‰, -0.33‰) and 2015-2016 (-1.13‰, -5.36‰, -0.61‰) (One-way ANOVA, $p < 0.05$; Tukey's post-hoc test, $p < 0.05$) (Table 6.1). This could be attributed to the 'amount effect' (Dansgaard 1964), as both annual weighted and arithmetic mean precipitation isotope ($\delta^{18}O$, $\delta^{2}H$ and $\delta^{17}O$) values were significantly inversely related to precipitation amount ($p < 0.05$, Fig. D6.2). One aspect of the 'amount effect' that could be important is sub-cloud evaporation (Salamalikis et al. 2016). In theory, drought conditions should enhance sub-cloud evaporation resulting in precipitation enrichment ($\delta^{18}O$, $\delta^{2}H$ and $\delta^{17}O$), lower ranges and lower *d* compared to normal years (Table 6.1). However, *d* was similar among the years (Kruskal Wallis, $p > 0.05$) (Table 6.1) and also similar between the normal (+7.5‰) and drought years (+7.1‰) (Mann Whitney Pairwise test, $p > 0.05$), suggesting that the degree of sub-cloud evaporation during droughts and normal years at this semi-arid site may not differ significantly.

Theoretically, longer travel times would allow for more equilibration time of raindrops with sub-cloud vapour (isotopic exchange) and sub-cloud evaporation resulting in higher $\delta^{18}O$, $\delta^{2}H$ and $\delta^{17}O$ values and lower *d* (Table 6.1). As expected, the median LCL for precipitation events during 2013-2014 (361 m) was significantly lower than that of the drought years (580 m) (Mann Whitney U, $p < 0.005$), indicating longer raindrop travel times from cloud base to the ground surface during droughts. To evaluate the degree of aridity effects between normal and drought years, *d* of drought and normal year precipitation events with LCL between 300 and 600 m (based on the median LCL) was evaluated. The *d* of drought year precipitation events (+10.2‰, range: -8.3‰ to +18.6‰) was significantly larger than for the normal year (+6.8‰, range: -5.2‰ to +15.4‰) (Mann

Whitney Pairwise test, $p < 0.05$), suggesting that some other mechanism maybe influencing *d* within this bin and this could be attributed to enhanced moisture recycling during droughts in the Kalahari ecoregion. Although the Kalahari ecoregion experiences a volumetric decrease in precipitation during droughts, it is accompanied by an increase in the recycling ratio (28% vs. 34% during wet and drought years), defined as the terrestrially derived precipitation divided by the total precipitation (Miralles et al. 2016). In the Amazon Basin, evaporation (E) accounts for about 40% of the evapotranspiration (ET) flux and the resultant precipitation is characterised by $d > +10‰$, suggesting a significant part was derived from evaporation (Gat and Matsui 1991, Martinelli et al. 1996, Victoria et al. 1991). This might explain the precipitation events with $d > +10‰$ observed in this study (Table 6.1). Therefore, the larger *d* during drought years (+10.2‰) in the 300-600 m LCL bin suggests an increase in the evaporative flux due to moisture recycling, indicating drier conditions for the region compared to the normal year (+6.8‰), whose *d* was probably influenced more by sub-cloud evaporation.

Table 6. 1 Annual weighted and arithmetic mean isotope ($\delta^{18}O$, $\delta^{2}H$ and $\delta^{17}O$) compositions of Windhoek precipitation (2012-2016) based on the hydrologic year, Oct-Sept.

		Mean $\delta^{18}O$‰			Mean $\delta^{2}H$‰			Mean $\delta^{17}O$‰			Mean *d*‰	
Time	**n**	**Ath**	**WA**	**Range**	**Ath**	**WA**	**Range**	**Ath**	**WA**	**Range**	**Ath**	**Range**
a	26	+0.94	-1.83	-9.74 - +7.36	+9.51	-7.55	-60.11 - +57.36	+0.48	-0.96	-5.36 - +4.03	+2.0	-18.9 - +18.6
b	37	-5.97	-9.03	-15.84 - +8.30	-42.44	-63.99	-122.19 - +51.98	-3.14	-4.76	-8.24 - +4.12	+5.3	-17.3 - +15.4
c	19	-0.41	-3.19	-9.80 - +9.31	+1.73	-15.48	-71.10 - +56.00	-0.33	-1.76	-5.38 - +4.69	+5.0	-36.2 - +19.8
d	27	-1.13	-2.83	-12.39 - +7.92	-5.36	-14.39	-85.29 - +48.21	-0.61	-1.46	-6.43 - +4.10	+3.6	-32.3 - +14.9
e	**109**	**-2.15**	**-5.17**	**-15.84 - +9.31**	**-13.16**	**-33.00**	**-122.19 - +57.36**	**-1.16**	**-2.73**	**-8.24 - +4.69**	+4.0	**-36.2 - +19.8**

Note: a is 2012-2013, b is 2013-2014, c is 2014-2015, d is 2015-2016, e is 20-2016,

Ath. is arithmetic mean and WA is weighted average

6.3.3 Key local drivers of precipitation isotope compositions

Precipitation isotopes are governed by several factors including but not limited to evaporation processes at the source, precipitation type and subsequent rain-out processes along the air mass-trajectory; however, correlations with local meteorological parameters suggest possible modification at the precipitation site (Coplen et al. 2015, Dansgaard 1964, Fudeyasu et al. 2011, Rindsberger et al. 1983, Salamalikis et al. 2016, Yurtsever 1975). The Windhoek precipitation isotope data at both event and monthly scales, exhibited significant relationships with local meteorological conditions (Table 6.2 and Table D6.4, respectively). Whereas event-scale precipitation isotopes were related to more local meteorological parameters than monthly isotopes (6 parameters vs. 3 parameters), suggesting loss of information on individual events through data aggregation (Noone and Simmonds 2002), these relationships were stronger at monthly scale (Risi et al. 2008, Vimeux et al. 2005, Wu et al. 2015). Therefore, event-scale comparisons with aggregated data will help define underlying uncertainties in relationships between isotopic composition of precipitation and climatic variables (Soderberg et al. 2013).

Table 6. 2 Significant relationships between event precipitation isotopes ($\delta^{18}O$, $\delta^{2}H$, $\delta^{17}O$ and *d*) and local meteorological data from the National Botanic Research Institute (NBRI), Windhoek 2012-2016.

	Regression equation	r	r^2	p-value
$\delta^{18}O$	y = -0.24 * (relative humidity) + 15.12	-0.63	0.39	**
	y = 0.01 * (lifted condensation level) - 8.79	0.61	0.37	**
	y =-0.25* (precipitation amount) - 0.03	-0.42	0.18	**
	y = 0.39 * (surface temperature) - 13.47	0.29	0.08	**
	y = 1.11* (wind speed) - 6.37	0.24	0.06	*
	y =0.56 * (air temperature) - 13.27	0.24	0.06	*
$\delta^{2}H$	y = -1.56 * (relative humidity) + 98.22	-0.56	0.31	**
	y = 0.06 * (lifted condensation level) - 55.44	0.54	0.29	**
	y = -1.69 * (precipitation amount) + 1.23	-0.39	0.15	**
	y =8.62(wind speed) - 45.29	0.26	0.07	*
	y = 2.47(surface temperature) - 83.02	0.25	0.06	*
$\delta^{17}O$	y =-0.13(relative humidity) + 7.86	-0.62	0.39	**
	y = 0.005 (lifted condensation level) - 3.71	0.61	0.37	**
	y = -0.13(precipitation amount) - 0.06	-0.42	0.18	**
	y = 0.21(surface temperature) - 7.06	0.29	0.08	**
	y =0.58(wind speed) - 3.37	0.24	0.06	*
	y =0.29(air temperature) - 6.94	0.24	0.06	*
d	y = -0.21 (lifted condensation level) + 14.89	-0.68	0.47	**
	y = 0.40(relative humidity) - 22.71	0.68	0.47	**
	y = -1.78(air temperature) + 38.97	0.50	0.28	**
	y = 0.34(precipitation amount) + 1.49	0.40	0.16	**
	y = -0.73(surface temperature) +24.76	-0.37	0.14	**

Note: * denotes significance at $p < 0.05$ and ** denotes significance at $p < 0.005$.

According to event-scale univariate analyses, the most significant local drivers of precipitation isotopes ($\delta^{18}O$, $\delta^{2}H$ and $\delta^{17}O$) in decreasing order were RH, LCL, precipitation amount, surface temperature, average wind speed and air temperature (Table

6.2). Precipitation isotopes were inversely related to RH, which reflected the influence of sub-cloud evaporation on isotopic composition (Berkelhammer et al. 2012, Salamalikis et al. 2016) (Table 6.2). This result was consistent with the Namibia precipitation isoscape that identified RH as a key driver of precipitation isotopes across Namibia (Kaseke et al. 2016). Precipitation isotopes were positively related to LCL and this could be attributed to the raindrop travel time between the cloud base and ground surface, the longer this was the more time available for raindrop isotopic equilibration with sub-cloud vapour and sub-cloud evaporation (Salamalikis et al. 2016, Sánchez-Murillo et al. 2016) (Table 6.2). Because LCL is a function of temperature and RH; RH and LCL are related ($RH = -0.04(LCL) + 99.00$, $r = -0.999$, $r^2 = 0.998$, $p < 0.005$), and this underlies the inverse relationship between *d* and LCL (Table 6.2). Precipitation isotopes were also inversely related to precipitation amount and this could be attributed to the "amount effect" (Dansgaard 1964). The 'amount effect' suggests that light precipitation events are more prone to equilibration with enriched sub-cloud vapour and or experience sub-cloud evaporation and are thus more enriched than larger volume events. Larger precipitation events increase sub-cloud RH, reducing evaporation resulting in depleted isotope compositions compared to smaller events. This would result in positive relationships between *d* and precipitation amount and *d* and RH (Table 6.2). These results were thus consistent with expected sub-cloud evaporation from low intensity precipitation events over Windhoek. Finally, precipitation isotopes ($\delta^{18}O$, $\delta^{2}H$ and $\delta^{17}O$) showed weak but positive relationships with site air and surface temperature similar to Treble et al. (2005), which would enhance isotopic exchange with sub-cloud vapour as well as sub-cloud evaporation (Table 6.2). This was however, in contrast to Dansgaard (1964) who did not observe a temperature effect using monthly data for the site.

At monthly time-scales, the significant drivers of local precipitation isotope composition in decreasing order were RH, precipitation amount and minimum temperature ($p < 0.05$; Table D6.4), while *d* was significantly related to a single local parameter RH (Table D6.4). Similar to the findings of Dansgaard (1964), volume weighted monthly precipitation isotope compositions detected the "amount effect" indicating much stronger relationships than either the unweighted event or monthly samples but did not detect the "temperature effect" (Table 6.2, Table D6.4 and Table D6.5). This suggests loss of

information through data aggregation, “temperature effect”, (Noone and Simmonds 2002), while at the same time indicating that aridity is a major driver of precipitation isotope compositions at the site. Similarly, the weighted LMWL slope for this study 7.9±0.35 (n=29) was similar to that determined earlier 8±1.5 (n=14) (Dansgaard 1964), indicating sub-cloud evaporation and consistent with the interpretations above and classification of the site as semi-arid (*BSh*).

Because multi-scale influences on precipitation isotopes do not conform well to univariate regression analysis in mid-latitude and subtropical locations (Alley and Cuffey 2001, Fricke and O'Neil 1999, Sturm et al. 2010), we applied multiple linear regression analysis (MLRA) at event scale (Table 6.3). The best performing models for $\delta^{18}O$, $\delta^{2}H$ and $\delta^{17}O$ combined air temperature, precipitation amount and RH, accounting for 47-53% of isotope variability at the site (Table 6.3). However, the best performing model for *d* included precipitation amount, LCL and average wind speed and accounted for 55% of the variation (Table 6.3). These MLRA models explained more precipitation isotope variation at event-scale compared to univariate analyses giving credence to the view that precipitation isotopes at mid-latitude and subtropical locations do not lend well to univariate analysis (Table 6.2 and Table 6.3). At the same time, these MLRA models suggest significant local modification of the precipitation isotope composition such that *d* cannot be considered a conservative environmental tracer of evaporation conditions at the source, at least for this semi-arid site (Lai and Ehleringer 2011, Welp et al. 2012, Zhao et al. 2014) (Table 6.3). However, it is important to acknowledge that no analyses of source conditions was performed in this study. The most influential local parameter on precipitation isotope compositions over Windhoek according to the MLRA models was RH, suggesting isotopic exchange and sub-cloud evaporation associated with cloud base to ground surface travel time enhanced by air temperature as the physical mechanism accounting for 47-53% of $\delta^{18}O$, $\delta^{2}H$ and $\delta^{17}O$ variability. However, for *d*, LCL was the most influential parameter suggesting cloud base to ground surface travel time and associated sub-cloud evaporation with windy conditions as the driving physical mechanism (Table 6.2 and Table 6.3).

Table 6. 3 Best performing multiple linear regression models between event precipitation isotopes and local meteorological data from the National Botanic Research Institute (NBRI), Windhoek 2012-2016. Only meteorological conditions with significant relationships from Table 2 were used.

	Multiple linear regression equation	AIC	RSME	r^2	p-value
$\delta^{18}O$	y = 43.26 - (1.03*air temp) - (0.01*amt) - (0.34*RH)	300.9	4.5	0.53	< 0.05
$\delta^{2}H$	y = 334.28 - (8.62*air temp) - (0.70*amt) - (2.45*RH)	704.2	34.4	0.47	< 0.05
$\delta^{17}O$	y = 22.67 - (0.54*air temp) - (0.06*amt) - (0.18*RH)	174.0	2.4	0.53	< 0.05
d	y = 8.39 + (0.13*amt) - (0.02 * LCL) + (1.68 *winspd)	364.9	6.2	0.55	< 0.05

Note: air temp is air temperature (°C), RH is relative humidity (%), amt is precipitation amount, LCL is lifted condensation level and winspd is wind speed (ms^{-1})

The unaccounted precipitation isotope ($\delta^{18}O$, $\delta^{2}H$ and $\delta^{17}O$) variability from the MLRA models could be related to several factors including but not limited to precipitation type, rain-out processes and source evaporation conditions (Aggarwal et al. 2016, Coplen et al. 2015, Crawford et al. 2013, Dansgaard 1964, Fudeyasu et al. 2011, Jouzel et al. 2013). Recently, stratiform and convective precipitation have been associated with depleted and enriched isotopic compositions, respectively (Aggarwal et al. 2016, Coplen et al. 2015, Fudeyasu et al. 2011, Kurita 2013). However, no significant relationships were observed between $\delta^{18}O$, $\delta^{2}H$, $\delta^{17}O$ and stratiform fraction at our study site, suggesting isotopic composition was independent of precipitation type (Table D6.6). This was supported by the significant inverse relationship between *d* and stratiform fraction (Fig. 6.3a), suggesting stratiform precipitation was more susceptible to sub-cloud evaporation than convective precipitation. Stratiform precipitation consists of small raindrops (~1 mm in diameter) which may partially evaporate or grow by accretion and coalescence depending on prevailing conditions: subsidence or uplift, respectively (Houze Jr 2014). Convective precipitation on the other hand consists of larger rain drops (> 2 mm in diameter) that do not experience much evaporation or growth (Houze Jr 2014, Schumacher and Houze Jr 2003, Steiner and Smith 1998). Therefore, an increase in stratiform fraction would diminish raindrop size, increase travel time from cloud base to ground surface, decrease average precipitation rate facilitating sub-cloud evaporation and isotopic exchange with below cloud vapour. Models estimate a 30-80% reduction in raindrop size due to sub-cloud evaporation in arid environments, resulting from a combination of high temperatures and low RH (Wang et al. 2016). At the same time, the weighted precipitation rate decreased with an increase in stratiform fraction (Fig. 6.3b), consistent with the predictions above enhancing equilibration with ambient vapour as well as enhancing sub-cloud evaporation. This would result in lower *d*, and higher $\delta^{18}O$, $\delta^{2}H$ and $\delta^{17}O$ values for stratiform compared to convective precipitation which is less susceptible to sub-cloud evaporation (Houze Jr 2014, Schumacher and Houze Jr 2003, Steiner and Smith 1998), although this was only significant for *d* (Table D6.7).

Applying MLRA to *d*, the best performing model was *d* = 4.0 - (0.12 * stratiform fraction) + (0.56 * amount) (AIC 82.9, r^2 0.61, RMSE 5.3, $p < 0.05$), with precipitation amount being the most influential parameter. These results suggest that sub-cloud

evaporation resulted in enrichment of ^{18}O, ^{2}H and ^{17}O in stratiform precipitation to the extent that it was more enriched or similar to convective precipitation at the site (Table D6.7). This would explain the observed $\delta^{18}O$, $\delta^{2}H$ and $\delta^{17}O$ independence of precipitation type and rate observed at the site (Table D6.6). This contradicts the suggestion that the relationship between precipitation isotopes and intensity may be more visible at event scale (Dansgaard 1964). This result could be related to the fact that precipitation type and intensity are related (Fig. 6.3), thus where both types occur the influence of sub-cloud evaporation on the isotopic composition of the different precipitation types is not equal (Table D6.7). Therefore, the effect of precipitation intensity will likely be best observed when each precipitation type is considered separately or *d* is used instead (Table D6.7). However, given the data reduction already incurred in differentiating precipitation type, such an analysis is not possible for this study. These results, therefore suggest that precipitation isotopes are independent of precipitation type at least at this site and possibly other dryland environments. However, it is important to acknowledge the complexity associated with these calculations, notably estimation of stratiform fraction is greater when shallow rain is significant and amounts are low (Funk et al. 2013, Schumacher and Houze Jr 2003), while isotope data at a sampling point could be biased towards stratiform precipitation (point vs raster data) (Aggarwal et al. 2016). Nonetheless, these calculations provide general trends of precipitation isotopes and precipitation type in a semi-arid environment.

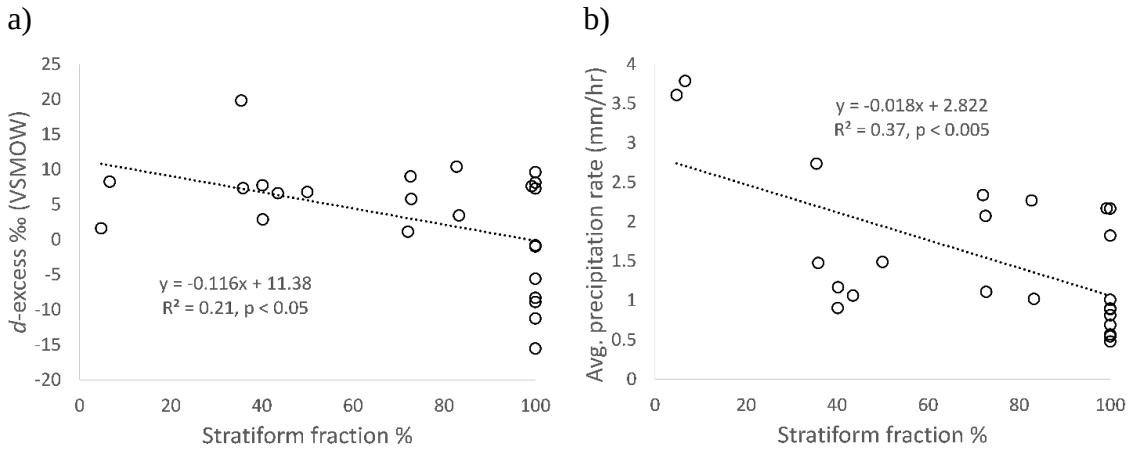

Figure 6. 3 Variation of a) d-excess as a function of stratiform fraction and b) average conditional precipitation rate as a function of stratiform fraction, for rain events observed over Windhoek, 2012-2016 (n = 24).

6.3.4 HYSPLIT air mass trajectories, cluster analysis and $\delta'^{17}O$-$\delta'^{18}O$

Ten day HYSPLIT (Stein et al. 2015) back-trajectory analyses suggest that Windhoek (2012-2016) precipitation originated from both the Indian and Atlantic Oceans (Fig. 6.4). However, the 140 hr trajectory cluster analysis grouped the sources into four clusters (Fig. 6.4), but no significant differences were detected among the precipitation clusters in $\delta^{18}O$, $\delta^{2}H$, $\delta^{17}O$ and *d*. This suggests precipitation isotopes underwent extensive modification at the precipitation site (47-53%) making them indistinguishable (Table 6.3). The results highlight the inappropriateness of *d* as a conservative tracer of evaporation conditions at the source region, as 55% of *d* variability was related to local meteorological conditions at the precipitation site (Table 6.3). However, $^{17}\Delta$ and $\delta'^{17}O$-$\delta'^{18}O$ could be used as conservative tracers of humidity changes at the vapour source independent of temperature and thus complement *d* interpretations (Angert et al. 2004, Barkan and Luz 2007, Li et al. 2015). $\delta'^{17}O$-$\delta'^{18}O$ slopes of 0.529±0.001 indicate a dominance of equilibrium fractionation processes, suggesting high RH conditions at the evaporation source (Luz and Barkan 2005). Therefore the $\delta'^{17}O$-$\delta'^{18}O$ slope of cluster 1 (0.529±0.003) suggests high RH conditions over the subtropical Indian Ocean evaporation source (Fig. 6.4 and Fig. 6.5). However, $\delta'^{17}O$-$\delta'^{18}O$ slopes of 0.506-0.5185 indicate a dominance of kinetic fractionation processes suggesting non-steady state conditions with low RH at the evaporation source (Angert et al. 2004, Barkan and Luz 2007). Thus the $\delta'^{17}O$-$\delta'^{18}O$ slopes

of clusters 2 (0.502±0.007) and 3 (0.507±0.019) suggest low RH conditions over the South Atlantic during evaporation (Fig. 6.4 and Fig. 6.5). The $\delta'^{17}O$-$\delta'^{18}O$ slope for cluster 4 (0.520±0.004) suggests non-steady state evaporative conditions at more than 50% RH (Li et al. 2015). It is important to note that these trajectories only indicate geographic origins of moisture and do not take in account any additional moisture picked during transport to the site. We acknowledge that there seems to be an association between trajectory distance and $\delta'^{17}O$-$\delta'^{18}O$, suggesting an influence of ET on $\delta'^{17}O$-$\delta'^{18}O$ (Landais et al. 2006, Li et al. 2017) (Fig. 6.4). However, given that moisture recycling is estimated at 28-34% (Miralles et al. 2016), how and to what extent ET would influence precipitation $\delta'^{17}O$-$\delta'^{18}O$ in the region is uncertain (Landais et al. 2006, Li et al. 2017) and beyond the scope of the current study.

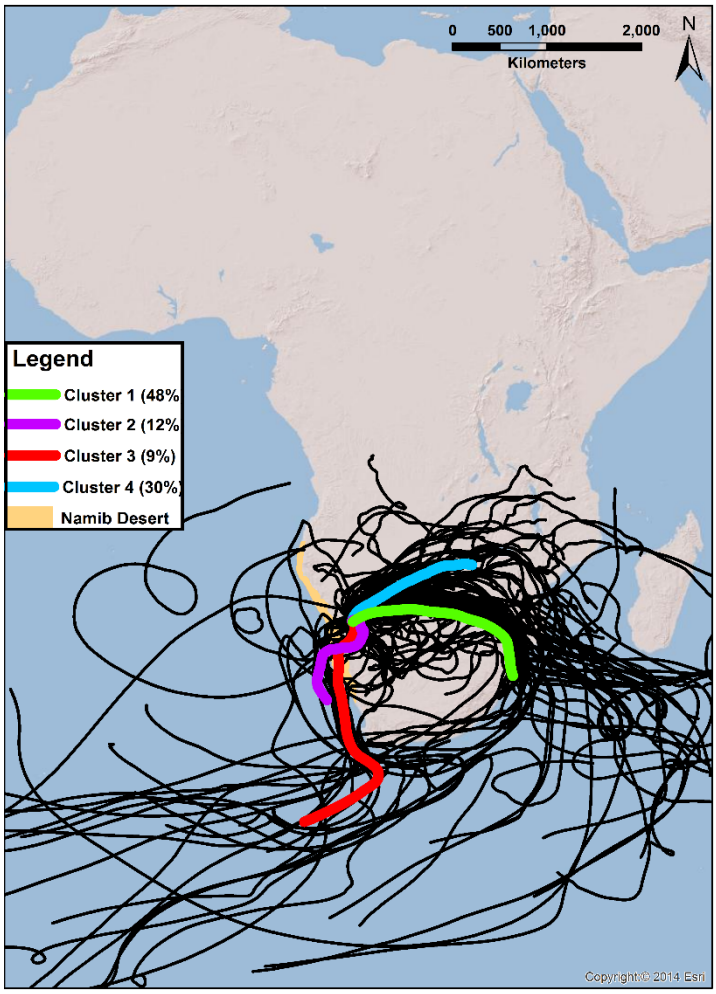

Figure 6. 4 Ten day (240 hr) atmospheric back trajectories of precipitation events received at Windhoek during the 2012-2016 period (n = 99). The associated mean trajectory clusters were based on ~six day (140 hrs) trajectories, which equate to the approximate travel time to Windhoek after intersecting land and atmospheric residence times for the region (Miralles et al. 2016).

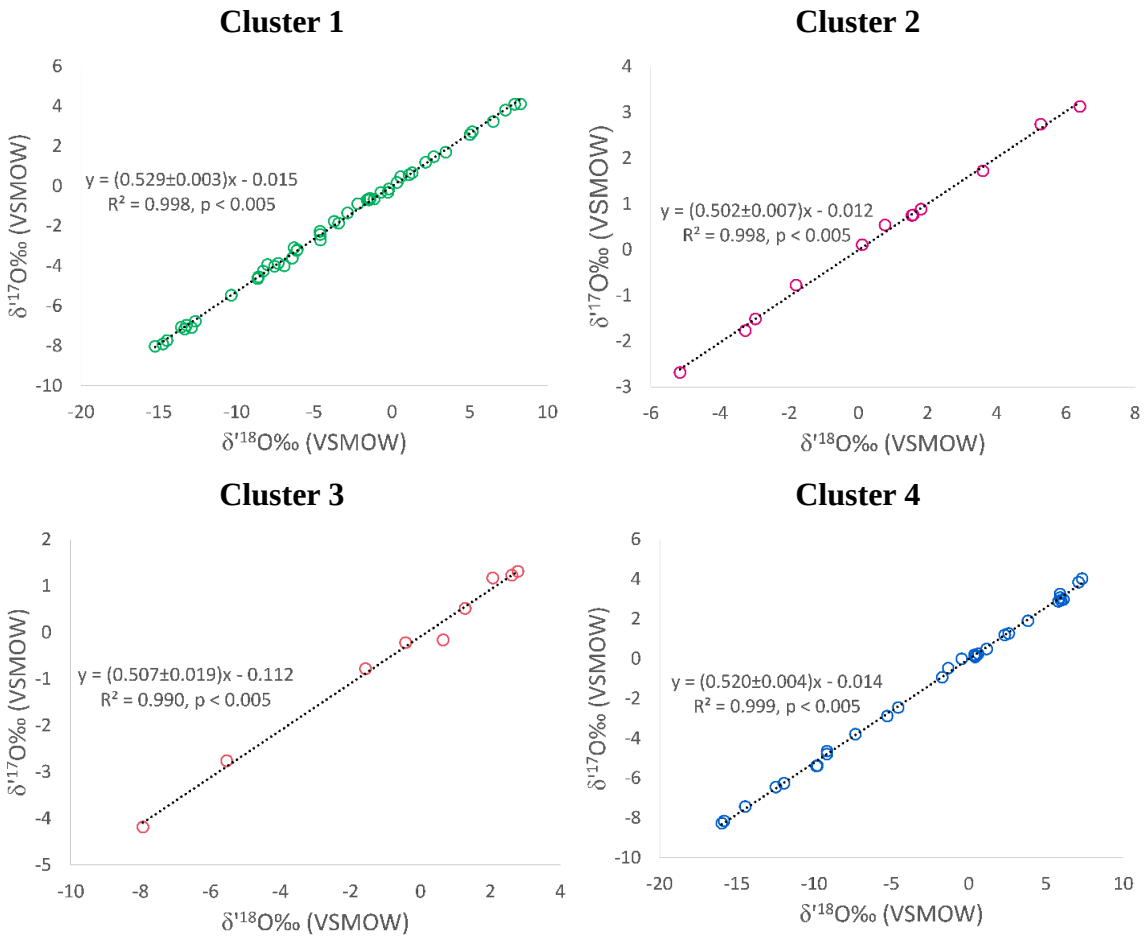

Figure 6. 5 The four trajectory clusters of Windhoek precipitation during 2012-2016 as defined by the $\delta'^{17}O$-$\delta'^{18}O$ relationships.

The origins of cluster 1 were consistent with the position of the Subtropical Indian Ocean dipole (SIOD) (Reason 2001) while cluster 4 origins were consistent with the position of the tropical Indian Ocean dipole (IOD) (Fig. 6.4). Sea surface temperatures (SST) around the origins of cluster 1 range from 23-26°C while those around cluster 4 origins range from 24-28°C (Oct-Apr) (Rao et al. 1989). Warmer SSTs would result in greater evaporation and result in higher RH over the tropical oceans (30°N-30°S) (Shie et al. 2006). However, the $\delta'^{17}O$-$\delta'^{18}O$ slope of cluster 4 (0.520) was smaller than that of cluster 1 (0.529) despite higher SST around cluster 4 origins. This suggests non-steady state conditions around cluster 4, resulting in lower RH than expected from the SST compared to cluster 1 origins. Summer precipitation in southern Africa has been associated with the tropical western Indian Ocean with the subtropical southwest Indian Ocean

thought to be a substantial source of moisture for the region (D'Abreton and Lindesay 1993, Reason and Mulenga 1999). However, the trajectory analyses results suggest that the subtropical Indian Ocean may contribute more moisture over the western parts of southern Africa or at least Windhoek (2012-2016) than the tropical Indian Ocean (Fig. 6.4).

The third potential source of moisture associated with summer precipitation over southern Africa is often regarded as the tropical South Atlantic Ocean (Fauchereau et al. 2003, Hermes and Reason 2005), although exact influences are unknown (Reason et al. 2006). However, our results suggest that clusters 2 and 3 originated from a region over the subtropical South Atlantic Ocean (Fig. 6.4). It is known that West African precipitation is influenced by a South Atlantic Ocean dipole (SAOD), defined as: north east pole, NEP (10°E–20°W, 0°S–15°S) and south west pole, SWP (10°W–40°W, 25°S–40°S) (Nnamchi and Li 2011, Nnamchi et al. 2011). However, simulations of this SAO also suggest a smaller south-east pole (SEP) in phase with the NEP (Nnamchi et al. 2011), consistent with the origins of clusters 2 and 3, defined as SEP 0°E-15°E and 30°-45°S (Fig. D6.4). However, because Nnamchi and Li (2011) focussed on SAOD influences on precipitation variability in West Africa, no attention was paid to possible influences on precipitation variability in southern Africa. Given that the results presented here and the simulations by Nnamchi et al. (2011) converge over the same region, suggests this SEP could be an extension of the SAOD or a secondary subtropical SAOD defined as SEP and SWP and may influence precipitation variability in southern Africa, at least over Windhoek (Fig. D6.4). However, Reason and Jagadheesha (2005) and Harris et al. (2010) also suggest the existence of a subtropical South Atlantic Ocean dipole influencing precipitation over the Southwestern Cape region of South Africa, although the location of the dipole is shifted slightly to the left of that proposed in Fig. D6.4. Therefore, the existence of a subtropical South Atlantic Ocean dipole is a distinct possibility although exact locations may be debatable and outside the scope of this study. This is in contrast to studies that have often exclusively associated precipitation anomalies over western parts of central and southern Africa to the tropical South Atlantic Ocean, Benguela Niño and the South Atlantic Ocean Dipole (SAOD) (Hermes and Reason 2005, Nnamchi and Li 2011, Reason and Smart 2015, Rouault 2003).

Applying a simple classification based on oceanic origins of precipitation events over Windhoek (2012-2016), precipitation events were grouped into two: Indian Ocean (clusters 1 and 4) and subtropical Atlantic Ocean (clusters 2 and 3) (Fig. 6.4 and Fig. 6.6). The resulting $\delta'^{17}O$-$\delta'^{18}O$ slope for precipitation from the subtropical Atlantic Ocean (0.506±0.009) was consistent with dominance of kinetic fractionation processes (0.506-0.5185), suggesting evaporation under non-steady state conditions at low RH (Angert et al. 2004, Barkan and Luz 2007, Li et al. 2015) (Fig. 6.6a). The $\delta'^{17}O$-$\delta'^{18}O$ slope for precipitation from the Indian Ocean (0.525±0.002) was close to the 0.5265 slope which indicates evaporation occurred at high RH (~85%) (Li et al. 2015) (Fig. 6.6b). According to Araguás-Araguás et al. (2000), high RH (~80%), warm temperatures (25°C) and low wind velocities result in *d* values of about +10‰. Therefore, the $\delta'^{17}O$-$\delta'^{18}O$ results were consistent with SST and RH conditions for the Indian Ocean (Araguás-Araguás et al. 2000, Rao et al. 1989). However, precipitation *d* from the Indian (+7.7‰) and subtropical Atlantic Oceans (+5.5‰) were significantly smaller than the GMWL (+10‰) (Kruskal-Wallis, $p < 0.05$; Mann-Whitney post-hoc test, $p < 0.05$). There were no significant differences between precipitation *d* from the Indian and subtropical Atlantic Oceans (Kruskal-Wallis, $p > 0.05$) nor between their respective LMWLs (One-way ANCOVA, $p > 0.05$) (Fig. 6.6c and Fig. 6.6d). These results suggest precipitation isotopes collected in Windhoek underwent significant modification by local meteorological conditions, consistent with earlier conclusions (Table 6.2 and Table 6.3). These local modifications, resulted in similar LMWLs (Fig. 6.6c and Fig. 6.6d) and may have altered precipitation *d* by as much as 55% such that its use as a conservative tracer of evaporation conditions at the source may be questionable, at least for this semi-arid environment (Table 6.3).

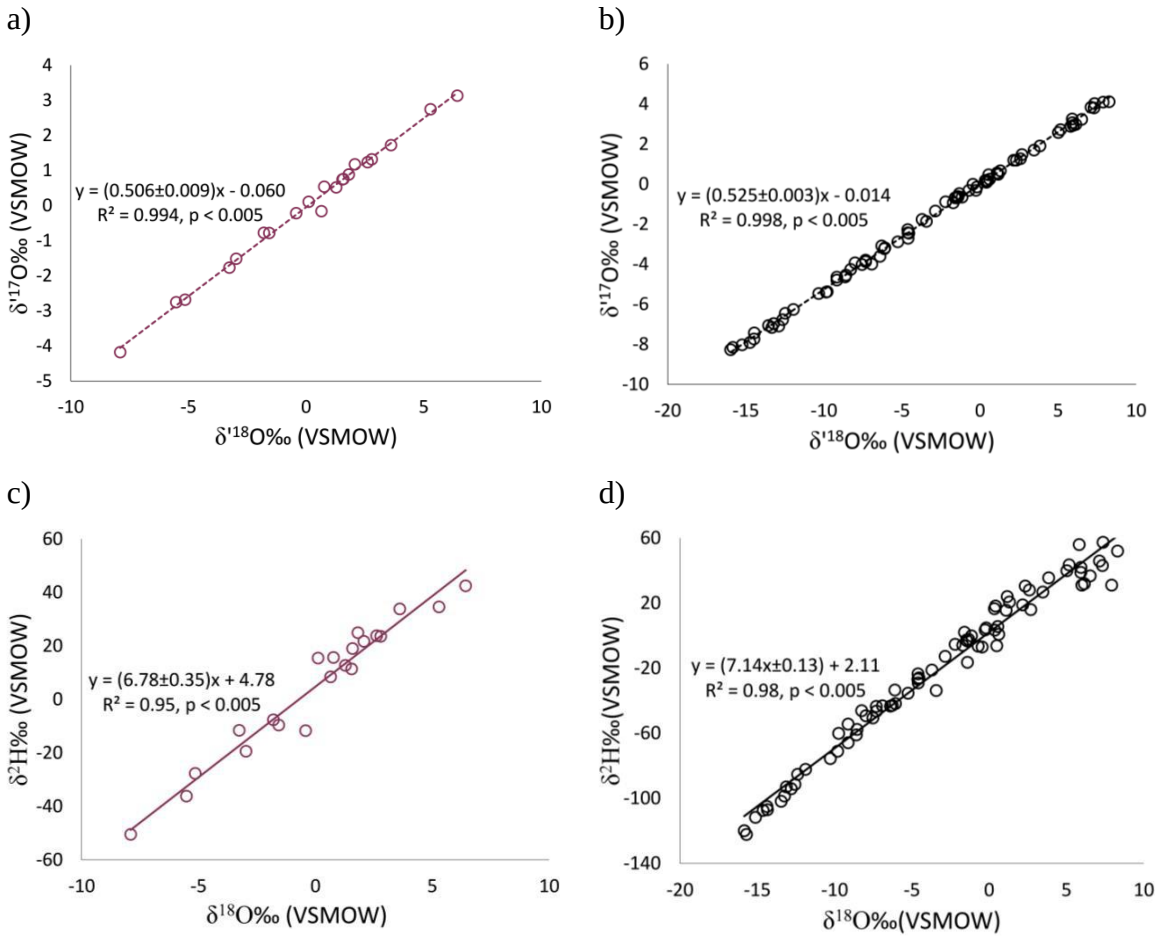

Figure 6. 6 Isotope relationships of combined trajectory clusters based on ocean source for Windhoek precipitation 2012-2016; a) subtropical Atlantic Ocean $\delta'^{17}O$-$\delta'^{18}O$, b) Indian Ocean $\delta'^{17}O$-$\delta'^{18}O$, c) subtropical Atlantic Ocean $\delta^{2}H$-$\delta^{18}O$ and d) Indian Ocean $\delta^{2}H$-$\delta^{18}O$.

Precipitation from the subtropical Atlantic Ocean was significantly enriched in $\delta^{18}O$ (+0.8‰), $\delta^{2}H$ (+12.7‰) and $\delta^{17}O$ (+0.5‰) than from the Indian Ocean $\delta^{18}O$ (-2.0‰), $\delta^{2}H$ (-9.9‰) and $\delta^{17}O$ (-0.9‰) (Kruskal-Wallis, $p < 0.05$). Because the Atlantic Ocean (~266 km) is located closer to Windhoek than the Indian Ocean (~1904 km) (Fig. 6.1 and Fig. 6.4), the observed precipitation enrichment in $\delta^{18}O$, $\delta^{2}H$ and $\delta^{17}O$ from events originating from the subtropical Atlantic Ocean could be reflecting the 'continental effect' (Dansgaard 1964). In addition, the isotope compositions of precipitation originating from the subtropical Atlantic Ocean presented here were generally more enriched in $\delta^{18}O$ and $\delta^{2}H$ compared to those reported for Cape Town (Harris et al. 2010). This could be attributed to the influence of sub-cloud evaporation at Windhoek as noted by Dansgaard (1964).

The Indian Ocean was the primary source of moisture for Windhoek precipitation during 2012-2016, accounting for 68-92% of annual precipitation events and 51-94% of the annual precipitation amount (Table 6.4). These results were consistent with studies that have concluded that the Indian Ocean was the primary source of moisture for precipitation over southern Africa (D'Abreton and Lindesay 1993, Reason and Smart 2015, Reason and Mulenga 1999). On the other hand, the results also indicate that the South Atlantic Ocean contributed a substantial amount of moisture to Windhoek during this period; 24-32% of annual precipitation events and 10-49% of annual precipitation amount during drought years and 6-8% during non-drought years (Table 6.4). Therefore, more research is needed to understand the influence and effects of the sub-tropical South Atlantic Ocean on precipitation in Windhoek, Namibia and southern Africa. It is important to acknowledge that the temporal isotopic variability for this subtropical semi-arid site (Table 6.1) is similar to that of tropical sites e.g., Puerto Rico with different moisture sources (Sánchez-Murillo et al. 2016), suggesting some other pan-tropical mechanism may influence precipitation isotope compositions in addition to those described by (Dansgaard 1964). Aggarwal et al. (2016) suggests that this mechanism could be the precipitation type, however, the results presented here contradicted this, suggesting that if such a pan-tropical mechanism exists, it requires further investigations.

Table 6. 4 Annual and total contribution of events and precipitation from the Indian and South Atlantic Ocean over Windhoek 2012-2016

	2012 - 2013		2013 - 2014		2014 - 2015		2015 - 2016		2012 - 2016	
	Indian	Atlantic	Indian	Atlantic	Indian	Atlantic	Indian	Atlantic	Indian	Atlantic
% frequency	71	29	92	8	76	24	68	32	79	21
% precipitation	67	33	94	6	90	10	51	49	79	21

6.3.5 Annual and inter-annual local meteoric water lines (LMWL)

Figure 6.7 displays the different LMWLs generated for the site based on 2012-2016 event-scale data from the Local Meteoric Water Line Freeware programme (Crawford et al. 2014). Crawford et al. (2014) notes that the calculation of LMWLs using different methods on the same data can result in wildly different LMWLs, complicating interpretation. However, for this particular site LMWLs based on the unweighted methods were similar while those based on the weighted versions were similar while both showed the same trends. The weighted LMWLs had larger slopes and intercepts than the unweighted LMWLs (Fig. 6.7). However, these LMWLs were similar to those calculated for Windhoek based on GNIP data, $y = 7.1013x + 8.0159$ (OLSR) and $y = 7.30x + 9.3594$ (PWLSR) (Crawford et al. 2014), except for the lower intercepts. The slope of the OLSR 2012-2016 LMWL (7.05) was significantly smaller than the global meteoric water line (GMWL) (8) (ANCOVA, $p < 0.05$) while GMWL *d* (+10‰) was significantly larger than that of the 2012-2016 Windhoek LMWL (+7.1‰) (Kruskal-Wallis, $p < 0.05$; Fig. 6.6). Local meteoric water lines with slopes < 8 are characteristic of arid and semi-arid environments (Araguás-Araguás et al. 2000), consistent with the classification of Windhoek as a hot semi-arid climate (*BSh*). Arid and semi-arid environments also suggest secondary processes such as sub-cloud evaporation (Ehhalt et al. 1963, Stewart 1975), consistent with the low *d* observed at the site (Table 6.1).

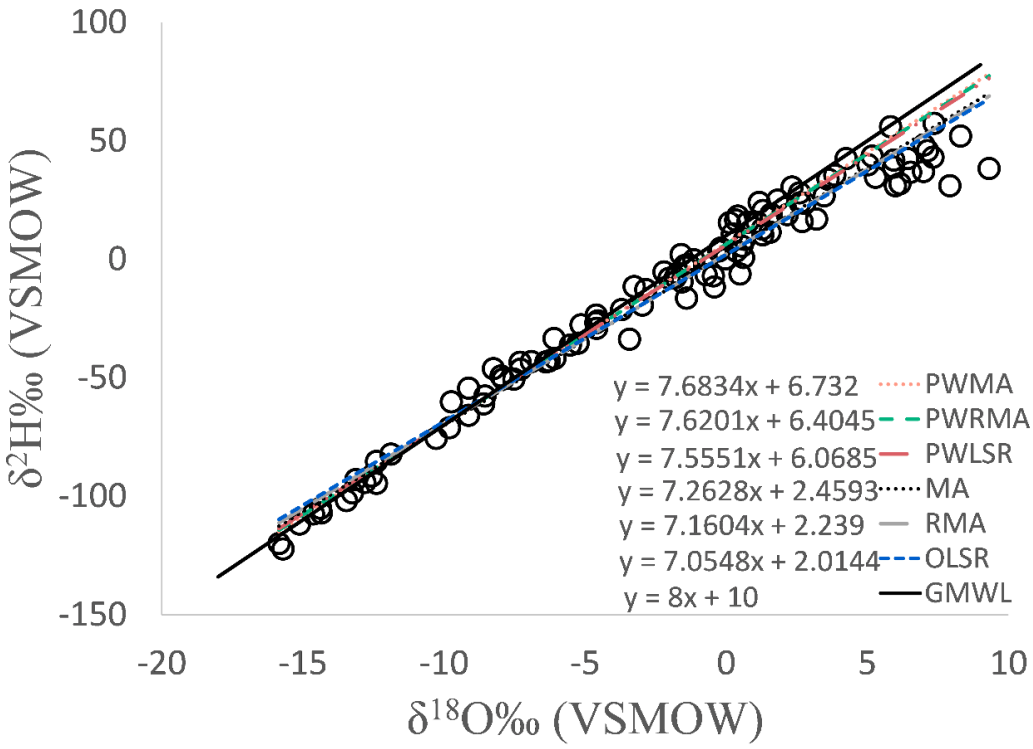

Figure 6. 7 Event scale local meteoric water lines for Windhoek (2012-2016) calculated using (Crawford et al. 2014) with the GMWL as a reference. Ordinary least square regression (OLSR), reduced major axis regression (RMA), major axis regression (MA) with precipitation weighted (PW) versions.

Whereas the 2012-2016 Windhoek LMWLs gave an overview of the general climate characteristics, they did not reflect annual variability e.g., wet vs. dry years (Fig. 6.8 and Table D1). There was no significant difference between the OLSR 2012-2016 LMWL (7.05) and 2013-2014 LMWL (7.36) slopes, suggesting 'normal' precipitation amounts for the site during 2013-2014 (ANCOVA, $p > 0.05$) (Fig. 6.8b). However, the slopes of the OLSR LMWLs for 2012-2013 (6.57), 2014-2015 (6.42) and 2015-2016 (6.53) were significantly smaller than that of the 2012-2016 LMWL (7.05) (ANCOVA, $p < 0.05$) (Fig. 6.8). The deviation of these annual LMWL slopes below the 2012-2016 LMWL reference suggest below 'normal' precipitation during these periods at the site, consistent with the meteorological droughts observed (Fig. 6.2 and Table D6.2). These results suggest that meteorological droughts caused abnormally dry conditions beyond the normal arid or semi-arid conditions at the site. This would have resulted in enhanced or intense sub-cloud

evaporation, significantly lowering annual LMWLs than the 2012-2016 LMWL (Fig. 6.8). Therefore the annual LMLs for 2012-2013, 2014-2015 and 2015-2016 were consistent with the cumulative precipitation totals which indicated meteorological drought conditions during these years (Fig. 6.2 and Table D6.2).

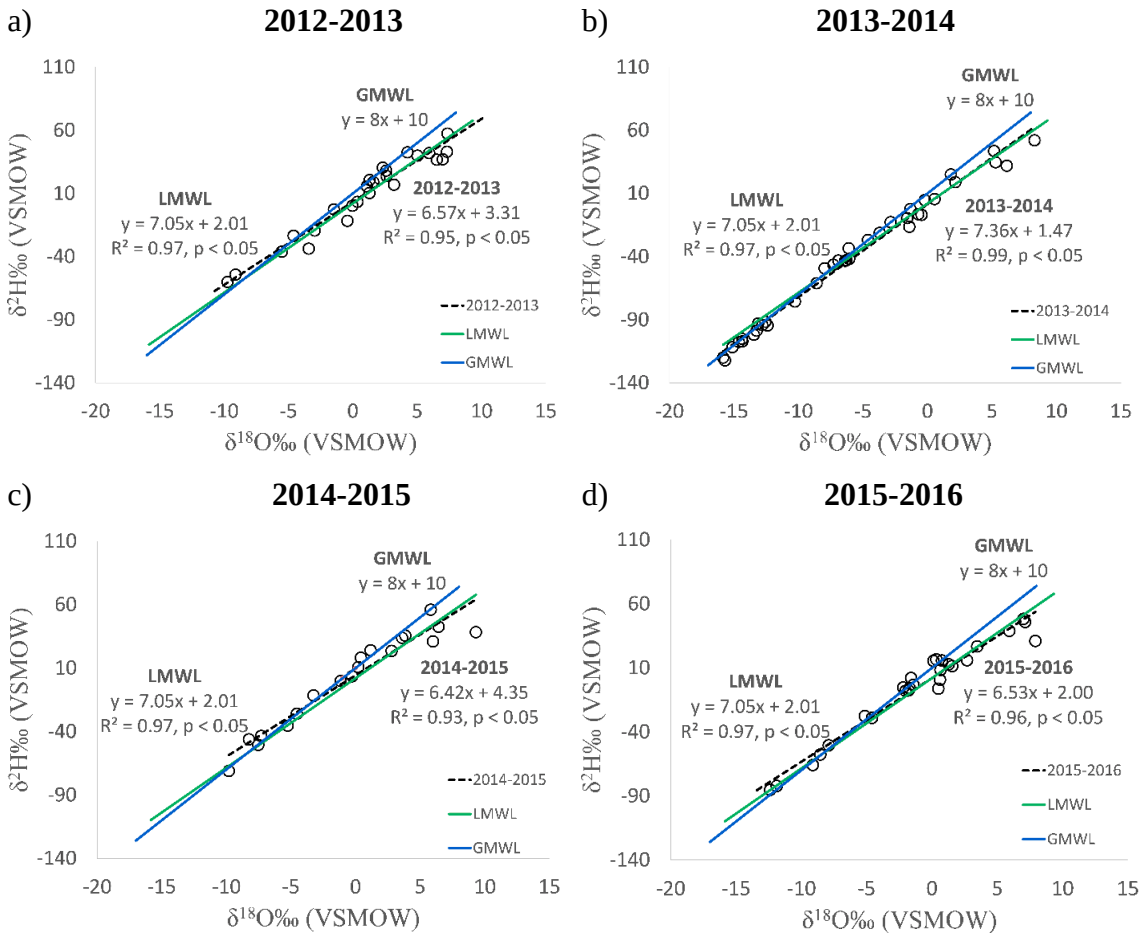

Figure 6. 8 Annual unweighted local meteoric water lines (LMWLs) for Windhoek (2012-2016) based on the rainfall year (Oct-Sep): a) 2012-2013, b) 2013-2014, c) 2014-2015 and d) 2015-2016. The GMWL and unweighted LMWL(2012-2016) were included as references.

6.3.6 Drought differentiation using $\delta'^{17}O$-$\delta'^{18}O$ relationship

There were no significant differences in precipitation *d* among the years 2012-2013 (+3.64‰), 2013-2014 (+7.33‰), 2014-2015 (+9.00‰), and 2015-2016 (+7.62‰) nor with the 2012-2016 LMWL (+7.13) (Kruskal-Wallis, $p > 0.05$). This suggests that the

precipitation isotopes were significantly altered by the local environmental parameters such that *d* was not a conservative tracer of evaporation conditions at the source. At the same time, there were no significant differences between LMWLs generated from precipitation events from the Indian Ocean ($y = 7.14\pm0.13x + 2.11\pm0.97$; $r^2 = 0.98$, $p < 0.05$) and those from the subtropical Atlantic Ocean ($y = 6.78\pm0.35x + 4.78\pm1.2$; $r^2 = 0.95$, $p < 0.05$) (One-way ANCOVA, $p > 0.05$), suggesting that origins of precipitation had no effect on isotopic composition at the site. The $\delta'^{17}O$-$\delta'^{18}O$ slopes for 2012-2013 and 2013-2014 were similar (Fig. 6.9a and Fig. 6.9b), suggesting high RH (~85%) evaporation conditions (Araguás-Araguás et al. 2000, Li et al. 2015) conducive for mass transport of moisture to the precipitation site (Fig. 6.1). While Windhoek received normal to above normal precipitation during 2013-2014 consistent with expectations of an El Niño neutral year, 2012-2013 was a drought (Fig. 6.2 and Fig. D6.1). However, the eastern and parts of central southern Africa (e.g., Mozambique, Zimbabwe, Botswana) experienced above normal precipitation and violent storms during 2012-2013 (Moyo and Nangombe 2015) while the western parts including Namibia experienced droughts. This suggests Windhoek should have received normal to above normal precipitation during 2012-2013 but mesoscale (western southern Africa) conditions may have caused the drought. On the other hand, 2014-2015 and 2015-2016 $\delta'^{17}O$-$\delta'^{18}O$ slopes were similar (Fig. 6.9c and Fig. 6.9d) and suggested low RH (~50%) non-steady state evaporation conditions at the sources (Li et al. 2015), conditions that would have resulted in less moisture transported to the precipitation site (Fig. 6.1). The 2014-2015 and 2015-2016 $\delta'^{17}O$-$\delta'^{18}O$ slopes thus possibly reflected El Niño (Fig. D6.1), a synoptic system associated with droughts in the region (Hoell et al. 2016). Because 2012-2013 was ENSO neutral while the 2014-2016 droughts were probably El Niño related, $\delta'^{17}O$-$\delta'^{18}O$ could be reflecting differences in the causes of these droughts; mesoscale vs. synoptic scale respectively (Fig. 6.9). These results were consistent with the increase (decrease) in recycled E/ET (T/ET) during 2014-2016 due to consecutive droughts that affected the entire region compared to the 2012-2013 drought which only affected the western parts of Southern Africa (Table D6.4). Interestingly, the origins of clusters 1 and 4 (Indian Ocean) were consistent with modelled source areas of precipitation deficits during droughts in the Kalahari ecoregion while clusters 2 and 3 (Atlantic Ocean) are not affected during droughts (Miralles et al. 2016) (Fig. 6.4). This

decrease in Indian Ocean contributions to precipitation could account for the percentage increase in South Atlantic Ocean contributions during droughts observed at Windhoek (Table 6.4).

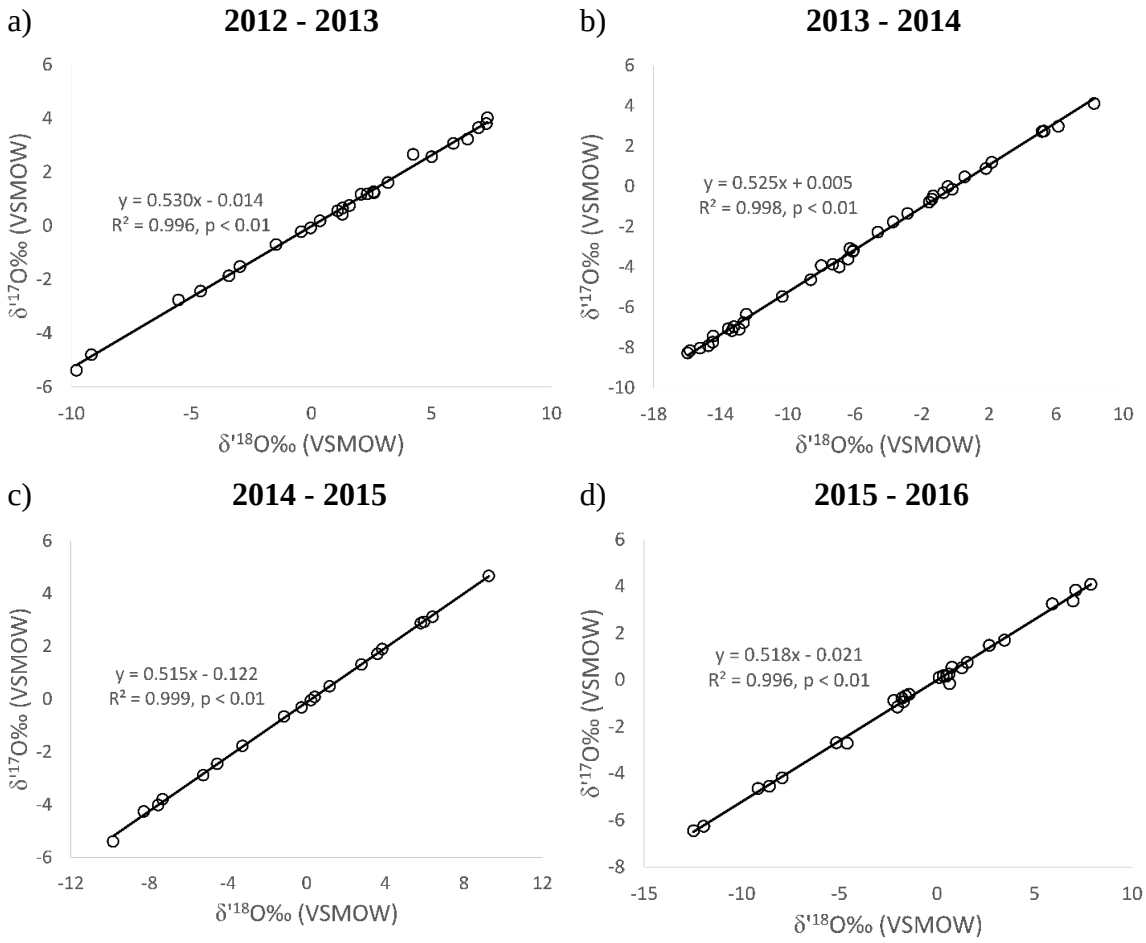

Figure 6. 9 Plots showing the annual $\delta'^{17}O$-$\delta'^{18}O$ of Windhoek precipitation over 4 years: a) 2012-2013, b) 2013-2014, c) 2014-2015 and d) 2015-2016.

Because the correlation between $\delta^{18}O$ and $\delta^{2}H$ is controlled by underlying physical properties, it has been argued that PWRMA and PWMA are more appropriate approaches than OLSR, especially the former (Crawford et al. 2014). According to the PWRMA and PWMA LMWLs, the meteorological drought severity increased in the following order 2014-2015, 2015-2016 and 2012-2013 (Table D6.1). However, this was in contrast to the precipitation totals which suggest drought severity increased in the following order 2015-2016, 2014-2015 and 2012-2013 (Fig. 6.2 and Table D6.2). Given the relationship between

El Niño and droughts in the region (Allan et al. 2003, Nicholson and Entekhabi 1986, Reason and Rouault 2002), the 2015-2016 drought was expected to be more severe than the 2014-2015 based on El Niño strength (Fig. D6.1). However, recent work suggests that precipitation response to drought in the region is related to ENSO and SIOD phase relationships (Hoell et al. 2016). A positive SIOD is characterised by warm waters on the south west Indian Ocean and cool tropical waters in the central and eastern Indian Ocean while a negative SIOD is reversed (Behera and Yamagata 2001, Hoell et al. 2016, Reason 2002). The warm waters of a positive SIOD increase evaporation and the moist air is advected over southern Africa (Behera and Yamagata 2001, Reason 2001). When ENSO and SIOD are in phase (++), El Niño induced droughts are moderate but when ENSO and SIOD are antiphase (+-), El Niño induced droughts are severe (Hoell et al. 2016). During early summer 2014-2015, El Niño and SIOD were antiphase (Fig. D6.1 and Fig. D6.3) and this may have enhanced the precipitation response to El Niño, less precipitation than expected (Fig. 6.2 and Table D6.2). On the other hand, 2015-2016 experienced a stronger ENSO (+) but was in phase with the SIOD (+) (Fig. D6.1 and Fig. D6.3) mitigating the precipitation response to El Niño, more precipitation than expected (Fig. 6.2 and Table D6.2).

Neither univariate analyses nor MLRA showed any significant relationships between precipitation amount, ONI and the SIOD as measured by the South Western Indian Ocean (SWIO) index (http://stateoftheocean.osmc.noaa.gov/sur/ind/swio.php) (OOPC 2016) ($p > 0.05$). This could be because ENSO is a result of complex interactions between several climate systems, thus the multivariate ENSO index (MEI) (https://www.esrl.noaa.gov/psd/enso/mei/table.html) (NOAA 2016) was substituted for ONI. MEI is considered the most representative ENSO index integrating multiple meteorological parameters measured over the Pacific Ocean (Mazzarella et al. 2013). Multiple linear regression analyses showed a significant relationship ($p < 0.05$) between precipitation amount, MEI and SWIO accounting for 17.4% of precipitation variability observed in Windhoek (2012-2016) (Table 6.5). These results suggest precipitation amount over the site may have been partly related to the interaction of the SIOD and ENSO nodes, consistent with (Hoell et al. 2016) (Fig. 6.2, Fig. D6.1 and Fig. D6.3). We did not perform a similar analysis for the South Atlantic Ocean (SAO) because the north-eastern pole of

the current SAO dipole indices are based on the north-eastern parts of the South Atlantic (http://stateoftheocean.osmc.noaa.gov/sur/atl/sat.php) (Nnamchi et al. 2011, OOPC 2017) versus the south eastern parts identified in this study (Fig. D6.4). Therefore the current South Atlantic Ocean Dipole (SAOD) Index does not represent the region of interest and is thus inappropriate for this study (Fig. D6.4). Furthermore, there is little research related to the influence of the subtropical Atlantic on precipitation across southern Africa.

Table 6. 5 Multivariate analysis of Windhoek precipitation as influenced by El Niño Southern Oscillation (ENSO) and the South Western Indian Ocean (SWIO) Index nodes (2012-2016).

	Multiple linear regression equation	AIC	RSME	r^2	p-value
ppt	y = 27.61 - (15.32* MEI) + (37.07*SWIO)	337.3	32.6	0.17	< 0.05

Note: ppt is monthly precipitation amount in mm

6.4 Conclusions

Precipitation isotopes sampled from Windhoek over the period 2012-2016 suggest significant modification by local meteorological parameters, accounting for 47-53% of the isotope variability. The most influential local meteorological parameters at both event and monthly scales indicated substantial sub-cloud evaporation at the site, consistent with the semi-arid classification of the site and the meteorological droughts that occurred during this period. At the same time, sub-cloud evaporation may have resulted in significant modification of stratiform precipitation such that it was indistinguishable from convective precipitation using individual isotopes, resulting in isotopic compositions ($\delta^{18}O$, $\delta^{2}H$ and $\delta^{17}O$) that were independent of precipitation type. This suggests that precipitation $\delta^{18}O$, $\delta^{2}H$ and $\delta^{17}O$ in arid and semi-arid environments could be independent of precipitation type, at least for Windhoek. However, it is still possible to differentiate stratiform precipitation from convection precipitation based on *d*. Trajectory analyses suggested that precipitation events experienced at the site could be broadly classified into two groups: Indian and subtropical South Atlantic Ocean sourced. Contrary to popular perception, these results suggest that the subtropical South Atlantic Ocean generates a non-negligible amount of precipitation events over Windhoek. Therefore the influence of the subtropical South

Atlantic Ocean on southern African precipitation and climate could currently be underestimated. At the same time, $\delta'^{17}O$-$\delta'^{18}O$ in conjunction with HYSPLIT back trajectories identified four precipitation source clusters. Two of these cluster sources were consistent with the positions of the Indian Ocean dipole and the subtropical Indian Ocean dipole while the remaining clusters had similar origins in the subtropical South Atlantic Ocean, consistent with simulations of a possible dipole in the subtropical South Atlantic Ocean (Nnamchi et al. 2011). If such a dipole exists, this could influence precipitation over southern Africa and understanding it would improve forecasting efforts over the region or at least Windhoek and parts of South Africa. $\delta'^{17}O$-$\delta'^{18}O$ appeared a much better tracer of environmental conditions at the evaporation site than *d* which was significantly influenced by meteorological conditions at the precipitation site. At the same time, $\delta'^{17}O$-$\delta'^{18}O$ appeared to reflect differences between El Niño and non-El Niño related droughts, suggesting $\delta'^{17}O$-$\delta'^{18}O$ could be a novel tool to differentiate drought causes; synoptic vs. mesoscale, respectively. Finally, the temporal isotope variability exhibited by this semi-arid site compared to tropical sites suggests pan-tropical mechanisms may be controlling precipitation isotope compositions but the nature of this mechanism(s) we believe is still elusive.

References

Aggarwal, Pradeep K, Ulrike Romatschke, Luis Araguas-Araguas, Dagnachew Belachew, Frederick J Longstaffe, Peter Berg, Courtney Schumacher, and Aaron Funk. 2016. "Proportions of convective and stratiform precipitation revealed in water isotope ratios." *Nature Geoscience* 9 (8):624-629.

Allan, RJ, CJC Reason, JA Lindesay, and TJ Ansell. 2003. "Protracted'ENSO episodes and their impacts in the Indian Ocean region." *Deep Sea Research Part II: Topical Studies in Oceanography* 50 (12):2331-2347.

Alley, Richard B, and Kurt M Cuffey. 2001. "Oxygen-and hydrogen-isotopic ratios of water in precipitation: beyond paleothermometry." *Reviews in Mineralogy and Geochemistry* 43 (1):527-553.

Angert, Alon, Christopher D Cappa, and Donald J DePaolo. 2004. "Kinetic ^{17}O effects in the hydrologic cycle: Indirect evidence and implications." *Geochimica et cosmochimica acta* 68 (17):3487-3495.

Araguás-Araguás, L, K. Froehlich, and K. Rozanski. 2000. "Deuterium and $\delta^{18}O$ isotope composition of precipitation and atmospheric moisture." *Hydrological Processes* 14 (8):1341-1355.

Baldini, Lisa M, Frank McDermott, James UL Baldini, Matthew J Fischer, and Martin Möllhoff. 2010. "An investigation of the controls on Irish precipitation $\delta^{18}O$ values on monthly and event timescales." *Climate dynamics* 35 (6):977-993.

Barkan, Eugeni, and Boaz Luz. 2007. "Diffusivity fractionations of $H_2{}^{16}O/H_2{}^{17}O$ and $H_2{}^{16}O/ H_2{}^{18}O$ in air and their implications for isotope hydrology." *Rapid Communications in Mass Spectrometry* 21:2999-3005.

Barras, Vaughan JI, and Ian Simmonds. 2008. "Synoptic controls upon δ18O in southern Tasmanian precipitation." *Geophysical Research Letters* 35 (2).

Barras, Vaughan, and Ian Simmonds. 2009. "Observation and modeling of stable water isotopes as diagnostics of rainfall dynamics over southeastern Australia." *J. Geophys. Res.* 114 (D23):D23308. doi: 10.1029/2009jd012132.

Behera, Swadhin K, and Toshio Yamagata. 2001. "Subtropical SST dipole events in the southern Indian Ocean." *Geophysical Research Letters* 28 (2):327-330.

Benson, Larry, and Harold Klieforth. 1989. "Stable isotopes in precipitation and ground water in the Yucca Mountain region, southern Nevada: Paleoclimatic implications." *Aspects of Climate Variability in the Pacific and the western Americas*:41-59.

Berkelhammer, M, L Stott, K Yoshimura, K Johnson, and A Sinha. 2012. "Synoptic and mesoscale controls on the isotopic composition of precipitation in the western United States." *Climate dynamics* 38 (3-4):433-454.

Bowen, G. J. 2017. "The Online Isotopes in Precipitation Calculator." http://www.waterisotopes.org.

Bowen, GJ, and J Revenaugh. 2003. "Interpolating the isotopic composition of modern meteoric precipitation." *Water Resources Research* 39:1299, doi:10.129/2003WR002086.

Burnett, Adam W, Henry T Mullins, and William P Patterson. 2004. "Relationship between atmospheric circulation and winter precipitation $\delta^{18}O$ in central New York State." *Geophysical research letters* 31 (22).

Conway, Declan, Emma Archer Van Garderen, Delphine Deryng, Steve Dorling, Tobias Krueger, Willem Landman, Bruce Lankford, Karen Lebek, Tim Osborn, and Claudia Ringler. 2015. "Climate and southern Africa's water-energy-food nexus." *Nature Climate Change* 5 (9):837-846.

Coplen, Tyler B, Paul J Neiman, Allen B White, and F Martin Ralph. 2015. "Categorisation of northern California rainfall for periods with and without a radar brightband using stable isotopes and a novel automated precipitation collector." *Tellus B: Chemical and Physical Meteorology* 67 (1):28574.

CPC. 2016. "Oceanic Nino Index (ONI)." Climate Prediction Center. http://www.cpc.ncep.noaa.gov/products/analysis_monitoring/ensostuff/ensoyears.shtml.

Crawford, Jagoda, Catherine E Hughes, and Spyros Lykoudis. 2014. "Alternative least squares methods for determining the meteoric water line, demonstrated using GNIP data." *Journal of hydrology* 519:2331-2340.

Crawford, Jagoda, Catherine E Hughes, and Stephen D Parkes. 2013. "Is the isotopic composition of event based precipitation driven by moisture source or synoptic scale weather in the Sydney Basin, Australia?" *Journal of hydrology* 507:213-226.

D'Abreton, PC, and JA Lindesay. 1993. "Water vapour transport over southern Africa during wet and dry early and late summer months." *International Journal of Climatology* 13 (2):151-170.

Dansgaard, W. 1964. "Stable isotopes in precipitation." *Tellus, 16*:436-468.

Ehhalt, D, K Knott, JF Nagel, and JC Vogel. 1963. "Deuterium and $\delta^{18}O$ in rain water." *Journal of Geophysical Research* 68 (13):3775-3780.

Fauchereau, Nicolas, S Trzaska, Yves Richard, Pascal Roucou, and Pierre Camberlin. 2003. "Sea-surface temperature co-variability in the Southern Atlantic and Indian Oceans and its connections with the atmospheric circulation in the Southern Hemisphere." *International Journal of Climatology* 23 (6):663-677.

Field, Robert D. 2010. "Observed and modeled controls on precipitation $\delta^{18}O$ over Europe: From local temperature to the Northern Annular Mode." *Journal of Geophysical Research: Atmospheres* 115 (D12).

Fricke, Henry C, and James R O'Neil. 1999. "The correlation between $^{18}O/^{16}O$ ratios of meteoric water and surface temperature: its use in investigating terrestrial climate change over geologic time." *Earth and Planetary Science Letters* 170 (3):181-196.

Friedman, Irving, Joyce M Harris, George I Smith, and Craig A Johnson. 2002. "Stable isotope composition of waters in the Great Basin, United States 1. Air-mass trajectories." *Journal of Geophysical Research: Atmospheres* 107 (D19).

Fudeyasu, Hironori, Kimpei Ichiyanagi, Kei Yoshimura, Shuichi Mori, Jun-Ichi Hamada, Namiko Sakurai, Manabu D Yamanaka, Jun Matsumoto, and Fadli Syamsudin. 2011. "Effects of large-scale moisture transport and mesoscale processes on precipitation isotope ratios observed at Sumatera, Indonesia." *Journal of the Meteorological Society of Japan. Ser. II* 89:49-59.

Funk, Aaron, Courtney Schumacher, and Jun Awaka. 2013. "Analysis of rain classifications over the tropics by version 7 of the TRMM PR 2A23 algorithm." *Journal of the Meteorological Society of Japan. Ser. II* 91 (3):257-272.

Gat, J. R., and I. Carmi. 1970. "Evolution of the isotopic composition of atmospheric waters in the Mediterranean Sea area." *Journal of Geophysical Research* 75 (15):3039-3048. doi: 10.1029/JC075i015p03039.

Gat, JR. 1996. "Oxygen and hydrogen isotopes in the hydrologic cycle." *Annual Review of Earth and Planetary Sciences* 24:225–262.

Gat, JR, and E Matsui. 1991. "Atmospheric water balance in the Amazon Basin: an isotopic evapotranspiration model." *Journal of Geophysical Research: Atmospheres* 96 (D7):13179-13188.

Hammer, Ø., Harper, D.A.T, Ryan, P.D. 2001. "PAST: Paleontological statistics software package for education and data analysis." *Palaeontologia Electronica* 4 (1):9.

Harris, C , C Burgers, J Miller, and F Rawoot. 2010. "O- and H-isotope record of Cape Town rainfall from 1996 to 2008, and its application to recharge studies of Table mountian groundwater, South Africa." *South African Journal of Geology* 113:33-56

Hermes, JC, and CJC Reason. 2005. "Ocean model diagnosis of interannual coevolving SST variability in the South Indian and South Atlantic Oceans." *Journal of Climate* 18 (15):2864-2882.

Hoell, Andrew, Chris Funk, Jens Zinke, and Laura Harrison. 2016. "Modulation of the Southern Africa precipitation response to the El Niño Southern Oscillation by the subtropical Indian Ocean Dipole." *Climate Dynamics*:1-12.

Houze Jr, Robert A. 2014. *Cloud dynamics*. Vol. 104: Academic press.

Hulston, JR, and HG Thode. 1965. "Variations in the S^{33}, S^{34}, and S^{36} contents of meteorites and their relation to chemical and nuclear effects." *Journal of Geophysical Research* 70 (14):3475-3484.

Jouzel, Jean, Gilles Delaygue, Amaëlle Landais, Valérie Masson-Delmotte, Camille Risi, and Françoise Vimeux. 2013. "Water isotopes as tools to document oceanic sources of precipitation." *Water Resources Research* 49 (11):7469-7486.

Kaseke, Kudzai Farai, Lixin Wang, and Mary K Seely. 2017. "Nonrainfall water origins and formation mechanisms." *Science Advances* 3 (3):e1603131.

Kaseke, Kudzai Farai, Lixin Wang, Heike Wanke, Veronika Turewicz, and Paul Koeniger. 2016. "An Analysis of Precipitation Isotope Distributions across Namibia Using Historical Data." *PloS one* 11 (5). doi: http://dx.doi.org/10.1371/journal.pone.0154598.

Kazmierz Rozanski, Luis Araguas-Araguas, and Roberto Gonftanttni. 1993. "Isotopic Patterns in Modern Global Precipitation."

Kurita, Naoyuki. 2013. "Water isotopic variability in response to mesoscale convective system over the tropical ocean." *Journal of Geophysical Research: Atmospheres* 118 (18).

Läderach, Alexander, and Harald Sodemann. 2016. "A revised picture of the atmospheric moisture residence time." *Geophysical Research Letters* 43 (2):924-933.

Lai, C. T., and J. R. Ehleringer. 2011. "Deuterium excess reveals diurnal sources of water vapor in forest air." *Oecologia* 165 (1):213-223.

Landais, A, E Barkan, D Yakir, and B Luz. 2006. "The triple isotopic composition of oxygen in leaf water." *Geochimica et cosmochimica acta* 70 (16):4105-4115.

Lawrence, Mark G. 2005. "The relationship between relative humidity and the dewpoint temperature in moist air: A simple conversion and applications." *Bulletin of the American Meteorological Society* 86 (2):225-233.

Lee, Jung-Eun, Inez Fung, Donald J DePaolo, and Cara C Henning. 2007. "Analysis of the global distribution of water isotopes using the NCAR atmospheric general circulation model." *Journal of Geophysical Research: Atmospheres* 112 (D16).

Lewis, SC, AN LeGrande, M Kelley, and GA Schmidt. 2010. "Water vapour source impacts on oxygen isotope variability in tropical precipitation during Heinrich events." *Climate of the Past* 6 (3):325.

Li, Shuning, Naomi E Levin, and Lesley A Chesson. 2015. "Continental scale variation in 17 O-excess of meteoric waters in the United States." *Geochimica et Cosmochimica Acta* 164:110-126.

Li, Shuning, Naomi E Levin, Keir Soderberg, Kate J Dennis, and Kelly K Caylor. 2017. "Triple oxygen isotope composition of leaf waters in Mpala, central Kenya." *Earth and Planetary Science Letters* 468:38-50.

Liu, J., G. Fu, X. Song, S. P. Charles, Y. Zhang, D. Han, and S. Wang. 2010. "Stable isotopic compositions in Australian precipitation." *Journal of Geophysical Research D: Atmospheres* 115 (23).

Liu, Jianrong, Xianfang Song, Guobin Fu, Xin Liu, Yinghua Zhang, and Dongmei Han. 2011. "Precipitation isotope characteristics and climatic controls at a continental and an island site in Northeast Asia." *Climate Research* 49 (1):29-44.

Lu, Xuefei, Lixin Wang, Ming Pan, Kudzai F Kaseke, and Bonan Li. 2016. "A multi-scale analysis of Namibian rainfall over the recent decade–comparing TMPA satellite estimates and ground observations." *Journal of Hydrology: Regional Studies* 8:59-68.

Luz, Boaz, and Eugeni Barkan. 2005. "The isotopic ratios $^{17}O/^{16}O$ and $^{18}O/^{16}O$ in molecular oxygen and their significance in biogeochemistry." *Geochimica et Cosmochimica Acta* 69 (5):1099-1110.

Martinelli, Luiz Antonio, Reynaldo Luiz Victoria, Leonel Silveira Lobo Sternberg, Aristides Ribeiro, and Marcelo Zacharias Moreira. 1996. "Using stable isotopes to determine sources of evaporated water to the atmosphere in the Amazon basin." *Journal of hydrology* 183 (3):191-204.

Mazzarella, A, A Giuliacci, and N Scafetta. 2013. "Quantifying the Multivariate ENSO Index (MEI) coupling to CO2 concentration and to the length of day variations." *Theoretical and applied climatology* 111 (3-4):601-607.

Merlivat, Liliane, and Jean Jouzel. 1979. "Global Climatic Interpretation of the Deuterium-18O Relationship for Precipitation." *J. Geophys. Res.* 84:5029-5033. doi: 10.1029/JC084iC08p05029.

Miller, Martin F. 2002. "Isotopic fractionation and the quantification of ^{17}O anomalies in the oxygen three-isotope system: an appraisal and geochemical significance." *Geochimica et Cosmochimica Acta* 66 (11):1881-1889.

Miralles, Diego G, Raquel Nieto, Nathan G McDowell, Wouter A Dorigo, Niko EC Verhoest, Yi Y Liu, Adriaan J Teuling, A Johannes Dolman, Stephen P Good, and Luis Gimeno. 2016. "Contribution of water-limited ecoregions to their own supply of rainfall." *Environmental Research Letters* 11 (12):124007.

Moyo, Elisha N, and Shingirai S Nangombe. 2015. "Southern Africa's 2012–13 violent storms: role of climate change." *Procedia IUTAM* 17:69-78.

Munday, Callum, and Richard Washington. 2017. "Circulation controls on southern African precipitation in coupled models: The role of the Angola Low." *Journal of Geophysical Research: Atmospheres* 122 (2):861-877.

Nicholson, Sharon E, and Dara Entekhabi. 1986. "The quasi-periodic behavior of rainfall variability in Africa and its relationship to the Southern Oscillation." *Meteorology and Atmospheric Physics* 34 (3):311-348.

Nnamchi, Hyacinth C, and Jianping Li. 2011. "Influence of the South Atlantic Ocean dipole on West African summer precipitation." *Journal of Climate* 24 (4):1184-1197.

Nnamchi, Hyacinth C, Jianping Li, and Raymond NC Anyadike. 2011. "Does a dipole mode really exist in the South Atlantic Ocean?" *Journal of Geophysical Research: Atmospheres* 116 (D15).

NOAA. 2016. "Multivariate El Niño Southern Oscillation (MEI) Index ". National Oceanic and Atmospheric Administration (NOAA). https://www.esrl.noaa.gov/psd/enso/mei/table.html.

Noone, David, and I Simmonds. 2002. "Associations between δ 18O of water and climate parameters in a simulation of atmospheric circulation for 1979–95." *Journal of Climate* 15 (22):3150-3169.

OOPC. 2016. "South Wester Indian Ocean (SWIO) SST." Ocean Observations Panel for Climate http://stateoftheocean.osmc.noaa.gov/sur/ind/swio.php.

OOPC. 2017. "South Atlantic Tropical (SAT) SST index." Ocean Observations Panel for Climate. http://stateoftheocean.osmc.noaa.gov/sur/atl/sat.php.

Rao, Rokkam R, Robert L Molinari, and John F Festa. 1989. "Evolution of the climatological near-surface thermal structure of the tropical Indian Ocean: 1. Description of mean monthly mixed layer depth, and sea surface temperature, surface current, and surface meteorological fields." *Journal of Geophysical Research: Oceans* 94 (C8):10801-10815.

Reason, Chris JC, and Sandi Smart. 2015. "Tropical south east Atlantic warm events and associated rainfall anomalies over southern Africa." *Frontiers in Environmental Science* 3:24.

Reason, CJC. 2001. "Subtropical Indian Ocean SST dipole events and southern African rainfall." *Geophysical Research Letters* 28 (11):2225-2227.

Reason, CJC. 2002. "Sensitivity of the southern African circulation to dipole sea-surface temperature patterns in the south Indian Ocean." *International Journal of Climatology* 22 (4):377-393.

Reason, CJC, and D Jagadheesha. 2005. "Relationships between South Atlantic SST variability and atmospheric circulation over the South African region during austral winter." *Journal of Climate* 18 (16):3339-3355.

Reason, CJC, W Landman, and W Tennant. 2006. "Seasonal to decadal prediction of southern African climate and its links with variability of the Atlantic Ocean." *Bulletin of the American Meteorological Society* 87 (7):941-955.

Reason, CJC, and H Mulenga. 1999. "Relationships between South African rainfall and SST anomalies in the southwest Indian Ocean." *International Journal of Climatology* 19 (15):1651-1673.

Reason, CJC, and M Rouault. 2002. "ENSO-like decadal variability and South African rainfall." *Geophysical Research Letters* 29 (13).

Richard, Y, S Trzaska, P Roucou, and M Rouault. 2000. "Modification of the southern African rainfall variability/ENSO relationship since the late 1960s." *Climate Dynamics* 16 (12):883-895.

Rindsberger, M, M Magaritz, I Carmi, and D Gilad. 1983. "The relation between air mass trajectories and the water isotope composition of rain in the Mediterranean Sea area." *Geophysical Research Letters* 10 (1):43-46.

Risi, Camille, Sandrine Bony, and Françoise Vimeux. 2008. "Influence of convective processes on the isotopic composition (δ18O and δD) of precipitation and water vapor in the tropics: 2. Physical interpretation of the amount effect." *Journal of Geophysical Research: Atmospheres (1984–2012)* 113 (D19).

Risi, Camille, Sandrine Bony, Françoise Vimeux, and Jean Jouzel. 2010. "Water-stable isotopes in the LMDZ4 general circulation model: Model evaluation for present-day and past climates and applications to climatic interpretations of tropical isotopic records." *J. Geophys. Res.* 115 (D12):D12118. doi: 10.1029/2009jd013255.

Romps, David M. 2017. "Exact Expression for the Lifting Condensation Level." *Journal of the Atmospheric Sciences* 74 (12):3891-3900.

Rouault, M. 2003. "Southeast Atlantic warm events and southern african rainfall." EGS-AGU-EUG Joint Assembly.

Salamalikis, V, AA Argiriou, and E Dotsika. 2016. "Isotopic modeling of the sub-cloud evaporation effect in precipitation." *Science of the Total Environment* 544:1059-1072.

Sánchez-Murillo, Ricardo, Christian Birkel, Kristen Welsh, Germain Esquivel-Hernández, J Corrales-Salazar, Jan Boll, E Brooks, Olivier Roupsard, O Sáenz-Rosales, and Irina Katchan. 2016. "Key drivers controlling stable isotope variations in daily precipitation of Costa Rica: Caribbean Sea versus Eastern Pacific Ocean moisture sources." *Quaternary Science Reviews* 131:250-261.

Sánchez-Murillo, Ricardo, Ana M Durán-Quesada, Christian Birkel, Germain Esquivel-Hernández, and Jan Boll. 2017. "Tropical precipitation anomalies and d-excess evolution during El Niño 2014-16." *Hydrological Processes* 31 (4):956-967.

SASSCAL. 2017. Southern Africa Science Service Centre for Climate Change and Adaptive Land-use

Schmidt, Gavin A, Georg Hoffmann, Drew T Shindell, and Yongyun Hu. 2005. "Modeling atmospheric stable water isotopes and the potential for constraining cloud processes and stratosphere-troposphere water exchange." *Journal of Geophysical Research: Atmospheres* 110 (D21).

Schumacher, Courtney, and Robert A Houze Jr. 2003. "Stratiform rain in the tropics as seen by the TRMM precipitation radar*." *Journal of Climate* 16 (11):1739-1756.

Shie, C-L, W-K Tao, and J Simpson. 2006. "A note on the relationship between temperature and water vapor over oceans, including sea surface temperature effects." *Advances in Atmospheric Sciences* 23 (1):141-148.

Sinclair, KE, SJ Marshall, and TA Moran. 2011. "A Lagrangian approach to modelling stable isotopes in precipitation over mountainous terrain." *Hydrological Processes* 25 (16):2481-2491.

Sjostrom, Derek J, and Jeffrey M Welker. 2009. "The influence of air mass source on the seasonal isotopic composition of precipitation, eastern USA." *Journal of Geochemical Exploration* 102 (3):103-112.

Soderberg, Keir, Stephen P. Good, Molly O'Connor, Lixin Wang, Kathleen Ryan, and Kelly K. Caylor. 2013. "Using atmospheric trajectories to model the isotopic composition of rainfall in central Kenya." *Ecosphere* 4 (3):art33. doi: 10.1890/ES12-00160.1.

Stein, AF, RR Draxler, GD Rolph, BJB Stunder, MD Cohen, and F Ngan. 2015. "NOAA's HYSPLIT atmospheric transport and dispersion modeling system." *Bulletin of the American Meteorological Society* 96 (12):2059-2077.

Steiner, Matthias, and James A Smith. 1998. "Convective versus stratiform rainfall: An ice-microphysical and kinematic conceptual model." *Atmospheric research* 47:317-326.

Stewart, Michael K. 1975. "Stable isotope fractionation due to evaporation and isotopic exchange of falling waterdrops: Applications to atmospheric processes and evaporation of lakes." *Journal of Geophysical Research* 80 (9):1133-1146.

Stumpp, C, J Klaus, and W Stichler. 2014. "Analysis of long-term stable isotopic composition in German precipitation." *Journal of Hydrology* 517:351-361.

Sturm, Christophe, Qiong Zhang, and David Noone. 2010. "An introduction to stable water isotopes in climate models: benefits of forward proxy modelling for paleoclimatology." *Climate of the Past* 6 (1):115-129.

Sturm, M, M Zimmermann, K Schütz, W Urban, and H Hartung. 2009. "Rainwater harvesting as an alternative water resource in rural sites in central northern Namibia." *Physics and Chemistry of the Earth, Parts A/B/C* 34 (13):776-785.

Terzer, S, LI Wassenaar, LJ Araguás-Araguás, and PK Aggarwal. 2013. "Global isoscapes for δ 18 O and δ 2 H in precipitation: improved prediction using regionalized climatic regression models." *Hydrology and Earth System Sciences* 17 (11):4713-4728.

Tian, C., Wang, L. and Novick, K. A. 2016. "Water vapor δ^2H, $\delta^{18}O$ and $\delta^{17}O$ measurements using an off-axis integrated cavity output spectrometer – sensitivity

to water vapor concentration, delta value and averaging-time." *Rapid Communications in Mass Spectrometry*:doi: 10.1002/rcm.7714.

Treble, PC, WF Budd, PK Hope, and PK Rustomji. 2005. "Synoptic-scale climate patterns associated with rainfall δ 18 O in southern Australia." *Journal of Hydrology* 302 (1):270-282.

Trenberth, Kevin E. 1998. "Atmospheric moisture residence times and cycling: Implications for rainfall rates and climate change." *Climatic change* 39 (4):667-694.

Victoria, Reynaldo L, Luiz A Martinelli, Jefferson Mortatti, and Jeffrey Richey. 1991. "Mechanisms of water recycling in the Amazon Basin: isotopic insights." *Ambio*:384-387.

Vimeux, Françoise, Robert Gallaire, Sandrine Bony, Georg Hoffmann, and John CH Chiang. 2005. "What are the climate controls on δD in precipitation in the Zongo Valley (Bolivia)? Implications for the Illimani ice core interpretation." *Earth and Planetary Science Letters* 240 (2):205-220.

Vuille, M, Raymond S Bradley, Martin Werner, R Healy, and F Keimig. 2003. "Modeling δ18O in precipitation over the tropical Americas: 1. Interannual variability and climatic controls." *Journal of Geophysical Research: Atmospheres* 108 (D6).

Wang, Lixin, Kelly Caylor, and Danilo Dragoni. 2009. "On the calibration of continuous, high-precision $\delta^{18}O$ and $\delta^{2}H$ measurements using an off-axis integrated cavity output spectrometer " *Rapid Communications in Mass Spectrometry* 23:530-536. doi: 10.1002/rcm.3905.

Wang, Shengjie, Mingjun Zhang, Yanjun Che, Xiaofan Zhu, and Xuemei Liu. 2016. "Influence of below-cloud evaporation on deuterium excess in precipitation of arid central Asia and its meteorological controls." *Journal of Hydrometeorology* 17 (7):1973-1984.

Welp, Lisa R., Xuhui Lee, Timothy J. Griffis, Xue-Fa Wen, Wei Xiao, Shenggong Li, Xiaomin Sun, Zhongmin Hu, Maria Val Martin, and Jianping Huang. 2012. "A meta-analysis of water vapor deuterium-excess in the midlatitude atmospheric surface layer." *Global Biogeochem. Cycles* 26 (3):GB3021. doi: 10.1029/2011gb004246.

Werner, Martin, Petra M Langebroek, Tim Carlsen, Marcus Herold, and Gerrit Lohmann. 2011. "Stable water isotopes in the ECHAM5 general circulation model: Toward high-resolution isotope modeling on a global scale." *Journal of Geophysical Research: Atmospheres* 116 (D15).

Wu, Huawu, Xinping Zhang, Li Xiaoyan, Guang Li, and Yimin Huang. 2015. "Seasonal variations of deuterium and oxygen-18 isotopes and their response to moisture source for precipitation events in the subtropical monsoon region." *Hydrological Processes* 29 (1):90-102.

Yurtsever, Yo. 1975. "Worldwide survey of stable isotopes i precipitation." *Rep. Sect. Isotope Hydrol., IAEA*.

Zhao, L, Lixin Wang, X Liu, H Xiao, Y Ruan, and M Zhou. 2014. "The patterns and implications of diurnal variations in the d-excess of plant water, shallow soil water and air moisture." *Hydrology and Earth System Sciences* 18 (10):4129-4151.

Zhao, Liangju, Honglang Xiao, Maoxian Zhou, Guodong Cheng, Lixin Wang, Li Yin, and Juan Ren. 2012. "Factors controlling spatial and seasonal distributions of precipitation $\delta^{18}O$ in China." *Hydrological Processes* 26 (1):143-152. doi: 10.1002/hyp.8118

CHAPTER 7: CONCLUSIONS

Stable water isotopes ($\delta^{18}O$, $\delta^{2}H$ and $\delta^{17}O$) are important tools that aide our understanding of dryland ecohydrological processes. We demonstrate for the first time, using novel isotope methods ($\delta^{17}O$ vs. $\delta^{18}O$), that fog and dew can be differentiated based on their different isotope fractionation processes. This distinction is important because vegetation may be differentially adapted to harvesting fog and dew (Roth-Nebelsick et al. 2012, Ebner et al. 2011, Esler et al. 1999), thus the increase of one of these components does not necessarily translate to the same species composition or distribution. These results suggest that fog and dew components in ecological models predicting the potential impact of global climate change in non-rainfall dominated ecosystems, should be considered separately.

It is generally assumed that advective fog is the architect of the Namib fog-zone, but isotope results suggest that multiple fog and dew types occur regularly in this area. Furthermore, groundwater may be recycled via evapotranspiration and redistributed in the upper few cm of the soil profile as fog and dew, where it becomes available to fauna and flora unable to directly tap into the groundwater. Therefore, the importance of groundwater in these dryland environments could be underestimated. The results also suggest a potential advection-radiation fog shift along the edges of the Namib fog-zone. Extension of fog up to 60 km inland, in the Central Namib Desert, could be related to evapotranspiration from the Kuiseb and Swakop Rivers as well as mixed and radiation fog formed in the area. If this advection-radiation shift hypothesis is true, then this might result in lower fog frequency, biodiversity and a shift in species composition and distribution along the current edge of the fog-zone. This is because radiation fog is spatially variable and its dominance along the edge of the fog-zone is probably related to a decrease in advective fog than an increase in radiation fog frequency. Consequently, fog input to the area is decreasing with frequency dropping 56% from 2001 (Henschel and Seely 2008) to the time of this study and is predicted to continue decreasing in the future due to global climate change (Haensler et al. 2011). In addition, radiation fog is confined to topographic lows and ephemeral channels (Eckardt et al. 2013), while fauna such as the fog-harvesting beetle (*Onymacris unguicularis*) position themselves on dune crests to harvest fog. Reports from the Gobabeb

Training and Research Centre corroborate this, suggesting *Onymacris unguicularis* range may be shifting closer to the coast. Furthermore, what may appear as a single fog event over the Central Namib Desert might actually consist of multiple fog types i.e., advective, mixed and radiation.

Fog and dew may be exploited as supplementary water resources and average yields could be improved substantially by adoption of materials designed specifically for fog and dew harvesting. However, we urge caution on potability of this water and advise trace metal and biological analyses before use, as these two tests are often ignored and yet they could be of major concern when fog and dew are considered. Fog and dew scrub atmospheric pollutants and when coupled with their acidity, may result in elevated trace metal concentrations that may be of concern to human health (Sträter et al. 2010). At the same time, by their nature as open collection water systems are prone to biological contamination. However, there are simple measures that can be taken to address these concerns without significantly impacting the cost of potable water from these systems (Sharan et al. 2017, Schemenauer and Cereceda 1992). For example, liming to increase pH, use of filters and disinfection (Muselli et al. 2006, Sträter et al. 2010, Sharan et al. 2017). After these corrective measures, we believe fog and dew to be potable and could play an important role in dryland systems, supplementing existing water resources. At the same time, the efficiency of fog and dew harvesting projects could be improved significantly by adopting materials and designs designed specifically for these tasks.

Despite the potential of fog and dew as potable water resources, they will likely always play a supplementary role to traditional water resources. Therefore, even though non-rainfall water harvesting may ameliorate water scarcity, there is need to understand precipitation patterns and controls in drylands as this is the main source of water even though unpredictable. Global isoscapes do not scale down well or capture local variations in data scarce regions but reflect global trends. Therefore, their application to drylands and developing nations should be treated with caution. However, these regions may have historical precipitation isotope data that may be used to generate isoscapes based on arithmetic means (Dutton et al. 2005). Although, absolute values generated from this method are questionable, the trends and variations were consistent with synoptic weather patterns that influence precipitation over the region and the country. This suggests that the

value of historical data and locally generated isoscapes is in deciphering trends and not absolute values. The results also suggest relative humidity and elevation as the key drivers of precipitation isotopes across Namibia, consistent with the classification of the country as semi-arid to arid climate. The locally generated isoscape also suggested that the Atlantic Ocean may contribute significantly to precipitation over Namibia and Southern Africa, in contrast to the accepted narrative where contributions are generally considered negligible.

Backward trajectory analyses of precipitation events over Windhoek was consistent with the local isoscape, which suggesting 21% of precipitation between 2012 and 2016 originated from the Atlantic Ocean. Interestingly, these precipitation events originated from the same region, subtropical Atlantic Ocean, consistent with an area of warming simulated by Nnamchi et al. (2011). These results therefore suggest the existence of a sub-tropical Atlantic Ocean dipole that may influence precipitation over Windhoek, Cape Town and possibly southern Africa. These results also suggest that the subtropical Indian Ocean may be the major source of precipitation events over southern Africa, at least Windhoek, in contrast to earlier studies which suggest the tropical Indian Ocean as the dominant source (D'Abreton and Lindesay 1993, Reason and Mulenga 1999). Similar to the locally generated precipitation isoscapes, relative humidity was the most significant isotope driver. However, multiple regression analysis suggests that 47-53% of $\delta^{18}O$, $\delta^{2}H$ and $\delta^{17}O$ variability and 55% of *d* variability was related to local meteorological conditions. Thus *d* cannot be regarded as a conservative environmental tracer of evaporation conditions at the origin (Welp et al. 2012, Lai and Ehleringer 2011). However, ^{17}O vs ^{18}O appeared a more conservative tracer of environmental conditions at the source and may be useful in differentiating drought causes: synoptic (El Niño) vs. mesoscale (local).

In conclusion, the use of stable water isotopes to investigate ecohydrological processes in Namibia suggest that multiple fog and dew types occur regularly in the Namib Desert and that the role of groundwater in dryland ecohydrology may be underestimated. Fog is spatially and temporally variable, and what may appear as a single fog event may comprise many different fog types. Fog and dew are controlled by different fractionation processes despite both being condensation reactions. The Atlantic Ocean may play a significant role in determining precipitation patterns in southern Africa, at least Windhoek, in contrast to popular perception. Global isoscapes do not scale down well in drylands and

developing nations, thus caution is advised when applied to these regions. Finally, ^{17}O vs ^{18}O may be a more conservative environmental tracer compared to *d* and may be a useful tool to differentiate different drought causes.

References

D'Abreton, PC, and JA Lindesay. 1993. "Water vapour transport over southern Africa during wet and dry early and late summer months." *International Journal of Climatology* 13 (2):151-170.

Dutton, Andrea, Bruce H Wilkinson, Jeffrey M Welker, Gabriel J Bowen, and Kyger C Lohmann. 2005. "Spatial distribution and seasonal variation in 18O/16O of modern precipitation and river water across the conterminous USA." *Hydrological Processes* 19 (20):4121-4146.

Ebner, M, T Miranda, and A Roth-Nebelsick. 2011. "Efficient fog harvesting by Stipagrostis sabulicola (Namib dune bushman grass)." *Journal of Arid Environments* 75 (6):524-531.

Eckardt, FD, K Soderberg, LJ Coop, AA Muller, KJ Vickery, RD Grandin, C Jack, TS Kapalanga, and J Henschel. 2013. "The nature of moisture at Gobabeb, in the central Namib Desert." *Journal of Arid Environments* 93:7-19.

Esler, Karen J, Phillip W Rundel, and Piet Vorster. 1999. "Biogeography of prostrate-leaved geophytes in semi-arid South Africa: hypotheses on functionality." *Plant Ecology* 142 (1-2):105-120.

Haensler, Andreas, Jan Cermak, Stefan Hagemann, and Daniela Jacob. 2011. "Will the southern African west coast fog be affected by future climate change? Results of an initial fog projection using a regional climate model." *Erdkunde*:261-275.

Henschel, Joh R, and Mary K Seely. 2008. "Ecophysiology of atmospheric moisture in the Namib Desert." *Atmospheric Research* 87 (3):362-368.

Lai, C. T., and J. R. Ehleringer. 2011. "Deuterium excess reveals diurnal sources of water vapor in forest air." *Oecologia* 165 (1):213-223.

Muselli, Marc, Daniel Beysens, Emmanuel Soyeux, and Owen Clus. 2006. "Is dew water potable? Chemical and biological analyses of dew water in Ajaccio (Corsica Island, France)." *Journal of environmental quality* 35 (5):1812-1817.

Nnamchi, Hyacinth C, Jianping Li, and Raymond NC Anyadike. 2011. "Does a dipole mode really exist in the South Atlantic Ocean?" *Journal of Geophysical Research: Atmospheres* 116 (D15).

Reason, CJC, and H Mulenga. 1999. "Relationships between South African rainfall and SST anomalies in the southwest Indian Ocean." *International Journal of Climatology* 19 (15):1651-1673.

Roth-Nebelsick, A, M Ebner, T Miranda, V Gottschalk, D Voigt, S Gorb, T Stegmaier, J Sarsour, M Linke, and W Konrad. 2012. "Leaf surface structures enable the endemic Namib desert grass Stipagrostis sabulicola to irrigate itself with fog water." *Journal of The Royal Society Interface*.

Schemenauer, Robert S, and Pilar Cereceda. 1992. "The quality of fog water collected for domestic and agricultural use in Chile." *Journal of Applied Meteorology* 31 (3):275-290.

Sharan, Girja, Anil Kumar Roy, Laurent Royon, Anne Mongruel, and Daniel Beysens. 2017. "Dew plant for bottling water." *Journal of Cleaner Production* 155:83-92.

Sträter, Ellen, Anna Westbeld, and Otto Klemm. 2010. "Pollution in coastal fog at Alto Patache, Northern Chile." *Environmental Science and Pollution Research* 17 (9):1563-1573.

Welp, Lisa R., Xuhui Lee, Timothy J. Griffis, Xue-Fa Wen, Wei Xiao, Shenggong Li, Xiaomin Sun, Zhongmin Hu, Maria Val Martin, and Jianping Huang. 2012. "A meta-analysis of water vapor deuterium-excess in the midlatitude atmospheric surface layer." *Global Biogeochem. Cycles* 26 (3):GB3021. doi: 10.1029/2011gb004246

CHAPTER 8: SUPPLEMENTAL MATERIALS

Appendix A: Non-rainfall water origins and formation mechanisms

Note A2.1: Wind direction and speed measurements.

Automatic wind measurements started in November 2015 therefore we made use of manual observations made three times daily at 08:00hrs, 14:00hrs and 20:00hrs. Kaseke *et al*. *2012* shows that fog and dew moisture advected to the site lags behind that of a site (Kleinberg) west of Gobabeb Research and Training Centre. Based on this, we made the assumption that relatively high wind speeds with a general westerly wind direction at 20:00hrs should give a general indication of the source of advective fog and dew observed at the study site. Kaseke *et al*. 2012 also shows that dew formation at the site generally occurs between 04:00 – 07:00hrs, therefore we made the assumption that wind direction at 08:00hrs generally reflects the source of locally derived fog and dew and that the speed would be generally low. Because mixed fog is a combination of both the advected and local moisture, we made the assumption that both observations at 20:00hrs and 08:00hrs were equally important thus we averaged the two (Table A2.2). We acknowledge the uncertainty of the wind data due to lack of automatic instrumentation; however, we present this data as an additional line of evidence to verify our fog and dew classification (methods).

In general advective fog originated from the south-west (median 230°), mixed fog from west-south-west (median 260°) while radiation fog originated from south (median 180°) of the site. This data is generally consistent with expectations indicating advective and mixed fog have westerly origins (Atlantic Ocean) while radiation fog originates from a southerly direction consistent with the position of the river at the study site. Wind speeds attributed to advective fog (4.0 ms^{-1}) were higher than both those for mixed (3.8 ms^{-1}) and radiation fog, which is also consistent with expectation. In general, advective dew originated from the south-west (median 205°) while the locally derived dew originated from the south-east (median 166°) (Table A2.2). We expected higher wind speeds would transport moisture to the site resulting in advective dew formation while locally generated dew would have slower speeds or calm conditions. The data generally supports this, 6.5 ms^{-1} vs 2.1 ms^{-1} for advective dew and locally generated dew, respectively (Table A2.2).

Table A2. 1 Isotopic composition and d-excess of individual precipitation events captured during 2014-2015.

Sample ID	Date	$\delta^{18}O$ ‰	$\delta^{2}H$ ‰	$\delta^{17}O$ ‰	*d* ‰
Rain 1	11/02/2014	3.41	30.04	2.62	2.79
Rain 2	13/02/2014	5.28	43.79	3.26	1.58
Rain 3	03/01/2014	1.72	12.05	0.88	-1.72
Rain 4	04/01/2014	-2.63	-32.63	-4.11	-11.57
Rain 5	24/09/2014	3.05	10.37	1.49	-14.02

Table A2. 2 Isotopic composition and classification of individual fog, dew, groundwater and river samples captured between 2014 and 2015. The wind direction (azimuth degrees) and speed (m/s) that may have influenced formation (Note A2.1) are also shown.

ID	$\delta^{18}O$ ‰	$\delta^{2}H$ ‰	$\delta^{17}O$ ‰	Classification	Wind direction	Wind speed	Date
F1	-1.5	-2.14	-0.62	Advective fog	130°	3.0	21-Sep-14
F2	-1.04	-1.12	-0.24	Advective fog	270°	4.0	2-Jan-14
F3	-0.52	+3.01	+0.03	Advective fog	230°	5.0	25-Nov-14
F4	0.00	+10.79	+0.25	Advective fog	180°	5.0	24-Oct-14
F5	-0.07	+7.69	+0.22	Advective fog	270°	3.0	4-Oct-14
F6	-0.49	+4.41	-0.08	Advective fog	180°	5.0	24-Oct-14
F7	-1.94	-7.34	-1.23	Advective fog	230°	5.0	23-Oct-14
F8	-0.94	-0.74	-0.69	Advective fog	230°	2.0	3-Oct-14
F9	-0.98	-0.78	-0.52	Advective fog	130°	6.0	9-Sep-14
F10	-0.33	+5.19	+0.41	Advective fog	230°	2.0	3-Oct-14
F11	-1.08	-2.61	-0.06	Advective fog	180°	6.0	29-Dec-14
F12	-0.97	-0.32	-0.43	Advective fog			
F13	-0.72	+1.04	+0.08	Advective fog	230°	4.0	12-Sep-14
F14	-0.94	-1.11	-0.56	Advective fog	230°	3.0	5-Mar-14
F15	+0.45	+10.42	+0.51	Advective fog			
F16	-0.84	-4.18	-0.81	Mixed fog	180°	3.5	10-Sep-14
F17	-0.43	-0.77	-0.27	Mixed fog	270°	4.5	11-Jan-15

F18	-0.02	+3.35	+0.12	Mixed fog	315°	4.5	7-Jan-15
F19	+0.09	+2.63	+0.08	Mixed fog	335°	6.5	25-Aug-14
F20	+0.54	+9.60	+0.45	Mixed fog	230°	3.5	23-Sep-14
F21	+0.25	+6.00	+0.42	Mixed fog	270°	4.0	23-Mar-14
F22	-1.47	-7.36	-0.86	Mixed fog	140°	3.0	4-Mar-14
F23	-0.82	-2.63	-0.26	Mixed fog	250°	3.0	1-Apr-14
F24	-0.55	-1.35	-0.40	Mixed fog	180°	4.5	25-Jun-14
F25	-1.01	-5.19	-0.80	Mixed fog	270°	3.5	22-Feb-14
F26	+3.89	+22.16	+1.10	Radiation fog (rain)	310°	3.0	29-Sep-14
F27	+3.20	+19.14	+1.84	Radiation fog (rain)	310°	5.0	18-Aug-14
F28	+4.26	+26.54	+2.30	Radiation fog (rain)			
F29	+0.88	+5.56	+1.08	Radiation fog (groundwater)			
F30	+0.98	+7.23	+0.81	Radiation fog (groundwater)	50°	3.0	6-Mar-14
F31	+0.14	+0.15	+0.39	Radiation fog (groundwater)	50°	0.0	22-Jan-14
F32	-0.78	-4.70	-0.21	Radiation fog (groundwater)	360°	4.0	21-Feb-14
F33	-1.31	-10.66	-1.10	Radiation fog (groundwater)	90°	2.0	4-Aug-14
F34	+6.98	+34.05	+3.56	*Radiation fog (groundwater)	130°	2.0	20-Jan-14
F35	+11.42	+56.28	+6.51	*Radiation fog (groundwater)	310°	3.0	29-Nov-14
F36	+10.99	+55.19	+6.16	*Radiation fog (groundwater)	360°	7.0	16-Dec-14
F37	+4.32	+22.67	+2.29	*Radiation fog (groundwater)			

F38	+9.64	+57.90	+4.74	*Radiation fog (groundwater)			
D1	-1.74	-10.73	-1.65	Groundwater sourced dew			28-Dec-13
D2	-2.9	-13.93	-2.07	Groundwater sourced dew	130°	3.0	31-Jul-14
D3	+0.30	+3.20	-0.33	Groundwater sourced dew	50°	2.0	10-Dec-14
D4	-6.76	-28.19	-4.11	Groundwater sourced dew	360°	2.0	16-Oct-14
D5	-3.34	-14.16	-2.10	Groundwater sourced dew	180°	2.0	30-Jul-15
D6	+0.34	+3.08	-0.24	Groundwater sourced dew	130°	2.0	4-Aug-15
D7	+0.88	-10.06	-0.23	Shallow soil sourced dew	230°	2.0	2-Aug-14
D8	+1.75	+1.38	+0.43	Shallow soil sourced dew	90°	2.0	4-Aug-14
D9	+2.24	+1.06	+0.51	Shallow soil sourced dew	130°	2.0	5-Aug-14
D10	-5.51	-37.21	-3.32	Shallow soil sourced dew	230°	1.0	7-Aug-14
D11	-1.17	-19.36	-1.13	Shallow soil sourced dew			
D12	+3.13	+5.60	+1.19	Shallow soil sourced dew	130°	3.0	31-Jul-15
D13	+0.04	+6.68	-0.91	Advective dew	180°	6.0	25-Jul-14
D14	-0.07	+8.72	-0.68	Advective dew	230°	7.0	26-Jul-14
D15	-6.01	-15.62	-3.71	Advective dew			
G1	-9.12	-65.38	-4.89	Shallow groundwater			6-Aug-14
G2	-8.98	-61.05	-4.44	Shallow groundwater			24-Jul-14
G3	-9.62	-64.72	-4.44	Shallow groundwater			5-Aug-15
G4	-9.62	-64.73	-4.40	Shallow groundwater			

G5	-6.67	-46.37	-3.59	Deep groundwater	5-Aug-14
G6	-6.93	-45.40	-3.26	Deep groundwater	6-Aug-15
R1	-11.49	-85.11	-6.51	River water	23-Dec-13

Note: 1. * refers to samples that show evidence of evaporative enrichment.

2. wind speed and direction are manual measurements

3. the river flowed for two days from the 23rd-25th December 2013

Table A2. 3 Monthly rainfall that could have influenced fog and dew formation at Gobabeb Research and Training Centre during the observation period.

	Rainfall amount (mm)		
Month	**2013**	**2014**	**2015**
January	0	2.16	4.93
February	0	7.92	0
March	21.70	0	0
April	0	2.69	0
May	0	0.36	0
June	0	0	0
July	0	0	0
August	0	4.4*	0.44
September	17.97	0.64	0
October	0	0	0.17
November	0	0.13	0
December	1.71	0	8.66

Note: *recorded in a weather station 13 km from the study site.

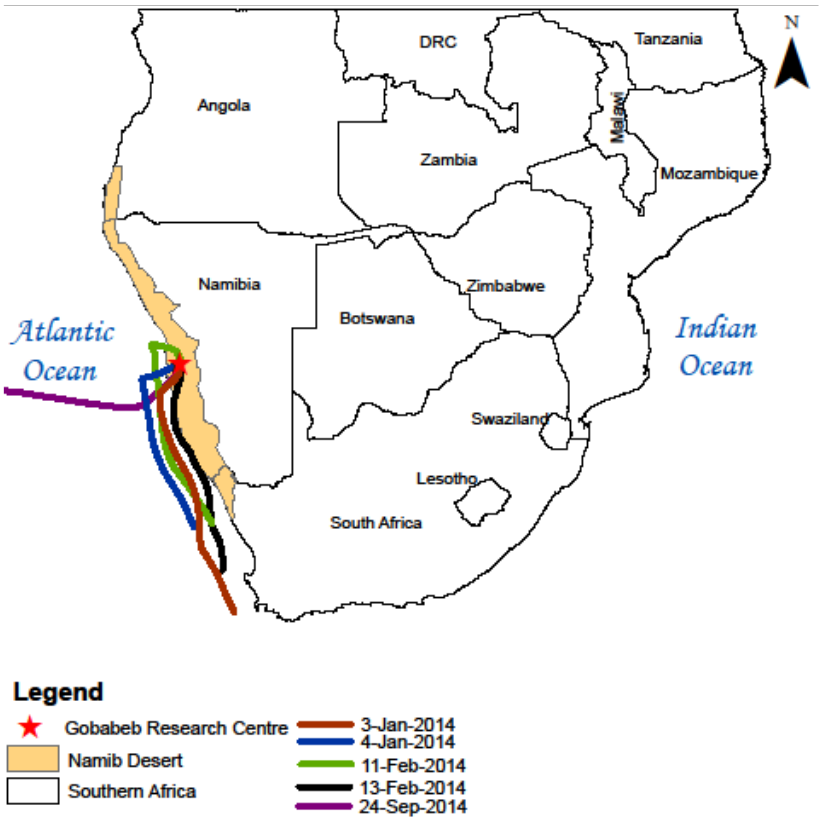

Figure A2. 1 Hybrid Single-Particle Langragian Integrated Trajectory (HYSPLIT) model (Stein, 2015) 48hr backward trajectory analysis of the five precipitation events captured at Gobabeb Research and Training Centre during the observation period.

References

Kaseke, KF, AJ Mills, K Esler, J Henschel, MK Seely, and R Brown. 2012. "Spatial Variation of "Non-Rainfall" Water Input and the Effect of Mechanical Soil Crusts on Input and Evaporation." *Pure and Applied Geophysics* 169 (12):2217-2229.

Stein, AF, RR Draxler, GD Rolph, BJB Stunder, MD Cohen, and F Ngan. 2015. "NOAA's HYSPLIT atmospheric transport and dispersion modeling system." *Bulletin of the American Meteorological Society* 96 (12):2059-2077.

Appendix B: Fog spatial distributions over the Central Namib Desert - an isotope approach.

Table B3. 1 The GPS coordinates of the FogNet (FN) and temporary stations used in the study.

Station name	latitude	longitude
Coastal MET_FN	-23.0563	14.625
Kleinberg_FN	-22.9893	14.7279
Soophies Hoogte_FN	-23.0068	14.8908
Marble koppie_FN	-22.9695	14.9897
Vogelfederberg_FN	-23.08	15.0289
Station 8_FN	-23.2653	15.05563
Aussinanis_FN	-23.4435	15.0459
Gobabeb_FN	-23.5603	15.0404
Station 1	-23.4719	14.97056
Station 2	-23.278	14.76598
Station 3	-23.0344	14.72111
Station 4	-23.0164	14.72389
Station 5	-23.5636	15.02222

Table B3. 2 Isotopic characteristics of fog at each observation site on each day when fog was recorded. The dashes (-) indicate insufficient sample for analysis, n/a indicates no fog was recorded and (*) means the site was not yet established.

	10 June 2016		17 June 2016		18 June 2016		19 June 2016	
ID	**$\delta^{18}O$‰**	**$\delta^{2}H$‰**	**$\delta^{18}O$‰**	**$\delta^{2}H$‰**	**$\delta^{18}O$‰**	**$\delta^{2}H$‰**	**$\delta^{18}O$‰**	**$\delta^{2}H$‰**
MET	-0.50	-5.22	-0.80	-9.82	-0.60	+1.59	-	-
KB	+0.11	+0.58	-1.33	-14.70	-0.70	-0.13	-0.89	-2.95
S3	-0.26	-3.49	-0.87	-12.12	-0.83	-1.15	-1.03	-3.20
S4	-0.37	-3.78	-0.61	-11.92	-0.78	+0.31	-0.67	-2.35
SH	-0.83	-6.73	-2.31	-19.41	-1.92	-11.79	-1.30	-6.91
MK	+0.66	+1.85	+2.02	+7.48	-2.60	-18.33	-1.76	-10.23
VF	-0.11	-2.73	-3.60	-28.19	-4.45	-33.19	-1.99	-15.80
S8	-	-	n/a	n/a	-	-	-0.83	-7.51
AU	+3.03	+22.43	n/a	n/a	+3.94	+9.99	-0.90	-6.97
GBB	-0.76	-0.58	n/a	n/a	-1.31	-14.36	-1.72	-12.14
S5	*	*	n/a	n/a	-0.70	-12.78	-1.40	-13.32
S1	-0.24	-1.02	n/a	n/a	-1.85	-15.83	-1.57	-11.34
S2	-0.15	-1.27	n/a	n/a	-1.29	-8.91	-0.86	-5.52

Note: MET: Coastal MET, KB: Kleinberg, SH: Sophies Hoogte, MK: Marble Koppie, VF: Vogelfederberg, S8: Station 8, AU: Aussinanis, GBB: Gobabeb. S1-S5 are five temporary stations.

Table B3. 3 Average air temperature (°C), soil temperature (°C) at 10 cm depth, relative humidity (RH %), dewpoint temperature (°C), wind speed (m/s) and median wind direction (°) during fog observation hours at each FogNet station on days with observed fog.

10/6/2016	MET	12.2	17.5	100	12.2	1.1	259
	KB	12.6	17.8	100	12.6	1.2	302
	SH	12.5	18.5	99	12.3	1.4	245
	MK	12.4	17.8	98	12.0	1.3	206
	VF	12.4	15.3	98	12.1	2.1	104
	S8	13.6	16.8	94	12.6	2.2	122
	AU	13.5	16.5	95	12.6	2.1	175
	GBB	13.4	18.2	94	12.5	1.4	279
17/06/2016	MET	8.8	15.0	98	8.5	2.3	59
	KB	8.6	15.2	98	8.2	1.7	108
	SH	10.6	16.8	87	8.5	2.2	67
	MK	14.6	16.6	75	10.2	2.1	78
	VF	11.4	12.8	75	7.1	3.2	45
18/06/2016	MET	10.0	15.4	99	9.8	1.1	266
	KB	10.2	16.2	99	10.1	1.9	327
	SH	8.2	15.4	99	8.1	1.4	342
	MK	8.1	14.5	97	7.6	0.8	265
	VF	8.0	11.4	91	6.7	2.0	45
	S8	6.4	12.4	83	3.8	2.0	84
	AU	7.1	11.7	92	5.9	1.5	299
	GBB	7.7	14.5	90	6.1	1.0	115
19/06/2016	MET	9.3	14.3	97	8.9	1.9	171
	KB	8.7	14.5	99	8.6	1.6	142
	SH	8.3	15.5	99	8.1	1.3	289
	MK	7.3	14.0	99	7.1	1.1	268
	VF	7.1	11.0	98	6.9	1.7	226

	S8	6.4	12.2	96	5.9	1.8	61
	AU	6.5	11.7	98	6.2	1.7	323
	GBB	6.5	13.9	96	6.0	0.9	93

Note: MET: Coastal MET, KB: Kleinberg, SH: Sophies Hoogte, MK: Marble Koppie, VF: Vogelfederberg, S8: Station 8, AU: Aussinanis, GBB: Gobabeb. S1-S5 are five temporary stations.

Table B3. 4 Fog yield in ml for each fog event observed over the sampling period. Two types of passive fog collectors were used: cylindrical for the FogNet (FN) stations with the exception of Gobabeb and flat 1 m^2 for Gobabeb and Stations 1-5 (in bold).

Coastal MET_FN	100	405	7.5	<2
Kleinberg_FN	100	30	100	22
Soophies Hoogte_FN	100	6	75	52
Marble koppie_FN	150	2	43	76
Vogelfederberg_FN	250	2	4	100
Station 8_FN	n/a	0	<2	46
Aussinanis_FN	60	0	<2	46
Gobabeb	**missing**	**0**	**650**	**550**
Station 1	**2000**	**0**	**600**	**600**
Station 2	**1900**	**0**	**1270**	**340**
Station 3	**1000**	**1600**	**2360**	**560**
Station 4	**1800**	**2900**	**1640**	**670**
Station 5	**n/a**	**n/a**	**65**	**350**

Note: Because different types of collectors were used we cannot compare the yields between the different types of collectors.

Figure B3. 1 Surface water ponding at Vogelfederberg on the 10th June 2016. Evidence of recent rainfall activity on the 6th and 7th June 2016. CREDIT: K.F.K./Indiana University–Purdue University Indianapolis

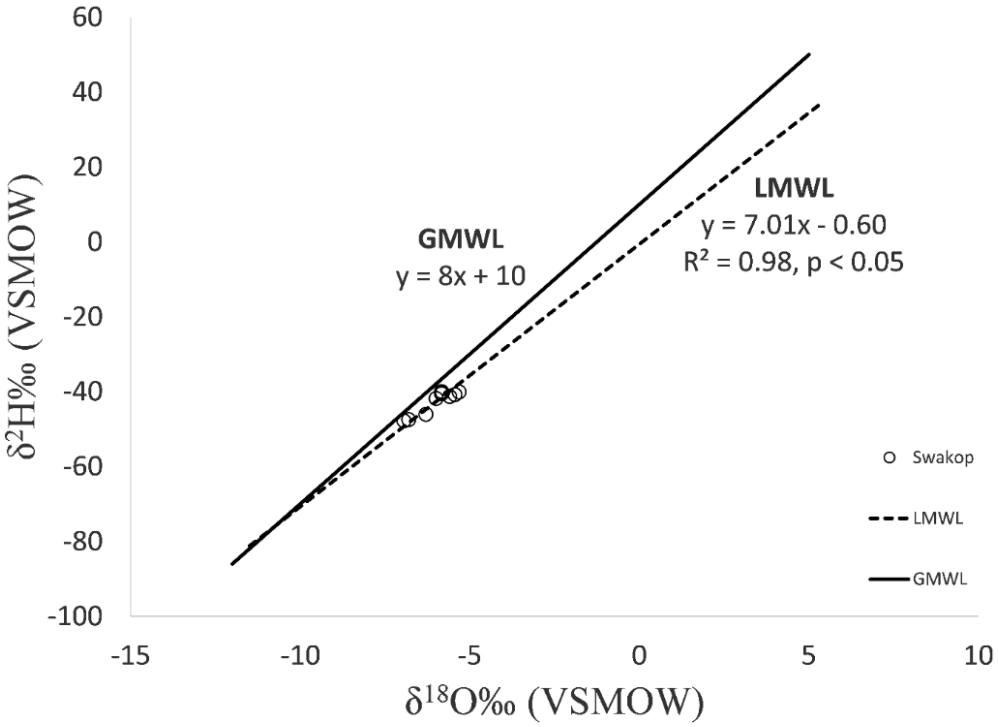

Figure B3. 2 The groundwater isotopic composition of the Swakop River and its relation to the Gobabeb local meteoric water line (LMWL). The GMWL is included as a reference, the LMWL is adapted from Kaseke et al (2017) and the Swakop River isotopic composition is from Marx (2009).

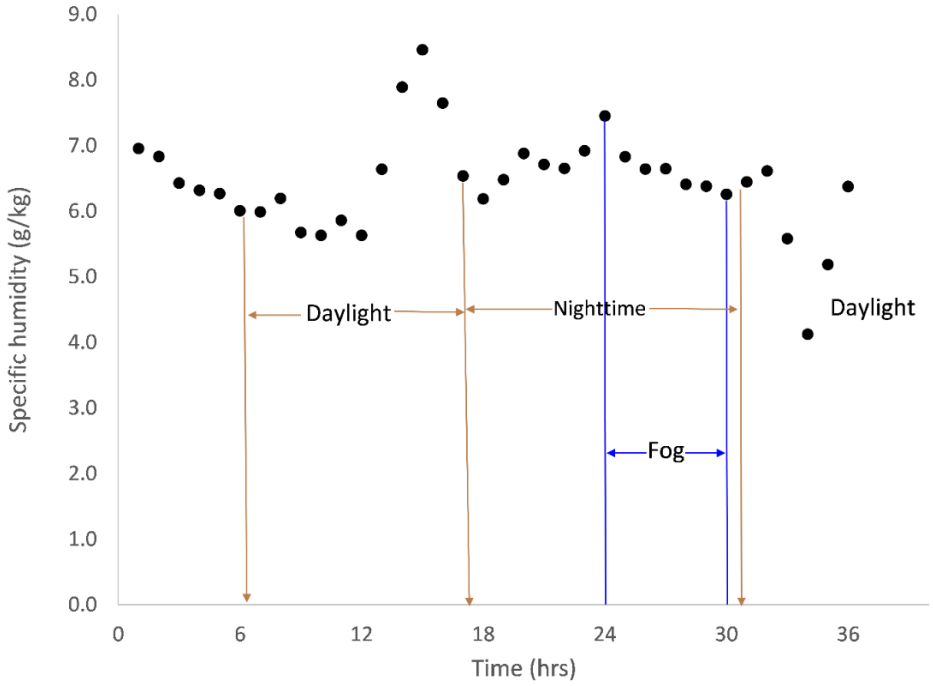

Figure B3. 3 Specific humidity changes at Vogelfederberg FogNet station with the fog hours for the 17th June 2016 fog indicated. The daylight (06:30 – 17:15 hrs) and night time hours are also indicated.

References

Kaseke, Kudzai Farai, Lixin Wang, and Mary K Seely. 2017. "Nonrainfall water origins and formation mechanisms." *Science Advances* 3 (3):e1603131.

Marx, V. 2009. "Impacts of upstream uses on the alluvial aquifer of the Swakop River, Namibia." *Germany: Diplomarbeit, Albert Ludwig University of Freiburg*.

Appendix C: An analysis of precipitation isotope distributions across Namibia using historical data

Dataset C1 Rainfall database with isotopic compositions and associated physical and meteorological conditions of the sampling sites
https://doi.org/10.1371/journal.pone.0154598.s001.

Appendix D: Precipitation origins and key drivers of precipitation isotope (^{18}O, ^{2}H, ^{17}O) compositions over Windhoek

Table D6. 1 The Windhoek weighted LMWLs at annual and inter-annual scale calculated using the Local Meteoric Water Line Freeware programme (Crawford et al. 2014).

Year	n	PWLSR	PWRMA	PWMA
2012-2013	26	y = 6.7163 + 4.8301	y = 6.8296 + 5.0283	y = 6.9401 + 5.2214
2013-2014	37	y = 7.8266 + 6.6796	y = 7.8490 + 6.8822	y = 7.8708 + 7.0789
2014-2015	19	y = 7.3435 + 7.9222	y = 7.4846 + 8.3717	y = 7.6233 + 8.8139
2015-2016	27	y = 6.9287 + 5.2171	y = 7.0266 + 5.4940	y = 7.1219 + 5.7638
2012-2016	**109**	**y = 7.5551 + 6.0685**	**y = 7.6201 + 6.4045**	**y = 7.6834 + 6.7320**

*Note: PWLSR (precipitation weighted ordinary least squares regression), PWRMA (precipitation weighted reduced major axis) and PWMA (precipitation weighted major axis)

Table D6. 2 Annual precipitation totals based on the hydrologic year (Oct-Sept) from the National Botanic Research Institute (NBRI), Southern Africa Science Service Centre for Climate Change and Adaptive Land-use (SASSCAL) weather station, Windhoek 2012-2016. The 'normal' precipitation is a long-term average from the Namibia Meteorological Services.

Year	Precipitation total (mm)
2012-2013	123.7
2013-2014	556
2014-2015	244.7
2015-2016	309
Normal	356.3

Table D6. 3 Distribution of Windhoek annual precipitation between early and late summer measured over 2012-2016.

Precipitation	2012-2013	2013-2014	2014-2015	2015-2016
Early summer, Oct-Jan	39.5	33.8	55.0	64.6
Late summer, Feb-Apr	49.9	65.7	41.8	29.3
Oct-Apr (% of annual)	89.4	99.5	96.8	93.9

Table D6. 4 Significant relationships between monthly precipitation isotopes and monthly weather data from the National Botanic Research Institute (NBRI), Windhoek 2012-2016.

Isotope	Regression equation	r	r^2	p-value
$\delta^{18}O$	y =-0.30(RH) + 8.89	-0.77	0.59	**
	y = -0.09(rainfall) + 1.86	-0.68	0.47	**
	y =-0.58(min. temp) + 5.34	-0.39	0.15	*
$\delta^{2}H$	y = -1.98(RH) + 62.73	-0.69	0.48	**
	y =-0.64(rainfall) + 18.61	-0.67	0.45	**
	y =-4.04(min. temp) + 42.76	-0.38	0.14	*
$\delta^{17}O$	y =-0.16(RH)+ 4.56	-0.77	0.59	**
	y = -0.05(rainfall) + 0.95	-0.69	0.48	**
	y =-0.30(min. temp) + 2.75	-0.39	0.15	*
d	y = 0.44(RH) – 8.40	0.52	0.27	**

Table D6. 5 Significant relationships between volume weighted monthly precipitation isotopes and monthly weather data from the National Botanic Research Institute (NBRI), Windhoek 2012-2016.

Isotope	Regression equation	r	r^2	p-value
$\delta^{18}O$	y =-0.10(rainfall) + 0.19	-0.93	0.86	**
	y = -0.20(RH) + 0.50	-0.60	0.36	**
$\delta^{2}H$	y = -0.07(rainfall) + 1.51	-0.89	0.80	**
	y =-0.14(RH) + 3.50	-0.55	0.30	**

Table D6. 6 Univariate analysis of event scale precipitation isotopes and stratiform fraction, Windhoek 2012-2016.

Isotope	Regression equation	r	r^2	p-value
$\delta^{18}O$	y = 0.07(stratiform) - 8.27	0.29	0.09	> 0.05
	y = 0.42(ppt. rate) - 4.20	0.05	0.00	> 0.05
$\delta^{2}H$	y = 0.41(stratiform) - 54.82	0.25	0.06	> 0.05
	y =6.63(ppt. rate) - 35.63	0.12	0.01	> 0.05
$\delta^{17}O$	y = 0.03(stratiform) - 4.29	0.29	0.08	> 0.05
	y = 0.24(ppt. rate) - 2.22	0.06	0.00	> 0.05
d	y = 3.25 (ppt. rate) - 2.01	0.37	0.14	> 0.05

Note: stratiform is stratiform fraction (%) and ppt. rate is precipitation rate (mm/hr)

Table D6. 7 Influence of precipitation type (convective and stratiform) on precipitation isotope compositions sampled from Windhoek between 2012 and 2016, (n = 24). Precipitation type was obtained from TRMM and GPM satellite data.

		Mean $\delta^{18}O$‰			Mean $\delta^{2}H$‰			Mean $\delta^{17}O$‰			Mean *d*‰	
ppt	**n**	**Ath**	**WA**	**RNG**	**Ath**	**WA**	**RNG**	**Ath**	**WA**	**RNG**	**Ath**	**RNG**
strat	16	+1.88	-2.63	-15.71 - +7.32	-14.36	-17.84	-122.19 - +45.83	-0.98	-1.36	-8.12 - +3.85	+0.70	-15.2 - +10.4
con	8	-6.88	-3.55	-15.84 - +2.62	-47.44	-25.23	-119.95 - +23.82	-3.60	-1.86	-8.24 - +1.23	+7.64	+1.6 - +19.8
com	24	-3.55	-6.18	-15.84 - +7.32	-25.39	-43.07	-122.19 - +45.83	-1.85	-3.21	-8.24 - +3.85	+3.0	-15.5 - +19.8

Note: strat. is stratiform, con. is convective, com. is combined (stratiform and convective), Ath is arithmetic mean, WA is weighted average and RNG is range.

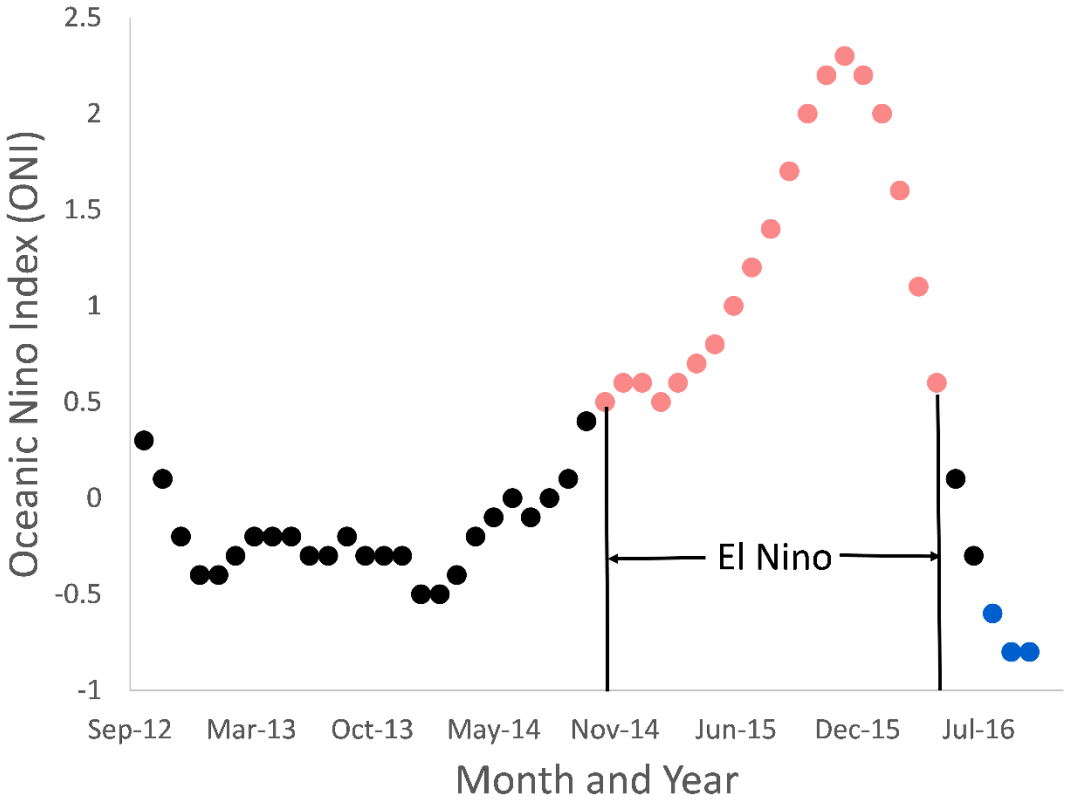

Figure D6. 1 El Niño Southern Oscillation (ENSO) trends measured using the Oceanic Nino Index for the period 2012-2016. An ENSO phase is defined by at least three months continuous data above or below ± 0.5, with months not satisfying this criteria considered neutral (black dots). A positive ENSO phase (+) is denoted by red dots while a negative ENSO (-) phase is denoted by blue dots.

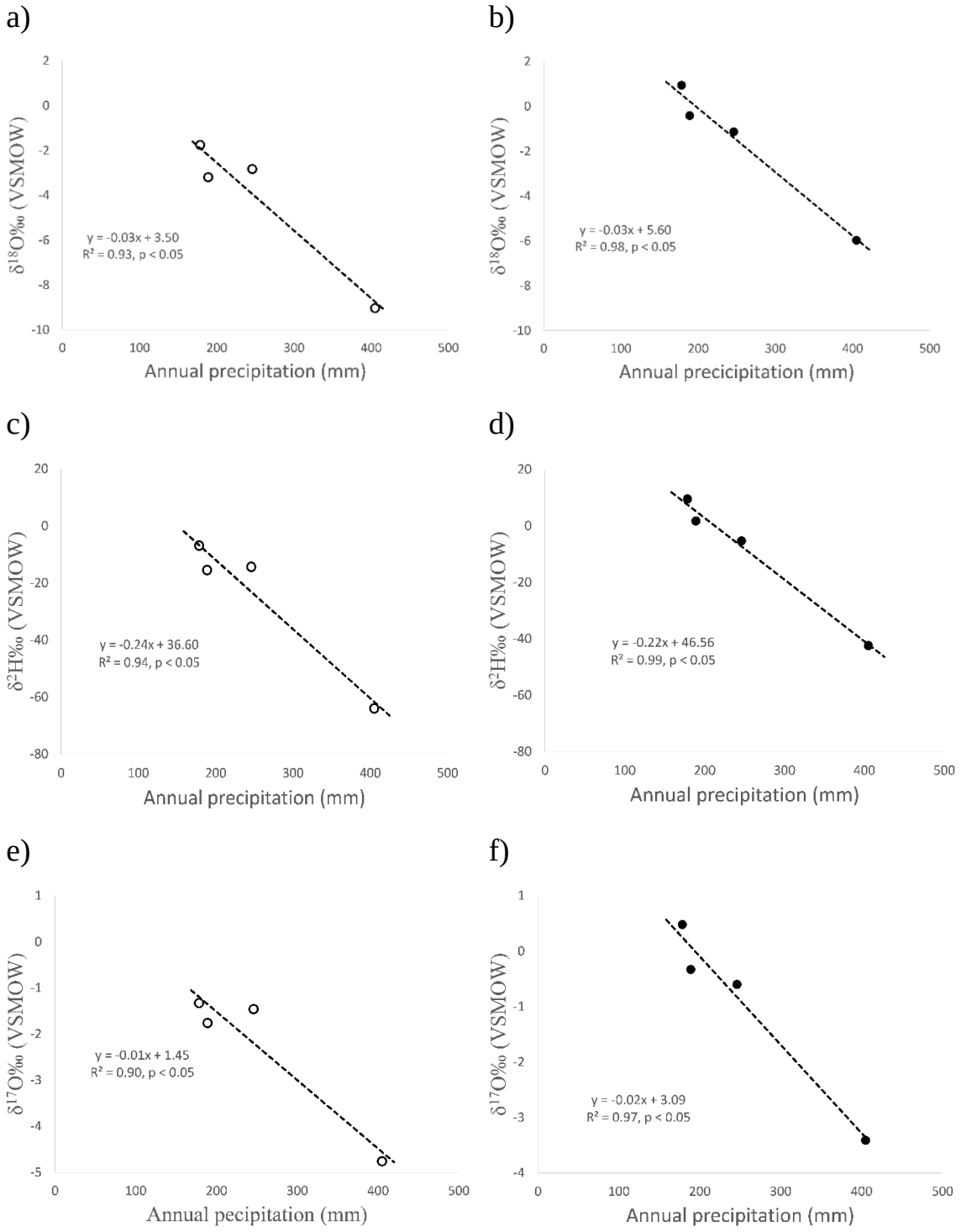

Figure D6. 2 The Annual weighted and unweighted precipitation isotopes vs precipitation amount: a) weighted δ ^{18}O, b) unweighted δ ^{18}O, c) weighted δ ^{2}H, d) unweighted δ ^{2}H, e) weighted δ ^{17}O and e) unweighted δ^{17}O.

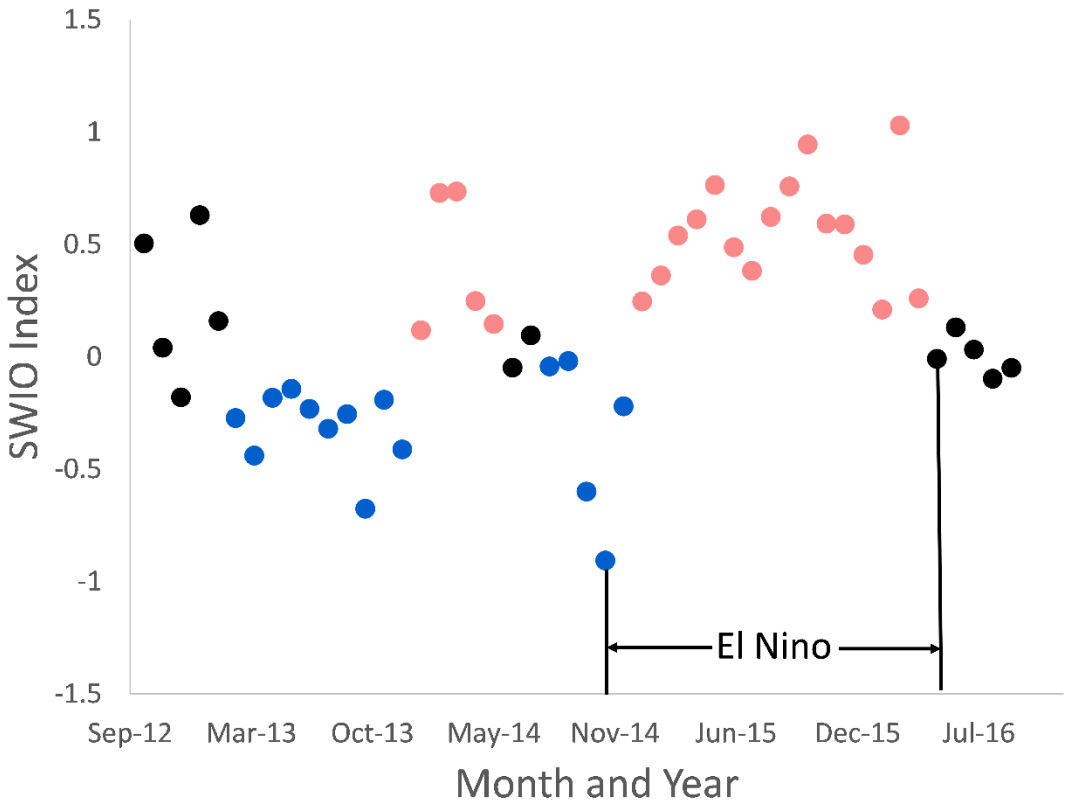

Figure D6. 3 The subtropical Indian Ocean dipole (SIOD) as measured by the South Western Indian Ocean Index for the period 2012-2016. An SIOD phase is defined by at least three months continuous + or -data, with months not satisfying this criteria considered neutral (black dots). A positive SIOD phase (+) is denoted by red dots while a negative SIOD (-) phase is denoted by blue dots.

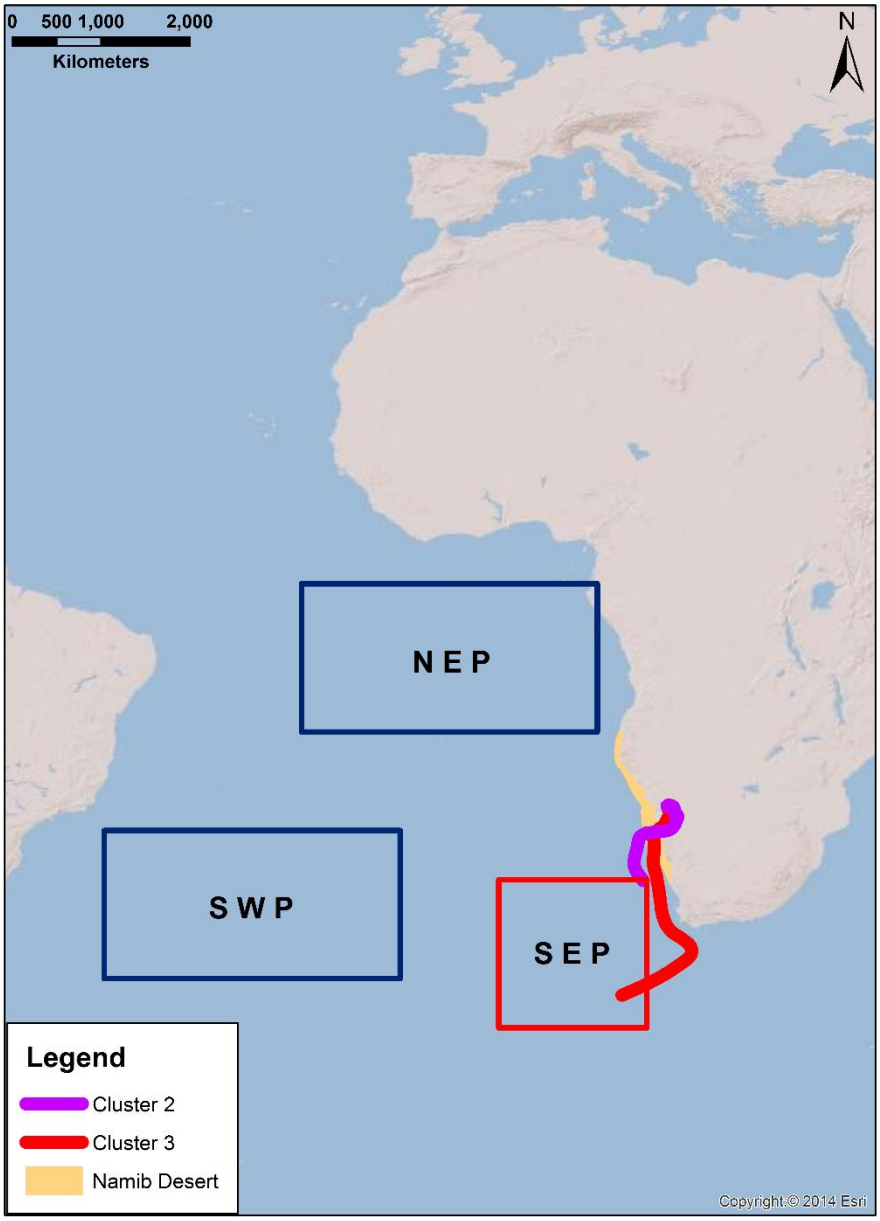

Figure D6. 4 The location of the South Atlantic Dipole (SWP (10°W–40°W, 25°S–40°S) and NEP (10°E–20°W, 0°S–15°S)) used for defining the South Atlantic Dipole Index (Nnamchi et al. 2011) and the position of the secondary dipole defined here as: SWP (10°W–40°W, 25°S–40°S) and SEP (0°–15°E, 30°S–45°S). Where SWP is the south-west position of the dipole, NEP is the north-east position and SEP is the south-east position.

Dataset D1 Event and monthly precipitation samples, isotopes and associated meteorological data used in the manuscript 2018JD028470-sup-0002-Data_Set_SI-S01.xls

References

Nnamchi, Hyacinth C, and Jianping Li. 2011. "Influence of the South Atlantic Ocean dipole on West African summer precipitation." *Journal of Climate* 24 (4):1184-1197.

CURRICULUM VITAE
KUDZAI FARAI KASEKE

Professional Preparation

December 2018	INDIANA UNIVERSITY – PURDUE UNIVERSITY INDIANAPOLIS **PhD Major: Applied Earth Sciences** (Advisor: Lixin Wang) A stable isotope approach to investigate ecohydrological processes in Namibia. **PhD Minor: Remote sensing and GIS** (Jeffery Wilson) Coursework completed: Introduction to GIS; Advanced GIS; Introduction to Remote Sensing; Advanced GIS
December 2009	STELLENBOSCH UNIVERSITY (SOUTH AFRICA) **MSc. in Conservation Ecology** (Advisors: Anthony Mills and Karen Esler) “Non-rainfall" atmospheric water in arid soil micro-hydrology and ecology.
August 2005	UNIVERSITY OF ZIMBABWE (ZIMBABWE) BSc. Honours Agriculture – Soil Science

Awards

IUPUI Graduate student travel fellowship	2017
IUPUI School of science graduate council travel award	2015
IUPUI Graduate student travel fellowship	2014

Nominations

John H. Edwards Fellowship	2017
Sherry Queener Graduate Student Excellence Award	2017

Sherry Queener Graduate Student Excellence Award 2016

Research and Teaching experience

Research Assistant: IUPUI Ecohydrology Lab, Department of Earth Sciences, Indianapolis, Indiana (August 2013 – August 2018)

Teaching Assistant: Principles of Ecology and Evolution Laboratory, IUPUI Biology Department, Indianapolis, Indiana (August 2014 – December 2016)

Research Assistant: Stellenbosch University, Soil Science Department, Stellenbosch, South Africa (August 2007 – December 2009)

Voluntary intern: Gobabeb Training and Research Centre, Namib Naukluft Park, Namibia (June 2006 – January 2007)

Publications

1. **Kaseke, K. F**. and Wang, L. Fog and dew as potable water resources - harvesting technique improvements and water quality concerns. *GeoHealth doi:10.1029/2018GH000171*

2. **Kaseke, K. F**., Wang, L., Tian, C., Wanke, H. and Lanning, M. Rainfall origins and key drivers of precipitation isotope (δ^2H, $\delta^{18}O$ and $\delta^{17}O$) compositions over Windhoek. *Journal of Geophysical Research-Atmospheres doi.org/10.1029/2018JD028470*

3. Tian, C., Wang, L., **Kaseke, K. F.** and Bird, B. W. (2018) Stable isotope compositions (δ^2H, $\delta^{18}O$ and $\delta^{17}O$) of rainfall and snowfall in the central United States. *Scientific Reports 8:6712, doi:10.1038/s41598-018-25102-7*

4. **Kaseke, K.F.,** Wang, L., Tian, C., Seely, M.K., Vogt, R., Wassenaar, T. and Mushi, R. (2018) Fog spatial distributions over the Central Namib Desert – an isotope approach. *Journal of Aerosol and Air Quality Research, doi: 10.4209/aaqr.2017.01.0062*

5. **Kaseke, K.F.,** Wang, L. and Seely, M.K. (2017) Non-rainfall water origins and formation mechanisms in the Namib Desert. *Science Advances 3 (3), e1603131 doi:10.1126/sciadv.1603131*

6. **Kaseke, K. F**., Wang, L., Wanke, H., Turewicz, V. and Koeniger, P. (2016) An analysis of precipitation isotope distributions across Namibia using historical data. *PloS one 11 (5), doi.org/10.1371/journal.pone.0154598*

7. Li, B., Wang, L., **Kaseke, K. F.,** Vogt, R. and Seely, M. K. (2018) The impact of fog on soil moisture dynamics in the Namib Desert. *Advances in Water Resources 113, 23-29 doi.org/10.1016/j.advwatres.2018.01.004*

8. Ravi S., Wang L., **Kaseke K. F.** and Buynevich I. V. (2017) Ecohydrologic interactions within "fairy circles" in the Namib Desert: Revisiting the self-organization hypothesis. *Journal of Geophysical Research: Biogeosciences 122 (2), 405-414 doi:10.1002/2016JG003604*

9. Wang, L., **Kaseke, K. F.** and Seely, M. K. (2016) Effects of non-rainfall water inputs on ecosystem functions. *WIREs Water 2017, 4:e1179, doi/10.1002/wat2.1179*

10. Lu, X., Wang, L., Pan, M. and **Kaseke, K. F**. (2016) A multi-scale analysis of Namibian rainfall over the recent decade – comparing TRMM satellite estimates and ground observations. *Journal of Hydrology: Regional Studies 8 (2016) 59-68 http://dx.doi.org/10.1016/j.ejrh.2016.07.003*

11. Li, B., Wang, L., Li, L., **Kaseke, K. F.** and Seely, M. K. (2016) The Impact of Rainfall on Soil Moisture Dynamics in a Foggy Desert. *PloS one 11 (10), e0164982, http://dx.doi.org/10.1371/journal.pone.0164982*

12. Warren-Rhodes, K. A., McKay, C. P., Boyle, L. Ng., Wing, M. R., Kiekebusch, E. M., Cowan, D. A., Stomeo, F., Pointing, S. B., **Kaseke, K. F**., Eckardt, F., Henschel, J. R., Anisfeld, A., Seely M. K and Rhodes, K. L. (2013) Physical Ecology of Hypolithic Communities in the Central Namib Desert: the Role of Fog, Rain, Rock Habitat and Light. *Journal of Geophysical Research: Biogeosciences 118 (4), 1451-1460, doi/10.1002/jgrg.20117.*

13. **Kaseke, K. F**., Mills, A. J, Esler, K. J., Henschel, J. R., Seely, M. K. and Brown. R (2012) Spatial variation of "non-rainfall" water input and the effect of mechanical soil crusts on input and evaporation. *Journal of Pure and Applied Geophysics 169 (12), 2217-2229, doi/10.1007/s00024-012-0469-5*

14. **Kaseke, K.F**., Mills, A.J., Brown, R., Esler, K.J., Henschel, J.R. and Selly, M.K (2012) The effects of desert pavements on soil micro-hydrology. *Journal of Pure and Applied Geophysics 169 (5), 873-880, doi/10.1007/s00024-011-0367-2*

15. **Kaseke, K.F**., Mills, A.J., Brown, R., Esler, K.J., Henschel, J.R. and Seely, M.K (2012) A method for direct assessment of the "non-rainfall" atmospheric water cycle: input and

evaporation from the soil. *Journal of Pure & Applied Geophysics, 169 (5), 847-85710, doi/10.1007/s00024-011-03289*

Selected Presentations and Conference contributions

1. **Kaseke, K. F**. Stable isotopes in dryland ecohydrology: what can $\delta^{17}O$ tell us? Oral. *Desert Research Institute, January 2018.*

2. **Kaseke, K. F**., Wang, L. and Wanke, H. Key drivers of precipitation isotopes in a dryland Windhoek, Namibia (2012-2016). Poster. *AGU-Fall Meeting, San Francisco, December 2016.*

3. **Kaseke, K. F**., Wang, L., Tian, C., Wanke, H. and Lanning, M. Rainfall origins and key drivers of precipitation isotope ($\delta^{2}H$, $\delta^{18}O$ and $\delta^{17}O$) compositions over Windhoek. Oral. *IAEA Coordinated Research Programme (F31004), Vienna Austria, Oct 2017*

4. **Kaseke, K. F**., Wang, L. and Wanke, H. The dynamics of rainfall isotopic compositions ($\delta^{2}H$, $\delta^{18}O$ and $\delta^{17}O$) from Windhoek, Namibia. Poster. *AGU-Fall Meeting, San Francisco, December 2016.*

5. Ravi, S., Wang, L., **Kaseke, K.F.** and Buynevich, I.V. Ecohydrologic interactions within "fairy circles" in the Namib Desert. Poster. *AGU-Fall Meeting, San Francisco, December 2016*

6. Daryanto, S., Wang, L., **Kaseke, K. F.** and Ravi, S. Integrating teaching and authentic research in the field and laboratory settings. Poster. *AGU-Fall Meeting, San Francisco, December 2016*

7. Li, B., Wang. L., **Kaseke, K.F.** and Seely, M. The soil moisture dynamics and its control in a foggy desert. Poster. *AGU-Fall Meeting, San Francisco, December 2016*

8. **Kaseke, K. F**., Wang, L., Wanke, H., Turewicz, V. and Koeniger, P. An analysis of stable water isotope distributions across Namibia: rainfall and groundwater isoscapes. Poster. *AGU-Fall Meeting, San Francisco, December 2015*

9. Wang, L., **Kaseke, K. F.,** Daryanto, S. and Ravi, S. Integrating teaching and research in the field and laboratory settings. Poster. *AGU-Fall Meeting, San Francisco, December 2015*

10. **Kaseke, K. F**., Wang, L., Wanke, H., Turewicz, V. and Koeniger, P. An analysis of stable water isotope distributions across Namibia: rainfall and groundwater isoscapes. Oral. *IAEA Coordinated Research Programme (F31004), Vienna Austria, Jun 2015*

11. **Kaseke, K. F. and Wang, L. (2014)** Stable isotope analysis of rainfall and "non-rainfall" inputs in the Namib Desert. Poster. *AGU-Fall Meeting, San Francisco, December 2014*

12. Lu, X., Wang, L., Pan, M. and **Kaseke. K. F.** A multi-scale analysis of Namibian rainfall-comparing TRMM satellite data and ground observations. Poster. *AGU-Fall Meeting, San Francisco, December 2014*

13. Wang, L. and **Kaseke, K. F.** Environmental monitoring without borders. Poster. *AGU-Fall Meeting, San Francisco, December 2014*

14. **Kaseke, K.F.** The effect of soil type on "non-rainfall" atmospheric water input into soil. Oral. *Namibia Scientific Society, July 2009*

15. **Kaseke, K.F.** Spatial variation of "non-rainfall" atmospheric water. Oral. *Namibia Scientific Society, July 2009*

16. **Kaseke, K.F.** The influence of quartz pebbles on "non-rainfall" atmospheric water input, preliminary results. Oral. *Interfaces, Oudtshoorn South Africa, oral presentation, August 2008*

17. **Kaseke, K.F.,** Henschel, J.R. and Berkowicz,S. Dew collection in the Namib Desert. Oral. *4th International Conference on Fog and Dew, La Serena Chile, July 2007*